Nuffield Department of Clinical Neurosciences

DPhil Clinical Neurosciences

The *in-vivo* study of Pain in Neuromyelitis Optica

George Tackley

St Edmund Hall

Supervisors:
Dr Jacqueline Palace
Prof Irene Tracey
Dr Yazhuo Kong

Trinity Term, 2017

Abstract

The in-vivo study of Pain in Neuromyelitis Optica

George Tackley, St Edmund Hall
Trinity Term, 2017

Neuromyelitis optica is a severe autoimmune neuroinflammatory disorder characterised by longitudinally extensive myelitis and severe optic neuritis. An oft-neglected symptom of the condition is severe, intractable chronic pain that can be detrimental to quality of life and is marked out by its severity and prevalence in comparison to the related disorder, multiple sclerosis.

The experiments within this thesis make use of both conventional and advanced MRI techniques applied to the spinal cord and brain, and ^{1}H NMR spectroscopy of blood plasma to explore the mechanisms driving chronic pain in NMO. The principle findings are:

i. Thoracic lesions are associated with greater pain, irrespective of lesion length or cervical lesion volume. They are associated with spinothalamic tract damage in the cervical cord that correlates with the severity of pain. A possible autonomic aetiology is proposed.

ii. Periaqueductal grey (PAG) to dorsolateral prefrontal cortex and to pregenual anterior cingulate cortex functional connectivity is correlated with pain severity, conversely PAG to rostroventromedial medulla connectivity is negatively associated with pain severity. Disruption of descending pain modulatory circuits is considered.

iii. PAG glutamate concentration is negatively correlated with pain scores and is higher in low pain patients compared to controls and high pain patients. The discussion includes consideration of pain vulnerability.

Chronic pain in NMO can devastate lives. The studies undertaken in this thesis are some of the earliest MRI imaging studies directed at understanding pain in NMO and the association of pain with thoracic lesions and the aberrations in the descending pain modulatory network are novel findings. There is more to be done and my hope is that this body of work will serve as a stepping-stone to a better understanding of chronic pain in NMO and the future development of effective treatments.

Table of contents

Acknowledgments

A huge debt of gratitude is owed to my supervisors, Dr Jaqueline Palace and Prof Irene Tracey, for creating the opportunity to study pain and neuromyelitis optica in Oxford, and for the unrelenting support that they and my third supervisor Dr Yazhuo Kong have provided over the last few years.

I need also to thank our funders, the Guthy-Jackson Charitable Foundation, without whom the imaging work would not have been possible.

I am indebted to Dr Faye Probert and Dr James Larkin for their guidance, collaboration and tutoring in metabolomics, and for their abundant NMR and analytical wizardry, and to Prof Daniel Anthony for the use of his laboratory.

The neuroimmunology team in the John Radcliffe also require my thanks, specifically Prof Angela Vincent and Dr Patrick Waters for their friendly input and advice, and Dr Mark Woodhall for his tireless assaying, expertise and friendship.

Of no lesser importance, my wife Emma for all those additional hours of childcare and for her willingness to let me follow my passion; my children Eva and Jessica for not disturbing Daddy in his study; my mother, father and parents-in-law, Alan and Joanne, for their tremendous support, and my good friend Kurt Dettman for his help proofreading.

George Tackley, October 2017

S.D.G.

Chapter 1a

Neuromyelitis optica: clinical features, pathology and treatment

Introduction and terminology

Neuromyelitis optica (NMO) is a severe neuroinflammatory disorder of the central nervous system, commonly manifesting with one or both of visual impairment due to optic neuritis and sensory or motor dysfunction as a results of transverse myelitis, and with blindness, paralysis, respiratory failure and coma at its most severe (Chalumeau-Lemoine et al., 2006; Wingerchuk et al., 1999). Alongside these disabling complaints, and hitherto relatively neglected by physicians, a large proportion of NMO patients suffer severe and chronic neuropathic pain (Kanamori et al., 2011). Understanding chronic NMO-related pain is the motivation for my thesis.

Historically, NMO has been considered a variant of the demyelinating disorder multiple sclerosis (MS), however since the discovery of the causative antibody, aquaporin 4 antibodies (AQP4Ab), a greater understanding of its pathophysiology has emerged and it is now clear that NMO due to AQP4Abs is primarily an astrocytopathy causing secondary demyelination (Lennon et al., 2004; Pittock and Lucchinetti, 2016).

Throughout the thesis, NMO will be used with reference to any participant with confirmed or suspected AQP4Ab positive disease. Where the inclusion of seronegative NMO examples are of relevance, these will be highlighted in the text.

Epidemiology and race

NMO affects at least twice as many women as men, with a ratio of 10 to 1 in some populations (Etemadifar et al., 2015). Mean age of onset is between 30 and 40 years (Etemadifar et al., 2015), but NMO can present at any age, from the very young to octogenarians (Absoud et al., 2015; Suchdev et al., 2017). Prevalence is between 0.5 and 4.4 per 100,000, with incidence between 0.05 and 0.4 per 100,000 per year; some of this range may be due in part to different prevalence and incidence figures for different racial groups, for example there is probably a higher incidence and prevalence in Afro-Caribbean compared to Caucasian and Japanese populations (Etemadifar et al., 2015). Relapse rates also appear to be higher in Afro-Caribbean compared with Caucasian and Japanese groups (Pandit et al., 2015; Tackley et al., 2016), and Afro-Caribbean groups tend to have lower age of onset and poorer visual (but not motor) outcomes (Kitley et al., 2012b).

Although published studies have yet to look at the interplay between race and pain within NMO, there is a large body of literature examining racial differences in other pain models and disorders. These have shown lower pain thresholds and tolerance levels in African-

Americans and Asian-Americans compared to non-Hispanic whites (Campbell et al., 2005; Rowell et al., 2011), however a large confounder is that enhanced physiological pain sensitivity may result from the psychosocial effects of being a member of a minority ethnic group (Edwards et al., 2001). There is a paucity of literature regarding the physiological mechanisms behind differing pain experiences across races, a few studies have shown differences in physiological measures, for example African-Americans have lower-threshold involuntary nociceptive flexion reflexes compared to non-Hispanic whites (Campbell et al., 2008), but anatomically precisely where these changes are actuated is unclear, i.e. are they a result of top-down modulation secondary to psycho-social factors, or do they reflect genetic or structural differences between races? Sociocultural factors certainly play an important role, altering (a) the experience of pain, for example the greater use of 'external' coping strategies in African-Americans compared to non-Hispanic whites, (b) the reporting of pain, for example Italian-born men are more likely to report back pain compared to a Caucasian Australian population, (c) the meaning of pain, from persecutory interpretations to something to be conquered, and (d) the access to (and take-up of) treatment, usually skewed in favour of ethnic *majority* populations (Campbell and Edwards, 2012; Portenoy et al., 2004; Stanaway et al., 2011; Tan et al., 2005; See Campbell and Edwards for review).

Presenting signs and symptoms

The common presenting symptoms of NMO can be broadly divided by lesion location: spinal cord (sensorimotor), optic nerve (visual) and brainstem (varied manifestations).

Acute myelitis in NMO commonly manifests with sensory or motor deficits, and can cause bladder and sexual dysfunction (the former presumably more common with lumbosacral

cord involvement as seen in non-NMO transverse myelitis) (Kalita et al., 2002; Mutch et al., 2014). Symptoms typically progress over days to varying degrees of dysfunction, at worst to anaesthesia, paralysis and anuria. Not uncommonly, these symptoms are heralded by back pain overlying and localising the causative area of myelitis; this pain commonly resolves but is frequently replaced by chronic neuropathic pain symptoms: spasm-evoked pain, allodynia, hyperalgesia and spontaneous pain (Pellkofer et al., 2013; Qian et al., 2012; Zhao et al., 2014), discussed in detail in Chapter 1c.

Equally common as sensorimotor deficits are visual disturbance and blindness (Tackley et al., 2016), unilateral more commonly than bilateral (Wingerchuk et al., 1999). These share characteristics of other optic neuritis aetiologies, such as pain evoked by eye movement, however unlike MS-related or idiopathic optic neuritis (ON), they are more frequently bilateral and more likely to incur poor visual outcome (Kim et al., 2017). Of note, as with the acute components of myelitis-related pain optic neuritis pain also resolves (usually within days), however, unlike with NMO spinal cord damage, a chronic optic / ophthalmic pain phenotype is not recognised.

The symptoms of brain involvement in NMO attacks are wide ranging and may relate partly to the distribution of AQP4 (see below, especially Figures 1 and 2). The commonest, and archetypal of NMO, is severe and protracted vomiting, plus or minus hiccoughs, attributable to lesions of the area postrema (Wingerchuk et al., 2015). Less common are the syndrome of inappropriate ADH secretion, caused by lesions of the hypothalamus (Pu et al., 2015) and encephalopathy caused by large lesions of brain parenchyma, very infrequent in adults but more frequent in children (Wingerchuk et al., 2015). Unusual symptoms of disordered

thermoregulation, daytime somnolence, memory disturbance and behavioural change have all been reported associated with brainstem and hypothalamic lesions (Viegas et al., 2009). Importantly there are no reports of pain modulation by NMO brainstem lesions involving the periaqueductal grey (PAG), an area not uncommonly lesioned in NMO and a key component of descending pain modulatory pathways (Matthews and Palace, 2014). Animal studies have shown that lesions of the PAG can both *produce* analgesia and *reduce* opioid mediated analgesia (Dostrovsky and Deakin, 1977; Melzack et al., 1958). Although not explicitly reported in the NMO literature, a related area, the rostral ventromedial medulla (RVM), is likely to on occasion be affected by lesions in NMO given the frequency of medullary lesions and might also play a role in NMO pain pathology. Again, the animal literature shows that lesions of the RVM produce resistance to opiate induced analgesia (Prieto et al., 1983). Electrical and pharmacological stimulation of these and other brainstem regions produce hugely varied effects on pain. These are discussed in greater detail in Chapter 1c within the context of the descending modulation of pain.

Disease course

NMO typically relapses if left untreated, probably about once a year (although natural history data are lacking), with each relapse carrying the risk of increased disability (Tackley et al., 2016). This is quite unlike MS where major disability accumulates progressively in the later stages of disease when relapses have ceased; in NMO there is no progressive phase and disability is all relapse related. Attack-dependent disability is the premise for maintaining lifelong immunosuppression in confirmed cases of NMO. Given the recommendations for lifelong treatment, the precise natural history off-treatment is not well defined, but has clearly improved since the 1990s where 31% (15/48) died within 5-

years, most frequently of acute respiratory failure (Wingerchuk et al., 1999); within the Oxford cohort less than 10% (7/76) of AQP4Ab positive patients died over a 3-year period between 2013 and 2016, and none of respiratory failure related to an acute myelitis episode (personal observation). It is important to note here that AQP4Ab negative NMO can be monophasic (whereas AQP4Ab positive NMO is invariably relapsing) and lifelong treatment for the seronegative group may not be appropriate (Kitley and Palace, 2016). It is also important to note that although AQP4Ab positive NMO is typically polyphasic (relapsing), chronic pain symptoms (outside of the acute relapse episode) are often permanent consequences (or near permanent consequences) of previous relapses (personal observation); chronic pain intensity may increase at the time of subsequent relapses but there is no available evidence to suggest it remains at a level greater than baseline thereafter and its natural history in relation to subsequent relapses is largely unknown (Zhao et al., 2014). Of those with pain in NMO, it is constant in nature in greater than 60% (Qian et al., 2012; Zhao et al., 2014).

Patients on immunosuppressive treatment relapse on average once every two years. Severity of relapse is largely unpredictable however it appears that immunosuppression may lessen the disabling effect of a relapse (Tackley et al., 2016). It should be noted that there is no clearly defined outcome measure with which to measure disease severity; the commonly used EDMUS (Confavreux et al., 1992) or EDSS (Kurtzke, 1983) are well recognised but do not incorporate information about other important outcomes such as fatigue and pain.

The site of attacks is varied. Onset attacks commonly affect the cord (typically longitudinally extensive transverse myelitis, LETM, with 3 or more contiguous spinal cord segments involved) and optic nerve, however multiple other lesion sites are recognised (Wingerchuk et al., 2006). As with presenting features, relapses can cause damage anywhere in the CNS. Isolated optic neuritis is probably relatively less common in relapses compared to onset attacks, though remains one of the commonest relapse types (Tackley et al., 2016).

It will thus be important to examine whether relapse frequency and number are important for developing chronic pain, and to explore the relationship between commonly used disability scores (such as EDMUS) and pain measures.

Diagnostic criteria

Table 1. (**A**) 1999 and, (**B**) 2015 diagnostic criteria

(Adapted from Wingerchuk et al., 1999, 2015{Citation})

A – 1999 Criteria
Diagnosis requires all absolute criteria *and* one major supportive criterion *or* two minor supportive criteria
Absolute criteria
1. Optic neuritis
2. Acute myelitis
3. No evidence of clinical disease outside of the optic nerve or spinal cord
Supportive criteria
Major
1. Negative brain MRI at onset (does not meet MS criteria of Paty et al.*)
2. Spinal cord MRI with signal abnormality extending over ≥3 vertebral segments
3. CSF pleocytosis of >50 WBC/mm^3 *OR* >5 neutrophils/ mm^3
Minor
1. Bilateral optic neuritis
2. Severe optic neuritis with fixed visual acuity worse than 20/200 in at least one eye
3. Severe, fixed, attack-related weakness (MRC grade ≤2) in one or more limbs

(table continued overleaf)

B – 2015 Criteria (abridged)

Criteria for NMOSD with positive AQP4Ab
1. At least 1 core clinical characteristic
2. Exclusion of all alternative diagnoses
Criteria for NMOSD *without* positive AQP4Ab result
At least 2 core clinical characteristics as a result of 1 or more attacks and meeting the following requirements: a. At least 1 of the core clinical characteristics must be optic neuritis, acute myelitis, or area postrema syndrome b. Dissemination in space c. Fulfillment of additional MRI requirements, as applicable
2. Exclusion of alternative diagnoses

Core clinical characteristics
1. Optic neuritis
2. Acute myelitis
3. Area postrema syndrome: Otherwise unexplained hiccoughs or nausea and vomiting
4. Acute brainstem syndrome
5. Symptomatic narcolepsy or acute diencephalic clinical syndrome with NMOSD-typical diencephalic lesions
6. Symptomatic cerebral syndrome with NMOSD-typical brain lesions

Additional MRI requirements for AQP4Ab negative NMOSD
1. Acute optic neuritis: A. normal brain MRI or non-specific findings, or B. optic nerve MRI with T2-weighted or T1-Gd enhanced lesions > half optic nerve length or involving optic chiasm
2. Acute myelitis: lesion extending over ≥ 3 contiguous segments (=LETM) or ≥ 3 contiguous segments of SC atrophy with history compatible with past myelitis
3. Area postrema syndrome: requires associated dorsal medulla or area postrema lesions
4. Acute brainstem syndrome: requires associated peri-ependymal brainstem lesions

MS, multiple sclerosis; *MS diagnostic criteria (Paty et al., 1988); MRC, Medical Research Council; CSF, cerebrospinal fluid; LETM, longitudinally extensive transverse myelitis; SC, spinal cord.

The discovery of AQP4Abs as a specific and sensitive marker for NMO (defined by 1999 diagnostic criteria; Table 1A) has enabled rapid diagnosis and has changed consensus over the disease's definition and scope (Wingerchuk et al., 1999). The place of the antibody test within the criteria has evolved from being a sub-criterion in 2006, to being of foremost

importance in the contemporary definition: NMO (or NMOSD) is now divided into “antibody positive” and “antibody negative” before any further criteria are evaluated, with the Ab-positive group no-longer requiring the demonstration of optic neuritis or spinal cord lesions on MRI to make a diagnosis (Wingerchuk et al., 2015; Table 1B). Despite the dominance of AQP4Abs in the diagnostic criteria, LETM remains an important and accurate marker of NMO and is especially useful for diagnosis in participants without AQP4Ab positive status (Kitley, 2013).

The discovery of AQP4Ab led to the recognition of a broader spectrum of anatomical involvement in NMO, including within the brain with abnormalities shown on MRI in about 50% of AQP4Ab positive cases (Kim et al., 2015) and within spinal cord where it is now recognised that short cord lesions can feature in the absence of LETM (Flanagan et al., 2015). Many NMO lesions are found in areas highly relevant to pain processing, notably the spinal cord dorsal horn, hypothalamus, periaqueductal grey, locus coeruleus, and medulla (conceivably affecting the rostral ventromedial medulla) (Blanc et al., 2012; Downer et al., 2012; Kim et al., 2010; Matthews and Palace, 2014; Pittock et al., 2006; see Figure 1 and Chapters 1b and 1c for further discussion).

Figure 1. Areas of lesion-based and 'hidden' damage with anatomical relevance to the processing of pain in NMO patients.

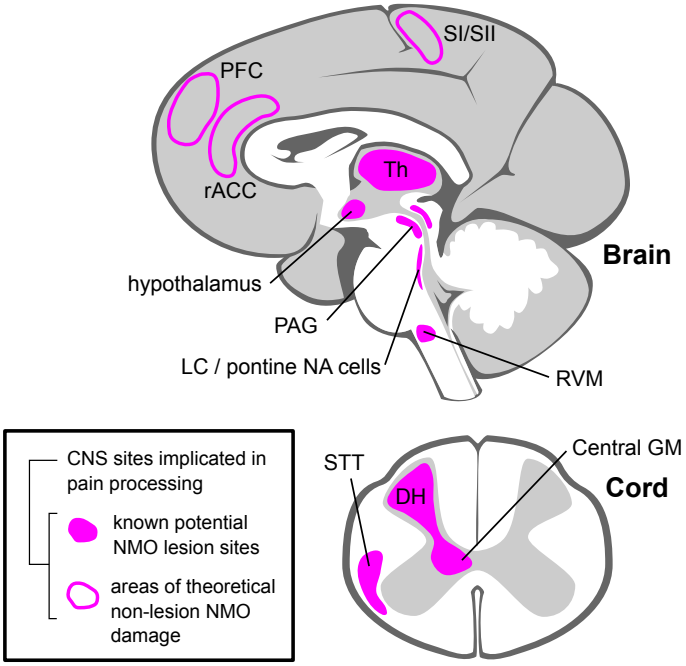

Lesions in NMO frequently coincide with CNS areas relevant to pain processing (filled pink areas). Additionally, areas not thought to be affected by lesions but nonetheless with evidence of non-lesion damage (for example MRI diffusion measure abnormalities in normal appearing neural tissue) may also occur at pain-relevant sites (unfilled pink outlines). These areas implicated in pain processing are discussed in more detail in the introductory chapters (1a, 1b and 1c). PFC, pre-frontal cortex; SI/SII, primary / secondary somatosensory cortex; rACC, rostral anterior cingulate cortex; Th, thalamus; PAG, periaqueductal grey; LC, locus coeruleus; NA, noradrenergic; RVM, rostral ventromedial medulla; STT, spinothalamic tract; GM, grey matter; DH, dorsal horn.

Relevant pathophysiology

<u>AQP4 expression has a complicated relationship with lesion location</u>

Ever since a role for anti-AQP4 antibodies was put forward in 2004 (Lennon et al., 2004), ongoing research has highlighted not only its relevance as a marker for the disease, but has demonstrated that it is (a) a necessary part of disease pathogenesis, is (b) sufficient for

limited damage, and that (c) AQP4Ab mediated astrocyte destruction is the inaugural step in lesion pathology (Pittock and Lucchinetti, 2016).

Figure 2. AQP4 expression in the brain, showing high levels of expression (**A**) on periependymal surfaces and (**B**) in astrocyte foot processes at the blood-brain-barrier

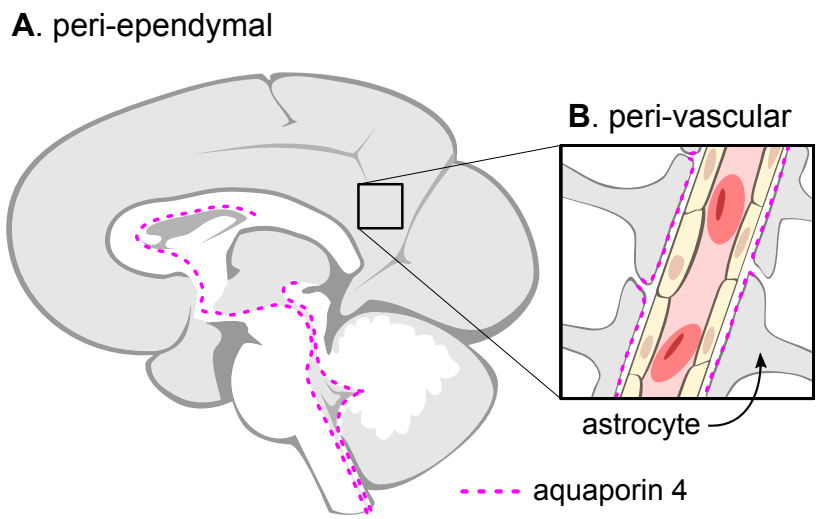

AQP4 expression (pink dashed line) is particularly dense in foot processes of astrocytes at the (B) blood-brain barrier and at (A) ependymal surfaces of the brain, a pattern largely reflected in the distribution of NMO lesions showing a predilection for the area postrema, periaqueductal grey, optic nerve and spinal cord grey matter.

AQP4 expression is particularly dense in foot processes of astrocytes at the blood-brain barrier (BBB) and at ependymal surfaces of the brain and this is reflected in the distribution of lesions in NMO with their predilection for sites of high aquaporin expression (for example area postrema, periaqueductal grey, optic nerve and spinal cord GM) (Pittock and Lucchinetti, 2016; see Figure 2). AQP4 is the most abundant water channel in the CNS, serving an important role in maintaining water homeostasis, however it is also found in other tissues throughout the body including the stomach, kidney, lung and skeletal muscle (Amiry-Moghaddam and Ottersen, 2003). It is of interest therefore that the damage in NMO

is confined to the CNS. Some have hypothesised that AQP4's co-expression and co-assembly with excitatory amino acid transporter 2 (EAAT2) in the astrocyte membrane optimises the antigen for AQP4Ab binding whilst others have shown that AQP4 expressed on astrocytes lacks the co-expression of compliment regulatory proteins you find expressed with AQP4 elsewhere (Pittock and Lucchinetti, 2016). Interestingly, there are a few case reports of extra-CNS features of NMO, for example myositis associated hyper-CK-aemia (Guo Y et al., 2014).

Within the cord, in contrast to MS, lesions tend to be central and involve grey matter, with 60% or more of lesions occupying more than half the cord cross-sectional area (Misu et al., 2007; Nakamura et al., 2008).

There is no evidence of cortical demyelination (unlike in MS) both pathologically and at high-field MRI (Kister et al., 2013; Lucchinetti et al., 2014). However, there *is* evidence of *damage* to the cortex: areas with loss of AQP4 reactivity in layer I astrocytes (in the absence of complement activation – see 'composition of lesions' below) and scattered loss of neurones in layers II – IV has been demonstrated (Figure 1). Some of this damage is certainly remote anterograde or retrograde degeneration, and some is related to loss of trophic support usually provided by healthy astrocytes (Lucchinetti et al., 2014; Popescu et al., 2010). Thus, cortical pain processing areas are unlikely to be directly damaged by NMO lesions but may suffer deafferentation and glial dysfunction. Pathological studies to date have not made comment on region specific cortical damage in NMO (in one study frontal neuronal loss was used as the exemplar location but not compared to other areas; Saji et al., 2013), however neuroimaging studies in NMO have shown increased mean diffusivity (MD, a surrogate

marker of damage; see Chapter 1b) in the parietal and occipital cortices (Yu et al., 2006) and a largely consonant thinning of the post-central and precentral gyri and calcerine sulcus (Calabrese et al., 2012). These imaging findings are probably correlates of non-demyelinating pathological changes in the cortex, and in light of their location could theoretically influence pain processing. The somatosensory cortex is consistently activated in human brain mapping studies of evoked pain and the motor cortex and occipital cortex also demonstrate changes in activity in certain contexts, the former most likely epiphenomenal and the latter in migraine where hypo-perfusion might contribute to visual aura (Apkarian et al., 2005; Denuelle et al., 2008). Evidence of maladaptive plasticity in the primary sensory cortex, for example shifting of cortical representations of somatotopic regions, has been found in functional investigations of pain states including phantom limb pain, syringomyelia and post-herpetic neuralgia (Flor et al., 1997; Karl et al., 2001; Pleger et al., 2006). Furthermore, in primates, there is building evidence that an anterior subregion (Brodmann's area, BA, 3a) of the primary sensory cortex (SI) receives input originating from unmyelinated nociceptors whilst the posterior SI (BA 3b and 1) receives input arising from myelinated afferents (including nociceptors) and that prolonged nociceptive stimulation alters the interactions between these sub-regions and may consequently alter the pain representation in SI in favour of unmyelinated (C nociceptor) input (Vierck et al., 2013). In the human example of chronic trigeminal neuralgia, reduced somatosensory cortical thickness has been found that co-localised to an area of somatosensory cortex shown to be active during induced allodynia (on fMRI). The reduced cortical thickness was thus hypothesised to be an effect of prolonged allodynic symptoms rather than a causative factor of pain experience (DaSilva et al., 2008). Therefore, it seems clear that pain alters cortical regions known to be affected in NMO, and that these pain related changes have the

potential to further modify the pain experience, but whether pain phenomenon have any role in causing the cortical changes seen in NMO, or how NMO related damage in these areas might alter the pain experience will need to be addressed in future studies.

Finally, an interesting hypothesis, related to the relatively frequent history of NMO manifesting after an inaugural episode of centrally mediated vomiting, perhaps often under-reported or dismissed as a bout of gastroenteritis, is that AQP4Ab might enter the CNS through areas of relative weakness in the BBB, such as exists in the area postrema, an area frequently affected by lesions in NMO (Popescu et al., 2011).

Composition of lesions

NMO lesions can be broadly characterised by (1) primary loss of AQP4 immunoreactivity on astrocytes, (2) activation of complement, and (3) infiltration with inflammatory cells including lymphocytes and plasma cells (Lucchinetti et al., 2002; Misu et al., 2007; Pohl et al., 2013; Roemer et al., 2007; see Kawachi and Lassmann, 2017 for review). The cytotoxic effects are hypothesised to involve AQP4Ab binding followed by complement activation, findings corroborated in animal models and astrocyte cultures (Herwerth et al., 2016; Sabater et al., 2009) (Figure 3).

Figure 3. NMO lesion pathological characteristics

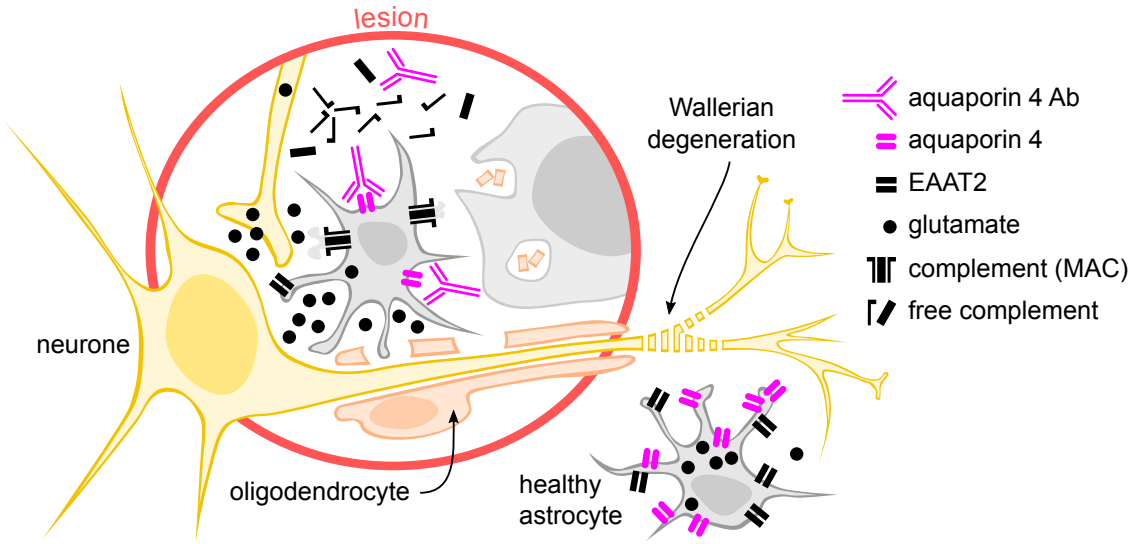

Numerous cellular and biochemical changes occur at the site of NMO lesions, many of which impact on neural processing (including nociception). Astrocytes damaged by AQP4Ab mediated complement activation show disrupted glutamate recycling (loss of EAAT2 and expulsion of glutamate into extracellular space). Infiltration of CNS tissue by macrophages containing myelin-fragments (grey cell top-right) are evidence of active demyelination. Other inflammatory cells are also present (though not represented above): lymphocytes, plasma cells and activated microglia, the latter particularly associated with pro-nociceptive cytokine release. MAC, complement membrane attack complex; Ab, antibody; EAAT2, excitatory amino acid transporter 2.

There is heterogeneity in the pathological characteristics of lesions in NMO, with some attempts by pathologists to define types of lesion (see Lucchinetti et al., 2014 for review). Broadly, lesions have one of the following two constellations of characteristics: perivascular demyelination, infiltration of myelin-laden macrophages, severe axonal loss, necrosis of grey and white matter, and loss of astrocytes (Lucchinetti et al., 2002); or, vacuolated myelin with relative absence of demyelination, reactive astrocytes, microglial activation, limited axonal injury and variable, granulocytic inflammation (Misu et al., 2007; Roemer et al., 2007). The latter constellation has been posited to show some scope for reversibility,

with features of re-myelination sometimes seen, and probably reflected in MRI studies showing brainstem lesion resolution (Misu et al., 2005; Roemer et al., 2007; see Chapter 1b).

Activation of complement is a typical feature of lesions, often evidenced by the presence of C9neo, an essential component of the complement membrane attack complex (Lucchinetti et al., 2002). Chronic lesions typically show gliosis, cystic degeneration and cavitation, and macroscopically show atrophy of the lesioned tissue (e.g. spinal cord and optic nerves) (Lucchinetti et al., 2002). There may also be an apparent increase in number and prominence of blood vessels with thickened hyalinised walls in necrotic or peri-necrotic lesions, selective loss of AQP4 immunoreactivity in the absence of structural damage, and a spectrum of astrocyte morphological abnormalities (Mandler et al., 1993; Roemer et al., 2007). Of note, patches of Wallerian degeneration can be seen in spinal cord WM tracts along with loss of myelin, oligodendrocytes and axons (Misu et al., 2013).

There is evidence of glutamate dysregulation in lesions, where loss of AQP4 immunoreactivity is associated with loss of EAAT2 staining (Hinson et al., 2008). This likely contributes to cytotoxicity and may influence pain processing at the level of the spinal cord. Additionally, microglia activation occurs in NMO lesions (Lucchinetti et al., 2002), which again may have implications for pain (see Chapter 1c).

Management

NMO is appropriately managed by a diverse multidisciplinary team, including but not limited to specialist nurses, physiotherapists, occupational therapists, pharmacists, psychologists, pain consultants, immunologists and sometimes psychiatrists. The neurologist's role is to diagnose NMO, detect evidence of relapse and crucially to manage patients' pharmacotherapy.

Pharmacological treatment

There is international agreement that immunosuppression should be started as early as possible and continue indefinitely (Kimbrough et al., 2012) however the exact form of immunosuppressive treatment is not universally decided upon. Some of this indecision reflects the difficulties in acquiring indisputable evidence for treatment options: the ethics of placebo controlled trials are contentious and there is little motivation to trial established, cheap and unprofitable agents (Cree et al., 2016; Greenberg, 2015; Palace, 2015; Weinshenker, 2015).

Acutely, attacks are managed with high dose steroids (usually IV) with escalation to intravenous immunoglobulin or plasma exchange in the absence of improvement; steroids are typically tapered as the patient is established on long-term treatment (Palace et al., 2012; Stellmann et al., 2017).

For long-term management, the pattern followed by most NMO clinics is to commence azathioprine (or similar steroid-sparing agent, such as mycophenolate mofetil) as soon as possible after diagnosis, with or without a trial of a second steroid-sparing agent in the

event of treatment failure (i.e. relapse) before escalating to rituximab, an anti-CD20 monoclonal antibody (Palace et al., 2012). As steroid-sparing agents take several months to reach maximum efficacy and the concomitant administration of prednisolone is recommended early on in treatment (at least 20mg daily for 6 months), in some centres, long-term low-dose prednisolone (5-15mg daily) is recommended in addition to steroid sparing agents (Kitley and Palace, 2016). Subsequent escalation is rarely needed but where necessary is tailored to the patient; options include alternative humanised monoclonal anti-CD 20 antibodies (e.g. ofatumumab), drug treatment trial therapies (e.g. anti-IL6 monoclonal Ab tocilizumab) and regular plasma exchange or intravenous immunoglobulin (Araki et al., 2014; Palace et al., 2012; Sedani et al., 2012).

A comprehensive review of all established and emerging NMO treatments is outside the scope of this chapter, however one monoclonal Ab currently being trialled is certainly of mention: Tocilizumab, an IL-6 receptor monoclonal antibody, is reported to be an effective treatment for NMO and by counteracting a common neuroinflammatory and pro-nociceptive mediator, IL-6, reduces relapse rates and lessens neuropathic pain (Araki et al., 2014) (Further discussion of IL-6 and its relevance in neuropathic pain can be found in Chapter 1c).

Summary

Neuromyelitis optica is an antibody mediated astrocytopathy causing secondary demyelination in the CNS. Consensus management involves long-term immunosuppression. Lesions are well recognised as occurring in structures relevant to pain modulation: the dorsal horn of the spinal cord, the periependymal structures of the brainstem (including the

periaqueductal grey and locus coeruleus) and diencephalon (i.e. the hypothalamus), the thalamus and the medulla oblongata (conceivably including the RVM) (Blanc et al., 2012; Downer et al., 2012; Kim et al., 2010; Matthews and Palace, 2014; Pittock et al., 2006; Pu et al., 2015; Viegas et al., 2009; Wingerchuk et al., 2015). Characteristics of lesions, such as disruption of glutamate homeostasis, may be of particular relevance to pain and are discussed further in Chapter 1c. Additionally, the effect of cord lesion extent (length, volume and location) and predilection for grey matter in ensuing pain symptoms is addressed in Chapters 1b, 4 and 5.

Chapter 1b

Review of MRI imaging in NMO

Introduction

MRI is central to the diagnosis of NMO, and although its pivotal place in the diagnostic criteria now sits below that of AQP4Ab detection, it is still vital to the early recognition of NMO and for identifying antibody negative disease wherein appropriate management relies on discrimination from MS to avoid the potentially deleterious effects of disease-modifying treatments (Juryńczyk et al., 2013; Palace J et al., 2010; Shimizu et al., 2010; Wingerchuk et al., 2015).

This chapter overviews the key clinical MRI findings in NMO and highlights where these might be relevant to pain. It also briefly describes non-conventional MRI techniques not covered elsewhere in the thesis.

The spinal cord

Longitudinally extensive transverse myelitis (LETM), the imaging hallmark of NMO, is 98% sensitive and 83% specific for distinguishing NMO from optico-spinal MS (using 2006 criteria) and when captured on clinical imaging should always prompt consideration of NMO (Wingerchuk et al., 2006, 2015).

In contrast to MS, where long spinal cord lesions are rare, seropositive NMO has significantly longer lesions spanning a mean of 4.5 – 8.7 SC segments (Kıyat-Atamer et al., 2013; Yonezu et al., 2013; Zhong et al., 2012). LETM is frequently oedematous in the acute stages (Kıyat-Atamer et al., 2013; Murchison et al., 2013) and predominantly central in the axial plane, involving grey as well as white matter with 60% occupying more than half the cord cross-section (Downer et al., 2012; Murchison et al., 2013; Nakamura et al., 2008; Yonezu et al., 2012; Zhong et al., 2012) (see Figure 1). It commonly involves the thoracic cord. In contrast, MS SC lesions tend to be short, predominantly located in the cervical cord, and transversely peripheral, asymmetrical and posterior (Calvo et al., 2013; Frohman and Wingerchuk, 2010). The relative differences in the location of lesions is noteworthy as central pain in MS is less prevalent and less severe (O'Connor et al., 2008; See Chapter 1c for further discussion and Chapter 4 for experimental work).

Figure 1. T2-weighted MRI of longitudinally extensive transverse myelitis (LETM) evolution and cross-sectional findings in aquaporin 4 antibody positive NMO. (**A**) Five segment oedematous LETM extending into medulla. (**B**) Subsequent 'break-up' and regression of same LETM lesion. Axial T2-weighted sections through image A showing, (**C**) full diameter cord lesion and, (**D**) central cord lesion, nicely demarcating central grey-matter.

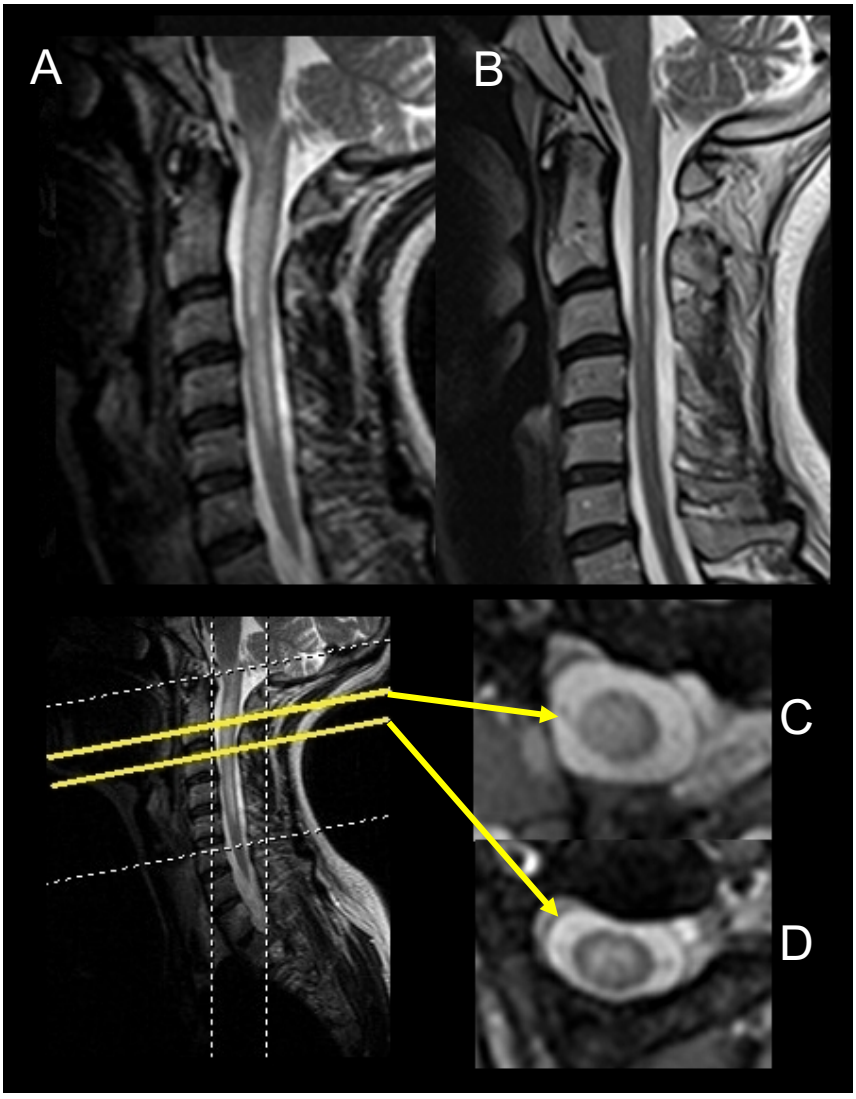

Approximately 72% of spinal cord lesions enhance with gadolinium during an acute myelitis relapse (Murchison et al., 2015; Figure 2).

Figure 2. Longitudinally extensive transverse myelitis lesion (T5-8) in an aquaporin 4 antibody positive patient with gadolinium (Gd) enhancement; (**A**) T1-weighted MRI with Gd; (**B**) T2-weighted MRI.

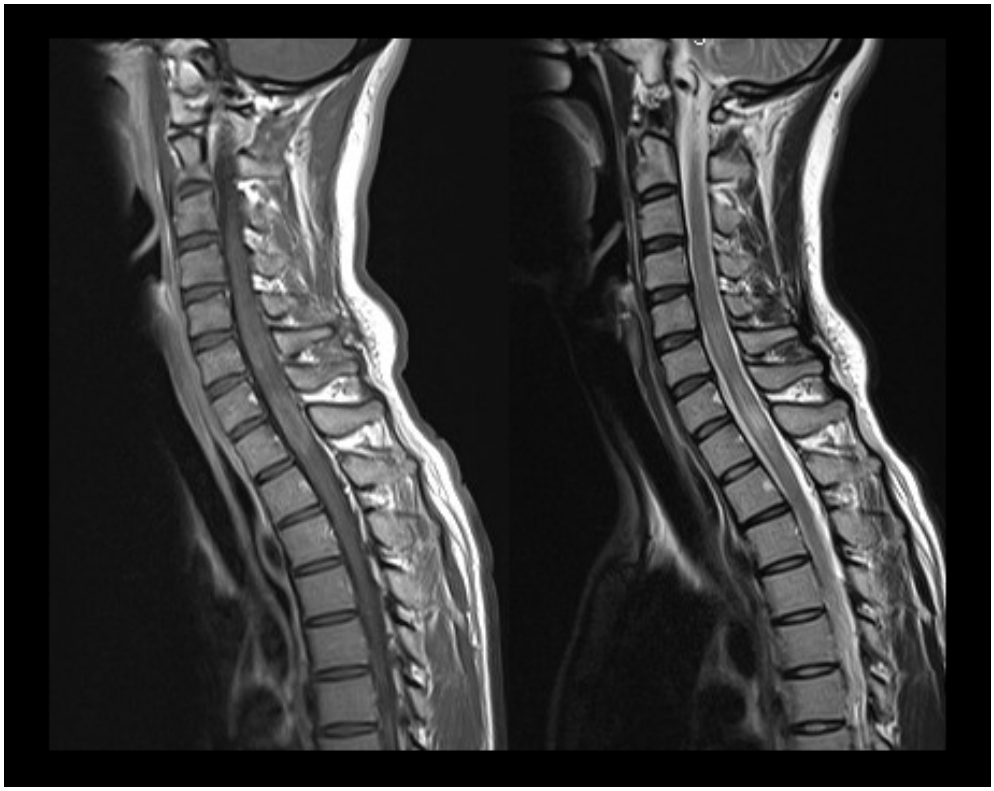

After treatment with high dose steroids and at follow-up, NMO LETM lesions frequently "fragment" into multiple shorter lesions (see Figure 1). Affected cords can also undergo focal or widespread atrophy two or more years post-myelitis, irrespective of AQP4Ab status (Asgari et al., 2013). Cord atrophy measures are analysed in Chapter 4. The Imaging Cohort (see Chapter 3) in this thesis is cross-sectional and therefore lesion number will likely be influenced by the lesion 'break-up' phenomenon.

Acute T1 hypointensity is not a typical feature in MS transverse myelitis, but is commonly noted in acute NMOSD spinal cord lesions (Downer et al., 2012; Murchison et al., 2013) though at a lower frequency in chronic lesions (Murchison et al., 2013; Nakamura et al.,

2008). The hypointensity tends to be central involving the grey matter and may be more common in thoracic than cervical regions (Nakamura et al., 2008; see Figure 3).

Figure 3. T1-weighted MRI hypointensities (arrows) within longitudinally extensive transverse myelitis lesion in an aquaporin 4 antibody positive patient.

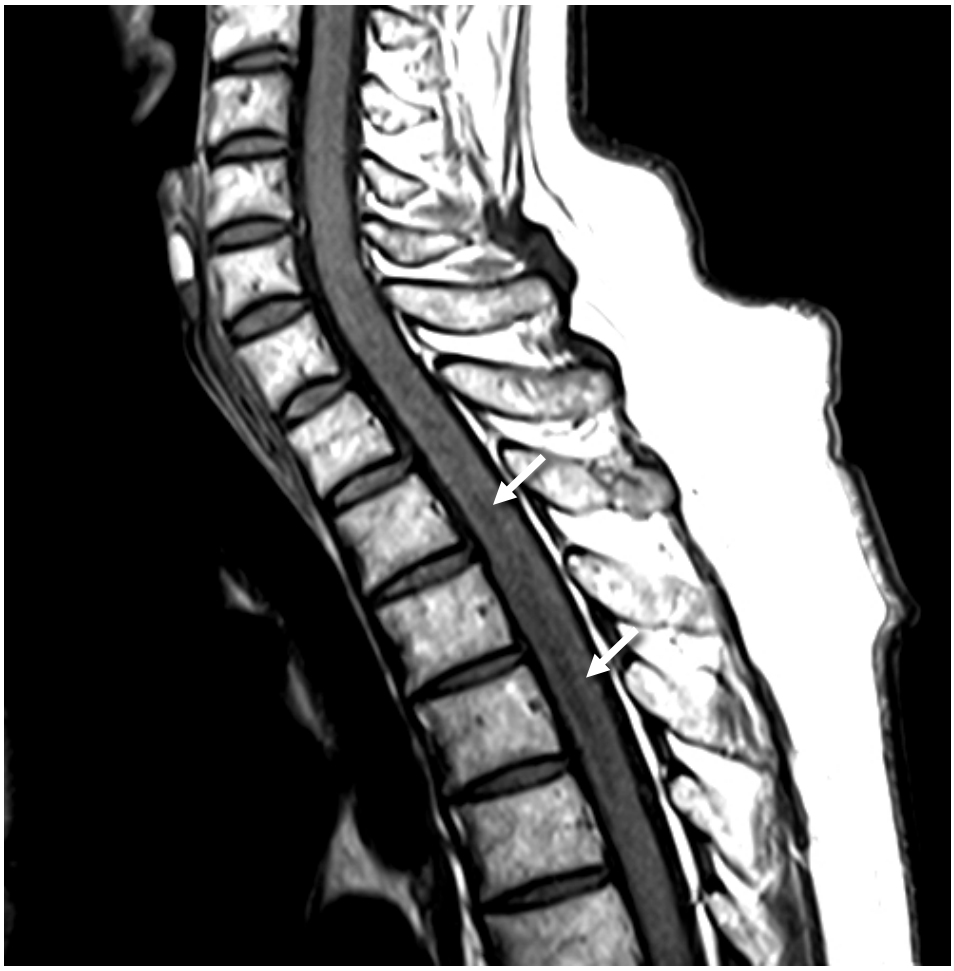

Not all inflammatory LETMs are due to NMO and long spinal cord lesions are also a feature of idiopathic acute transverse myelitis with or without acute disseminated encephalomyelitis (ADEM). As an isolated phenomenon, LETM is associated with AQP4Abs in 32-80% of cases (see Kitley et al., 2012a for review) with their presence predicting a higher risk of relapse (Kitley, 2013; Weinshenker et al., 2006). Notably, antibody negative

LETM seldom progresses to “true NMO” (5/44) and is more often part of a monophasic illness, such as ADEM (Kitley, 2013).

The brain

Although brain MRI is frequently normal on T1/T2-weighted MRI (a feature made use of in early diagnostic criteria, see Wingerchuk et al., 1999), it is now well recognised that brain lesions do occur in NMO, although they are frequently non-specific in nature. Indeed, brain lesions are present in about half of patients at presentation (Kıyat-Atamer et al., 2013; Pittock, 2006) increasing to 60% on follow-up with as many as 16% fulfilling MS-diagnostic criteria (Matthews et al., 2013; Wingerchuk et al., 2015). NMO-typical brain lesions, though not pathognomonic in NMO but rare in MS, are now included as part of the core characteristics of the NMO diagnostic criteria and are shown in Figure 4.

Brainstem and cerebellar lesions commonly occur in NMO patients (26-81%), involving the medulla most frequently but with lesions in the pons, cerebellar peduncles, mesencephalon and diencephalon also recognised (Asgari et al., 2013; Downer et al., 2012; Jarius et al., 2012) (see Figures 5, 6 & 7).

As highlighted in Chapter 1a (see especially Chapter 1a Figure 1), areas critical to central pain processing are commonly affected by NMO lesions: the periaqueductal grey, locus coeruleus, hypothalamus, thalamus and medulla oblongata (and thus conceivably the RVM) (Blanc et al., 2012; Downer et al., 2012; Kim et al., 2010; Matthews and Palace, 2014; Pittock et al., 2006; Pu et al., 2015; Viegas et al., 2009; Wingerchuk et al., 2015). As no cortical areas are lesioned, no pain-relevant areas of cortex are lesioned, however hidden damage revealed by diffusion and morphometry studies have shown changes in the parietal and frontal cortices that may be relevant to pain (Calabrese et al., 2012; Yu et al., 2006).

Figure 4. Diencephalic and cerebral lesions in NMO

https://www.ncbi.nlm.nih.gov/pmc/articles/PMC4515040/

NMO 'typical lesions' in the brainstem coincide with sites of high AQP4 expression (Pittock et al., 2006), and are listed in the diagnostic criteria as the dorsal medulla (especially area postrema) and periependymal surfaces of the third and fourth ventricle (or cerebral aqueduct, including the hypothalamus and PAG) (see figures 6 & 7). Taken together, forebrain and brainstem 'NMO typical' lesions are only seen in a minority (7-9%) of patients (Matthews and Palace, 2014; Pires et al., 2012; Pittock, 2006; Pittock et al., 2006) however their diagnostic power is noteworthy: hypothalamic and PAG lesions are relatively specific for AQP4Ab positive disease (although they can be seen in myelin oligodendrocyte glycoprotein Ab positive disease, see Jurynczyk et al., 2017a) and area postrema lesions are more frequent in AQP4Ab positive versus seronegative NMO (Asgari et al., 2013; Downer et al., 2012). The brainstem lesions seen in NMO are notable for involving sites of particular relevance to pain: the PAG, locus coeruleus (LC), and medulla are all well-described components of the dorsolateral funicular (DLF) descending modulatory pathway that projects to the dorsal horn of the spinal cord to inhibit or facilitate pain transmission via noradrenergic and serotonergic* pathways respectively (Eide and Hole, 1993; Eippert et al., 2009a; Jones and Gebhart, 1986; Suzuki et al., 2004) (See Chapter 1a Figure 1 and Chapter 1c Figure 2).

* When assuming that dorsal horn 5-HT effects are mediated via a facilitatory receptor, e.g. 5-HT3 R.

Figure 5. Medullary lesion in aquaporin 4 antibody positive patient.

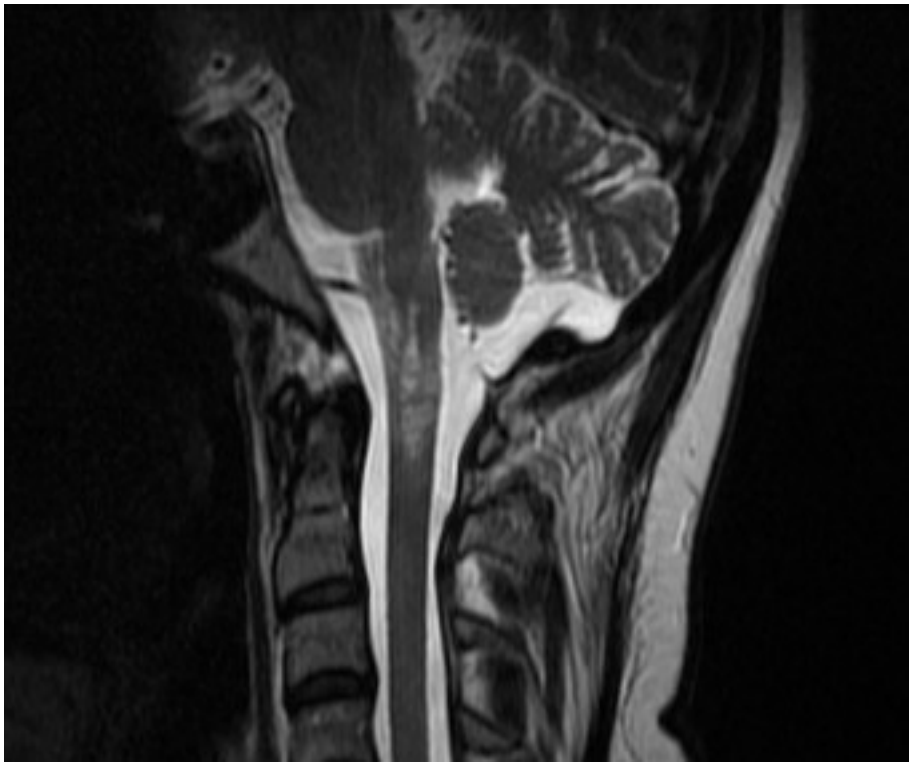

Figure 6. 'Typical-NMO' MRI with T2-weighted hyperintensities seen in peri-ependymal areas and the diencephalon, including bilateral hypothalamic lesions (red arrows)

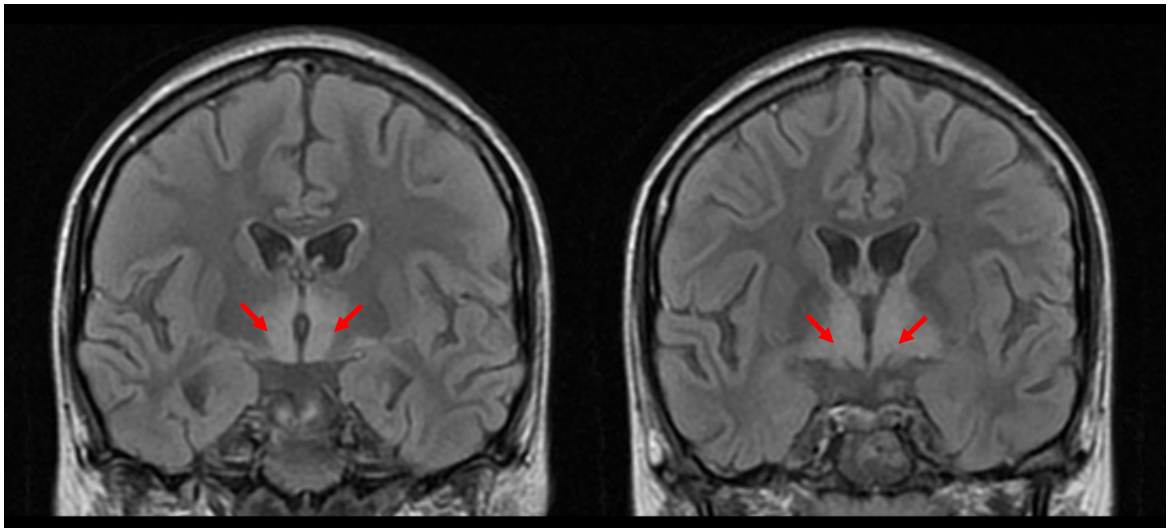

Figure 7. 'Typical-NMO' MRI with T2-weighted hyperintensities seen in the floor of the fourth ventricle, including bilateral area postrema lesions (red arrows).

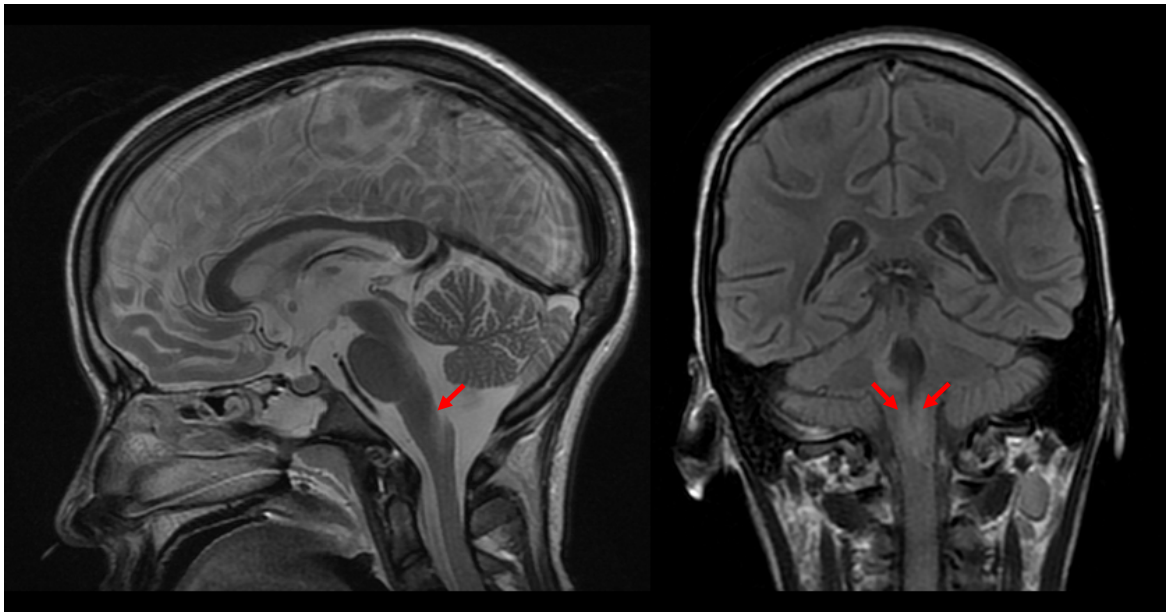

Area postrema (vomiting centre or chemoreceptor trigger zone) lesions are often associated with episodes of intractable vomiting and hiccoughs that not uncommonly herald the onset of NMO (Apiwattanakul et al., 2010), however radiographic lesions of the area postrema and surrounding structures frequently disappear on follow-up imaging (Popescu et al., 2011). These early symptoms that result from transient damage to a brainstem area with a relatively open blood-brain barrier (BBB) might provide clues to NMO pathogenesis (see 'MRI insights into pathogenesis' below).

Ethnicity appears to influence the age of onset, onset phenotype and outcome of NMO (Kitley et al., 2012b) and this influence is also seen in the imaging features. Acute extensive brain lesions are frequently reported in Japanese (Cabrera-Gomez and Kister, 2012; Ito et al., 2009; Matsushita et al., 2009) and Korean (Huh et al., 2013) studies but are near absent in Western case series, with the exception of Afro-Caribbean patients where extensive white matter lesions and diencephalic and brainstem signal abnormalities are sometimes

seen (Pittock, 2006; Pittock et al., 2006). T2-hyperintense cortical lesions, a common feature in MS, are absent from MRI studies using double inversion recovery sequences in Italian and Korean NMO participants (Calabrese et al., 2012) and on ultra-high field (7 tesla) MRI in Caucasian and Afro-Caribbean participants (Kister et al., 2013; Sinnecker et al., 2012). Post-mortem analysis has also confirmed their absence in a US/Cuban cohort (Popescu et al., 2010). However, cortical lesions visible on conventional imaging *have* been reported in two case series of Japanese NMO patients: a small series of 3 cortical lesion patients (Tahara et al., 2012) and another showing two of 18 participants with cortical lesions (Ito et al., 2009). Peculiarly, in the latter study, the comparison MS population (n=39) reportedly had no cortical lesions which is somewhat at odds with the MS literature (Kidd et al., 1999). A recent Korean study further validates the findings of acute cortical lesions in eastern populations but stresses their rarity (6 of 215 patients enrolled in their study had cortical lesions) (Kim et al., 2016). The relationship between NMO pain and ethnicity is examined in Chapter 3, and more generally discussed in Chapter 1a.

In contrast to MS where sub-clinical MRI activity is the norm and the majority of relapsing patients develop progression over time, NMO appears to be active only during relapses, with no inter-relapse accrual of disability (Matthews et al., 2015). However, asymptomatic forebrain lesions are sometimes seen and less commonly, mesencephalic and diencephalic lesions may also be asymptomatic (Asgari et al., 2013; Pittock, 2006), yet whether these represent silent disease progression is not established.

The optic nerve

Akin to the longitudinally extensive nature of transverse myelitis in NMO, optic nerve lesions are also frequently extensive, an apparent difference with MS (Storoni et al., 2013). There is a trend towards a higher frequency of posterior anterior visual pathway lesions in NMO compared to MS (Khanna et al., 2012; Storoni et al., 2013) and chiasmal enhancement is found in NMO–related ON but not in MS (Khanna et al., 2012) (see Figure 8). Acute optic neuritis is known to cause pain, however no chronic optic nerve pain is recognised in NMO.

Figure 8. Chiasmal lesion in NMO Aquaporin 4 antibody positive patient (A) with gadolinium enhancement (red arrow) and (B) T2-hyperintensity (red arrow).

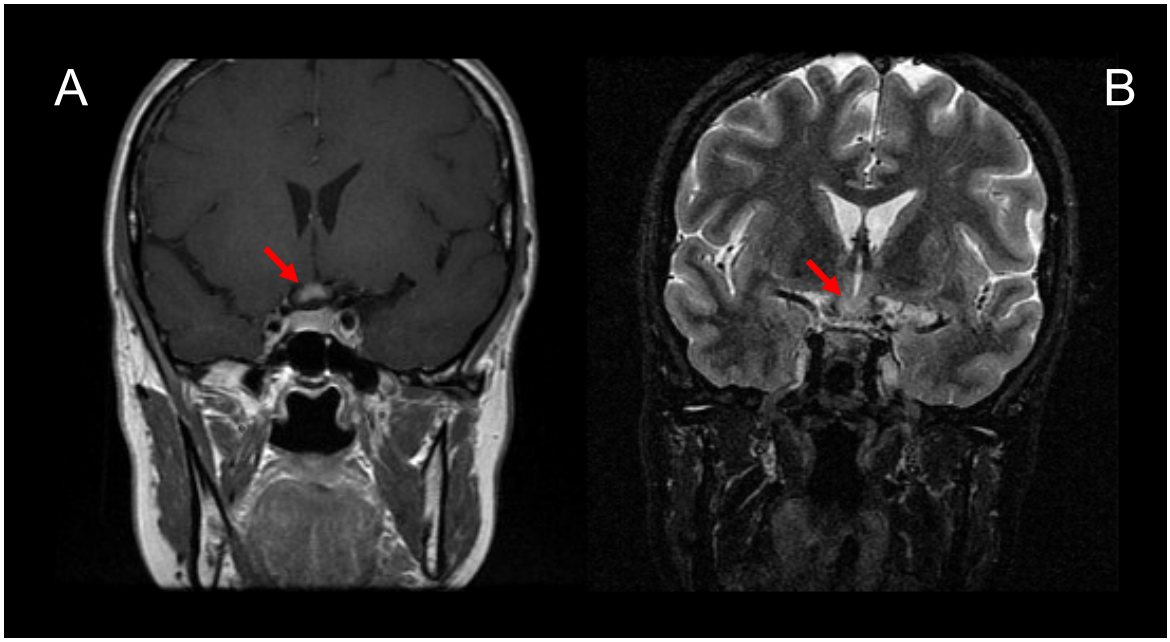

MRI insights into pathogenesis

As discussed in Chapter 1a, AQP4 is found throughout the CNS and is expressed in high concentrations on perivascular and subpial end-feet portions of astrocyte membranes, and consequently found in high concentrations on periependymal surfaces, the glia limitans and at the blood brain barrier. NMO brain lesions have been described as having a predilection

for these sites (Amiry-Moghaddam and Ottersen, 2003; Pittock et al., 2006; Wingerchuk et al., 2007), however the non-specific white matter lesions of the brain can be widely distributed (Matthews et al., 2013) and not solely in AQP4 rich zones. Conversely, the cortex, which is rich in AQP4, is generally spared (at least from 'visible' MRI lesions) and extra-CNS sites of expression, the kidneys, stomach and airways, are also seemingly unaffected by the NMO disease process (Papadopoulos and Verkman, 2011; Popescu et al., 2010); NMO-associated myopathy may however prove to be an exception to the rule (Cosgrove et al., 2014; Guo Y et al., 2014). Explanatory hypotheses for this selective distribution of lesions include regional variations of BBB integrity (Papadopoulos and Verkman, 2011), AQP4 epitope configuration (Lennon et al., 2005), spatially differing AQP4 isomer ratios (Saini et al., 2010) and tissue-differences in compliment regulatory protein expression (Yao and Verkman, 2017). Providing some support for the former, the area postrema, in addition to being rich in AQP4 is a CNS region where the ependymal lining does not form a tight blood–CSF barrier (Apiwattanakul et al., 2010; Jarius et al., 2012; Popescu et al., 2011). This local deficiency of the BBB may provide a portal for circulating AQP4Ab to access other sites in the brain and upper cord (Papadopoulos and Verkman, 2011; Popescu et al., 2011).

Another interesting facet of medullary floor lesions (especially those of the area postrema) is that they often undergo complete radiographical resolution, which could be related to regional CNS differences in complement-regulatory protein expression and/or a lack of excitatory amino acid transporter 2 (EAAT2) in this region reducing local tissue damage (Popescu et al., 2011).

Non-conventional imaging techniques

Non-conventional techniques relevant to pain in NMO will be covered in detail in Chapter 2, including diffusion imaging. This section will briefly summarise other relevant areas.

Ultra-high Field (7T) structural MRI Studies

Ultra-high field MRI has been increasingly utilised in research where because of the high signal-to-noise ratio (SNR) it offers superior anatomical definition of lesions. Using ultra-high field MRI it has been shown that supratentorial NMO lesions are generally small round and subcortical without a central venule or hypointense ring in contrast to the signature lesion found in MS that is oblong, periventricular, and traversed centrally by a venule (corresponding to the MS “Dawson's finger” lesion) (Kister et al., 2013; Sinnecker et al., 2012).

MR Spectroscopy

Spatially targeted nuclear magnetic resonance (NMR) spectroscopy can be used to measure the metabolomic composition of the whole brain (usually one metabolite at a time) or discrete regions (looking at multiple metabolites). More recently, this has been applied to the spinal cord and within this thesis is applied to the brainstem (see Chapter 2). N-acetyl aspartate (NAA), a marker of ‘neuronal integrity’, is the commonest metabolite analysed in studies of MS where its loss is posited to correlate with neurodegeneration (Narayana et al., 1998). Myoinositol, a putative measure of astrocyte function, is better placed to reflect the underlying astrocytopathic pathology of NMO (see Chapter 1a) (Ciccarelli et al., 2013). In support of DTI studies showing no evidence of tract damage outside NMO lesions (see chapters 2 & 5), MR spectroscopy has found no abnormalities in NAA, choline or myoinositol

in the normal appearing white or grey matter of NMO brains (De Seze et al., 2010). Within NMO cord lesions, low myoinositol levels have been found compared to MS lesions and controls, whereas MS cord lesions have low NAA levels compared to NMO lesions and controls (Ciccarelli et al., 2013). Targeted spectroscopy of the midbrain PAG, a novel technique used in this thesis, is described in detail in Chapter 2 and utilised in Chapter 7.

Conclusion

MR imaging is a powerful non-invasive tool for studying disease *in vivo*. Using different but complimentary techniques, it can assess diverse disease-related features including anatomical changes, tissue integrity and metabolite concentrations.

The majority of current NMO MRI research is retrospective and qualitative, and prospective and quantitative studies with longer-term follow-up, during and outside relapses, are required. There is huge potential for improving our ability to diagnose, monitor disease activity and better understand NMO disease pathogenesis and there are clear applications for broadening our understanding of NMO pain.

Longitudinally extensive transverse myelitis (LETM) is the archetypal MRI lesion of neuromyelitis optica (NMO) featuring high up in the diagnostic criteria, and along with the presence of aquaporin 4 antibody (AQP4Ab), provides one of the two most specific non-clinical markers for this disease entity. Whether lesion location, length and volume (and subsequent atrophy) are relevant to pain in NMO is addressed in Chapter 4.

Previous studies have shown no relationship between pain severity and the presence or absence of detectable AQP4Ab in NMO groups (Kong et al., 2014; Zhao et al., 2014) and

implies that the aetiology of pain in NMO is not mediated directly by the AQP4Ab but that a histopathological or macropathological feature common to these disorders is the cause. However the caveat to this reasoning is that AQP4Ab negative NMO is a poorly defined entity, ranging from AQP4Ab-related disease with presumed undetectable levels of AQP4Ab, to disorders caused by entirely different autoantibodies and those with disparate aetiologies (Wingerchuk et al., 2015).

The timing of MRI acquisition influences findings. Oedematous LETM may evolve into multiple shorter spinal lesions in an atrophied cord. Conversely, normal brain MRIs may accrue lesions at follow up and even fulfil MS criteria. Brainstem lesions often resolve, especially lesions of the medullary floor where a compromised blood brain barrier is posited as an entry site for AQP4Abs. These features must be taken into account when investigating the relationship of cross-sectional MRI findings to pain – for example long lesions that don't fragment might predict pain, or brainstem lesions (that subsequently disappear on conventional imaging) might be an important starting point for chronic pain pathology (see Chapters 4, 5, 6 and 7).

A number of imaging features are more common in NMO than MS and may have relevance to pain, given the difference in pain phenotype between the two diseases; the high frequency of thoracic involvement and the greater extent of lesions is explored in Chapter 4 and T1-hypointensities seen in thoracic NMO cord lesions warrants future investigation.

Search methodology

The MEDLINE database (pubmed.gov) was queried using MeSH terms for NMO and MRI: "("Neuromyelitis Optica"[Mesh]) AND ("Magnetic Resonance Imaging"[Mesh])". This retrieved in excess of 400 articles. These results were filtered by publication date for the current and preceding year resulting in 114 articles. An update search has since been performed prior to thesis submission. Studies that didn't clearly define antibody status were excluded, key NMO studies from dates outside of the search range but known to the author were included and pain references separately added. Fifty-three papers were eventually deemed suitable for inclusion.

Use of clinical images

All example MRI images in this chapter were obtained from patients under the care of the Oxford NMO National Clinic, except where specified in the figure legend. For all images, written informed consent was obtained under the NMO tissue bank protocol (Oxford REC no: 10/H0606/56).

Relevant personal publications

Tackley G, Kuker W, Palace J. Magnetic resonance imaging in neuromyelitis optica. Mult Scler. 2014 Aug;20(9):1153-64: *a number of text excerpts and figures are reused in an adapted form in the body of this chapter*.

CHAPTER 1c

Review of pain in NMO

Introduction

In health, pain is the alarm that alerts an organism to actual or potential tissue damage. It is a highly salient signal, motivating behaviour directed at removing the source of pain. This is clearly essential for an animal's survival, however this deep-rooted and phylogenetically ancient pain system can malfunction and leave unfortunate individuals suffering pain in the absence of threat or avoidable damage. At least one form of pain homeostasis malfunction is apparent in neuromyelitis optica (NMO). The known details of its aetiology are rudimentary and implore the research community to further investigate

what is a chronic and severe problem that has a detrimental effect on quality of life. Exploring the chronic central neuropathic pain syndrome of NMO is the focus of this thesis, with this review serving as an introduction to what is known about pain in NMO and what can be gleaned from related conditions.

NMO: one disease, multiple pain syndromes

Clinicians have been late to recognise and treat pain in NMO, despite its high prevalence (80%) and severity (Kanamori et al., 2011). Indeed, the evidence suggests pain is more detrimental to an NMO sufferer's quality of life than physical disability (Kong et al., 2016), an uncomfortable truth, more burdensome in light of the current absence of effective NMO pain treatments and lack of clinician and pharmaceutical focus (Qian et al., 2012).

Table 1. Pain traits in NMO

Pain trait	Characteristics	Assessment
Acute myelitis pain*	Corresponds to level of myelitis[1] Often precedes other symptoms of myelitis[2] Recovers in some (probably over weeks to months – personal observation), and in some progresses to chronic pain[3,6]	Patient report Clinical assessment
Post-myelitis chronic pain	Severe (22%-50%)**[4,7] Prevalent (84%-86%)[4,7] Temporal nature: - Constant (64-68%)[5,7] - Intermittent (25%)[5] - Constant with exacerbations (7%)[5] Location:[4] - chest (36%) - waist (32%) - legs (entire) (29%) - back (29%) Common subjective characteristics:[6,7] "burning", "aching", "prickling", "hot", "exhausting", "sharp", "sickening", "wretched"	BPI PainDetect McGill QST Clinical assessment Patient report

(table continued overleaf)

	Sensory characteristics:[6] - Hypoaesthesia (thermal and vibratory) - Hyperalgesia (esp. to heat) - Allodynia (to non-noxious stroking) - Paradoxical heat sensation to alternating hot and cold stimuli Largely refractory to standard anti-neuropathic pain treatments[7]	
Spasm-induced pain	Prevalent (25-90%)[7,8,9] Attributable to myelitis in at least 90%[8] Spontaneous or precipitated by movement[8] Upper and lower limbs involved[8,9] Onset ~20-50 days post-myelitis Favourable response to carbamazepine[8,9]	Patient report Clinical assessment
Retrobulbar pain*	Prevalence ~ 55%[7] Resolves over days to weeks (personal observation)	Patient report Clinical assessment
Headache and facial pain*	Rare (exact prevalence unknown): - trigeminal neuralgia, 3/258 (1%)[10] - cervicogenic headache, single case-report[10]	Patient report Clinical assessment
Myalgia	Very rare (2 case reports)[11,12] Associated clinical characteristics: - Hyperthermia - Elevated creatine kinase (CK)[11,12] Proximal muscle pain[12] Can be recurrent[12]	Patient report Clinical assessment

1: Holtås et al., 1993; 2: Dunne et al., 1986; 3: Barakat et al., 2015; 4: Kanamori et al., 2011 n=37; 5: Zhao et al., 2014, n=50, NB subset of "neuropathic" pain patients investigated, determined with DN4; 6: Pellkofer et al., 2013, NB sensory characteristics determined in hands and feet only, irrespective of site of pain; 7: Qian et al., 2012, n=29; 8: Kim et al., 2012, n=40 (10 with spasm pain); 9: Carnero Contentti et al., 2016, n=15; 10: Masters-Israilov and Robbins, 2017; 11: Cosgrove et al., 2014; 12: Guo Y et al., 2014.

BPI, brief pain inventory (Cleeland and Ryan, 1994); QST, quantitative sensory testing (Rolke et al., 2006); McGill, McGill pain questionnaire (Melzack, 1987).

* these pain syndromes have not been well characterised in NMO

** severe defined as 7-10 on 0-10 pain scale

At least six distinct forms of pain are reported in NMO patients (see Table 1). First is a dysaesthetic band (often referred to in the multiple sclerosis field as the "MS hug"), that

frequently heralds (and clinically localises) a spinal cord lesion. This typically subsides over days to weeks, but is commonly substituted over the subsequent weeks and months by a second and most troublesome pain syndrome (and the focus of this thesis): chronic central neuropathic pain, exhibiting a constellation of allodynia and dysaesthesia at both the level of the "hug", and within the trunk and limbs anywhere below the level of the lesion, most frequently the legs, feet, buttocks, perineum but also sometimes the arms, hands and shoulders (Kanamori et al., 2011; Zhao et al., 2013). The characteristics of this pain are not specific to NMO, and may be experienced in many causes of myelitis, however the extreme severity of central pain and its frequency and persistence in NMO sufferers is noteworthy (Kanamori et al., 2011).

Third is spasm-induced pain, which often compounds the second type of pain described above and may be relatively specific to NMO (Kim et al., 2012). Promisingly, unlike chronic central pain, this spasm-induced pain seems to be responsive to carbamazepine treatment (Carnero Contentti et al., 2016). Carbamazepine is thought to exert its analgesic actions through sodium channel blockade thereby reducing neuronal excitability, a mechanism potentially important for peripheral and central forms of pain including the phenomenon of central sensitisation (see discussion below) (Dib-Hajj et al., 2009). Within MS, painful spasms akin to those in NMO have been described and are hypothesised to result from ephaptic conduction from partially demyelinated CNS neurones involving sensory and motor tracts (Osterman and Westerberg, 1975). A general tempering of excitability in these neurones by carbamazepine's sodium-channel blockade might thus be responsible for improvement in spasm-induced pain symptoms. In pain guidelines, carbamazepine is almost exclusively recommended for the management of trigeminal neuralgia (Zakrzewska, 2010), primarily due to lack of high-quality studies of carbamazepine in other

forms of pain (McMahon, 2013), but its ineffectiveness in chronic (non-spasm-related) NMO pain is noteworthy (personal observation) and suggests neuronal excitability, or indeed an ephaptic transmission aetiology, might not be primary factors in this NMO pain trait.

Fourth is retrobulbar pain preceding or coinciding with optic neuritis (ON) relapses and occurring in about 50% of patients (Qian et al., 2012). This usually resolves with or without the recovery of any visual deficit; this pain has not been shown to differ from that of other causes of optic neuritis.

Fifth is headache and facial pain, outside the remit of ON but including trigeminal neuralgia and cervicogenic headache amongst others (Masters-Israilov and Robbins, 2017); there is little in the literature, or anecdotally in clinic, to suggest this is commonly a chronic problem in NMO.

Last, more recently described and exceedingly rare, is myalgia where raised creatinine kinase and evidence of peripheral AQP4Ab induced myopathy have led researchers to hypothesise that this may be an extra-CNS antibody mediated feature of NMO (Cosgrove et al., 2014; Guo Y et al., 2014).

Of all the pain syndromes described above, central neuropathic pain and spasm-related pain are the most life altering. Central neuropathic pain is the focus of the remainder of this chapter and is the focal topic of the thesis.

What are the known characteristics of central neuropathic pain in NMO?

Truncal and limb sited neuropathic pain is thought to only occur in NMO where evidence of spinal cord injury can be found (usually confirmed radiologically) and thus by IASP definitions the pain is a form of 'central neuropathic pain' ("IASP Taxonomy - IASP," 2016).

The prevalence of central neuropathic pain in NMO patients with evidence of myelitis is around 60%; there is no known predilection for gender or age, and no relationship has been shown between pain and disease duration or number of relapses (Bradl et al., 2014; Pellkofer et al., 2013; Zhao et al., 2013).

Of the few available studies, one explores the central neuropathic pain sensory phenotype in detail: Pellkofer et al's Quantitative Sensory Testing (QST) paper (Pellkofer et al., 2013). QST seeks to quantise sensory deficits through metered testing of sensory modalities, for example graded pressures applied until (a) detected and (b) pain elicited. Compared to controls, neuropathic pain sufferers in general show lower thresholds for nociceptive parameters (hyperalgesia) and higher thresholds for non-nociceptive parameters (hypoaesthesia); about a fifth exhibit paradoxical heat sensation (a sensation of intense heat in response to a stimulus of alternately cool and warm bars; posited as resulting from impaired central inhibition) and dynamic mechanical allodynia (pain when skin is stroked; posited as resulting from central sensitisation) (Craig et al., 1996). Common findings in central causes of neuropathic pain include a loss of function across a range of modalities without positive sensory findings, or with isolated mechanical hyperalgesia, along with paradoxical heat sensations (Maier et al., 2010).

Pellkofer et al's study of eleven AQP4Ab-positive NMO participants revealed the expected features of heat-induced hyperalgesia on a background of thermal hypoaesthesia, with ongoing pain strongly correlating with sensory loss; all interpreted as evidence of deafferentation. There was also, as expected, evidence of dynamic mechanical allodynia and paradoxical heat sensations, (proposed as evidence of central sensitisation and disinhibition), the former shown to be conveyed by large-diameter myelinated afferents

that do not convey peripheral pain information and thus implicating central integration of sensory information (Campbell et al., 1988) and the latter reflecting disintegration of heat, cold and pain-relevant thermal information disinhibiting heat sensing pathways (Susser et al., 1999). Central sensitisation and disinhibition are discussed further below. Interestingly, patients with cervical lesions were significantly more likely to have lower heat pain thresholds in the hands and feet compared to controls, with a similar trend found for cold pain thresholds, suggesting information from the extremities conveyed by the spinothalamic tract is in some way altered by cervical lesion (note, however, that those with cervical lesions were significantly closer to their latest relapse). One drawback of the study is that only the hands and feet were assessed, irrespective of whether these were painful areas, to allow meaningful comparison with The German Network for the Study of Neuropathic Pain (DFNS) standardised QST test battery (Rolke et al., 2006).

Clues to pathogenesis from other central neuropathic pain conditions

Spinal cord injury

At least 40% of spinal cord injury (SCI) patients suffer neuropathic pain in one form or another. Pain in SCI is broadly divided into 'at level' or 'below level' to distinguish between sensory symptoms within the dermatome of the injured segment, or below; it is noteworthy that at-level pain might be central or peripheral (e.g. nerve root injury) whilst below-level pain is exclusively central. As in other neuropathic pain conditions, pain may be spontaneous (unrelated to stimulus) or evoked (stimulus-dependent) (Finnerup, 2013). Below-level neuropathic pain, experienced in about 25% of pain sufferers is often described as severe or excruciating and develops months to years after injury, giving some credence to neuroplastic pain aetiologies and in many ways reflecting what we see in the

NMO clinic. Those experiencing pain at 3-6 months post-injury are likely to continue to experience pain at 3-5 years (Siddall et al., 2003).

A few recurring themes in SCI might provide insight into the pain's pathogenesis. Firstly, neuropathic pain seems to be more common in patients with incomplete lesions (Davidoff et al., 1987) which may tie-in with observations in the NMO clinic whereby pain appears to coincide with recovery of function. Secondly, lesions of the spinothalamic tract (STT) are thought necessary but are shown to be insufficient to cause neuropathic pain: two patients with anatomically similar STT lesions can suffer severe pain or no pain at all (again, anecdotally similar to pain in NMO). Third and probably most important is the concept of central sensitisation. First described by Woolf in animal models of peripheral nerve injury (described in detail below under 'contemporary theories of central neuropathic pain mechanisms'), central sensitisation as defined by the IASP is an "increased responsiveness of nociceptive neurones in the central nervous system to their normal or subthreshold afferent input" ("IASP Taxonomy - IASP," 2016; Woolf, 1983). This is sometimes referred to as a 'spinal pain generator', a dysfunctional dorsal horn network with resultant central sensitisation, and has support from (a) animal models showing that the preservation of the superficial dorsal horn is required for SCI pain (Yezierski et al., 2004), (b) the analgesic effect of surgical ablation of specific dorsal horn structures in SCI patients (Falci et al., 2002) and (c) at-level sensory hypersensitivity demonstrated in below injury level pain patients (Finnerup et al., 2007). A range of overlapping causative factors have been proposed in SCI and show support for earlier findings in central sensitisation research (again see later section and Figure 1), they include imbalanced inhibition caused by GABAergic dysfunction and interneuron loss (Meisner et al., 2010), increased

glutamatergic excitatory activity (Finnerup, 2013), anatomical and morphological rewiring (over a longer timescale) (Kalous et al., 2007) and microglial activation with their associated array of secreted downstream inflammatory mediators and growth-factors (Hains and Waxman, 2006).

It is also apparent that changes occur in supra-spinal areas after the development of a SCI pain syndrome, including within the thalamus, anterior cingulate cortex (ACC) and prefrontal cortices (Lenz et al., 1989; Stanwell et al., 2010); as of yet the precise relevance of these changes for SCI pain are not fully understood (Finnerup, 2013).

Multiple Sclerosis

As the closest disease analogue to NMO, the findings of research into multiple sclerosis (MS) central neuropathic pain may lend vital clues to the aetiology of pain in NMO. Pain prevalence in MS is far lower than in NMO (less than 50% versus 80%); additionally, the percentage with severe pain in MS (rated as 7-10 on a 0 to 10 pain score) is lower: 4% compared to 22% of NMO patients (Kanamori et al., 2011). At least half of pain sufferers in MS have central neuropathic pain (O'Connor et al., 2008). Of the central pain sufferers, other than 5% with trigeminal neuralgia, pain is located primarily in the lower extremities (87%), is mostly bilateral (76%) and is constant (Österberg et al., 2005). Sensory examination of MS pain patients reveals mechanical hyperalgesia, hyperaesthesia to pinprick, hypoaesthesia to touch and vibration, and a high frequency of cold and mechanical allodynia (very similar to sensory findings in NMO), suggestive of both deafferentation of multiple spinal tracts, including the spinothalamic tract, and CNS sensitisation. QST results are variably significant across studies, but where differences are

shown, they affirm the same pattern of deficits (Österberg and Boivie, 2010; Svendsen et al., 2005).

Regarding lesion location, an MRI study of MS participants with and without pain showed no significant difference in location of lesions along candidate sensory tracts (including dorsolateral columns, dorsal columns and thalamocortical projections) or discrete CNS areas (including cord grey matter, thalami and brainstem divisions). There was, however, a trend towards fewer lesions in thalamocortical projections in pain participants. Remarkably, although it seems the rostrocaudaul distribution of lesions was documented, this was not analysed in relation to pain (Svendsenl et al., 2011). Indeed, there is only one study to my knowledge to make reference to rostrocaudal location of lesions and their relationship with pain in MS pathogenesis (Okuda et al., 2014); their study suggests that thoracic cord lesions may play an important role in pain aetiology (see Chapter 4).

Unfortunately, the vast majority of pain studies in MS have limited numbers, low-powered designs or do not focus on central neuropathic pain, instead tending to focus on less common pain syndromes such as trigeminal neuralgia and migraine, and so the commonest form of pain in MS, that of central neuropathic pain, has remained relatively under researched (Seixas et al., 2014).

Syringomyelia

Although aetiologically distinct from NMO, syringomyelia provides a disease model of relatively selective STT damage causing chronic central pain (in about 60% of patients). Additionally, the anatomically central cord lesions might theoretically cause a high degree of grey matter damage and thus share features with NMO cord lesions. Studies have shown neither a difference in the extent or magnitude of sensory deficits between pain

and non-pain participants, nor a difference in the magnitude of thermal or mechanical deficits between intra-participant areas with and without pain and thus posit that STT damage may be necessary but is not sufficient for central pain development (Ducreux et al., 2006).

Within syringomyelia participants with pain, two subgroups can be clearly distinguished: those with exclusively spontaneous pain and those with a mixture of spontaneous and evoked pain (i.e. allodynia and hyperalgesia). The former is associated with greater sensory abnormalities than those with evoked pain, with severe mechanical and thermal deficits in the area of pain, put forward as evidence for supraspinal deafferentation. Additionally, the intensity of burning pain in the spontaneous pain group correlated with the degree of thermal deficits and is suggested to support a thermosensory disintegration model (Craig, 1998) (see later for further discussion). The evoked pain subgroup had minimal sensory deficits in the area of pain, providing little evidence for deafferentation and instead the authors propose central sensitisation or pain modulatory system dysfunction as its cause (Ducreux et al., 2006). No discernible correlations between DTI measures or spinothalamic tract function are found in evoked pain patients, yet interestingly, there is less cervical cord tissue damage on structural imaging and less impairment of STT function, in line with incomplete spinal lesions causing pain in SCI and animal models (Davidoff et al., 1987; Finnerup et al., 2003; Hatem et al., 2010).

Insights from animal models of NMO and related conditions

Animal models designed to investigate neuroinflammatory conditions manifest coincident pain phenotypes

Pain in animal models of NMO, that is NMO-IgG inoculated experimental autoimmune encephalomyelitis (EAE), have not looked specifically for pain effects (Jones et al., 2012) however, a related model, that of MOG-induced EAE, has shown spontaneous tactile and cold allodynia, a sign that emerges before other characteristics (Olechowski et al., 2009), whilst a subtly different proteolipid protein peptide (PLP) induced EAE model demonstrated chronic thermal hyperalgesia after a brief initial phase (days) of thermal hypoalgesia, implicating a dynamic CNS change in pain processing (Aicher et al., 2004). The dynamic changes may be sub-served by an initial loss of serotonin containing terminals in the dorsal horn, lowering descending facilitatory tone, and then a subsequent re-sprouting of serotonin terminals shifting the balance in favour of increased facilitatory tone (White et al., 1985).

SCI animal models manifest pain from induced excitotoxity and from isolated spinothalamic tract damage

It is worth mentioning work in animal models of spinal cord injury (SCI), as the adopted mechanism of injury in some models may parallel features of acute inflammation in NMO (for example induced excitotoxicity) and indeed some models of cord transection result in tract damage that is hypothetically apparent in NMO cords after severe inflammation (e.g. hemi-section or isolated spinothalamic tract damage) (Nakae et al., 2011).

An example of induced excitotoxicity via spinal cord injection of an AMPA-metabotropic receptor agonist (quisqualic acid) into rodent cord grey matter produced a model of pain where spinal sensory lamina I neurons showed increased excitability, bursting discharges

and long after-discharge responses as a result of excitotoxic damage; deep lesions affecting primarily dorsal horn interneurons have been shown to be sufficient to produce the pain model (Yezierski et al., 1998). Cord hemisection produces motor dysfunction ipsilaterally and mechanical and thermal hyperalgesia bilaterally (Nakae et al., 2011); interestingly, contrary to the findings in the diseases described above, it seems that unilateral lesions exclusively involving the spinothalamic tract are sufficient to induce a similar bilateral pain syndrome (Wang and Thompson, 2008).

Current management adopts generic neuropathic pain guidelines and lacks efficacy

The mainstay of anti-neuropathic therapy in NMO is pregabalin, gabapentin, amitriptyline and duloxetine (or medications of the same class) which is broadly in line with current anti-neuropathic recommendations (Finnerup et al., 2015). Pregabalin and gabapentin, both anti-epileptics, bind to $\alpha_2\delta$ subunits of voltage-gate calcium channels (Field et al., 2006; Wang et al., 1999) and prevent trafficking of the channel subunit to presynaptic terminals (Bauer et al., 2010; Hendrich et al., 2008), theoretically counteracting its upregulation in states of central sensitisation (Luo et al., 2001). The number needed to treat (NNT) to see a single patient with 50% pain relief (across a spectrum of neuropathic disorders) has been reported as 7.3 for gabapentin and 7.7 for pregabalin (Finnerup et al., 2015). Amitriptyline, a tricyclic antidepressant, may exhibit a range of analgesic mechanisms including peripheral anti-inflammatory effects via prostaglandin pathways, however for neuropathic pain its action as a monoamine (noradrenaline and serotonin) re-uptake inhibitor is thought to be most important. Interestingly, it seems to be the dual monoamine re-uptake action, i.e. re-uptake inhibition of both NA and 5HT, that mediates

its efficacy (Vrethem et al., 1997) suggesting that it influences both noradrenaline and serotonin mediated descending modulation. For their anti-allodynic properties, there is increasing evidence that tricyclics exert their effects at β2 receptors (Yalcin et al., 2009). There is also evidence that tricyclic antidepressants have sodium-channel blocker capabilities and consequent local anaesthetic-like properties, proposed by some as important for neuropathic pain reduction (Sudoh et al., 2003; Wang and Strichartz, 2001). The NNT to see a single patient with 50% pain relief is around 3.6 (Finnerup et al., 2015). Duloxetine, a newer antidepressant, inhibits serotonin and noradrenalin reuptake and in this regard may have a similar analgesic mechanism to amitriptyline (Bymaster et al., 2005). This and other SNRIs are reported as having a NNT of 6.4 (Finnerup et al., 2015), notably less effective than tricyclic antidepressants, perhaps due to a narrower range of therapeutic mechanisms.

Patients are usually commenced on one agent, and switched to another if ineffective or intolerable; many patients end up on multiple anti-neuropathic drugs, however the evidence for anti-neuropathic polypharmacy is non-existent (Bennett, 2015). Although there have been no formal trials of anti-neuropathic efficacy in NMO, persistently high pain scores despite administration of a range of the above therapies is commonly reported in the literature and alternative therapies are eagerly sought (Kanamori et al., 2011; Kong et al., 2016; Qian et al., 2012).

The treatment outlook is not entirely bleak. A recent trial of tocilizumab (an anti-IL-6 monoclonal antibody) for NMO treatment relapse management shows that it may also be effective at partially relieving neuropathic pain (Araki et al., 2014; Ringelstein et al., 2015),

and changes in the delivery of medications, for example topical lidocaine plasters for allodynia (although often not funded under the NHS; Bennett, 2015), hold some promise in NMO sufferers; there is also the use of carbamazepine in NMO, an anti-epilepsy sodium channel blocker, that seems to be effective at least for spasm-induced neuropathic pain (Carnero Contentti et al., 2016), however many patients find temporary improvement and not complete relief.

Contemporary theories of central neuropathic pain mechanisms: Disinhibition, central sensitisation and neuroplastic change

It is clear that central neuropathic pain is not an indivisible entity: there are constellations of different symptoms, from spontaneous pain with or without evoked pain to variable degrees of sensory dysfunction, and so teasing out mechanisms and finding therapeutic solutions is not a case of one size fits all (Bennett, 2015). There are three broad areas that encompass current thinking on the mechanisms driving central neuropathic pain; they are: disinhibition (Craig, 1998; Head and Holmes, 1911), sensitisation (Woolf, 1983) and neuroplastic change (for example Kalous et al., 2007).

Disinhibition, originally formulated by Head and Holmes and adapted by Craig posits that central pain results from the loss of inhibitory control of structures within the brain (Craig, 1998; Head and Holmes, 1911). The thermal-grill illusion of pain, whereby cool sensation (mediated by modality specific peripheral COOL C-fibres) is reduced disproportionately to tonic noxious cold input (mediated by polymodal C-fibres) and leads to the uncovering (or disinhibition) of noxious cold sensation (Craig and Bushnell, 1994). From anatomical evidence, Craig proposes that innocuous cold and noxious cold, carried in the STT

pathways, have unique terminations in medial and posterolateral portions of the thalamus, respectively. Damage to the lateral lamina I spino-thalamo-cortical pathway (which further projects to parietoinsular cortex), at any point along the pathway, disinhibits polymodal nociceptive activity in the medial lamina I spino-thalamo-cortical pathway (with projections to the anterior cingulate) via cortico-cortical or descending output from the insula, and engenders the 'thermoregulatory (homeostatic) motivation', consciously experienced as pain. A possible example of this is described above in the burning pain of syringomyelia and the hypothesis could well be relevant to NMO if lesions in some way selectively disrupt the lateral lamina I spino-thalamo-cortical pathway.

Central sensitisation phenomena are hypothesised to exist in both the brain and spinal cord of central pain patients and have a well-established research basis (Figure 1). Described first by Woolf, he demonstrated increased nociceptor synaptic efficiency in the dorsal horn in response to brief stimulation of peripheral nociceptors (Woolf, 1983). This was both homosynaptic and heterosynaptic, that is, amplification occurred for both the conditioning nociceptive input (hyperalgesia) but also for non-conditioned nociceptive (secondary hyperalgesia) and non-nociceptive (allodyndia) inputs (see Woolf, 2011 for review). Synaptic strength has been shown to be modulated by presynaptic and post-synaptic mechanisms (Woolf and Thompson, 1991), and also by changes in inhibition (Sivilotti and Woolf, 1994) and membrane excitability. Recent animal models have demonstrated that astrocytes, microglia and inflammatory mediators all play a part in sensitisation (Chacur et al., 2009; Gao et al., 2009; Samad et al., 2001). Peripherally induced central sensitisation has been observed in human capsaicin experiments (LaMotte et al., 1991) and again is shown to be heterosynaptic (Ziegler et al., 1999). In healthy

volunteers, peripherally induced central sensitisation manifests immediately but can last for many hours beyond the withdrawal of a conditioning stimulus, however it is fully reversible and sensory findings eventually return to baseline (Woolf, 2011).

Figure 1. Central sensitisation – NMO-relevant dorsal horn mechanisms

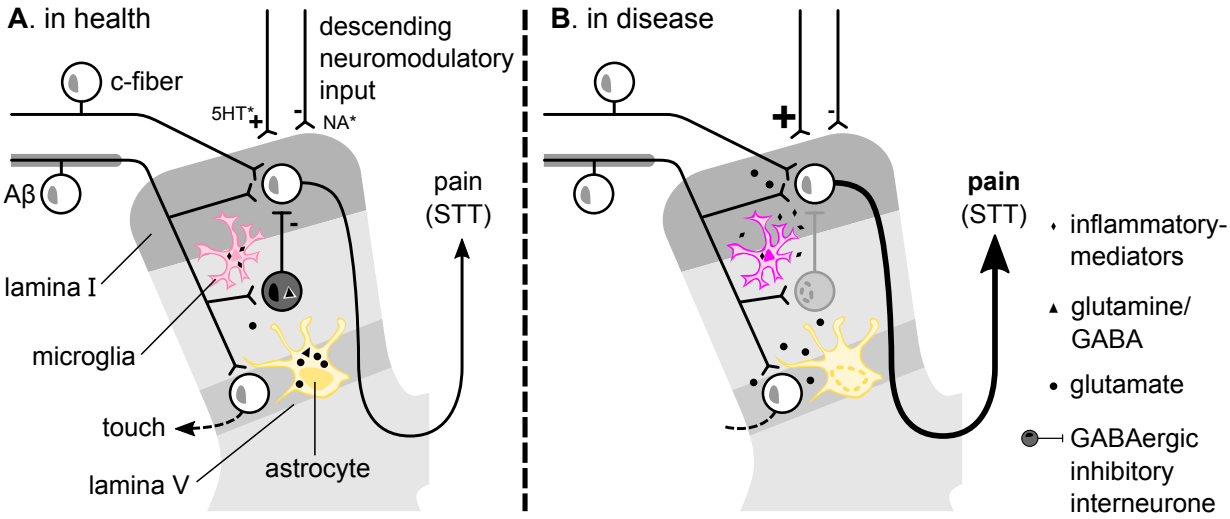

(A) In health glutamate-glutamine-GABA cycle maintained by astrocytes; microglia inactive. (B) In disease, astrocyte damage / loss causing (i) disrupted glutamate-glutamine-GABA cycle and subsequent dysfunction of inhibitory interneurons and (ii) excitotoxicity; imbalanced descending modulatory input, likely reduced descending inhibition outweighed by descending facilitation; activated microglia releasing pro-inflammatory and pro-nociceptive mediators and growth factors, including IL1-β and IL-6. *The diagram simplifies the actions of NA and 5HT. In reality, the contribution of 5HT mediated descending modulation is predominantly facilitatory and the contribution of NA is predominantly inhibitory, however there are many examples of exceptions not least instances of different receptor subtypes mediating opposing effects (Bannister and Dickenson, 2016).

Aβ, myelinated mechanoreceptor; STT, spinothalamic tract; NA, noradrenergic descending modulatory input; 5HT, serotonergic descending modulatory input.

Influences rostral to the dorsal horn can also modulate spinal pain processing, and these are summarised in Figure 2. In animals, early experiments stimulating the brainstem reticular formation and rostroventromedial medulla (RVM) produced analgesia and were

shown to inhibit spinal nociceptive transmission at the dorsal horn (Mayer and Price, 1976). These early experiments spawned further electrical and pharmacological studies of the RVM (and related structures). Pharmacological investigations with focal application of μ-receptor agonists or opioids to the RVM (or PAG) produced analgesia, an effect reversible by the application of opioid antagonists (Yaksh et al., 1988); similarly, cannabinoid agonists injected into the PAG or RVM also produced analgesia (Meng et al., 1998). Interestingly, hyperalgesia induced by naloxone-mediated opioid withdrawal in rat showed heightened RVM activity (where one might expect reduced activity) (Bederson et al., 1990; Kim et al., 1990), providing evidence (amongst other examples) that descending outputs of the RVM can be both facilitatory and inhibitory with regards to nociceptive processing at the dorsal horn (DH). The opposing facilitatory and inhibitory actions of the RVM on nociception are thought to be mediated by distinct cell-types within the RVM, termed 'ON' (facilitatory) and 'OFF' (inhibitory) cells, whilst a third cell-type, 'NEUTRAL', have less clearly defined roles (Fields et al., 1983). About 20 per cent of neurons in the RVM are serotonergic, and there is evidence that serotonin is involved in the central modulation of nociception, eliciting both facilitatory and inhibitory effects on nociceptive processing at the dorsal horn, probably via differential serotonin receptor subtypes (Bannister and Dickenson, 2017).

Figure 2. Descending pain modulatory pathways

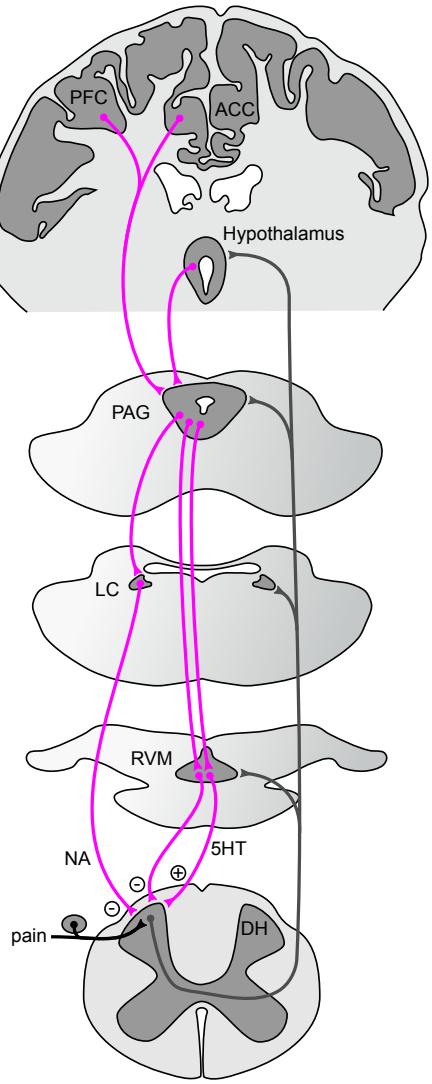

The brainstem, under the direction of rostral structures, significantly alters pain processing at the level of the dorsal horn via descending pathways (pink lines) and is in turn modulated by ascending nociceptive information (grey lines). The PAG-RVM descending pain modulatory system is well studied in humans and known to exert bidirectional control, mediated by RVM 'ON' and 'OFF' cells, at the level of the dorsal horn, thought primarily to be via descending serotonergic efferents (see text for discussion). Another descending source of modulation is the locus coeruleus (and related pontomedullary noradrenergic nuclei) that exerts antinociceptive (and probably pronociceptive, not shown on diagram) effects via noradrenergic efferents (see text). Pink lines, descending modulatory pathways; Black line, primary nociceptive afferent; Grey lines, ascending nociceptive information. PFC, prefrontal cortex; ACC, anterior cingulate cortex; PAG, periaqueductal grey; LC, locus coeruleus; RVM, rostral ventromedial medulla; NA, noradrenergic; 5HT, serotonergic; DH, dorsal horn (Adapted from McMahon, 2013).

The RVM is the final common output for most (if not all) descending facilitatory effects on pain (at least in the murine brain). Areas rostral to the RVM, including the ACC and periaqueductal grey (PAG), clearly play a role in providing both facilitatory and inhibitory input (for review, see Porreca et al., 2002; Urban and Gebhart, 1999). In humans, fMRI studies in healthy participants have shown that areas consistent with the RVM and mesencephalic pontine reticular formation (which includes the nucleus cuneiformis) and project extensively to the RVM (Zemlan and Behbehani, 1988), are active in capsaicin/heat models (Zambreanu et al., 2005) and injury-free opioid withdrawal models (Wanigasekera et al., 2011) of central sensitisation, at a magnitude that correlates with pain intensity (Lee et al., 2008), indicating a role for the RVM and its rostral inputs in pain facilitation in humans. This brainstem activity can be modulated by gabapentin which suppresses stimulus induced deactivations in the brainstem (an action dependent on a state of serotonin activation and $\alpha_2\delta$ upregulation at the dorsal horn) (Iannetti et al., 2005; Suzuki et al., 2005). Interestingly, these brainstem effects of gabapentin can be separated on fMRI from compounds ineffective in neuropathic pain (Wanigasekera et al., 2016).

Descending modulation has been studied in animal models of chronic pain where descending facilitation, particularly coordinated via the RVM, plays an important role (Gebhart, 2004). In humans with chronic pain conditions, a role for brainstem driven facilitation is increasingly recognised, as a functional MRI study in osteoarthritis demonstrates, showing that the degree of PAG activation correlated with neuropathic pain component scores when receiving noxious stimuli (Gwilym et al., 2009).

Another major modulatory system arises from noradrenergic cell groups in the lateral pontine tegmentum, in particular the locus coeruleus (LC), but also autonomic areas A5 and A7. Stimulation of the LC produces descending inhibition and antinociception mediated by spinal α_2-adrenergic receptors (Danzebrink and Gebhart, 1990; Hentall et al., 2003; Pertovaara, 2006). Akin to the bidirectional action of the PAG-RVM system, there is evidence that α1-adrenergic receptors in the dorsal horn might facilitate nociception and feature as part of a noradrenergic-mediated descending facilitatory system (Holden et al., 1999). Although distinct from the PAG-RVM descending circuits, interestingly all of these catecholaminergic nuclei are interconnected with the PAG (Bajic and Proudfit, 1999) and RVM (Yeomans and Proudfit, 1990) and have common rostral inputs, including the limbic system, hypothalamus and anterior cingulate cortex (Aston-Jones and Waterhouse, 2016).

Neuroplastic change certainly warrants consideration as a possible pain aetiology where pain onset is delayed for months or years after CNS insult, as is frequent in SCI patients. These neuroplastic changes might occur locally, as in the example of peripheral nerve injury in rats showing sprouting across dorsal horn laminae (Woolf et al., 1992), or at a supraspinal site distant to damage, as in the example of changes in Na-channel expression in the thalami of rats with SCI (Hains et al., 2005). As a mechanism, neuroplastic changes clearly overlap with central sensitisation.

Candidate central neuropathic pain hypotheses in NMO

What follows in this section is a collation of the findings discussed above to highlight aspects of particular relevance to NMO and to outline the investigatory steps taken to address them in this thesis.

NMO pain aetiology 1: Sensory pathway disruption

The concept of sensory pathway disruption has been covered in the discussions of MS, SCI, syringomyelia and animal models above. In brief: lesions to the spinothalamic tract, although probably not sufficient to cause chronic pain, are sometimes required, whilst incomplete tract disruption, lesion-free cervical cords and evidence of thermosensory deficits may all be factors predicting chronic pain (Craig, 1998; Ducreux et al., 2006; Finnerup et al., 2003). There is also evidence for rostro-caudal differences in cord pathology impacting on sensory and pain outcomes: within NMO, foot hyperalgesia associates with cervical lesions; in syringomyelia evoked pain associates with less cervical cord structural damage; and in MS, thoracic cord lesions are hypothesised to associate with pain (Hatem et al., 2010; Okuda et al., 2014; Pellkofer et al., 2013).

To explore these various aspects, detailed structural imaging of the cord (Chapter 4) is used to analyse the effects of lesion location and cord atrophy on pain, whilst diffusion imaging (Chapter 5) is used to probe for tract-specific pain related damage with particular focus on the STT.

NMO pain aetiology 2: Pain modulatory system dysfunction

In health output from descending pain modulatory systems projecting from the brainstem (for example, the PAG via RVM, or output from noradrenergic nuclei) to the dorsal columns act to facilitate or inhibit nociceptive transmission. This ensures that pain information reaching supraspinal structures is kept under close homeostatic control (see discussion above; and Figure 2; Millan, 2002; Pertovaara, 2006; Porreca et al., 2002). NMO is known to cause MRI-detectable lesions at a number of CNS locations critical for the

descending pain modulatory system (see Chapter 1a: Figure 1, Chapter 1b and Chapter 6), not least the dorsal horn, the periaqueductal grey (PAG) and the rostroventromedial medulla (RVM; Barnett et al., 2014; Tackley et al., 2014). Firstly, it is conceivable that lesions at any of these locations could interfere with the normal functioning of one of the descending pain modulatory systems and become a factor in inducing a chronic pain state (e.g. through disinhibition or central sensitisation). Secondly, it is also quite possible that long-term neuroplastic change, triggered by an initial NMO insult, could alter the balance of pain homeostasis in these key pain regulatory systems. Lastly, there is growing evidence that vulnerability to developing chronic pain varies between individuals and it may be that this intrinsic variability is the cause of pain in susceptible participants (Denk et al., 2014).

To address some of these questions, I studied resting state brain networks to see if and how they are altered in NMO pain, particularly focussing on PAG-related activity (Chapter 6); additionally, MRS analysis of detectible PAG neurotransmitters (primarily glutamate and GABA) are analysed to further unravel PAG neurochemistry in relation to NMO pain (Chapter 7).

Proposed NMO pain aetiology 3: Inflammatory-mediated

Within acute NMO lesions, activation of microglia and recruitment of macrophages, and the subsequent release of cytokines (including IL-1, IL-6 and TNF), chemokines and growth factors could all conceivably exert pro-nociceptive effects at the site of spinal cord lesions (Bradl et al., 2014). An interleukin of especial interest in NMO is IL-6, consistently found to be increased in NMO cerebrospinal fluid (CSF) and potentially implicated in its pathogenesis (e.g. through destruction of the blood-brain barrier, exacerbating CNS inflammation, and possibly mediating the production of AQP4Ab) (Uzawa et al., 2010). IL-6

is also found to be upregulated and necessary for the development of some components of peripheral and central neuropathic pain in animal models, possibly via decreased expression of astrocytic glutamate transport, GLT-1, and the subsequent disturbance of glutamate homeostasis (Sung et al., 2003). Glutamate receptor agonists are known to cause allodynia and hyperalgesia in rats, mainly via spinal NMDA receptors but also via prostaglandin dependent mechanisms (Minami et al., 2001) and thus IL-6 mediated disturbance of glutamate homeostasis may impact on pain behaviour. Indeed, IL-6 antibodies restore the expression of GLT-1 and reverse the pain phenotype seen in animal models. Furthermore, human trials of an IL-6 monoclonal antibody in NMO have not only shown a reduction in relapse rate, but also a reduction in neuropathic pain (Araki et al., 2014). Glutamate excitotoxicity seen in NMO lesions is probably exacerbated by poor uptake of glutamate by AQP4Ab-induced damaged astrocytes (Hinson et al., 2012) and as demonstrated in the animal models discussed in an earlier section, excitotoxicity can certainly induce locally sustained neuronal excitability and potentiate pain (Nakae et al., 2011) (see Chapter 1a Figure 2).

In chronic NMO cord lesions, the notable loss of astrocytes disrupts the glutamate-glutamine cycle and reduces available glutamine, GABA's precursor. As GABAergic interneurones are implicated in antinociceptive actions in the DH, for example the antinociceptive effects of intrathecal baclofen (Von Heijne et al., 2001), including mediating some of the modulatory actions of descending inputs (Millan, 2002), this may contribute to a pro-excitatory state (Bradl et al., 2014) (see Figure 1). These might all play a role in central sensitisation and the development of a spinal 'pain generator'. Downstream effects of activated microglia and related cytokines and growth factors could also conceivably mediate neuroplastic changes in the cord.

To investigate these many factors, the broad-brushed technique of proton NMR metabolomics is employed to profile NMO patients' sera and analyse them alongside pain scores in the hope of finding downstream (or upstream) markers of these cell-mediated changes (see Chapter 8).

Conclusion

NMO central neuropathic pain is poorly understood, highly prevalent, treatment refractory and detrimental to quality of life: it is an area that urgently needs addressing by the clinical research community.

Examining what is known about pain in NMO, related conditions (MS, syringomyelia and spinal cord injury), and from relevant animal models, reveals that NMO neuropathic pain is likely underpinned by a broad constellation of mechanisms including, but not limited to components of central sensitisation, disinhibition and neuroplastic change.

To prise out how these varied mechanisms might drive central neuropathic pain in NMO is the goal of this thesis, wherein particular focus is paid to spinal sensory pathway disruption (Chapters 4 & 5), dysfunction of the brainstem pain modulatory system (Chapters 6 & 7) and the effects of inflammation (Chapter 8).

Search methodology

The MEDLINE database (pubmed.gov) was queried with the following search string "((pain[Title] AND myelitis[Title])) OR (pain[Title] AND neuromyelitis[Title])", this retrieved 14 articles, seven of which were considered the core publications on pain in NMO. A further unrestricted query with string "pain AND neuromyelitis" produced a further 90 unique results, six of which were deemed relevant for inclusion. Articles describing pain in related conditions were found using disease Medical Subject heading (MeSH) terms and 'pain' as an additional search term, for example: "Spinal Cord Injuries"[Mesh] AND pain"; These were then filtered for reviews. Other articles relevant to the field and known to the author have also been referenced.

Chapter 2

MRI and analytical methods for the investigation of NMO pain

Introduction

This chapter describes the hardware, imaging modalities and associated analytical techniques used in the thesis, and provides a rationale for their application to the investigation of NMO pain. Detailed analytical pipelines used in the thesis are described in the relevant experimental chapters.

Scanner and protocols

All imaging was performed in Oxford's Functional Magnetic Resonance Imaging Centre for the Brain (FMRIB) on a 3-tesla Siemen's MAGNETOM® Verio MR scanner. The scanner was fitted with a 12-channel head coil, 4-channel neck coil and 8-channel spine coil. Physiological data, including respiratory movements and cardiac cycle, were measured with respiratory bellows and a pulse oximeter, and recorded using BIOPAC software with scanner trigger timing. The imaging protocols are shown in table 1 below.

Table 1. MRI protocol details

Sequence	*Anatomy*	*Details*
3D T1-weighted	Cervical cord and brainstem	3D isotropic MP-RAGE. 12-channel head coil, 4- channel neck coil and multi-channel spine coil. TR: 2.3s; TE: 3.9ms; flip angle 8^{o}; voxel=1.0x1.0x0.9mm
Sagittal T2-weighted	Cervical cord	TSE. 12-channel head coil, 4-channel neck coil and multi-channel spine coil. TR=4.6s, TE=67ms, voxel=0.6x0.6x3.0 mm
	Thoracic cord	TSE. 4- channel neck coil and multi-channel spine coil. TR=4.6s, TE=67ms, voxel=0.7x0.7x3.0 mm
Axial T2-weighted	Cervical cord	TSE. 12-channel head coil, 4- channel neck coil and multi-channel spine coil. TR=9.17s, TE=70, voxel=0.6x0.6x4mm
Diffusion-weighted	Cervical cord	EPI. 12-channel head coil, 4- channel neck coil and multi-channel spine coil. 30 diffusion directions. B0 and B=700s mm^{-2}. AP and PA phase encode directions. Echo-spacing 1.25ms. TR=7.6s. TE=92ms. 54 slices. Voxel=1.3x1.3x3mm.
Resting-state functional MRI	Brain	EPI. 12-channel head coil, 4- channel neck coil. GRAPPA acceleration factor 2. Phase encode direction AP. 44 slices. 128 measurements. FOV 192 x 192mm. TR 2.4s, TE 30ms, voxel=3x3x3mm.
MRS	Brainstem (PAG)	T1 MPRAGE used to localise VOI (1x1x1cm). B0 shimming using GRE shim[1]. Modified semi-LASER sequence. TE=28 ms, TR=3s, 192 averages[2].

1: (Shah et al., 2009)

2: (Oz and Tkáč, 2011)

Structural MRI of the cord

Despite a growing literature of structural imaging used in the investigation of neuroinflammatory cord disease, very few have used T1 and T2 weighted imaging to investigate pain. With the exception of Okuda et al., cord T2-hyperintense lesion mapping of the cord has not been considered in MS pain (Okuda et al., 2014). Another common measure, cervical cord cross-sectional area, a particular form of which, Mean Upper Cervical Cord Area (MUCCA), is popular in MS studies, has been shown to correlate with cervical cord lesion metrics and disability in MS and NMO (Daams et al., 2014; Mann et al., 2007) but again has not been studied with relation to neuroinflammatory pain (see Chapter 1b for more on conventional imaging in NMO). The advent of dedicated automated spinal cord analysis software, such as the spinal cord toolbox (De Leener et al., 2017), have made the routine analysis of cord anatomy more practicable than ever and so I take the opportunity here to look at T2 lesion characteristics and cervical cord cross-sectional area in relation to pain. Detailed methods and results can be found in Chapter 4.

Diffusion MRI of the cord

MRI diffusion imaging measures the diffusion dynamics of water within the imaged sample. It was developed in the early '90s and has become a sophisticated technique with wide-reaching clinical and research applications, not least in MS and NMO (Beaulieu, 2002). A diffusion tensor model is commonly fitted to diffusion-weighted data and from this a number of parameters can be derived. Within this thesis, two will be used: mean diffusivity (MD), a measure of the average amount of diffusion, and fractional anisotropy (FA), a measure of directionality. High MD represents unrestricted water diffusion whereas high FA suggests diffusion confined along a linear path (such as is found along myelinated white

matter tracts). Diffusion imaging in the spinal cord is made challenging by the inhomogeneous anatomy of the spine, however recent advances such as the reduced field-of-view 2D-selective radiofrequency excitation technique have made the acquisition of high quality cord diffusion data possible (Finsterbusch, 2012). Diffusion measures have been shown to be massively abnormal in inflammatory cord lesions where increased MD and reduced FA are commonly found and interpreted as reflecting demyelination (Klawiter et al., 2012); there are also reports of abnormal diffusion measures in areas of NMO cords without lesions (Pessôa et al., 2012; Qian et al., 2011), however it is not clear whether these changes are the consequences of lesions remote to the measurement site. Tract-specific measures are also reported, for example in the cervical posterior columns where changes correlate with clinically measured vibration sense thresholds (Naismith et al., 2013). Such a technique has clear relevance for understanding pain aetiology however no studies known to the author examine pain in neuroinflammatory disease using cord diffusion imaging. These techniques are applied here in Chapter 5.

Resting state functional MRI of the brain

Spatially-defined temporally-synchronised low-frequency fluctuations in blood oxygen level dependent (BOLD) signals of the 'resting' brain were first described in the early '90s within areas of the somatomotor cortex (Biswal et al., 1995). 'Resting brain activity' really refers to mean activity outside of task related activity (and commonly deactivated by participation in tasks). Studies have repeatedly reinforced the existence and spatial reproducibility of resting state networks (RSNs) (Beckmann et al., 2005) and have described multiple RSNs attributed to various resting cognitive functions that can be perturbed by disease and experimentally-induced states (Raichle, 2015). Perhaps the best known of these is the

default mode network (DMN), a network including the ventro- and dorsomedial prefrontal cortex, the posterior cingulate cortex, adjacent precuneus and the lateral parietal cortex; functions attributed to this network range from balancing attention and emotional state, bodily homeostasis and, most relevant to this work, the evaluation of pain (Baliki et al., 2008; Raichle, 2015). There are many ways to analyse resting-state networks, however the two broad methods of analysis used in this thesis are probably amongst the commonest: data-driven independent component analysis (ICA) and seed-based analysis. ICA analysis applied to resting-state fMRI data was first described by Beckmann and Smith (Beckmann and Smith, 2004) and utilises a data-driven technique to identify spatially distinct components of resting-state activity, results that can be compared across groups using the technique of dual-regression (Filippini et al., 2009), a technique that regresses the spatial maps (RSNs) of interest into individual participant data. Seed-based analysis of resting state data is more intuitive but less exploratory, it follows the conventional general linear model centred approach used in task-based fMRI (Woolrich et al., 2009) however rather than using a stimulus-modelled regressor, the mean resting-state activity of the seed of interest is used instead. The technique thus reveals whole-brain (or statistically masked) resting-state activation coincident with the activity of the seeded area. The application of these techniques to NMO pain can be found in Chapter 6.

MRS of the brainstem PAG

In-vivo magnetic resonance spectroscopy (MRS) was first described in the early '90s focussing on the ^{31}P nucleus, however the majority of MRS work currently performed focusses on ^{1}H. At 3.0 tesla and with advances in techniques (including the semi-LASER technique employed herein; see Oz and Tkáč, 2011), signals from choline, creatine, N-

acetylaspartate (NAA), lactate, alanine, glutamate, glutamine, and myo-inositol (mI) are reliably detectable (Zhu and Barker, 2011). Metabolites with potential relevance to pain in NMO include NAA, an amino-acid derivative synthesised almost exclusively in axons (Narayana et al., 1998), mI, a polyol that acts as an osmolyte and relatively specific astrocyte marker (Davie et al., 1994) and members of the glutamate-glutamine cycle, neurotransmitters that play central roles in neuronal excitation, inhibition and excitotoxicity (Duncan et al., 2014; Marignier et al., 2010). NAA and mI are frequently assessed in neuroinflammatory disease where, as a simplistic summary, NAA is commonly reduced in MS lesions and mI commonly reduced in NMO lesions (Tackley et al., 2014). Targeted MRS of the PAG in a neuroinflammatory model of chronic pain has not previously been performed and is applied in Chapter 6.

Summary

The diverse imaging techniques described above covering a range of CNS regions are used in this thesis to explore the aetiology of chronic pain in NMO.

CHAPTER 3
Cohort and assessments

Introduction

A cohort of prospectively recruited NMO participants (and age and sex-matched healthy controls) underwent prospective MRI imaging and a battery of clinical measures and forms the primary experimental cohort of this thesis (referred to hereon in as the 'Imaging Cohort'); this cohort is described in detail below. An additional cohort, the 'Metabolomics Cohort', is a cohort of prospectively recruited NMO and RRMS patients who donated plasma samples for metabolomics analysis; this cohort is described in detail in Chapter 8.

Ethics

Informed consent was obtained for all participants under a research protocol approved by the local ethics committee (Berkshire REC 13/SC/0238) and the local health board (Oxford University Hospitals NHS Foundation Trust).

Overview of statistics

Except where otherwise specified, two levels of significance are reported for statistical outcomes within the thesis: 'significant', or $p<0.05$, and 'highly significant', or $p<0.01$. 'Borderline' significance is considered $0.05 < p < 0.1$.

All statistical tests performed were parametric except where the Shapiro-Wilk normality test was violated; in these instances, a non-parametric alternative was used (see table 1). For a number of imaging analyses, permutation tests are utilised that make no assumptions about the underlying data structure; details of these can be found in the relevant chapters.

Table 1. Non-parametric alternatives to parametric tests

Parametric	*Non-parametric equivalent*
Student's T-test	Mann-Whitney U test
ANOVA	Kruskal-Wallis test
Post-hoc Tukey HSD test	Post-hoc Dunn test

Participants

Thirty-three NMO patients and 24 healthy age and sex-matched controls were recruited. A single control was later excluded from analyses upon later disclosure of a chronic pain condition.

Patients were recruited through Oxford's NMO Neuromyelitis Optica national clinic, whilst controls were recruited locally (in Oxford) via non-coercive advertisement. NMO participants with known pain were preferentially selected (which may skew the pain score distribution and provide some explanation for its biphasic shape; see Figure 2 below).

Recruitment criteria

The inclusion and exclusion criteria for NMO participants are listed below. Of note, only AQP4Ab positive NMO patients were recruited because of the possible ambiguity of diagnosis in antibody negative NMO cohorts (Jarius et al., 2012; Kitley et al., 2012a).

Inclusion:

- AQP4 Ab positive (Waters et al., 2012)
- Previous episode of transverse myelitis (TM)
- No TM relapse within last 6 months

Exclusion:

- Electrophysiological evidence of peripheral neuropathy
- History of surgery not compatible with FMRIB MRI safety protocols (primarily intervention with risk of metallic components being left in-situ without evidence to the contrary)
- Severe claustrophobia
- Geometric incompatibility with MRI bore / coils

Healthy controls were excluded if they had a current history of a pain causing problem and any of the MRI related contraindications listed in the exclusion criteria for patients above.

Although NMO participants with concurrent pain conditions were not excluded (to avoid low numbers), concomitant pain conditions were noted and their effects analysed (see 'Concomitant pain conditions' below).

Participant demographics

Patients and controls were well matched for age and gender, however there was a notable disparity in ethnicity (Table 2). Race plays an important role in pain experience and measurement (see Chapter 1a), and this is discussed further below with regards to pain scores and ethnicity.

Table 2. Patients and controls

	Age, mean(sd)[ns]	Female, n(%)[ns]	Ethnicity* Caucasian, n(%)	Afro-Caribbean, n(%)	Asian, n(%)
patients	53 (14.4)	26 (78.8)	19 (57.6)	6 (18.2)	8 (24.2)
controls	53.9 (16.5)	14 (60.9)	23 (100)	0 (0)	0 (0)

* $p<0.01$ for Chi square comparison of ethnic groupings across pts and controls

ns, no significant difference between patients and controls

Participant assessments

All NMO participants were assessed with the following pain, mood and disability scores (details of these measures are described in subsequent sections):

Pain:

- Brief pain inventory (BPI; from which the Pain Severity Index, PSI, is obtained)
- PainDetect

Mood

- Hospital anxiety and depression score (HADS)

- Center for Epidemiologic Studies depression scale (revised) (CESD)

Disability

- European Database for Multiple Sclerosis grading scale (EDMUS)

Controls were age and sex matched as best as possible and were confirmed to have no current pain condition.

Pain measurement: Brief Pain Inventory PSI is primary outcome measure

Two pain scores were utilised, a generic measure of pain in the form of the Brief Pain Inventory (BPI) and a neuropathic measure in the form of painDetect (Cleeland and Ryan, 1994; Freynhagen et al., 2006). Patients were requested to score the pain related to their myelitis rather than any coexisting non-myelitis pain problems (see section 'Concomitant pain conditions'), focusing on non-spasm related neuropathic pain. This is practicable up and to a point, but where concomitant pain conditions have altered a participant's central processing of pain, for example via central sensitisation thought to occur in osteoarthritis and migraine (Goadsby, 2005; Gwilym et al., 2009) (two of the concomitant pain conditions reported in the present cohort; see Table 6) this will impact on their pain experience globally (i.e. of any aetiology) and will almost certainly alter both the experience and report of NMO post-myelitis chronic pain, and influence experimental findings.

The scores from the first four questions of the BPI were combined to form a Pain Severity Index (PSI) and this measure is the primary outcome used for all studies in the thesis. The four components that make up the PSI are separately rated between 0, no pain, to 10, worst pain imaginable, and ask about: pain on average, pain "now", maximal pain in the last 24 hours and minimal pain in the last 24hrs (Cleeland and Ryan, 1994).

The full BPI also gathers information regarding the functional impact of pain. These data are examined below.

Pain was confirmed 'neuropathic' in line with the International Association for the Study of Pain (IASP) definitions ("IASP Taxonomy - IASP," 2016): all patients had pain attributable to a radiologically confirmed central lesion (current or historical). To glean further information not captured by the BPI, painDetect, was used to capture data about the character of pain (burning, sudden electric shock, etc.). These data are also examined below.

Definition of pain categories: low, meaningful, moderate and high

For many of the analyses included in the thesis, a pain classifier was useful. Therefore, pain is divided into 'low' ($PSI \leq 12$) and 'meaningful' ($PSI > 12$), with the latter category further divisible into 'moderate' ($12 < PSI < 23$) and 'high' ($PSI > 23$). This division is not arbitrary but based on the distribution of pain scores (see subsequent section and table 3).

The term 'meaningful' in the context of pain sufferers is potentially contentious, perhaps implying that those with 'non-meaningful' pain don't suffer. This was neither my intention nor my belief; the term is used here to try and define pain of a severity not seen in day to day life and particularly relevant to quality of life outcomes. Indeed, my definition of 'low' pain is consistent with numerous studies validated with pain-interference scores performed

across a range of diseases including diabetic peripheral neuropathy, spinal cord injury and phantom limb pain (Hanley et al., 2004; Jensen et al., 2001; Zelman et al., 2005) and aligns with the range of 'acceptable' pain in the cancer field (Dalal et al., 2012; Oldenmenger and van der Rijt, 2016). Furthermore, pain equivalent to the 'meaningful' cut-off defined herein has been associated with increased risk of admission in cancer sufferers (Fainsinger et al., 2009; Wagner-Johnston et al., 2010; Zelman et al., 2005).

Brief Pain Inventory (BPI)

The full BPI "short form" score (Cleeland and Ryan, 1994) consists of the PSI (out of 40; described above) and an additional functional interference score (out of 70); the maximum attainable score is therefore 110. The functional interference score incorporates seven questions rated from 0 to 10 regarding pain's impact on activity, mood, walking, work, relationships, sleep and enjoyment of life. Within this cohort, the two components of the score were strongly and significantly correlated ($r=0.79$, $p<0.01$; Figure 1). Mean BPI was 40.9 (s.d. 31.5; range 1-104).

The tight correlation between the PSI and the functional component score suggested NMO sufferers have pain-related functional deficits in-line with the severity of their pain and consequently little information is lost by using PSI as the primary outcome measure in place of the full BPI (see Figure 1); PSI is also in theory a cleaner measure of current pain intensity. Interestingly, the outlying points (pink filled circles in Figure 1; $r=0.92$ without outliers) were patients with diametrically opposed coping strategies; the first admitted to having severe pain issues but resiliently engages in multiple social and physical activities, whilst the second denies any effect of pain on her ability to function, despite much evidence to the contrary.

Figure 1. BPI component correlations

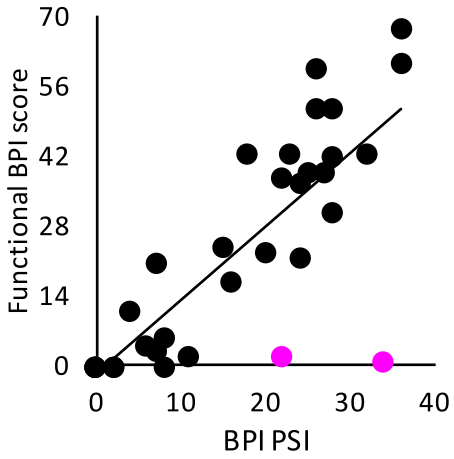

The severity and functional impact components of the BPI score were strongly correlated (r=0.79) in the Imaging Cohort. Two outliers (pink circles) had unusual and contrasting coping strategies (described in text). BPI, Brief Pain Inventory (/70); PSI, Pain Severity Index (/40); Pink filled circles: outliers.

PSI SCORE DISTRIBUTION: CLASSIFICATION OF LOW AND MEANINGFUL PAIN

The distribution of PSI scores was plotted and is shown in the histogram below (Figure 2). The distribution was biphasic and significantly non-parametric (Shapiro-Wilk test of non-normality, $p<0.01$).

Using the dividing point of the two clusters, 'low' pain was designated anything below the mid-point of the central minimum (i.e. bin '10 to 15', average=12.5, rounded up to 13; n=13), 'meaningful' pain was then defined as ≥13 (n=20). For symmetry, the 'high' pain group (a sub-group of the meaningful pain group) incorporates the 13 patients with the highest PSI scores (PSI>23 in this group) (see Table 3).

Figure 2. PSI histogram

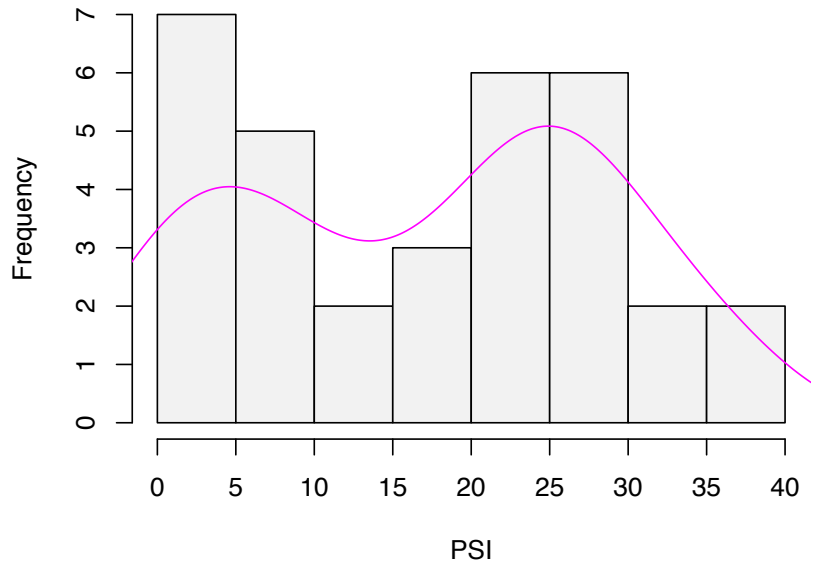

PSI scores were biphasic and non-parametric. PSI, pain severity index; Pink line: overlaid probability density function curve.

Table 3. Pain score groupings

Low (n=13)	PSI ≤12			
Meaningful (n=20)	PSI >12	**Moderate** (n=7)	12< PSI ≤23	
		High (n=13)	PSI >23	

PSI, Pain Severity Index

SPATIAL DISTRIBUTION OF PAIN: BPI BODY MAPS

As part of BPI (and painDetect) assessments, participants were asked to annotate the location of their pain on a body outline. These were collated and are displayed here in two ways: firstly, as a plot representing the percentage of patients with pain in a given area by depth of grey (Figure 3A) and secondly, as a plot representing the same data with each participant's contribution multiplied by their pain severity (PSI, normalised to range 0 to 1; Figure 3B).

The gross spatial pattern of pain was symmetrical, predominantly affecting the legs, back (including shoulders posteriorly and medially), hands and posterolateral neck. The upper arms, head and buttocks were relatively spared. The pain lay in the approximate dermatomal distribution of C7 downwards with relative sparing of sacral dermatomes.

Figure 3. (**A**) Pain distribution by reported site; (**B**) Pain distribution by reported site, scaled by pain severity

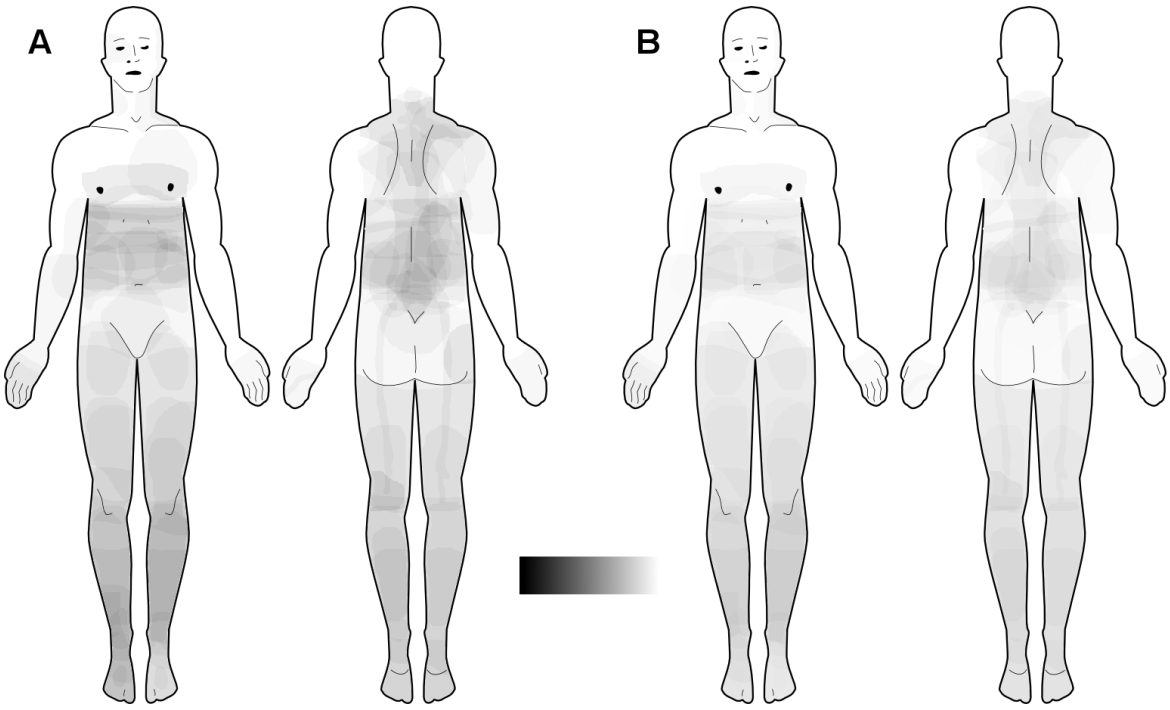

Scale bar indicates maximum (black) to minimum (white) possible greyscale shade.

A: greyscale = percentage with pain (black = 100% with pain in underlying area)

B: greyscale = percentage with pain *x* severity of pain (black = 100% with maximal pain in underlying area)

(Intensity maps generated with custom matlab script)

PainDetect score

PainDETECT (Freynhagen et al., 2006) was designed as a screening tool to detect a neuropathic pain aetiology in settings where limited investigations are available, for example primary care. It was employed here to add further descriptors to a patient's pain. It has two components, the first captures similar information to BPI's PSI; the second is a score out of 37 with predefined reference ranges for nociceptive (0 to 12), neuropathic (19 to 38) and undetermined (13 to 18) pain phenotypes. An array of seven questions probing neuropathic symptoms forms the bulk of the second component (see figure 5 below).

Unsurprisingly painDetect's PSI (the score's first component, not the neuropathic scale) and BPI's PSI were nearly perfectly correlated ($r=0.95$, $p<0.01$) and BPI PSI (referred to simply as 'PSI' in other chapters) is used exclusively in this thesis. The mean painDetect neuropathic score (the score's second component) was 15.9 with a standard deviation of 11.2 and range 0-37. The distribution of painDetect's neuropathic score is shown below for interest, bearing in mind that in this cohort, those below the "neuropathic" cut-off of 19 still have IASP-defined neuropathic pain (Figure 4).

More informative were the frequency of responses to the pain phenotype options in the painDetect score (summarised in Figure 5). These showed neuropathic symptoms across the board, with burning (25/33) and numbness (24/33) featuring highest and spontaneous electric shock like pain lowest (18/33) but still present in >50% of patients.

Figure 4. PainDetect neuropathic score histogram

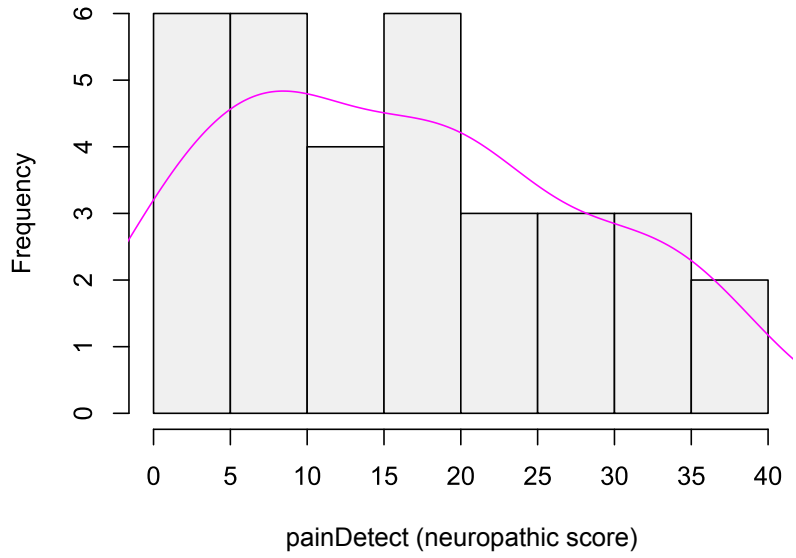

Although a cut-off of >19 is reserved for identifying neuropathic pain for the purpose of screening, all patients with pain in this cohort had neuropathic pain as defined by IASP, even if they fall below this score on painDetect. Pink line: overlaid probability density function curve

Figure 5. painDetect neuropathic symptom frequencies

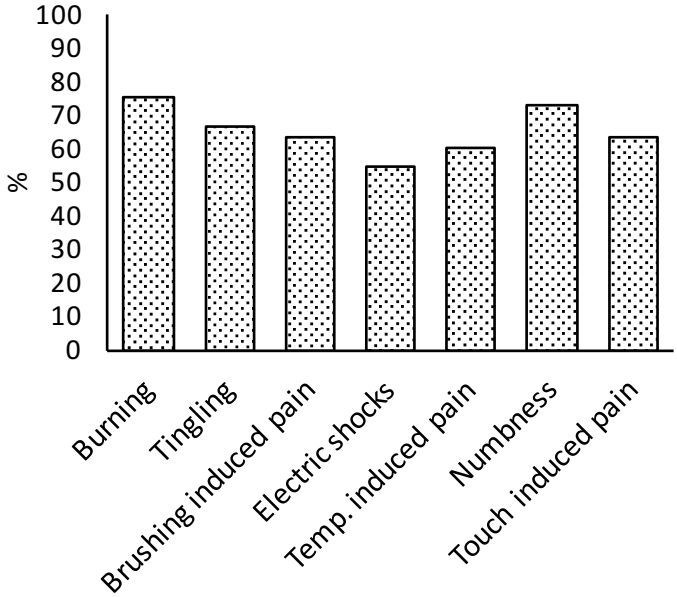

The majority of paitients had neuropathic symptoms, most frequently 'burning' (25/33, 76%). %, percentage of participants with pain symptom.

Clinical measurements and their relationships with PSI

Descriptive statistics of clinical measurements are shown in Table 4. Correlations between clinical measurements and PSI, calculated with Pearson's r, are shown below in Figure 6; noteworthy were the strong correlations between EDMUS, onset age and depression scores (HADS D and CESD). Clinical measures are further discussed in sub-sections below.

Table 4. Descriptive statistics for clinical measures

	mean (sd)	median (range)
PSI*	17.1 (11.6)	20 (0-36)
EDMUS*	3.9 (2.2)	3 (1-8)
Age	53 (14.4)	54.1 (23.5-80.4)
DD	9.5 (5.8)	8.9 (1-22.2)
Onset age	43.5 (16.4)	42.4 (12.4-74.6)
HADS A**	5.5 (4)	5 (0-14)
HADS D**	5.1 (3.3)	4 (0-12)
CESD*	12.3 (10.1)	11.5 (0-39)

sd, standard deviation; PSI, pain severity index; EDMUS, European database for MS disability grading; DD, disease duration; HADS, hospital anxiety (A) and depression (D) scale; CESD, centre for epidemiological studies depression score.

* Shapiro-Wilk normality test significant ($p<0.05$), suggestive of non-normally distributed data

** Shapiro-Wilk normality test borderline ($p=0.05$), possibility of non-normally distributed data

Figure 6. PSI correlations with clinical measures

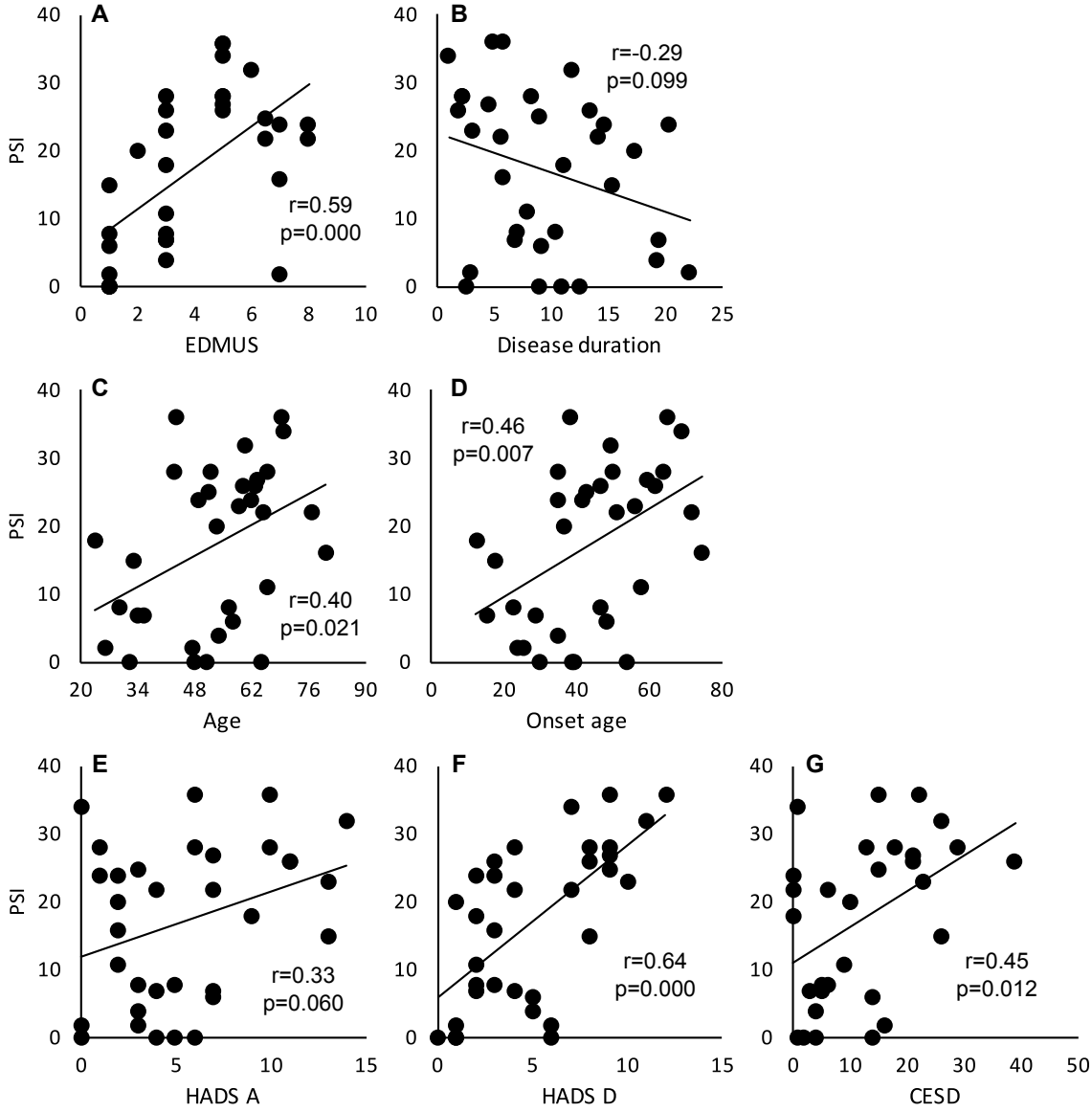

Pain (PSI) showed strong positive correlations with disability (EDMUS), onset age and measures of depression (HADS D and CESD). p-values not corrected for multiple comparisons, Bonferroni-corrected significance levels for $p<0.05$: $\alpha<0.007$, and for $p<0.01$: $\alpha<0.001$.
Note, three participants' CESD scores were unusable, therefore n=30 for plot G.

EDMUS

The EDMUS grading scale (EDMUS), is an integer score from 0 (no disability) to 9 (helpless and bed-bound), with two levels for a score of 6 (6.0/6A: ambulatory with permanent unilateral support; 6.5/6B: ambulatory with permanent bilateral support) that parallels and

is validated against the more commonly used expanded disability status score (EDSS) (Amato et al., 2004; Confavreux et al., 1992; Kurtzke, 1983). It is known to have non-linear properties, with unit-increases above 6 representing greater jumps in disability (Meyer-Moock et al., 2014). It is efficiently calculable in clinic and was the only measure of disability used in this cohort. As noted in Figure 6A, there was a strong correlation between PSI and EDMUS (r=0.59).

Depression and Anxiety

Two scores were used to assess depression, one of which incorporates an additional measure of anxiety (HADS). The Center for Epidemiologic Studies depression scale (CESD) was created primarily as a tool for investigating depression epidemiology in the community mental health setting but has been widely applied elsewhere (Eaton et al., 2004; Radloff, 1977). It consists of 20 graded questions (each 0 to 3) that enquire about various depressive symptoms, generating a composite score out of 60 (maximum equates to maximum severity of symptoms). The Hospital Anxiety and Depression Scale (HADS) was developed as a self-assessment scoring system for the hospital or medical outpatient setting; it comprises seven graded questions (scored 0 to 3) for both anxiety and depression with theoretical maxima of 21 each (maximum again equates to maximum severity of symptoms; Zigmond and Snaith, 1983).

Pain and mood have a complicated relationship, with neuroinflammatory pain being no exception (Alschuler et al., 2013). Interestingly, a recent in-house study showed depression (HADS) had only a borderline correlation with PSI in AQP4-Ab positive participants (r=0.38, p=0.07) but a strongly significant relationship in AQP4Ab negative participants (r=0.78,

p=0.01) (Kong et al., 2016). There is therefore the suggestion that NMO pain may be less mood confounded. That said, there were correlations within the present cohort between depression and pain (see Figure 6, F & G) and this complicated relationship is explored where relevant in subsequent chapters.

Race

Race was crudely categorised into three broad groups: Afro-Caribbean, Asian and Caucasian. These groups had significantly different pain scores (Table 5).

Table 5. PSI by racial grouping

	PSI, mean (sd) *	n
Afro-Caribbean	14.7 (11.9)	6
Asian **	8.9 (8.4)	8
Caucasian **	21.4 (10.5)	19

sd, standard deviation

* $p<0.05$ across groups by Kruskal-Wallis

** $p<0.05$ for post-hoc Dunn test

There are known ethnic disparities between pain response, management and physiology (discussed in Chapter 1a; for review see Campbell and Edwards, 2012). Given the low group numbers and the absence of non-Caucasian controls in this thesis, further insights into these areas are limited and the precise contribution of race to pain processing in NMO will be impossible to elucidate fully here. It is however interesting to note that the pain scores recorded in the present cohort go *against* the trend seen in the pain literature: that of greater pain in chronic disorders amongst ethnic minority groups (Edwards et al., 2001). This may suggest differing NMO pathophysiology determined by race ultimately drives the

pain differences seen here, over and above direct racial physiological and psychosocial influences on the pain experience seen elsewhere.

Concomitant pain conditions

Nine patients reported concomitant pain problems and a list of these is presented in Table 6. Mean PSI was 26.7 in those with confounding conditions versus 13.5 without (Mann-Whitney U test $p<0.01$).

Table 6. Concomitant pain conditions across n=9 patients.

Osteoarthritis (3)
Rheumatoid arthritis (2)
Historic shingles (3)
Migraine (1)
Sickle-cell trait (1)
Scoliosis (1)

Bracketed number = frequency (NB two participants suffered from two conditions)

Participants with concomitant pain were not excluded given the rarity of NMO (all patients were asked to score only their NMO-attributable pain at time of assessment, however as discussed above, where central pain processing changes are engendered by concurrent disease, NMO-attributable pain will be less separable and almost certainly altered). The concomitant conditions reported are heterogeneous in aetiology and associated pain phenotypes, and in so being may be less likely to imbue structured bias into the results.

Summary

The cohort has well matched patients and controls across age and gender and has a wide range of pain severity scores that are neatly sub-dividable into pain severity groups; it is thus well suited to the experiments in this thesis.

Strong confounding factors, such as concomitant pain conditions, cannot be overlooked when interpreting outcomes and along with gender and race related pain effects, these are discussed later in the thesis especially in relation to future work.

Chapter 4

Experimental chapter: Conventional cord imaging and lesion characterisation in NMO pain

Introduction and background

Chronic pain in NMO develops after at least one episode of myelitis and consequently examining the location and extent of myelitis lesions, along with detailed pain measures, has the potential to provide insights into pain pathogenesis. It is noteworthy that multiple sclerosis (MS) cord lesions are predominantly cervical and that NMO cord lesions often involve the thoracic cord, and it is quite possible that the location of the lesion might be associated with the increased pain noted post-myelitis in NMO as compared to MS (see Chapter 1c). Remarkably, the influence of the rostro-caudal location of spinal myelitis in NMO has not to my knowledge been previously studied and in fact, somewhat surprisingly, has barely been considered in other myelopathic pain conditions, such as MS and spinal cord injury (see Chapter 1c). In this chapter, sagittal cervical and thoracic T2-weighted MRIs

are utilised to document precisely this: the rostro-caudal location of NMO lesions in the spinal cord in relation to pain. Additional cervical axial images provided the means to quantify cervical lesion volume.

Cord atrophy is a recognised feature in NMO cords in areas of previous (or persistent) lesions (Tackley et al., 2014) and has been shown in MS and NMO cohorts to correlate with disability (Losseff et al., 1996; Wang et al., 2014; Yiannakas et al., 2015). Alongside lesion profiling, to investigate cord cross-sectional area's (CSA) possible relationship with pain, dedicated cervical axial images were examined.

Objectives / Aims

1. To ascertain the properties of T2-hyperintense lesions (location, length, volume or chronicity) that most influence chronic pain severity.
2. To determine if differences in cervical cross-sectional area (CSA) are exclusively related to the presence of lesions, both current and historical, or whether cervical CSA can independently predict pain.

Methods

Of the 33 NMO Imaging Cohort participants, 29 had T2-weighted imaging of the whole cord in the sagittal plane and T2-weighted scans of the cervical cord in the transverse plane (see Chapters 2 & 3 for cohort characteristics and imaging protocols). Of the 29 participants, 26 had historical MRI data that confirmed the location of cord lesions at the time of onset of their chronic pain. Thirty-two patients of the NMO Imaging Cohort had 3D T1 (MPRAGE)

structural imaging of the cord suitable for volumetric analysis (and includes the 29 participants mentioned above).

Current pain was assessed at the time of the study by the brief pain inventory's (BPI) pain severity index (PSI, 0-40).

T2 weighted lesion analysis

T2-weighted axial cord images were manually lesion masked in FMRIB's software library v5.0 (FSL) using FSLeyes (included in FSL v5.0.10; Jenkinson et al., 2012). Variability in participant cervical cord length meant axial coverage sometimes ended at C5 therefore this was used as the lower cut-off for volumetric lesion analysis. Documentation of lesion location (non-volumetric) was recorded using all available T2-weighted cord imaging (axial and sagittal cervical cord and sagittal thoracic cord).

Cord segmentation and cross-sectional area (CSA) calculation

T1-weighted cervical spinal cord images were segmented (the area of cord tissue masked) using a three-step algorithm based on the propagation of a deformable model implemented in the Spinal Cord Toolbox (SCT v3.0; De Leener et al., 2014). SCT was then used to calculate cross-sectional area (CSA): a probabilistic spinal level mask is first applied to the cord segmentation (Cadotte et al., 2015) and CSA calculated along the plane orthogonal to the cord centerline (De Leener et al., 2017; Yiannakas et al., 2015).

Spinal level C5 was used as the lower cut-off for CSA assessment for a few reasons; firstly, this is consistent with the cut-off set for other analyses (diffusion in Chapter 5, and T2-lesion volumetric below); secondly, visual inspection of segmentations demonstrates reliable

segmentation down to this level, with occasional errors thereafter; thirdly and importantly, my healthy-control CSA data is within the range shown in other imaging and cadaveric cohorts (Frostell et al., 2016; Ko et al., 2004) across the C1 to C5 interval but falls-off slightly thereafter.

Statistics

All statistical analyses were performed in R (R Core Team, 2017).

For the analysis of rostro-caudal lesion location effects, participants were grouped by gross location of transverse myelitis (isolated cervical, isolated thoracic or cervicothoracic). For axial comparisons, participants were grouped by transverse lesion location (central, whole-diameter or peripheral). Groups were compared by ANOVA with post-hoc pairwise comparisons evaluated by Tukey's Honest Significant Difference (Tukey's HSD) test, or by Kruskal-Wallace test with post-hoc Bonferonni corrected Dunn's test for non-parametric variables; chi-square was used to evaluate gender and race comparisons. The 'lesions mid-point' was calculated, mathematically equivalent to the lesion load 'centre of mass', to provide a helpful univariate measure in selected correlations and regression analyses; it does not encapsulate the extent or distribution of the lesion/s (for example, a lesion from C3 to C7 gives a C5 mid-point; for two lesions, a C5-6 lesion and a T1-2 lesion gives a C7 mid-point). Pearson's r was calculated to evaluate the strength of correlations.

Lesion burden was evaluated with three variables: maximum vertebral segments affected by any lesion ('Max segments per lesion'), the total number of segments affected by lesions per participant ('Total lesion segments') and the lesion volume across segments C1 to C5

('C1 to C5 lesion volume'). These were statistically compared using Kruskal-Wallis across pain groups ('low' and 'meaningful'). Correlations between lesion burden measures and PSI were evaluated with Pearson's r.

Statistical tests on CSA were limited to the first 5 spinal cord segments as the ability to accurately segment lower than this level is increasingly variable (see above); CSA measures were acquired for the following: patients and controls, and groups determined by current or historical cervical and/or thoracic lesions. Groups were compared with ANOVA and post-hoc Tukey HSD and correlations were calculated with Pearson's r. Bonferroni correction was not applied when testing multiple cervical levels as the measures from cervical levels themselves are strongly interrelated (i.e., if at C1 there is a significant difference for pain, it is very likely to be at or near significant at other cervical levels, therefore Bonferroni correction is overly harsh in quashing the unsurprising nature of differences at subsequent levels). Bonferroni correction is however applied where multiple groups are compared.

Where significant correlations were found in the above analyses, predictors of pain (PSI) and / or predictors of cross-sectional area (CSA) were further assessed using multiple regression models.

Results

T2-weighted hyperintense cord lesions

Twenty-nine participants had appropriate imaging data for lesion evaluation; their clinical characteristics can be found in Table 1. Detailed attributes of the NMO Imaging Cohort, from which this 29 is a large subset, are described in detail in Chapter 2.

ROSTRO-CAUDAL LOCATION OF LESIONS PREDICT CHRONIC PAIN OUTCOMES, PARTICULARLY PERSISTENT LESIONS

For variables grouped by cord lesion location, both EDMUS and PSI showed significant differences: greater disability in the cervicothoracic lesion group compared to cervical alone and higher pain in the thoracic alone lesion group compared to cervical alone or no-lesion groups (see Table 1).

When alternatively grouped by historical rostro-caudal lesion location and persistent lesion location, PSI was distributed similarly; most strikingly with persistent lesion location where, along with current lesion location, the isolated cervical and isolated thoracic groups dissociate entirely when plotted against PSI (see Figure 1). The mean duration between pain onset myelitis MRI and current MRI was 3.77 years (s.d. 3.63).

Of note the only participant with a current low pain score associated with an isolated thoracic lesion at pain onset had a distinct cervicothoracic lesion at the time of the current MRI (participant ‘a’ on Figure 1). The participants with the two highest current pain scores had cervicothoracic lesions associated with pain onset however only thoracic portions of

these lesions persisted until the time of the current study (participants 'b' & 'c' in Figure 1; note 'c' had developed a new cervical lesion by the time of the current study).

Table 1. Patient characteristics by lesion location

	Full cohort	Cervical alone	Thoracic alone	Cervico-thoracic	No lesion
n	**29**	3	6	15	5
Female, n (% of subgroup)	**24 (82.8)**	2 (66.7)	6 (100)	12 (80)	4 (80)
Age, mean(sd)	**53 (14.8)**	56.5 (6.8)	60.3 (8.2)	51.7 (16.5)	46 (14.5)
Onset age, mean(sd)	**43.1 (16.6)**	46.9 (6)	51.8 (10.8)	40.1 (19.5)	39.4 (12.7)
DD, mean (sd)	**9.9 (5.9)**	9.6 (0.9)	8.6 (6.1)	11.6 (5.8)	6.6 (5.7)
No. of attacks, median(range)	**4 (1-28)**	5 (4-7)	5 (1-10)	7 (1-28)	3 (1-4)
No. of TM attacks, median(range)	**3 (1-26)**	5 (3-5)	4.5 (1-10)	3 (1-26)	2 (1-3)
EDMUS, median(range)*	**3 (1-8)**	1 (1-1)	5 (3-7)	5 (1-8)	2 (1-5)
PSI, mean(sd)**	**17.5 (11.5)**	2 (2.8)	28.8 (4)	17.8 (10.2)	12.2 (10.6)
Afro-Caribbean, n(%)	5 (17.2)	1 (33.3)	0 (0)	2 (13.3)	2 (40)
Asian, n(%)	6 (20.7)	1 (33.3)	0 (0)	4 (26.7)	1 (20)
Caucasian, n(%)	18 (62.1)	1 (33.3)	6 (100)	9 (60)	2 (40)

* Kruskal-Wallis $p<0.05$; Dunn post-hoc test $p<0.05$ for cervicothoracic vs cervical; ** Kruskal-Wallis $p<0.01$; Dunn post-hoc test $p<0.01$ for cervical vs thoracic and $p=0.05$ for thoracic vs no lesion. Characteristics of lesion location groups at time of imaging across un-starred rows are non-significant; TM, transverse myelitis

To compute correlations within the same data, the lesions midpoint was utilised. This correlated convincingly with PSI and was strongest for persistent lesions ($r=0.72$ $p<0.01$; Figure 2).

Figure 1. Pain (PSI) versus cord lesion location group

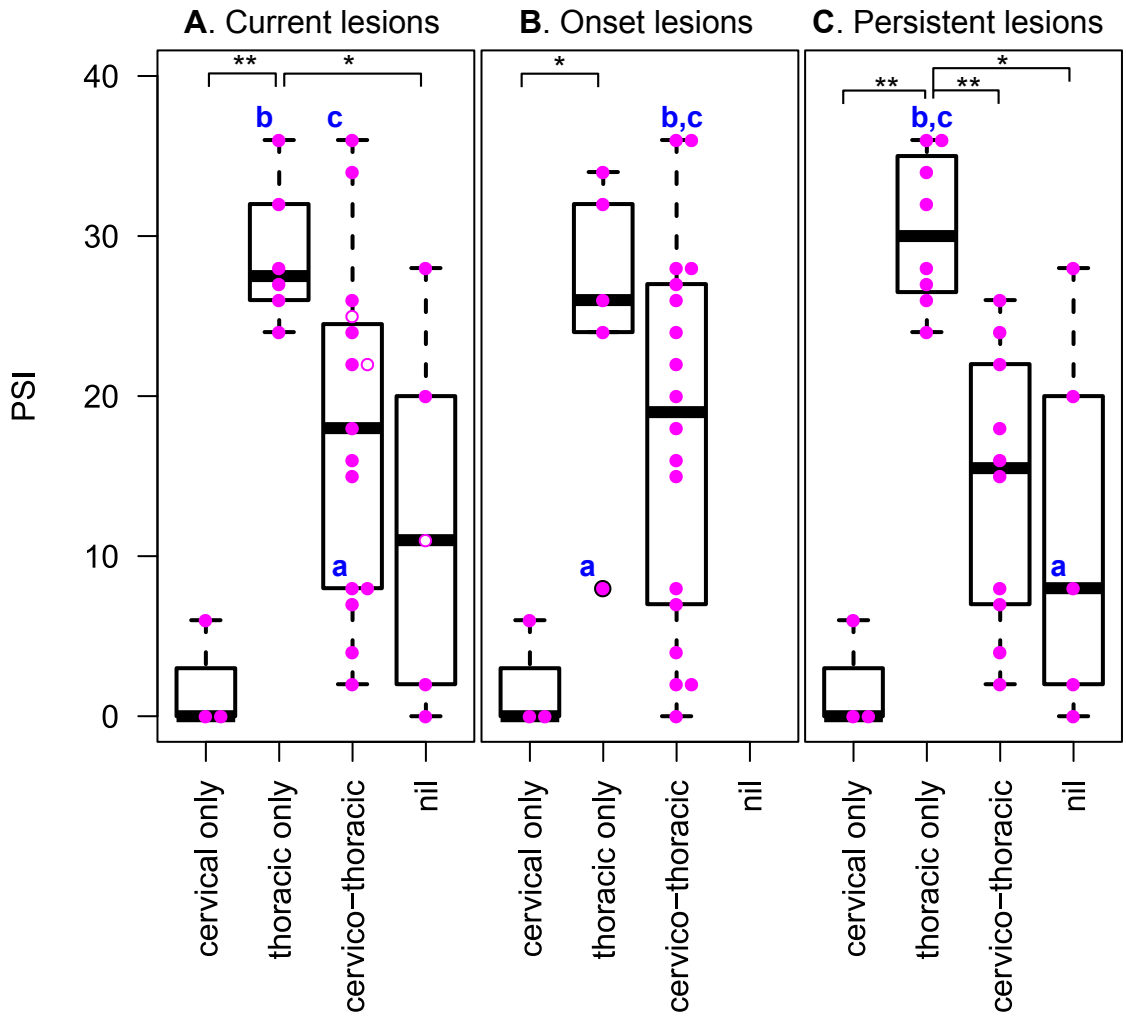

High pain scores (PSI) associated with isolated thoracic cord lesions, whereas low pain scores associated with isolated cervical cord lesions; those with cervico-thoracic cord lesions (and none) had a broad range of pain scores. Definitions: 'Current lesions' (A) – lesions present at study scan time; 'Onset lesions' (B) – lesions present at or near the time of pain onset when the pain causing myelitis was first imaged; 'Persistent lesions' (C) – lesions present in both A and B. PSI, pain severity index; **p≤0.01; *p≤0.05; a,b,c: see text for details. Boxplot elements: Box = interquartile range; thick horizontal line = median; upper whisker = maximum value (or 1.5-times inter-quartile range if less than maximum); lower whisker = minimum value (or 1.5-times inter-quartile range if greater than minimum); black open circle = outlier; o, white-filled pink circles (only in 'A. Current lesions') – no historical scans available to determine onset and persistent lesion location

Figure 2. Pain (PSI) versus lesions midpoint for (**A**) current lesions, (**B**) onset lesion, and (**C**) persistent lesions

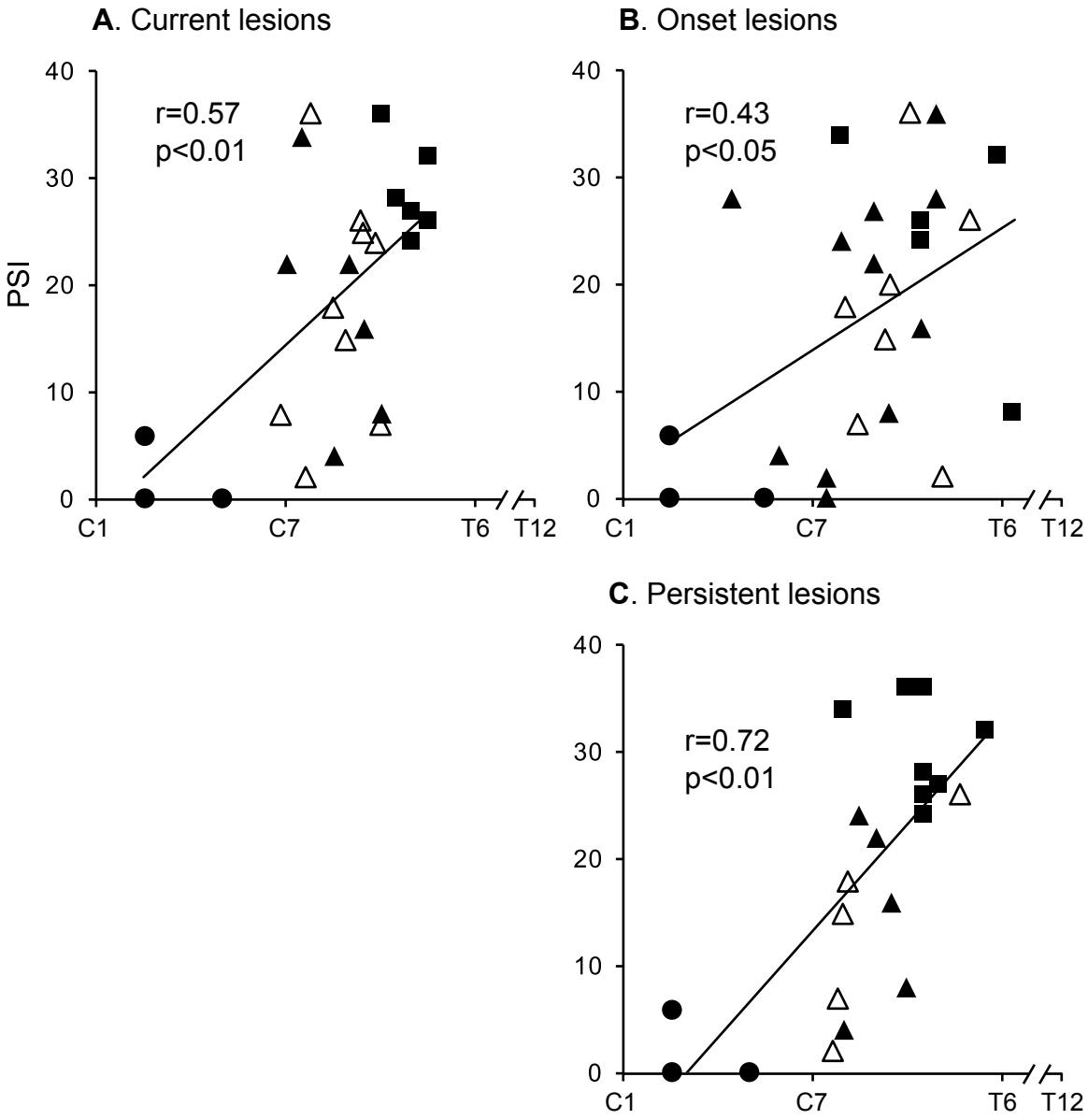

Lesions midpoint, equivalent to all lesions centre of mass, was used as a measure of lesions' cervical or thoracic tendency and was correlated, positively and significantly, with pain (PSI). Definitions: 'Current lesions' (A) – lesions present at study scan time; 'Onset lesions' (B) – lesions present at or near the time of pain onset when the pain causing myelitis was first imaged; 'Persistent lesions' (C) – lesions present in both A and B. PSI, pain severity index; C, cervical; T, thoracic; ■, continuous isolated thoracic lesion; ●, continuous isolated cervical lesion; ▲, continuous cervicothoracic lesions; △, discontinuous cervicothoracic lesion.

r, Pearson's correlation coefficient

Inspection of Figure 2 reveals an apparent clustering of the isolated cervical lesions (filled circles) and isolated thoracic lesions (filled squares) at low and high PSI, respectively, especially for current and persistent lesions (Figure 2A & C) and as expected from the grouped pain results. The cervicothoracic lesions (continuous and discontinuous; filled and empty triangles, respectively) have heterogeneous PSI scores with no clear pattern.

A multiple regression analysis with PSI as the dependent variable, and EDMUS, current age, age of onset, persistent thoracic lesions (y/n) and persistent cervical lesions (y/n) as independent variables produced a robust (adjusted r^2 0.64) and significant ($p<0.01$) model, with highly significant ($p<0.01$) opposing contributions from cervical lesions (standardised coefficient -0.46) and thoracic lesions (standardised coefficient 0.48; Table 2).

Table 2. Summary of linear regression with thoracic and cervical variables; PSI is the dependent variable

	Standardised co-efficient	St. error	p
EDMUS	0.227	0.981	0.231
Age	-0.346	0.326	0.412
Age at onset	0.537	0.274	0.188
Persistent thoracic lesion	0.482	4.029	**0.005**
Persistent cervical lesion	-0.46	3.336	**0.003**

NB, thoracic and cervical lesions are not mutually exclusive.

Significant coefficient p values in bold.

Regression model adjusted $r^2=0.64$, $p<0.01$.

Where persistent lesions midpoint was used in place of cervical and thoracic lesion variables, an equally predictive regression model resulted (adjusted r^2 0.66, $p<0.01$) with

significant factors ($p<0.05$) for lesions mid-point and current age, and a highly significant ($p<0.01$) effect from age of onset (Table 3).

Table 3. Summary of linear regression with lesions midpoint variable; PSI is the dependent variable

	Standardised co-efficient	St. error	p
EDMUS	0.334	1.059	0.118
Age	-1.31	0.412	**0.024**
Age at onset	1.475	0.315	**0.008**
Lesions mid-point	0.483	0.784	**0.012**

Significant coefficient p values in bold

Regression model adjusted $r^2=0.66$, $p<0.01$

THE EFFECT OF AXIAL LESION LOCATION IS HARD TO ASSESS DUE TO LOW NUMBERS IN NON-CENTRAL LESION GROUP

Aware that MS and NMO have differing transverse lesion locations, the effect of transverse lesion location on pain was analysed. There were 16 current (cervical) axial scans (two excluded due to movement artefact) and 22 historical (cervical and thoracic) axial scans (7 without historical axial imaging) suitable for this analysis. However, of the available axial images through lesions only a single patient in both current and historical scans had a non-central lesion (dorsally located). Thus, although there were too few to statistically assess the average pain score disparities, they were not markedly different (Table 4).

Table 4. Pain-onset-attack axial lesion location[a]

	N (lesion locations)	PSI, mean (sd)
Whole diameter	**7** (all CT)	15.7 (11.3)
Central	**14** (2C, 2T, 10 CT)	18.1 (12.3)
Peripheral	**1** (C)	0 (0)

[a] Seven patients excluded, three without any historical imaging available and four without T2 weighted axials available.

C, isolated cervical lesion/s; T, isolated thoracic lesion/s; CT, cervicothoracic lesion/s.

LESION BURDEN DOES NOT INFLUENCE PAIN

Lesion burden was not significantly different across pain groups (Table 5).

Table 5. Lesion burden measures by pain severity subgroups

		Full cohort	Low pain	Meaningful pain
	n	**29**	11	18
Max segments per lesion, mean(sd)[ns]		**4.9 (3.5)**	4.1 (3.7)	5.3 (3.3)
Total lesion segments, mean(sd) [ns]		**6.2 (4.5)**	5.1 (4.5)	6.8 (4.4)
C1 to C5 lesion volume, mm^3, mean(sd) [ns]		**143.1 (182.5)**	168.9 (159.9)	127.4 (193.3)

ns, non-significant difference across pain groups

There was no correlation between any of the lesion burden measures and PSI.

<u>Cervical cross-sectional area is strongly influenced by cervical lesions, current and historical, but does not correlate with pain outcomes</u>

Thirty-two participants had suitable imaging for calculating cross-sectional cervical cord areas (CSA) (further details of the NMO Imaging Cohort can be found in Chapter 3). Over the first 5 cervical segments, CSA averaged 60.4 mm^2 (sd 9.5) and ranged between 38.1 and 78.4 mm^2 for patients, and averaged 71.3 mm^2 (sd 6.6) with a range of 57.6 to 82.0 mm^2 in controls (see Figure 3 for actual size illustration).

Figure 3. Actual-size mean cross-sectional area (CSA) for levels C1 to C5

Actual-size representations of the cross-sectional area of both diseased NMO cords and control cords. Black line outlines = circumference of mean CSA; Grey doughnut, inner edge = circumference of minimum CSA, outer edge = circumference of maximum CSA; NB idealised circular cord area used.

Patients had significantly lower ($p<0.01$) CSA compared to controls. Current and historical cervical lesions have a dramatic and significant negative effect on mean CSA across multiple levels (see Figure 4).

Those never to have suffered a cervical lesion had mean CSA's comparable to controls (Figure 4, B1) and those with current exclusively thoracic lesions were comparable to those without any current lesions (Figure 4, B2); these together suggest that thoracic lesions play little part in determining the CSA of the cervical cord and were thus not included in further CSA analyses.

There was no statistically significant difference between low and meaningful pain and the mean CSA for all participants (Figure 4, C1), however, when only participants without current cervical lesions were analysed, a statistical difference emerged for the first cervical level (Figure 4, C2; note, comparison not performed for thoracic lesions for reasons stated in preceding paragraph).

To further investigate this and other relationships, I examined correlations of PSI, alongside other variables, with mean CSA (C1 to C5) (Figure 5).

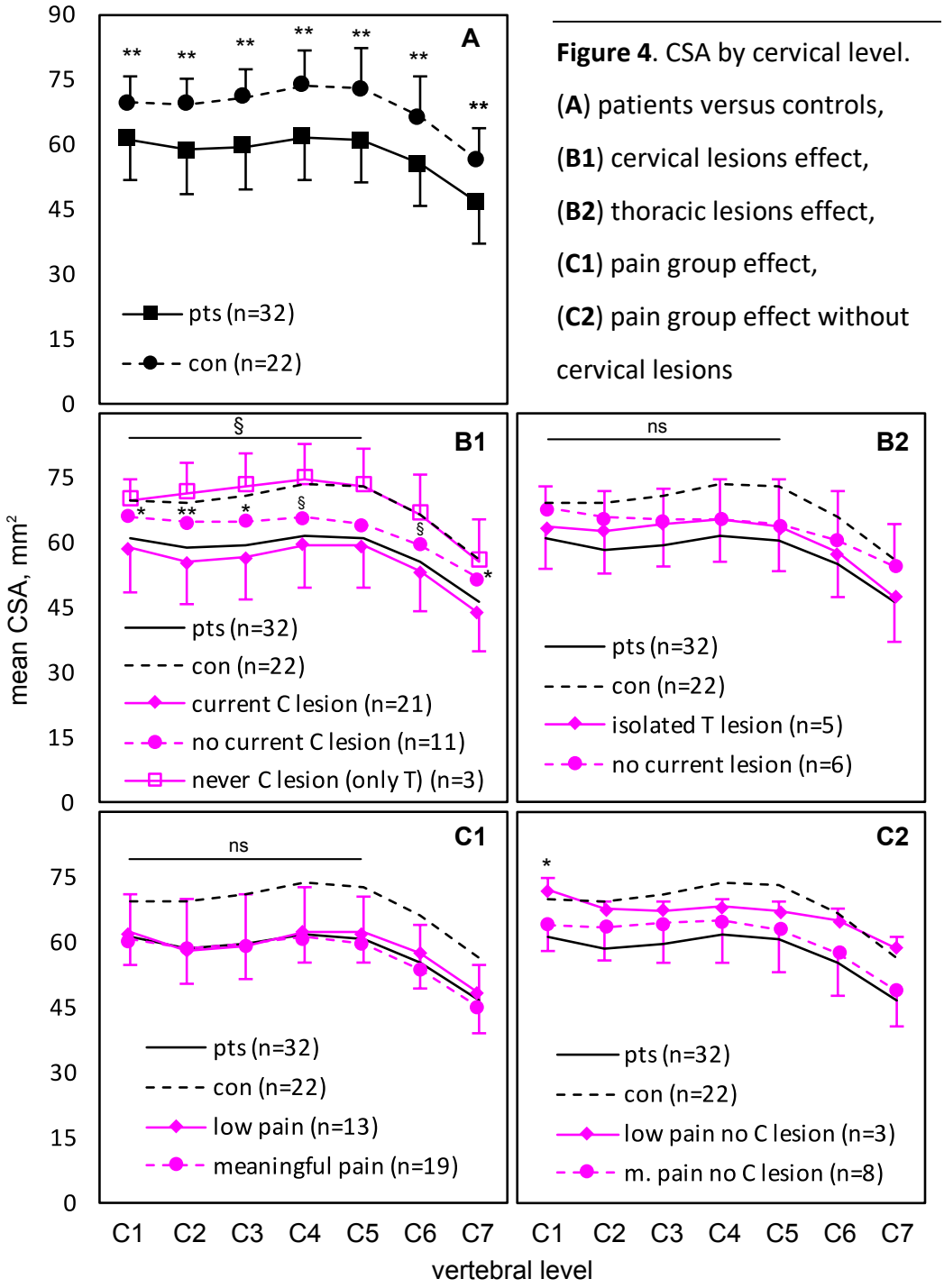

Figure 4. CSA by cervical level. (**A**) patients versus controls, (**B1**) cervical lesions effect, (**B2**) thoracic lesions effect, (**C1**) pain group effect, (**C2**) pain group effect without cervical lesions

Mean cross-sectional areas, grossly different for patient and controls (A), were largely influenced by the presence of current and historical cervical lesions (B1), and less so (if at all) by thoracic lesions (B2). No difference between pain groups was shown for mean CSA (C1) except for the first cervical level of subjects without cervical lesions (C2). A: **, $p<0.01$; B1: §, borderline significant ($p<0.1$) C1-5 average for 'never had cervical lesion' vs. 'current cervical lesion'; §, borderline significant (individual levels) for 'no current cervical lesion' vs 'current cervical lesion'; Bonferroni corrected. C2: *, $p<0.05$; m. pain, meaningful pain; CSA, cross-sectional area; pts, patients; con, controls; m. pain, meaningful pain.

Figure 5. Mean CSA (C1 to C5) versus: (**A**) PSI, (**B**) PSI (only lesion free cervical cords), (**C**) disease duration, (**D**) Age, (**E**) EDMUS, (**F**) onset age.

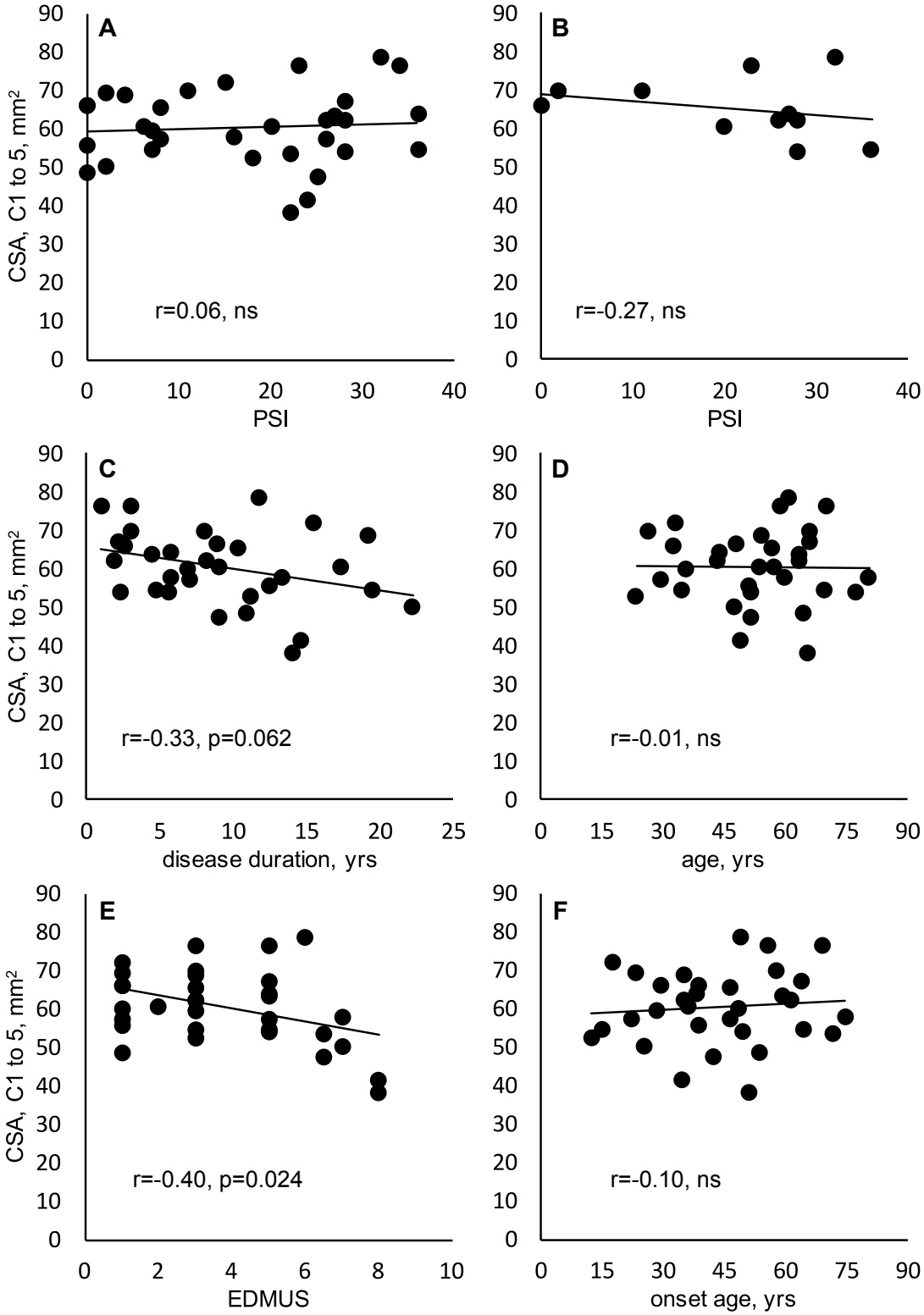

Cross-sectional cervical cord area correlated with disability (EDMUS), but not with measures of pain, disease duration, or age. CSA, cross-sectional area; PSI, pain severity index; ns, non-significant; r, Pearson's correlation coefficient.

Figure 5B shows the correlation equivalent of the relationship seen between pain group and lesion-free CSA (Figure 4, C2), and visually conveys the expected relationship, i.e. that CSA reduces as pain increases, but without reaching significance. Indeed, the only significant correlation found for the variables tested was for disability (EDMUS) where CSA reduced with increasing disability, as one would expect from existing research (Figure 5E). It can be seen from the figure that the relationship with EDMUS is not linear; a polynomial function produces a much tighter fit but would be less interpretable (see Chapter 3 for discussion of EDMUS).

To tease out the possible PSI-CSA relationship further, two regression models were built, the first with all available data and the second using only those with lesion-free cervical cords (Table 5, A and B).

Table 5. Regression CSA (C1 to 5)

A. all participants

	Standardised co-efficient	St. error	p
EDMUS	-0.592	0.892	**0.008**
Disease duration	-0.173	0.305	0.341
PSI	0.351	0.18	0.122

Regression model adjusted r^2=0.241, $p<0.05$

(Table continued overleaf)

B. lesion-free cervical cords

	Standardised co-efficient	St. error	p
EDMUS	-0.671	1.02	**0.021**
Disease duration	-0.161	0.414	0.516
PSI	0.432	0.251	0.167

Regression model adjusted r^2=0.279, $p<0.05$

Significant coefficient p values in bold

PSI, pain severity index

The regression models further reinforce CSA's lack of power in predicting chronic pain, and again reveal a significant relationship with disability.

Discussion

In this chapter, a significant relationship between the rostro-caudal location of myelitis lesions and the severity of neuropathic pain is described: the presence of thoracic lesions predicts greater myelitis-associated chronic pain than the presence of cervical lesions. This relationship is strongest with persistent lesions and suggests that MRI evidence of chronic thoracic lesions represents lingering cord pathology responsible for heightening pain, with a converse and perhaps protective effect seen with some cervical lesions.

The results also suggest that cervical cord atrophy, when measured in lesion free cervical cords, is greater in the upper cervical cord of patients with meaningful pain. However, this can most likely be discounted as PSI didn't correlate with cross-sectional area (CSA), and regression models with PSI alongside other variables revealed disability as more relevant (although given disability and pain's collinearity, this may represent EDMUS's usurpation of PSI). This fits neatly with the existing literature that shows cervical cord CSA decreases with

increased disability in MS and NMO (Losseff et al., 1996; Wang et al., 2014; Yiannakas et al., 2015).

Disability also appeared greater in those with thoracic cord lesions, however linear regression models did not preserve disability as a significant predictor of pain, but instead reported that grouped cord location, and lesion mid-point and age (current and at onset) were more important (again, caution is advised in the interpretation of EDMUS and PSI's relationship given their moderate collinearity).

I propose that one reason NMO transverse myelitis sufferers experience more pain than MS patients might relate to the differing proportions of cervical and thoracic cord involvement in the two conditions (Hua et al., 2015). In support of this hypothesis, Okuda et al. have reported that pain in MS associates with upper/mid-thoracic damage and propose an autonomic aetiology (Okuda et al., 2014). A large number of autonomic areas receive information about the body's sensory state, including pain, directly from ascending lamina I neurons of the spinal dorsal horn. These autonomic sites include the main homeostatic integration sites of the brainstem, that is the ventrolateral medulla, catecholaminergic cell groups (including the locus coeruleus, A5 and A7), the parabrachial nucleus and the PAG (Craig, 1995). Importantly, lamina I receives direct descending modulatory input from a number of these, not least the locus coeruleus whose descending noradrenergic inputs complete a feedback loop and can inhibit pain processing at the level of the dorsal horn of the spinal cord (see Chapter 1c) (Danzebrink and Gebhart, 1990). There is a respected caucus of work that posits this afferent autonomic information as the source of the body's representational state of wellbeing, motivating behaviour to maximise comfort or to

minimise pain (Craig, 2002). Ascending lamina I afferents project directly to the sympathetic cell columns, autonomic nuclei found exclusively in the thoracolumbar cord, and there is evidence to suggest that some of these connections are bidirectional (Okuda et al., 2014). Damage to these autonomic thoracolumbar nuclei or their projections may have a dysregulating effect on pain information processing in the cord and a knock-on effect on one's qualitative experience of pain (Okuda's findings are summarised in Figure 6).

My study had limitations. The absence of sequential pain scores during the period intervening pain onset and current MRI makes it harder to confirm the effects of additional myelitis attacks. I instead focused on the myelitis attack to which the patient attributed the start of their current pain, in effect making the assumption that only one attack causes chronic pain. Indeed, perhaps surprisingly, patients rarely do recall more than one myelitis attack having a long-lasting effect on their chronic pain (personal observation); pain intensity may temporarily increase at the time of subsequent relapses, but as discussed in Chapter 1a, there is no evidence to suggest it remains at a level greater than baseline thereafter, but studies in this area are notably lacking (Zhao et al., 2014). In any case, this should not produce a bias towards one cord region unless lesion location was related to first or subsequent attack and this was not the case.

Thoracic cross-sectional areas, lesion volumes and axial lesion locations were not assessed and it is likely that a thoracic lesion or atrophy effect on pain has been missed. The limited cervical axial imaging and historical whole-cord axial imaging available did not show an effect but possibly due to poor data resolution. These both warrant further detailed study.

CSA was not normalised for spinal cord length, intra-cranial volume, height or weight, as is common in studies of CSA, however these standardisation techniques have not been shown

to improve reliability of CSA related outcomes (Healy et al., 2012).

Figure 6. Autonomic mechanism of spinal cord sensitisation proposed by Okuda et al.

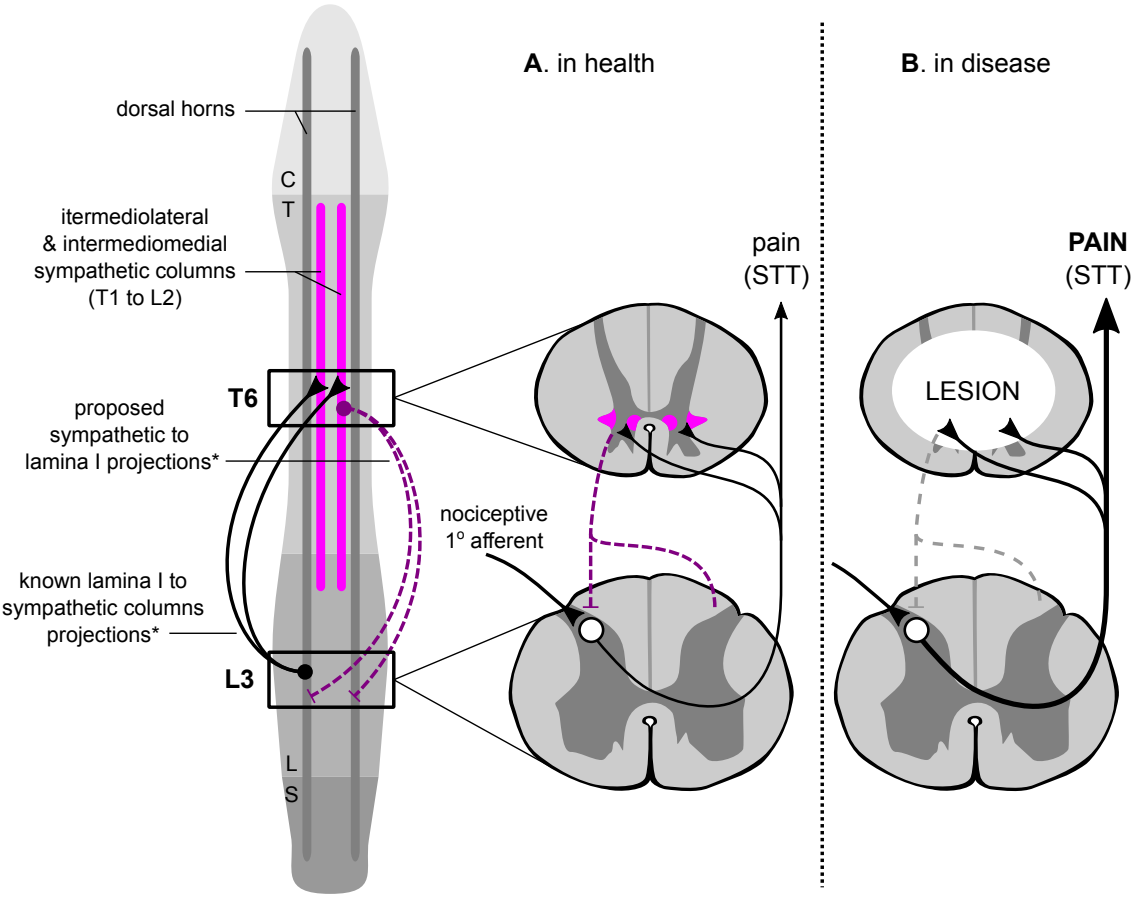

'LESION' in column B represents a central NMO inflammatory lesion causing intermediomedial and intermediolateral nuclei cell body loss (e.g. via necrosis) or efferent axonal loss (e.g. via demyelination) with the subsequent loss of innervation of remote areas of the dorsal horn (by these nuclei), hypothesised by Okuda et al. to alter pain processing at these remote sites, perhaps by influencing descending modulatory tone. * The known projections from lamina I originate at multiple spinal levels (including cervical levels) and terminate bilaterally at multiple levels of the sympathetic cell columns; likewise, the sympathetic column to lamina I projections proposed by Okuda et al. originate from multiple levels of the sympathetic cell column however retrograde tracers were only injected in the lumbar cord and thus terminations in the dorsal horn at other spinal levels are possible but currently have no literature basis (one level of origin and termination are shown here for clarity). C, cervical; T, thoracic; L, lumbar; S, sacral; STT, spinothalamic tract. T6 and L3 are exemplar segments, the same circuitry exists for multiple spinal levels (see text).

Conclusion

The rostro-caudal location of lesions may be an important determinant of post-myelitis chronic pain severity, seen most vividly in the relationship between severe pain and isolated thoracic lesions. The possibility of cervical involvement playing a role in modifying pain is of interest and needs validating in further cohorts. The potential role of the autonomic nervous system in post-myelitis pain is intriguing and could provide alternative therapeutic targets in future pain studies.

Relevant personal publications

Tackley G, Vecchio D, Hamid S, et al. Chronic neuropathic pain severity is determined by lesion level in aquaporin 4-antibody-positive myelitis J Neurol Neurosurg Psychiatry 2017;88:165-169: *some text excerpts and figures are reused in an adapted form in the body of this chapter*.

Chapter 5

Experimental chapter: Spinal cord diffusion imaging and tract-specific measures in NMO pain

Introduction

Diffusion imaging has been used extensively in the neuroinflammatory field because it provides a measure of tissue integrity and damage that is not conveyed by conventional sequences (i.e. T1 and T2-weighted) (Griffin et al., 2002). In this way, 'normal appearing' white or grey matter can be shown to be damaged, which within the brain is a diffusion imaging hallmark of multiple sclerosis (MS; this is more controversial in NMO where brain diffusion differences are probably less diffuse and more likely related to local or remote tract pathology; Kremer et al., 2015). The technique can and has been used in the spinal cord (see Chapter 2) and importantly in NMO shows differences in areas with and without lesions (Pessôa et al., 2012; Qian et al., 2011) and has shown tract-specific differences related to functional measures (Naismith et al., 2013).

From the literature, it is unclear whether diffusion differences in normal appearing tissue are related to remote lesions or whether these differences are tract specific; this is investigated below. Furthermore, how these measures relate to pain is virtually unexplored and lies untouched in the neuroinflammatory field; herein, these various diffusion measures are analysed alongside pain severity.

Objectives / Aims

1. To determine if diffusion measures are different across pain severity groups within spinal levels and tracts (with particular focus on the spinothalamic tract).

2. To determine the effect of lesions (cervical or thoracic; past or present) on diffusion measures across spinal levels and tracts.

3. To explore the interaction of (1) and (2).

Methods

Twenty-nine patients and 23 healthy controls from the Imaging Cohort had useable diffusion imaging data. Their characteristics are tabulated in Table 1.

Image pre-processing

Diffusion data was processed in FMRIB's software library v5.0 (FSL; Jenkinson et al., 2012) with the following steps: B0 images (with opposite phase-encode directions) were used to generate a fieldmap applied to all diffusion data for correction of susceptibility-induced distortion (FSL's *topup*). FSL's *dtifit* was then used to fit tensors to the data (NB FSL's *eddy* not used due to complications of 'brain' extracting cord data).

Table 1. Participant baseline characteristics

	Patients	**Controls**
n	29	23
Female, n(%)	23 (79.3)	15 (65.2)
Age, mean(sd)	53.8 (14.4)	53.9 (16.5)
Onset age, mean(sd)	44.7 (16.6)	
DD, mean(sd)	9.1 (5.1)	
No. of attacks, med(range)	4 (1-28)	
No. of TM attacks, med(range)	3 (1-28)	
EDMUS, med(range)	3 (1-28)	
PSI, mean(sd)	17.6 (11.4)	
Afro-Caribbean, n(%)	4 (13.8)	
Asian, n(%)	8 (27.6)	
Caucasian, n(%)	17 (58.6)	

sd, standard deviation; med, median

Registration and data extraction

A number of techniques were trialled. Firstly, FSL's *FLIRT* was used to register T1 to diffusion space (manually fine-tuned using FSL's *Nudge*) which produced excellent rostral-cord/brainstem co-registration but because of the nature of whole volume registration (versus slice-wise or 'slice-by-slice') it produced alignment errors caudally in the cord (see axial images in Figure 1). Secondly, SCT was used to register T1 to diffusion space utilising T1 and diffusion space segmentations which worked well with the exception of a handful of participants with large rostro-caudal malalignments (see sagittal images in Figure 1).

The chosen method segmented the cord directly in diffusion space with reverse registration of templates as this proved the most accurate and is least prone to user imbued bias. Registration of template (PAM50; see below) to diffusion space (distortion-corrected B0 image) follows the same protocol as for T1 imaging outlined in Chapter 4 (i.e. level identification, segmentation, straightening and registration). Fractional anisotropy and

mean diffusivity were then averaged across spinal cord levels using SCT level masks registered in diffusion space. A summary of the registration process relevant to extraction of diffusion measures from cord segments is shown in Figure 2.

Tract-specific masks were used for the spinothalamic tract (the principle tract of interest), corticospinal tract (CST), fasciculus gracilis (FG) and fasciculus cuneatus (the dorsal columns). An example of these tract masks in diffusion space is shown in Figure 3.

T2-lesions were excluded for a number of analyses below. Level specific exclusion refers to exclusion of an isolated level of a participant's data containing a lesion, but inclusion of the remaining non-lesioned segments of the same participant. Conversely, where participants are grouped by lesion (e.g. current cervical lesions present y/n), all of a participants' data were either included or excluded dependent on lesion group membership. It should be noted that many patients had T2-hyperintense thoracic lesions but no thoracic cords were assessed with diffusion imaging. Note, lesioned areas are included in analyses except where specified.

EDMUS was divided into two groups, EDMUS <4 and EDMUS ≥4. A score of EDMUS (or EDSS) 4 or above equates to impaired walking distance; scores below 4 equate to unlimited walking distance. It is thus a reasonable choice for a mild / moderate disability differentiation and it is commonly used cut-off for EDSS in MS where it heralds the progressive phase of the disease (Confavreux et al., 2000).

Figure 1. Registration errors and their solutions.

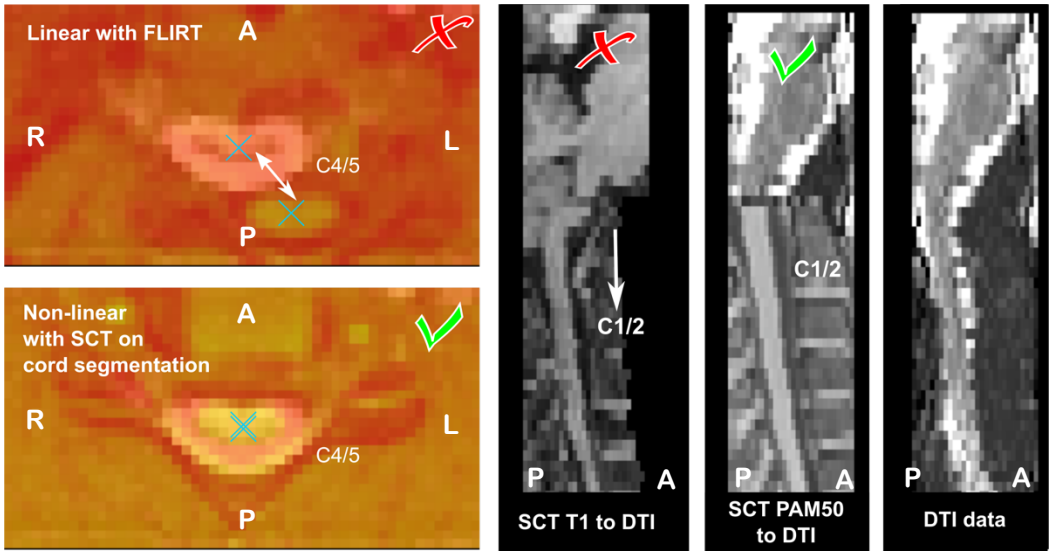

Various registration errors were encountered with different spinal cord processing techniques. Direct registration of diffusion space to PAM50 templates using the spinal cord toolbox was the eventual technique used. Blue Xs mark centre of the spinal cord; R, right; L, left, A, anterior; P, posterior. SCT, spinal cord toolbox; FLIRT, FMRIB's linear image registration tool.

Figure 2. Methods overview.

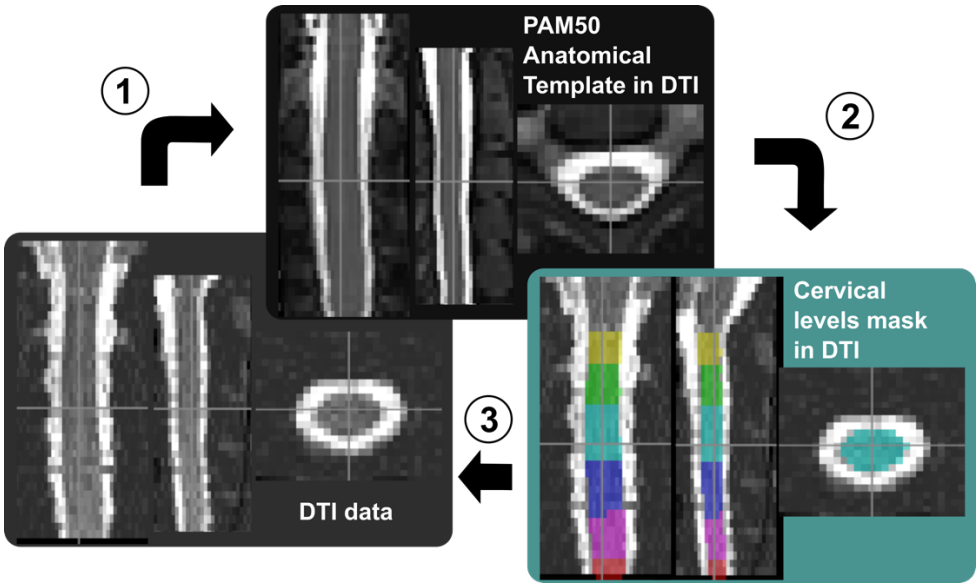

1. Register PAM50 spinal cord template to diffusion data using diffusion space segmentation
2. Load PAM50 template cervical segment level masks into diffusion space
3. Extract FA and MD metrics in diffusion space using segment mask, level by level

Figure 3. Axial sections of tract masks in diffusion space, cervical level C3 and C6 examples

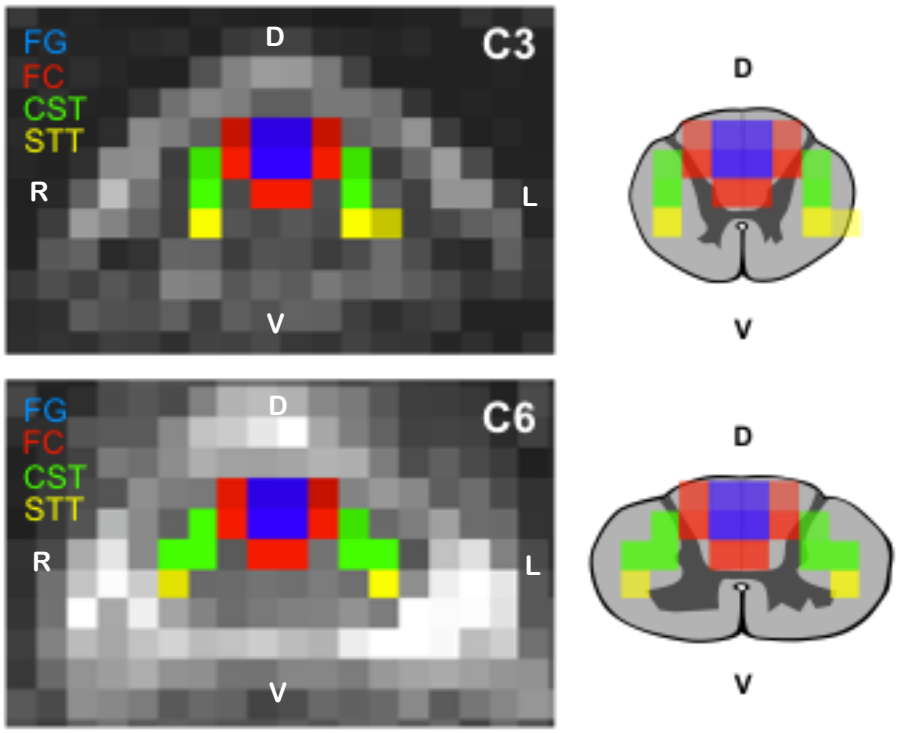

Example tract masks at levels C3 and C6 for a single subject on the left, with pictographic representations of the spinal cord anatomy to the right. Each coloured square represents a single voxel. FG, fasciculus gracilis (blue); FC, fasciculus cuneatus (red); CST, corticospinal tract (green); STT, spinothalamic tract (yellow); D, dorsal; V, ventral; R, right; L, left. C3, cervical level 3; C6, cervical level 6.

Statistics

For comparison of groups, the first five cervical spinal segments were used as these contained diffusion information from the majority of participants, whereas C6 and especially C7 consistently had unusable data due to either absence (field of view, FOV, not covering lower cervical cord because of anatomical differences), poor data quality at lower reaches (increased tissue interference in certain participants) or poor registration (significant distortions or unusual anatomy). Dedicated diffusion studies of the cord might overcome these problems in the future with longer scan times (and thus more repeats) to

improve the signal-to-noise ratio, a dedicated cervical field-of-view (mine incorporated the brainstem and this sometimes restricted lower cervical cord coverage) and with improved automated spinal cord registration tools (Cohen-Adad, 2017). All mean comparisons are performed using two-way student's T-tests, unless otherwise stated.

Numbers per group are shown in Table 2. This is not an exhaustive list and where appropriate, further sample size numbers are reported in the text.

Table 2. Sample numbers for whole cord and tract-specific analyses

A. patients and controls

	C1	C2	C3	C4	C5	C6	C7
All measures							
Patients, n	29	29	29	29	29	27	13
Controls, n	23	23	23	23	23	21	9
Excluding lesions							
Patients, n	14	14	14	13	12	17	9
Controls, n	23	23	23	23	23	21	9

B. meaningful and low pain groups

	C1	C2	C3	C4	C5	C6	C7
All measures							
Low Pain, n	18	18	18	18	18	17	8
Meaningful pain, n	11	11	11	11	11	10	5
Excluding lesions							
Low pain, n	9	9	10	9	9	11	5
Meaningful pain, n	5	5	4	4	3	6	4

Results

FA significantly lower in patients and those with meaningful pain

Mean fractional anisotropy (FA) was significantly different between patients and controls across multiple cervical levels (Figure 4A), even when taking account of current cervical lesions suggesting that there is diffusion-measure related damage that is detectable even in the absence of visible T2-hyperintense lesions (Figure 4B).

A similar but only borderline significant effect was seen for meaningful versus low pain (Figure 5A): the meaningful pain group has lower FA. The significance of the effect improved marginally when lesioned segments were excluded (Figure 5B).

Figure 4. (**A**) FA, patients and controls, (**B**) FA, patients and controls excluding lesioned segments

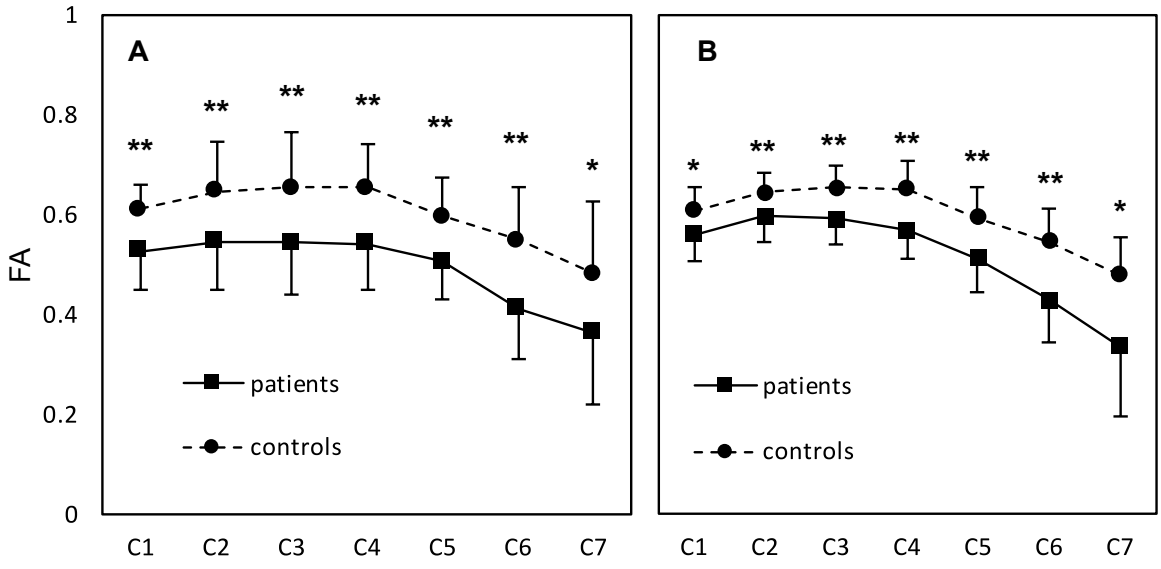

Cervical cord fractional anisotropy was lower in patients compared to controls (A), even with visible cervical lesions excluded from the analysis (B). **, p<0.01; *, p=0.05; Error bars = standard deviation, this is symmetrical about the data point however only half is shown for visual clarity (the same is true of subsequent figures except where specified)

Figure 5. (**A**) FA, low and meaningful pain, (**B**) FA, low and meaningful pain excluding lesioned segments **C**. FA vs pain score (PSI) correlation plot

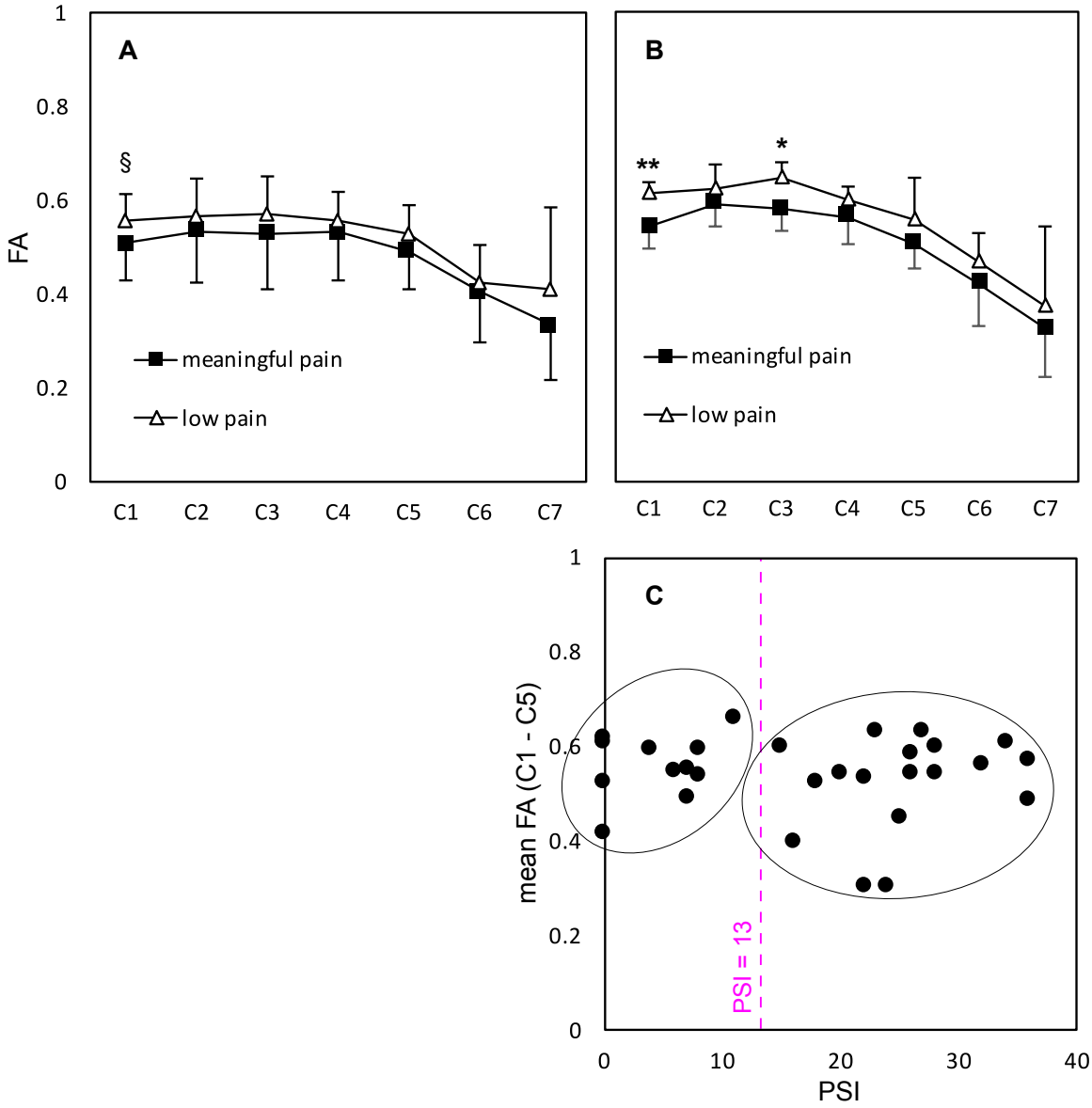

Cervical cord fractional anisotropy was lower in the high pain patient subgroup compared to the low pain subgroup (A), the difference was more apparent where analysis focussed on areas without lesions (B). Although no linear relationship exists between mean cervical FA and pain (Pearson's r=-0.06), there appear to be two clusters with different mean FA values separable by the low and meaningful pain cut-off (PSI=13) (see C; ellipses added for group visualisation purposes only); §, $p<0.1$; *, $p<0.05$; **, $p<0.01$.

To further explore the relationship between PSI and mean cervical (C1 to 5) FA, the data were plotted and Pearson's r calculated (see Figure 5C). There was no correlation (r=-0.06), however two distinct clusters were discernible to the right and left of the low / meaningful PSI limit (PSI=13), with overlapping but obviously different mean FA (this relationship is explored further below).

Analysing *only* segments containing lesions produced visually striking differences for comparisons of patients versus controls and meaningful versus low pain groups. The direction of difference was the same as for all participants in earlier analyses, however because of greater variance (as one might expect sampling lesioned areas) there was consequently less (or no) significant difference (Figure 6).

Figure 6. (**A**) FA, patients and controls including *only* lesioned segments (**B**) FA, low and meaningful pain including *only* lesioned segments

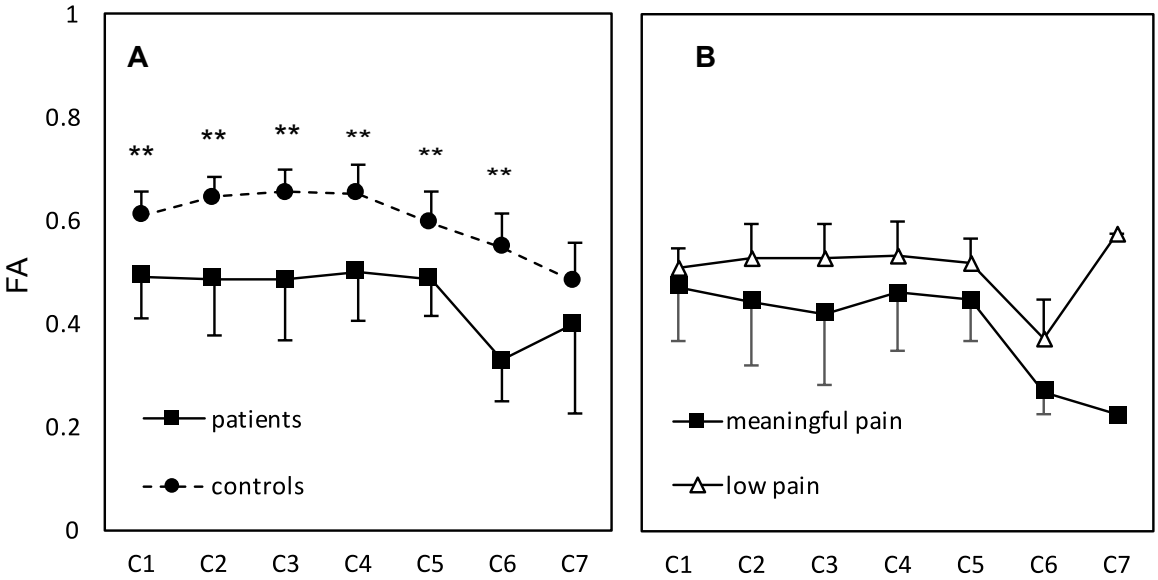

Comparing only segments with lesions for patients and controls, and pain sub-groups, produced visually stark differences but less significant effects, probably due to increased variance in areas of lesions; **, p<0.01.

When FA was subdivided by the gross location of lesions present anywhere in the cord (i.e. cervical only, thoracic only, cervicothoracic or none), a consistent and not wholly unexpected pattern emerged (Figure 7A). Participants with no lesions had FA similar to controls, participants with only current thoracic lesions had reduced FA compared to controls but not as low as those with only current cervical lesions; however, those with both cervical and thoracic lesions had the lowest FA. One can imagine damage to the cervical cord creating greater disruption to cervical diffusion measures than remote damage in the thoracic cord, but that the combination of both would be most disruptive of all. Interestingly, if these lesion location classifiers are added to the PSI vs mean FA correlation plot drawn above (in Figure 5C), an explanation for the distribution of FA by PSI also becomes apparent (Figure 7B): low mean FA is visibly characteristic of the cervicothoracic (CT) lesion group especially in participants above the low pain threshold (PSI>12) and these CT participants with meaningful pain and low FA bring down the average for the meaningful pain group.

This pattern of pain severity related to T2-lesion location mirrors what was found in the analyses of Chapter 4. What is new and interesting is that the data show that thoracic lesions (alone or as part of cervicothoracic lesions) have an effect on cervical FA. Indeed, current isolated thoracic lesions had lower mean cervical FA compared to controls ($p<0.05$) and compared to participants without current lesions (C6 & 7, $p<0.05$; C5, $p=0.08$; Figure 7A) which could be an effect of old cervical lesions, however, current cervicothoracic lesions appeared to have lower FA than cervical lesions alone (though not significant) and, importantly, participants who've never had cervical lesions had lower FA than controls (i.e. those patients who have only ever had thoracic lesions show cervical FA damage compared

to controls; borderline significant at p=0.06; data not shown). That is, we are not just seeing the presence of isolated thoracic lesions increasing the likelihood of previous cervical lesions causing currently reduced FA, instead it appears we are seeing remote damage from thoracic lesions reflected in cervical cord diffusion measurement (this is discussed later with regard to tract-specific damage and pain).

Figure 7. (**A**) Cervical and thoracic lesions effect on FA; (**B**) FA vs. PSI coded by lesion location group

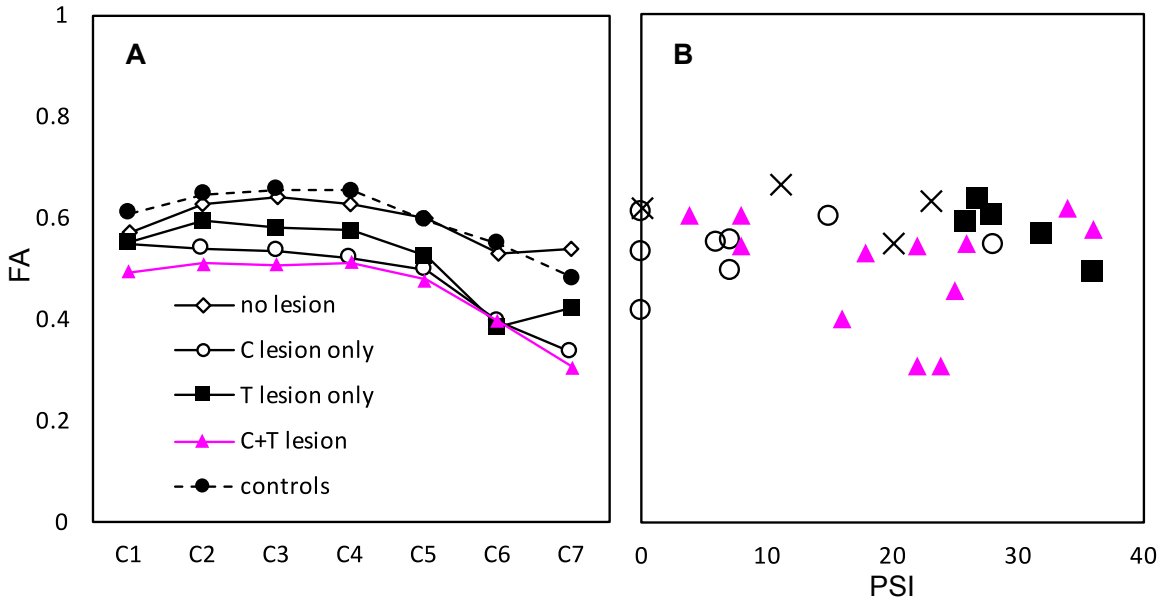

Cervicothoracic lesions (A, pink triangles) were associated with the lowest mean cervical FA values, and a subgroup of the cervicothoracic group pulled down the average cervical FA in those with meaningful (PSI>12) pain (B, pink triangles). C, cervical; T, thoracic. All lesion groups C1 to C5 averages were significantly different to controls ($p<0.05$). The 'no lesion' group C1 to C5 combined average was significantly different from the cervicothoracic and cervical lesion only group ($p<0.05$). Standard deviation error bars not shown for clarity. B: X, no current lesion; open circles, only cervical lesions; pink triangles, cervicothoracic lesions; black squares, only thoracic lesions.

High EDMUS also associated with lower FA

High levels of disability (EDMUS) were associated with lower mean FA (C1 to 5, lesions not excluded, $p<0.05$; Figure 8A). Unlike PSI, when plotted against mean FA, EDMUS showed a significant correlation ($r=0.54$, $p<0.01$; Figure 8B) which would be stronger if fitted with a polynomial regression line (EDMUS, like EDSS, is known to be non-linear, especially at higher scores; see Meyer-Moock et al., 2014).

Figure 8. (**A**) FA, low and high EDMUS, (**B**) C1 to C5 mean FA vs EDMUS correlation plot.

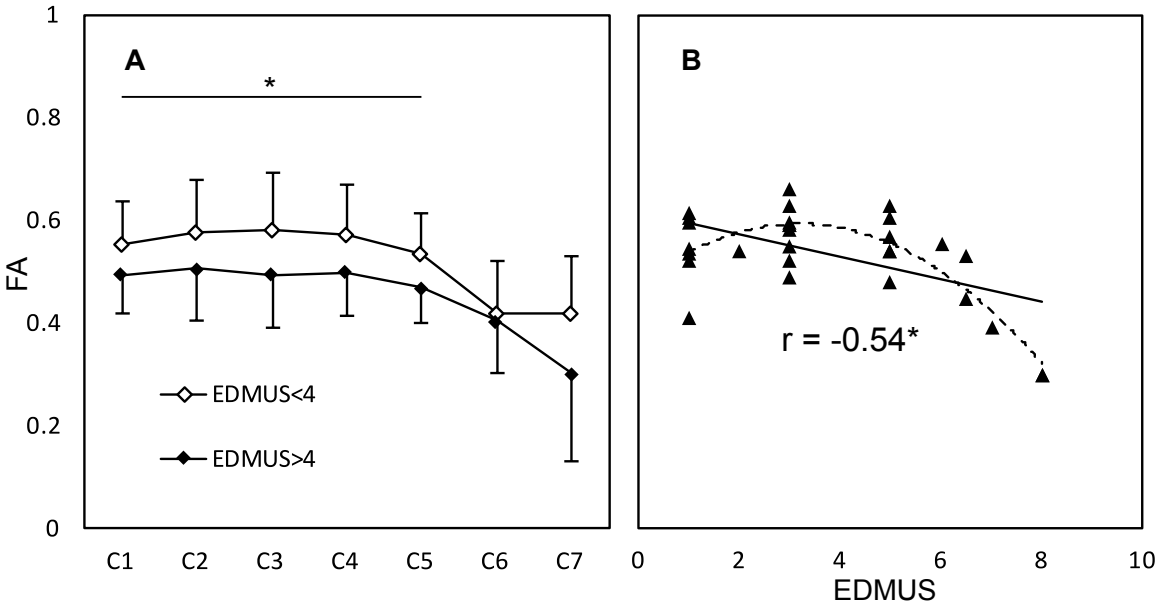

Higher disability (EDMUS) scores were associated with lower FA (A); disability and FA negatively correlated (B). *, $p<0.05$ for C1 to C5 combined average; *, $p<0.01$ for Pearson's r

---, example polynomial line of best fit

FA in grey and white matter

Differences between patients and controls remained significant ($p<0.01$) when the cord was sub-divided (by mask) into grey and white matter (Figure 9A & C). Meaningful pain versus low pain showed a pattern of lower FA for white matter analyses (at C1, $p=0.13$) that was

less striking for grey matter (Figures 9B & D); although the pattern of difference was similar, the degree of difference was appreciably different.

Figure 9. (**A**) FA, white matter (WM), patients and controls, (**B**) FA, WM, meaningful vs. low pain, (**C**) FA, grey matter (GM), patients and controls, (**D**) FA, GM, meaningful vs. low pain.

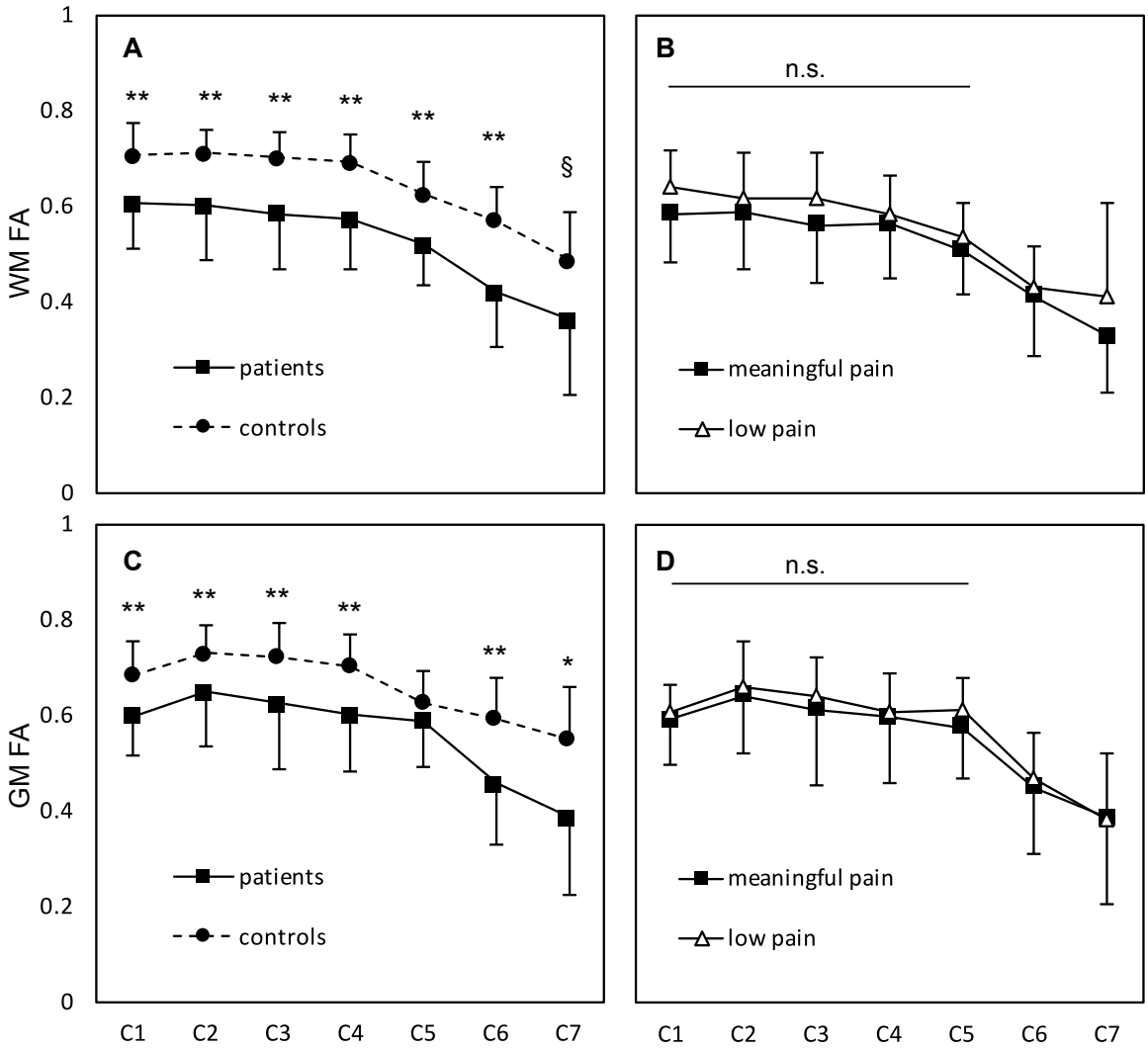

FA differences between patients and controls remained for both white-matter and grey-matter only analyses (A+C) but did not reach significance for pain subgroups (B+D). *, p<0.05; **, p<0.01; n.s., not significant for group average or individual levels.

Dorsal columns and spinothalamic tracts show pain related differences in FA

White matter was further subdivided by tract: spinothalamic (STT), corticospinal (CST) and the fasciculi cuneatus and gracilis (FC/FG, or dorsal columns). The same comparisons of patients versus controls and meaningful versus low pain were made and are summarised in Figure 10. Patients had significantly lower FA than controls across all tracts (Figure 10A, C, E, G) whilst meaningful pain participants showed significantly lower FA compared to low pain participants in the levels C1 and C7 of the FG, FC and CST. No significant differences were found for the STT for 'all participant' analyses when including and excluding intersecting lesions.

Having found that thoracic lesions can produce meaningful differences in cervical FA measures (see Figure 7A and surrounding narrative), and with the *a priori* knowledge that thoracic lesions are important for pain (see Figure 7B and Chapter 4), two techniques were used to determine the unique effect of thoracic lesions on cervical FA in relation to pain.

Firstly, as all participants with current isolated thoracic lesions have 'high' pain (PSI>23), no cord location subgrouping was possible. Therefore, instead of using the current isolated thoracic group, the 'never cervical lesion' group was analysed; these are patients who have never (from review of clinical notes) had a cervical lesion which in the Imaging Cohort means they've only ever suffered thoracic lesions. Of this small group of 3 patients, 2 had no visible current lesion and 1 had an isolated thoracic lesion. Their pain scores were dichotomised into moderate ($12<PSI\leq23$; n=2) and high (n=1) pain. Their data is plotted in Figure 11 and interestingly showed lower cervical FA in the STT, an apparent but lesser difference in the dorsal columns and very little difference in the CST; that is thoracic lesions

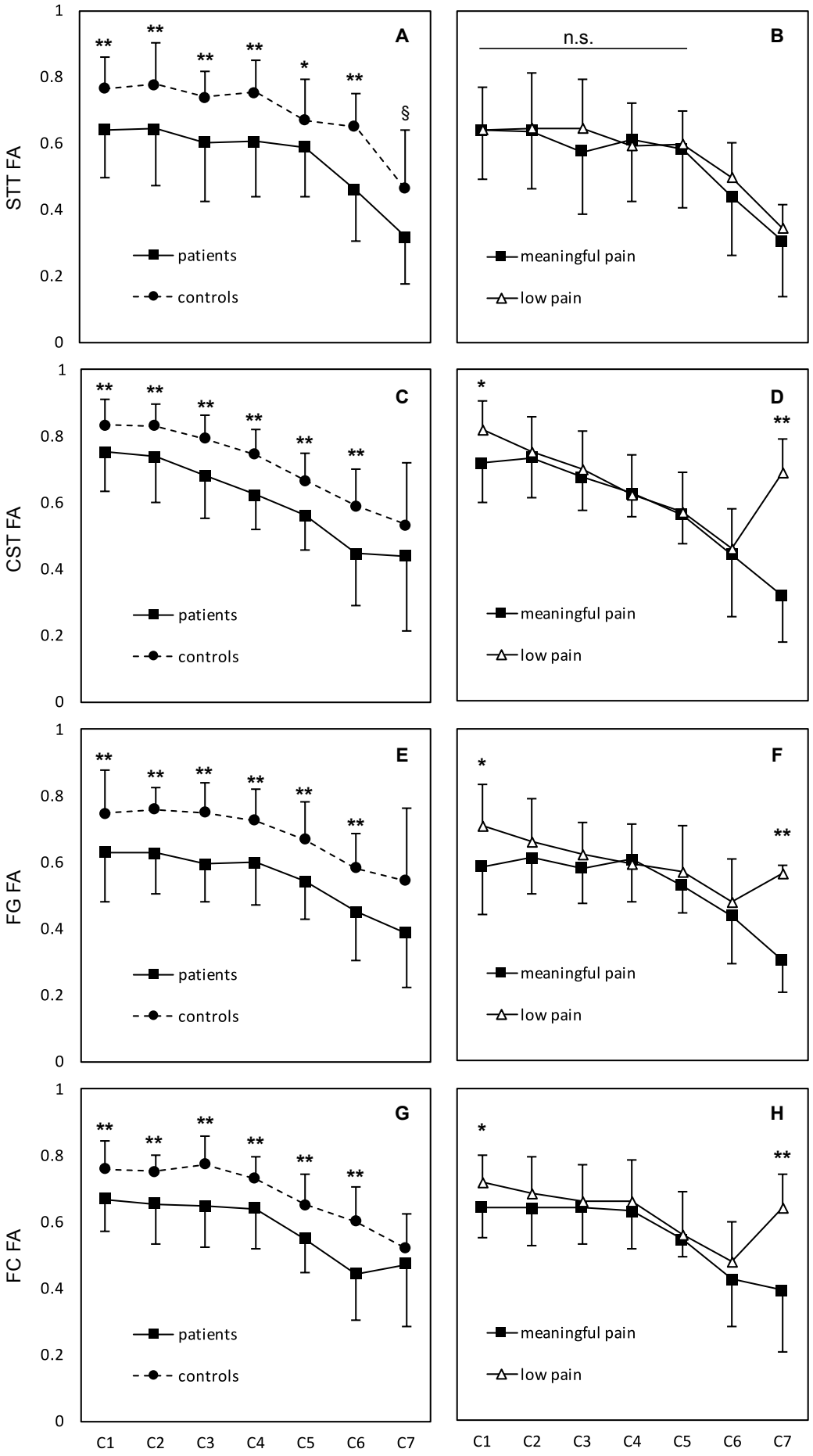

Figure 10. Tract-specific FA measures. (**A**) STT, patients and controls; (**B**) STT, meaningful vs. low pain; (**C**) CST, patients and controls; (**D**) CST, meaningful vs. low pain; (**E**) FG, patients and controls; (**F**) FG, meaningful vs. low pain; (**G**) FC, patients and controls; (**H**) FC, meaningful vs. low pain.

FA differences were found across all tracts for patients vs. controls, however differences were only found for dorsal columns and corticospinal tracts for pain sub-groups, not the spino-thalamic tract.

§ p<0.1
* p<0.05
** p<0.01

n.s., non-significant for C1 to 5 average or individual levels

(past or present) associating with greater cervical STT 'damage' had more pain (meaningful significance cannot be determined with the n=1 subgroup).

Figure 11. FA, no current or previous cervical lesion

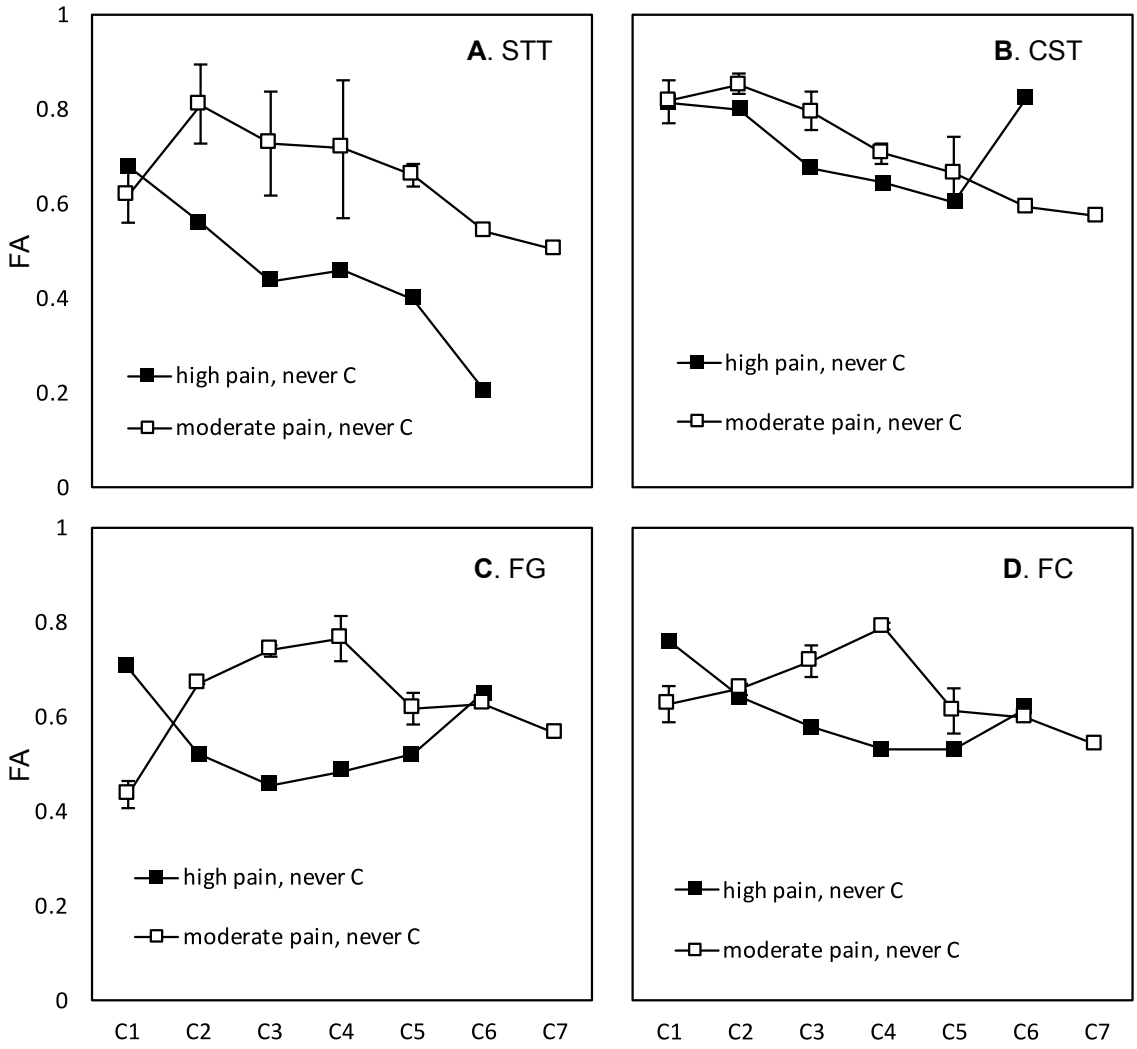

Three participants who had never suffered cervical lesions were dichotomised into moderate (n=2) and high (n=1) pain scores; differences seem to be more apparent in the STT where high pain associates with lower FA across all cervical levels (except C1; plot A). STT, spinothalamic tract; CST, corticospinal tract; FG, fasciculus gracilis; FC, fasciculus cuneatus.

Secondly, as the isolated thoracic patients' PSIs could not be subdivided into lesion location or pain groups, correlation tests with mean FA were performed (Figure 12). These revealed

strong significant negative correlations between pain and FA for both STT and FC (Figure 12A and D), with borderline significance for FG (Figure 12C) and no clear effect of pain on FA in CST (Figure 12B). Although both STT and FC showed significant correlations, it is evident from the correlation plots that PSI is explaining more FA variance than FG; indeed, an F-test showed significantly different variances for STT and FG FA ($p<0.01$).

Figure 12. Tract-specific FA measures versus pain for isolated thoracic lesion participants

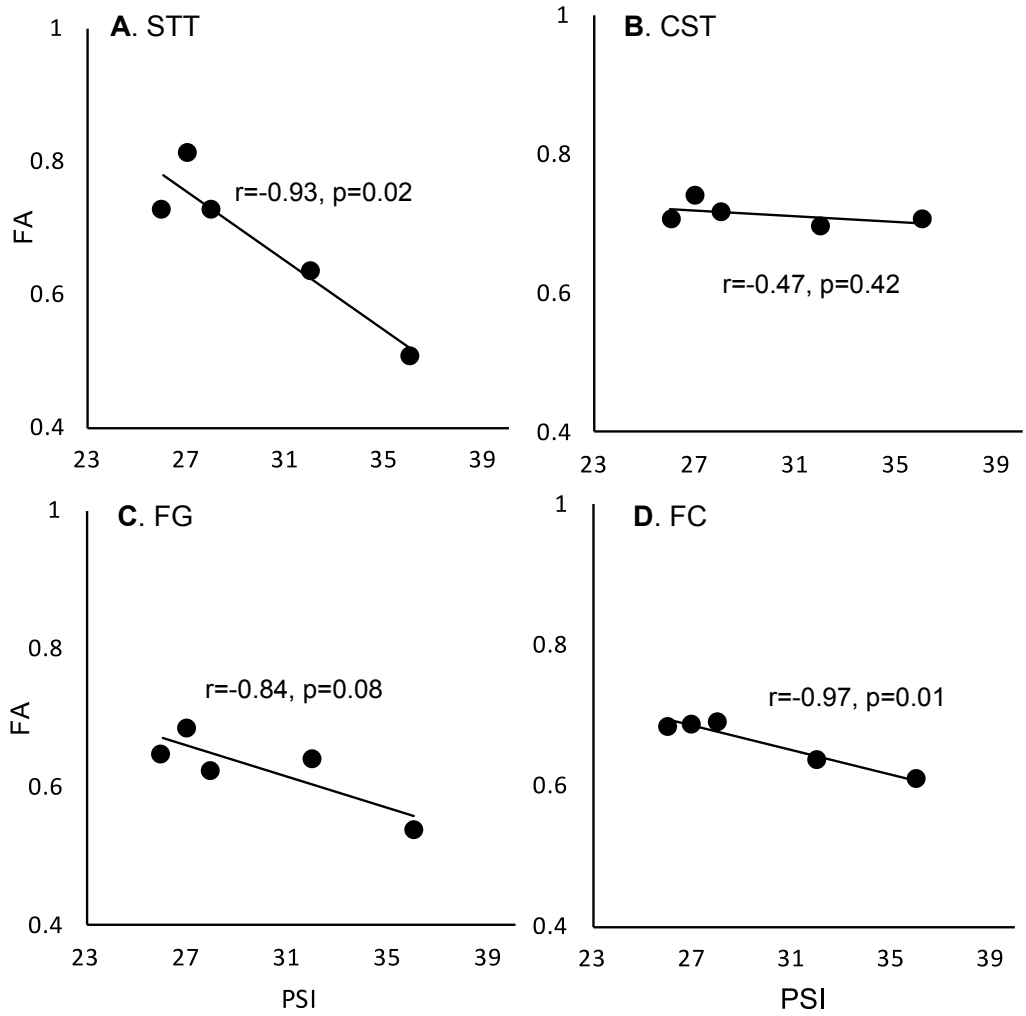

Five subjects with isolated thoracic lesions showed striking mean cervical FA correlations with pain score (PSI; A-D); the explained variance of these correlations was greatest for spinothalamic tracts (STT; plot A). FA, fractional anisotropy; PSI, pain severity index; STT, spinothalamic tract; CST, corticospinal tract; FG, fasciculus gracilis; FC, fasciculus cuneatus.

MD Results Summary

The pattern of results for mean diffusivity (MD) mirrored those of FA and are summarised in Figure 13.

Figure 13. Mean diffusivity summary results

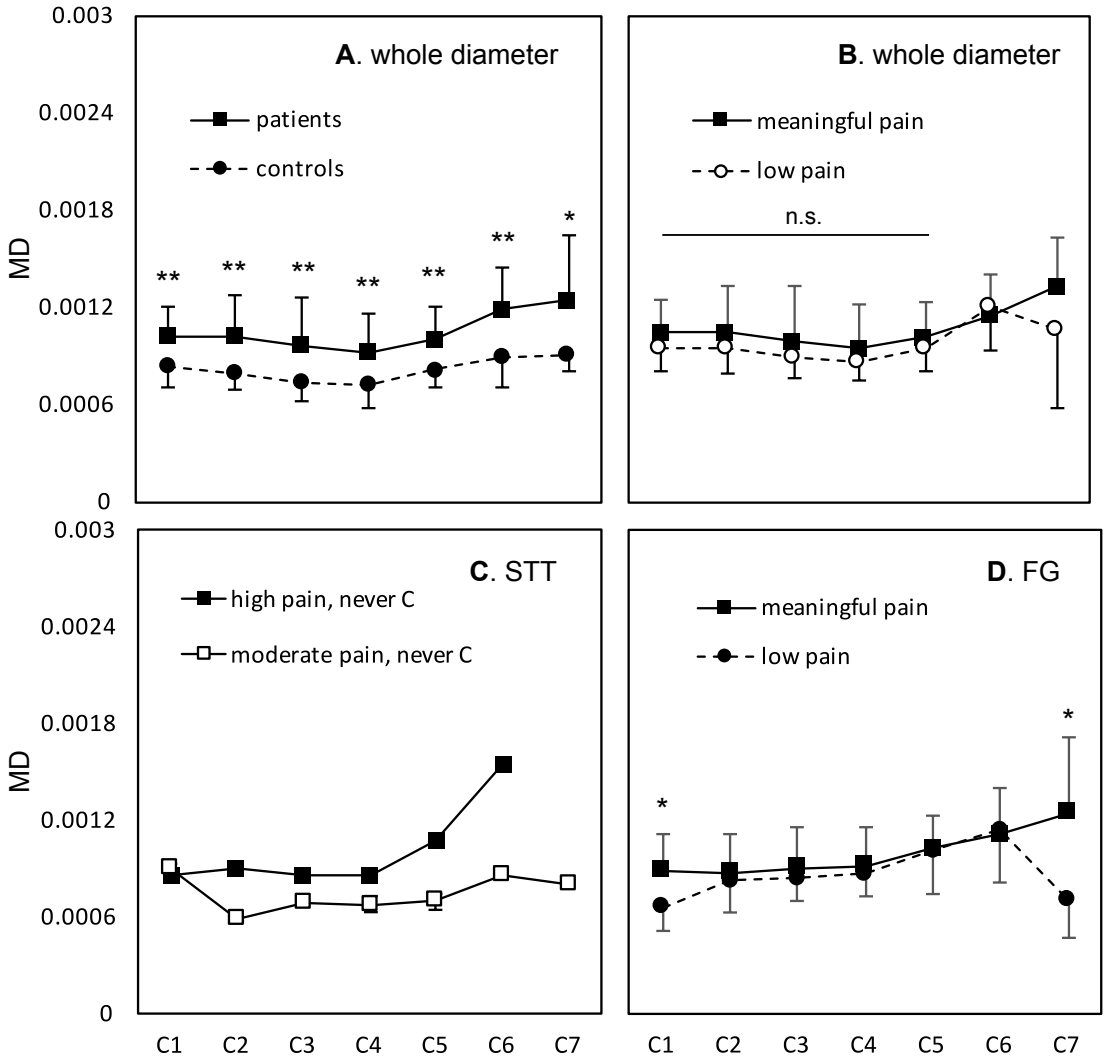

Mean diffusivity (MD) results mirrored those found using fractional anisotropy (FA): significant differences in mean MD for patients vs. controls (A) not found with pain sub-groups (B), except for further subdivisions – those with no history of cervical lesions showed higher MD values with greater pain (akin to lower FA indicating damage; plot C) and dorsal columns and corticospinal tracts showed higher MD for those with greater pain (plot D: FG shown as example). STT, spinothalamic tract; FG, fasciculus gracilis; **, $p<0.01$; *, $p<0.05$; n.s., not significant for C1 to 5 average or individual segments

Discussion

Participants with thoracic lesions and no cervical cord lesion have an average spinothalamic tract (STT) FA that negatively correlates with pain severity; in this chapter I directly relate tract-specific differences in diffusion measures to pain and demonstrate tract-specific evidence of Wallerian or retrograde degeneration. Within the select group without cervical lesions, these differences are almost exclusive to the STT: no relationship is found between corticospinal tract (CST) FA and pain, and the relationship between the dorsal column and pain, although there, explains significantly less variance.

This is not the whole story. Dorsal columns and corticospinal tracts (but *not* the spinothalamic tract) show significant differences between pain groupings when all patients are studied (irrespective of lesion location). A possible explanation follows. It must be noted that across all patients, average cervical FA is lower in high pain groups and it appears that this difference can be explained by the relative proportion of lesion locations (cervical / thoracic / cervicothoracic) within pain groups. Indeed, lesions (be they cervical or thoracic, current or historical) clearly account for most (if not all) of the diffusion measure differences seen between patients and controls and between meaningful and low pain groups. For pain groups, there is the suggestion that this difference is largely confined to white matter and is predominantly tract damage, however, no difference is seen across all participants in the spinothalamic tract (where one might suppose this pain related 'damage' to have occurred) but on the contrary, as mentioned, the dorsal columns and corticospinal tracts show a significant effect. Theories of imbalanced dorsal column and spinothalamic tract function causing chronic pain (Berić et al., 1988) have been largely discounted (Defrin et al., 2002); indeed the pattern here of greater dorsal column damage than spinothalamic tract damage

is in any case the wrong way around. Perhaps what it does reveal is that dorsal columns and corticospinal tracts are significantly damaged by whatever process is leading to pain, even if dorsal column damage *per se* is not causative. Drawing from Chapter 3 showing the importance of thoracic lesions, and in light of the evidence above, it may be that thoracic lesions are a central part of this pathological pain process and that the relatively preserved (or perhaps newly re-wired) cervical STT are also important in facilitation of the NMO pain state (as seen in incomplete spinal cord injury patients (Davidoff et al., 1987)).

Alternatively, it is possible that selective changes in the dorsal columns and corticospinal tracts are direct causes (or consequences) of disordered pain processing, but this is not well supported in the literature. Dorsal columns are implicated in pain transmission for visceral pain, in particular a subset of the dorsal columns: the post-synaptic dorsal column system, that runs deep in the dorsal column originating from second-order lamina IV-VI and X dorsal horn cells, and terminating in the ventral and rostral areas of the dorsal column nuclei (Berkley et al., 1986; Palecek, 2004). This pathway is activated by noxious visceral stimuli in rats (Al-Chaer et al., 1996) and lesions to the pathway provide analgesia from pelvic viscera pain in humans (Hirshberg et al., 1996). Interestingly, pain states affecting this pathway can alter *cutaneous* pain and sensory processing, as shown by the abolition of allodynia and mechanical hyperalgesia in the presence of a bone pain in rats following bilateral fasciculus gracilis lesions (Houghton et al., 1999). Relative dorsal column damage, as seen here, would be more likely to be analgesic and doesn't seem to provide an explanatory mechanism. Whether corticospinal tracts have a role in modifying pain is less clear and again, relative damage probably does not provide a viable explanation for pain modification seen in this thesis. It has been known for some time that stimulation of the sensorimotor cortex can suppress dorsal horn nociceptive activity (Lindblom and Ottosson, 1957) and is used as a

rationale for the efficacy of motor cortex stimulation in humans with chronic pain (Fontaine et al., 2009). This analgesic effect has more recently been shown to be mediated by a descending-inhibitory serotonergic RVM pathway, and not via the corticospinal tract (Viisanen and Pertovaara, 2010).

A further explanation is the potential confound of diffusion image resolution (discussed further below) and relative individual spinal tract mask size. Looking at Figure 3, one can see that the spinothalamic mask is represented by fewer voxels (depicted by small yellow squares) compared to the fasciculus cuneatus and gracilis and corticospinal tracts. This could produce a relative difference in signal-to-noise across tract diffusion measures and subsequently result in the inability to reach significance for comparisons of spinothalamic tract measures by pain groupings.

One exciting finding is that diffusion imaging might be able to reveal tract-specific remote degeneration. A well conducted study by Naismith and colleagues relates dorsal column and corticospinal tract diffusion abnormalities in neuroinflammatory patients to specific abnormalities in the sensorium and increased disability, respectively (Naismith et al., 2013). The lesions in their study were 'remote' in time, but not in space: all diffusion measures were cervical and participants were only recruited with a history of cervical cord lesions. The current chapter provides evidence that cervical tract-specific diffusion measures correlate with thoracic cord lesion damage and that within the spinothalamic tract this correlates with the degree of pain.

Non-pain findings reflected in the literature substantiate my findings. Average cervical FA is lower in patients than controls, and fits with many examples in neuroinflammatory diseases

where differences in both brain and cord FA are found in both lesioned and non-lesioned areas (Inglese and Bester, 2010). Additionally, the inverse correlation between disability and mean cervical FA measures has previously been reported (Naismith et al., 2013; Pessôa et al., 2012; Qian et al., 2011) and it's interesting to observe that the shape of the disability (EDMUS) vs FA correlation is apparently non-linear; it even suggests that FA of cervical cord might increase slightly from zero to mild disability, before precipitously falling off with worsening disability. EDMUS (or its counterpart EDSS) is known to be non-linear and a relationship between the score and disability has previously been proposed whereby integer changes at the higher end of the scale (≥6) represent greater jumps in disability (Meyer-Moock et al., 2014); this mirrors the appearance of my EDMUS data where above an EDMUS of 5, the mean FA measures precipitously fall (Figure 8B), however it is opposite to what has been found when relating MS disability to quality of life measures (Twork et al., 2010), all of which reinforces the difficulty of discerning what denotes equal changes in disability at different starting points.

One limitation of the analyses performed in this chapter is that of image resolution. Although the diffusion images were cleanly segmented, the underlying diffusion data remains of low resolution (1.3x1.3x3mm; see Figure 3) and thus the tract masks suffer from partial-voxel effects. Furthermore, because tracts were only applied as masks based on the geometry of the whole cord segmentation (i.e. not based on sub-segmentation of grey / white matter, or tracts), their anatomical positions, especially in a diseased cord (with variably severe and possibly asymmetrical atrophy), will in many cases be approximate. It must therefore be born in mind that when looking for differences in the dorsal columns or

STT, it may in fact be changes in the dorsal horn, or ventral horn and spinocerebellar tracts, respectively.

The primary results showing a relationship between FA and pain for those with current isolated thoracic cord lesions and those with a history of only isolated thoracic cord lesions have low numbers, n=5 and n=3, respectively. This clearly reduces the impact of my findings, however the fact that the differences were statistically significant in such small groups implies that these relationships will be readily verifiable in future work if they exist.

There are clearly more tracts to explore and increasingly refined techniques available for their exploration. Foremost must be to image the thoracic cord (where most of the lesions occur) in concert with the cervical cord to establish if thoracic damage is producing distal cervical cord effects, and whether STT measures indeed correlate with pain measures for these participants. It would also be fascinating to look at the damage to descending tracts, for example the dorsolateral funiculus conveying the tonic output of opioidergic RVM-mediated pain modulation to lamina I neurones of the dorsal horn (Basbaum and Fields, 1979; Fields and Basbaum, 1978). This will of course be affected by the same limitations discussed above, however dedicated cord sequences, advances in sequences for grey and white matter differentiation, and ever improving automated segmentation tools will make this increasingly feasible (Cohen-Adad, 2017). Furthermore, tractography methods have the potential to improve ascending and descending tract specific diffusion measures by providing the means to create participant-specific tract masks based using an individual's diffusion data (seeded at a site within the tract of interest), but also to unravel some of the complexities of brainstem-cord circuitry and provide additional measures in disease to further unpick network effects on pain (Ciccarelli et al., 2007).

Conclusion

Participants with thoracic lesions and no cervical cord lesions have an average spinothalamic tract (STT) fractional anisotropy (FA) that negatively correlates with pain severity. Furthermore, the pattern of cord lesions (cervical, thoracic, cervicothoracic) are reflected in mean FA measures of the cervical cord and synchronise with the findings of Chapter 4 whereby high pain scores associate with isolated thoracic lesions.

Chapter 6:
Experimental chapter: Brain resting state imaging and the pain network in NMO

Introduction and background

Resting-state networks are reproducible temporally synchronous spatial networks of neuronal brain activity apparent in the absence of task-related activity, and visualisable with fMRI techniques (see Chapter 2). These networks were first encountered as brain areas that consistently *deactivated* at the onset of tasks used in experimental functional imaging and it was these areas of consistent deactivation that were later shown to be tonically active at "rest", i.e. in the absence of task-related activity. The first resting-state network was thus appropriately entitled the 'default-mode' network (DMN), coined by Raichle et al., (Raichle et al., 2001) and subsequent experiment has revealed multiple other distinct brain networks that are also active "at rest" (Raichle, 2015). The DMN includes, amongst other areas, the precuneus, adjacent posterior cingulate cortices (PCC), medial pre-frontal cortices (PFC), and superior and lateral occipital cortices. The PCC and precuneus are implicated in background monitoring of events in the internal environment whilst the medial PFC may

evaluate an events associated salience (Raichle et al., 2001); it is thus unsurprising that DMN dynamics might be altered in acute and chronic pain states. Indeed strengthened connections between the periaqueductal grey (PAG, a key component of descending pain modulation) and the medial PFC have been associated with attentional disengagement from pain (Kucyi et al., 2013) perhaps engaging descending inhibition systems via the RVM, whilst greater connectivity between the DMN and the dorsolateral PFC, rostral anterior cingulate cortex (ACC) and insula have been shown in fibromyalgia patients suffering chronic pain (Napadow et al., 2010) and may represent ACC encoding of affective components of pain, the insula serving as a site of integration for the homeostatic behavioural drive and the dorsolateral PFC encoding anticipation of pain (Craig, 2003; Wager et al., 2004; Zubieta et al., 2001).

Areas of the opioidergic descending pain modulatory network (DPMN), a network including the PAG, RVM, insula, rostral anterior cingulate (ACC), dorsolateral prefrontal cortex (dlPFC) and hypothalamus, a network conceivably altered or damaged by the disease process in NMO, are all potential targets for DMN interactions (Eippert et al., 2009a; Wager et al., 2004) (see Chapter 1c, especially Figure 2). This chapter explores the relationship between resting-state brain connectivity and NMO chronic pain with particular focus on the resting-state connectivity of the PAG and its connections with the DPMN.

Objectives / Aims

1. To investigate differences in resting-state connectivity using a data driven approach across (a) NMO patients and healthy controls groups, (b) NMO meaningful pain and low pain groups, the latter including both NMO participants and controls, and (c) continuous PSI scores.

2. To determine how periaqueductal grey (PAG) seeded resting-state connectivity changes across the same groups with statistics focussed on other elements of the DPMN.

Methods

Twenty-seven of the Imaging Cohort's 33 participants (demographics shown in Table 1 below) had resting-state brain compatible with ICA and seed-based analysis. These were all acquired alongside physiological noise-modelling (PNM) measures, except in one individual for whom PNM recording failed. This individual is included in the ICA-based analyses but excluded from PAG-seeded analyses.

For higher level ICA and dual-regression, another single patient was excluded because of artefactual activations (primarily CSF) revealed in their lower level PAG-seeded GLM analysis. The same participant was included in higher-level seed-based analyses with PNM corrected data (patient's data shown as example of PNM correction in Figure 1). Imaging protocols are provided in Chapter 2.

Image pre-processing

FMRIB's software library v5.0 (FSL) tools were used to perform brain extraction (FSL's *BET*), B0 unwarping (*FUGUE*/*BBR*) and motion correction (*MCFLIRT*) (Jenkinson et al., 2012). Participant's functional data was registered to their T1 structural data before non-linear registering to standard space (FSL's *FLIRT* and *FNIRT*). Slice timing correction was not performed, in line with previous work showing little or no benefit in resting-state analysis (Wu et al., 2011). Spatial smoothing was set to a full-width half maximum (FWHM) of 5mm and high-pass filtering to 100s.

Table 1. Participant baseline characteristics

	Patients	Controls
n	27	21
Female, n (%)	23 (85.2)	14 (66.7)
Age, mean (sd)	54.5 (14.5)	55.8 (16)
Onset age, mean (sd)	45.1 (16.8)	
DD, mean (sd)	9.5 (5.6)	
No. of attacks, med (range)	4 (1-28)	
No. of TM attacks, med (range)	3 (1-28)	
EDMUS, med (range)	5 (1-28)	
PSI, mean (sd)	19.4 (11)	
Afro-Caribbean, n (%)	4 (14.8)	
Asian, n (%)	6 (22.2)	
Caucasian, n (%)	17 (63)	

sd, standard deviation; med, median

ICA and dual-regression

Single participant ICA was performed using FSL's *MELODIC* with the optimal number of components calculated by automated model order selection using prior principle component analysis (PCA) of the data. Variance normalisation was applied. FSL's *FIX* (Salimi-Khorshidi et al., 2014) was then run on the ICA results for all participants individually, with visual confirmation in FSL's FSLeyes that 'noise' components were excluded and 'signal' components preserved. (Note, this 'cleaned' functional lower level data is also used in the seed-based analyses below). Subsequent concatenation multi-participant ICA was performed (FSL's *MELODIC*).

Dual regression

Data were processed using dual-regression analysis to determine participant-specific differences in shared network maps (Filippini et al., 2009). Across all networks identified as potentially important to pain and NMO (n=14, includes those illustrated in Figure 2, and

three related networks), the following comparisons were analysed with FSL's *randomise*: patients versus controls, meaningful pain versus low pain, and effect (positive and negative) of PSI. Exclusively for the DMN, the effect of HADS A, HADS D and CESD were evaluated. And exclusively for visual networks (dorsal visual stream left and right, visuospatial and medial visual), the effect of visual acuity was assessed. For this, patients were classified as 'unimpaired' (decimal VA ≥ 1, equivalent to Snellen 6/6) or 'visual deficit present' (decimal VA < 1 in either eye).

PAG seed-based connectivity

The periaqueductal grey (PAG) was defined using a PAG mask developed in Oxford (Ezra et al., 2015) and the mean PAG resting-state time-series extracted for every participant. Sub-divisions of the PAG were not individually seeded because of image resolution limitations. Lower level GLM analyses were performed in FSL's FEAT on 'cleaned' individual participant functional data (*FIX* after single-participant ICA – see section above) with mean PAG time-series set as the explanatory variable of interest. Mean time series from linear masks in lateral ventricle CSF and periventricular white matter were included as confound explanatory variables, and all data were physiological noise model (PNM) corrected (See example in Figure 1; note especially improvement in lateral ventricle CSF artefacts). All higher-level analyses were performed using FSL's *randomise* with 5000 permutations and statistics reported as threshold-free cluster enhancement maps (Smith and Nichols, 2009).

Figure 1. PAG-coincident resting-state connectivity, pre- and post-PNM correction

A. Before PNM correction

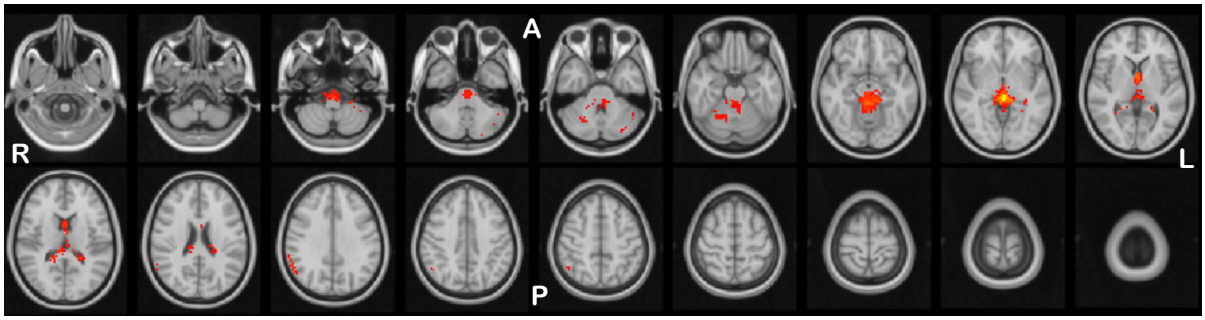

B. With PNM correction

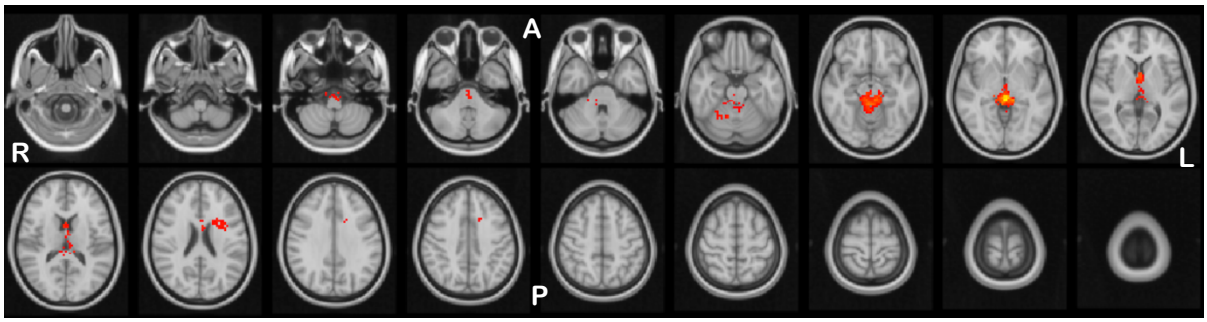

An example of the utility of physiological noise model correction, note especially the reduction in lateral ventricular artefact between A and B, an artefact probably caused by cardiac pulsation and consequently removed by regressing with PNM.

Statistics

Raw Z-statistic images are maps of z-scores (a score of the number of standard deviations a value is from the mean), uncorrected for multiple comparisons. An arbitrary threshold of $z>2.3$ is utilised in most z-stat figures below, equivalent to an uncorrected p-value of <0.05. All seed-based analyses were performed firstly brain-wide, and then with statistics masked by a combined DPMN mask (incorporating the ACC, paracingulate, dlPFC, insular, amygdala, hypothalamus, and brainstem). The core of the mask components (the ACC, paracingulate, insula, amygdala, brainstem) were obtained from the Harvard-Oxford atlas (Desikan et al., 2006) and generously thresholded at 10% (i.e. at least 10% of people would label area as named) to ensure the area of interest is included and to reduce bias. The other masks were

drawn manually, the hypothalamus as a 10mm radius sphere around the coordinates of the centre of the hypothalamus (Eippert et al., 2009a) and the dlPFC based on the middle frontal gyrus between inferior and superior frontal sulci and including only grey matter >25mm away from the midline.

Statistical contrasts were performed for: patients vs controls, low vs. meaningful pain, low vs. high pain and for pain as a continuous variable. All pain measurements were PSI based; pain groupings are defined in Chapter 3. Threshold-free cluster enhanced (TFCE) statistics were used to identify significant clusters of voxels (Smith and Nichols, 2009). For statistically robust comparisons of the target-masked TFCE tested contrasts, where 2 areas are reviewed (for example whole brain and DPMN) for each participant, a Bonferroni corrected significance of $p<0.05$ would require an alpha level of $\alpha<0.025$; likewise, for 3 areas an alpha level of $\alpha<0.0167$ is required. Given the exploratory nature of this work, these thresholds have not been robustly enforced and most results are thresholded at $p<0.01$ or $p<0.05$, unless stated otherwise.

Results

ICA determined resting state networks

Independent component analysis (ICA) of patients and controls resting-state data at participant and group level identified 60 independent networks. Sixteen were classified as noise. Eleven of the remaining 44 are shown as exemplars in Figure 2 and are described in detail below.

Figure 2: Resting state networks in all data

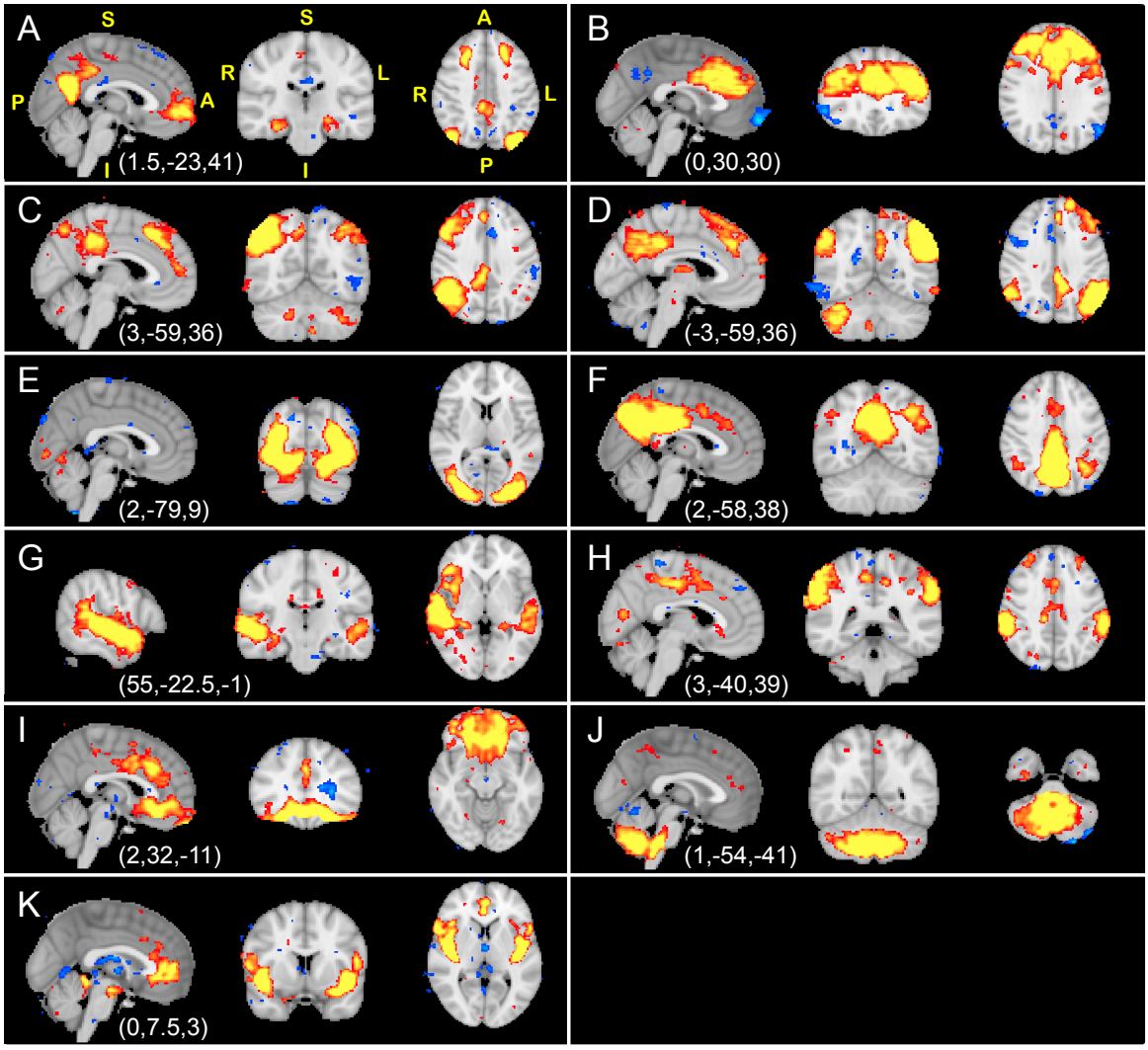

A-K results of undirected ICA of resting-state fMRI data; Bracketed numbers denote slice coordinates. A. Default-mode network; B. Salience network; C & D. Dorsal visual stream (lateralised); E. Medial visual; F. Visio-spatial; G. Auditory; H. Sensori-motor; I-K. Possible pain-associated networks. See text for detailed description. Yellow letters in A denote orientation of all image triplets; A, anterior; P, posterior; R, right, L, left; S, superior; I, inferior.

Network A consisted of large concerted activations in the precuneus cortices, adjacent posterior cingulate cortices (PCC), medial PFC, superior lateral occipital cortices, hippocampi and amygdalae. These areas are consistently described together in the default mode network wherein the PCC and precuneus are implicated in monitoring sensory information whilst the medial PFC evaluates associated salience (Raichle et al., 2001), the

latter receiving projections from the amygdala to its limbic areas (Barbas, 1995) and together forming part of a circuit processing fear (Marek et al., 2013). Network B again involved the medial prefrontal cortices but this time was associated with a large concerted activation involving the middle and anterior cingulate cortices (ACC) and paracingulate cortices, lateral prefrontal cortices, and smaller areas in the left primary motor cortex and insular cortices. This network thus incorporated areas involved in salience processing, overlapping with some of those in the DMN, in-particular areas involved in quantifying non-modality specific aversion (and by extension, often activated by pain) (Hayes and Northoff, 2012). Networks C and D showed right and left lateralised concerted activations in the lateral occipital cortex, the superior lobule, angular and supramarginal gyri of the parietal cortex, bilateral intraparietal sulci, middle and superior frontal gyri and frontal pole – in C this was right lateralised and in D left. This most likely represents the dorsal visual stream and is commonly lateralised (Beckmann et al., 2005). Network E showed concerted activations in the occipital poles, lateral occipital cortices, lingual gyri and fusiform gyri and probably the medial visual network (ventral visual stream) (Beckmann et al., 2005; Damoiseaux et al., 2006). Network F involving a large medial activation in the precuneus and adjacent PCC in concert with smaller activations in the lateral occipital cortices, angular gyri, middle and anterior cingulate cortices, frontal poles and thalami most likely represents a visuospatial system encoding spatial representations of the environment (again, areas overlap with DMN) (Beckmann et al., 2005). Network G showed concerted activation in the planum polare and planum temporale, superior temporal gyrus, Heschl's gyri and right insular. The network was slightly rightward skewed, and incorporated many parts of the auditory network (Beckmann et al., 2005). Network H included activation in parts of the pre- and post-central gyri and may represent a sensori-motor network (Biswal et al., 1995).

Network I exhibited concerted activations in the middle cingulate cortices, frontal poles, the orbitofrontal prefrontal cortices, and the subgenual rostral ACC, the latter two (at least) thought to be crucial components of the descending pain modulatory network (DPMN) (Eippert et al., 2009a). J is an example of one of the networks found with cerebellar activation, of which there were many, this one with concerted activation in areas relevant for pain: the right posterior insular, the L thalamus, the pons and medulla (incorporating RVM) and the ACC. Network K again interestingly showed many DPMN-associated activations, including the dorsolateral pre-frontal cortex (PFC), bilateral insular cortices, and the pregenual rostral ACC, and also concerted deactivations in the vicinity of the RVM, thalami and PAG and could be involved in the tonic descending modulation of pain information at rest (Eippert et al., 2009a).

Dual-regression reveals multiple significant differences between groups and across pain scores

The numerous activations associated with different contrasts across the 14 RSNs examined are summarised in Table 2.

Table 2. Activations associated with networks (p<0.05 unless otherwise stated).

Statistical contrast	Network (Figure 2 assigned letter)	cluster no.	size (voxels)	max (1-p value)	max X	max Y	max Z	COG X	COG Y	COG Z	Atlas anatomy
patients > controls	medial visual (**E**)	2	22	0.986	35	20	32	36	20	32	R occipital fusiform gyrus
		1	8	0.970	21	30	37	21	30	37	R lat. occipital cortex, inf. division
	salience / executive (**B**)	8	227	0.992	46	81	34	46	81	36	L ACC [F]
		7	109	0.984	34	76	41	32	76	43	WM, adj. R frontal operculum
		6	75	0.988	41	90	37	41	91	38	R frontal pole
		5	72	0.986	46	83	44	48	83	45	L ACC
		4	56	0.988	36	85	32	37	87	35	WM, adj. R paracingulate gyrus
		3	29	0.974	32	82	38	31	82	39	WM, adj. R frontal pole
		2	17	0.956	32	78	33	32	80	34	WM, adj. R frontal orbital cortex
		1	1	0.950	45	95	33	45	95	33	R frontal pole
	Auditory (**G**)	2	613	0.998	17	44	33	18	49	34	R middle temporal gyrus
		1	1	0.950	29	46	37	29	46	37	WM, adj. R hippocampus
controls < patients	All (**A-K**)	nil									
meaningful > low pain	All (**A-K**)	nil									
low > meaningful pain	All (**A-K**)	nil									

(table continued overleaf)

PSI effect	medial visual (**E**)	5	14	0.964	60	16	34	60	16	34	L occipital pole
		4	13	0.978	40	19	39	40	19	40	R intra-calcarine cortex
		3	7	0.960	59	15	30	59	15	30	L occipital pole
		2	1	0.950	51	27	39	51	27	39	L intra-calcerine cortex
		1	1	0.956	47	28	36	47	28	36	L lingual gyrus
	Visio-spatial (**F**)	5	200	0.994	53	49	20	57	46	19	L lobule V of cerebellum
		4	53	0.988	43	55	54	45	55	55	R PCC [F]
		3	22	0.984	38	52	55	39	54	56	R PCC
		2	3	0.966	52	23	48	53	23	48	L cuneal cortex
		1	2	0.960	59	40	67	60	40	67	L superior parietal lobule
PSI negative effect	All (**A-K**)	nil									
HADS A effect	DMN (**A**)	nil									
HADS A negative effect	DMN (**A**)	nil									
HADS D effect	DMN (**A**)	1	4	0.958	24	34	46	24	35	47	R angular gyrus [F]
HADS D negative effect *	DMN (**A**)	1	5	0.932	57	95	32	57	95	31	L frontal pole [F]
CESD effect	DMN (**A**)	NA									
CESD negative effect	DMN (**A**)	NA									
normal > impaired VA	All visual (**C-F**)	NA									
impaired > normal VA	medial visual (**E**)	1	4	0.964	50	41	23	50	42	23	Lobules I, II & III of cerebellum [F]

* p<0.9 threshold used

F, see example images of activations below; COG, centre of gravity for statistical cluster map

SIGNIFICANT DIFFERENCES EXIST BETWEEN PATIENTS AND CONTROLS IN VISUAL (NETWORK E), AUDITORY (NETWORK G) AND EXECUTIVE CONTROL (NETWORK B) NETWORKS

Significant effects were found in three networks exploring network-related activity greater in patients than controls (Table 2). One of these, a network likely involved in salience and executive function, showed multiple large significant clusters in the anterior cingulate, frontal and prefrontal cortices, opercula, and insular cortices the largest of which sat in the pregenual rostral anterior cingulate (Figure 3).

Figure 3. Patients > controls, dual-regression result in "salience" network (Network B).

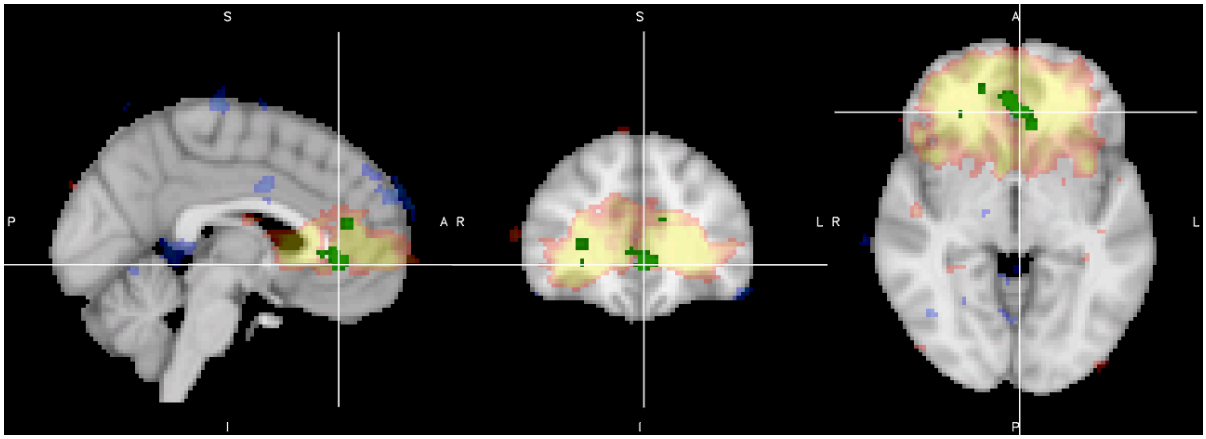

Red/yellow and blue/light-blue represent the salience network's group-wise concerted activations and deactivations; dual-regression results are overlaid in green, here representing the areas that patients activated in concert with this network more than controls. In this example, an area of the rostral anterior cingulate cortex is shown that demonstrated activity in concert with the group salience network in patients greater than in controls (Network B).

VISUOSPATIAL NETWORKS (NETWORKS E & F) ASSOCIATED WITH PAIN SEVERITY

Two networks were significantly associated with differences in PSI scores, the medial visual network and the visuospatial network. The latter showed multiple areas associated with PSI score, most notably the PCC (Figure 4).

Figure 4. PSI effect, dual-regression result in "visuo-spatial" network (Network F).

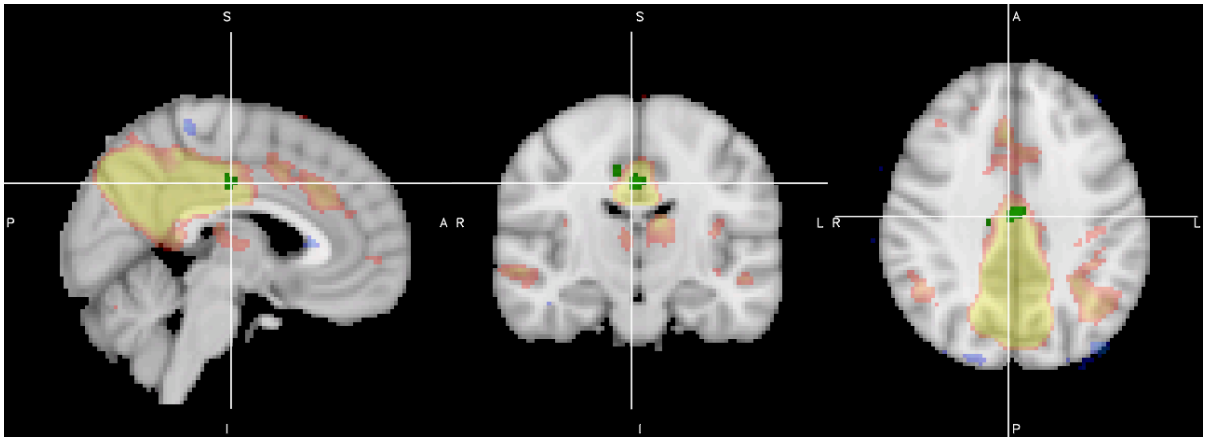

Red/yellow and blue/light-blue represent the visuo-spatial network's group-wise concerted activations and deactivations; dual-regression results are overlaid in green, here representing the areas that patients activated in concert with this network in line with the severity of their pain. In this example, an area of the posterior cingulate cortex is shown that demonstrated activity in concert with the group visuo-spatial network correlated with pain severity (Network F).

DMN NETWORK (NETWORK A) AFFECTED BY DEPRESSION NOT ANXIETY

There were no significant differences with anxiety scores, however the depression component of HADs (but not CESD) highlighted an area of increased connectivity in the R angular gyrus (of the lateral parietal lobe) associated with increasing depression scores (Figure 5A), and a borderline significant area of increased connectivity in the L frontal pole associated with decreasing depression scores (Figure 5B).

Figure 5. DMN activation related to depression score (HADS-D).

A – increased activity in the R angular gyrus associated with "DMN" (network A) that relates to increasing HADS-D

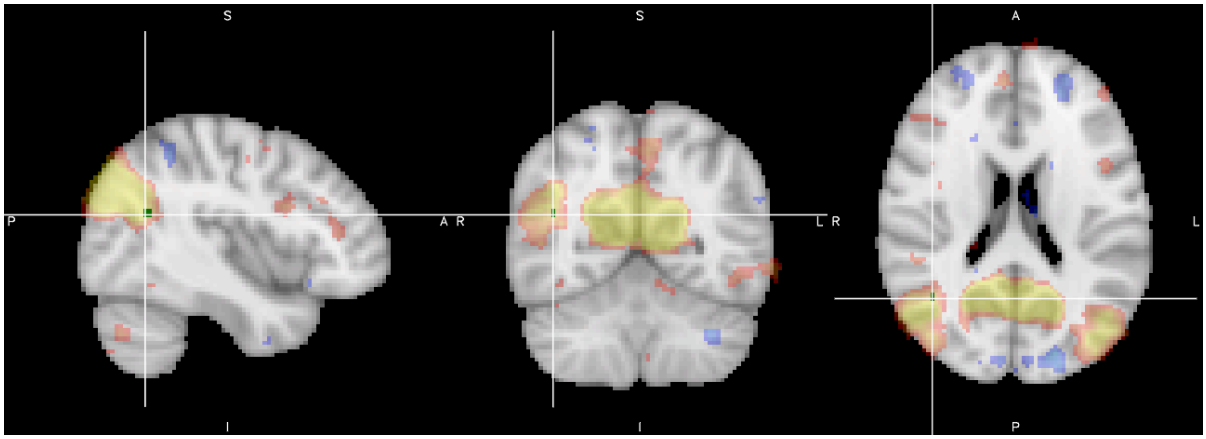

B – increased activity in the frontal pole associated with "DMN" (network A) activity that relates to decreasing HADS-D

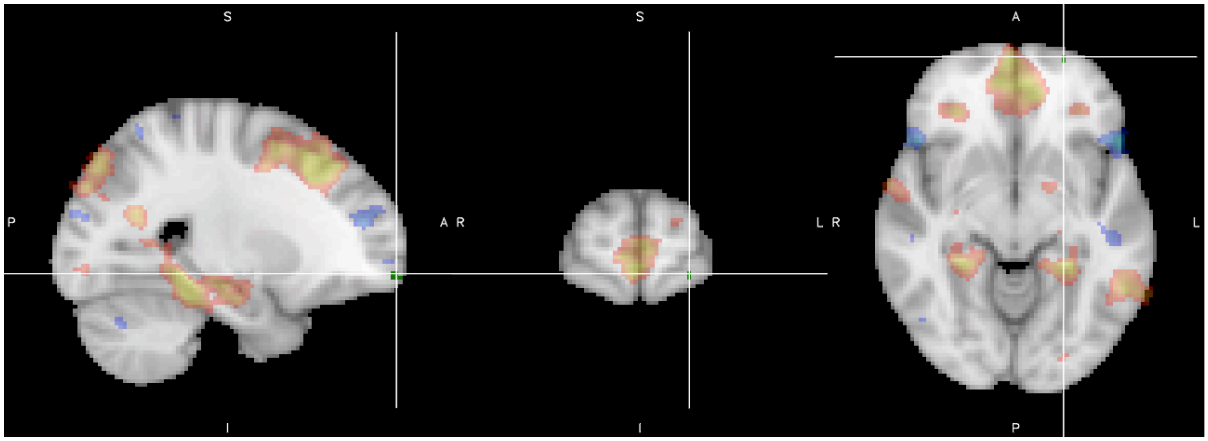

Red/yellow and blue/lightblue represent the DMN's concerted activations and deactivations; dual-regression results are overlaid in green, here representing the areas within which HADS-D correlated with DMN activity (network A). In 5A, an area of the R angular gyrus is shown that demonstrates activity in concert with the DMN correlated with HADS-D. In 5B, an area of the L frontal pole is shown that demonstrated activity in concert with the DMN negatively correlated with HADS-D. R, right; L, left; A, anterior; P, posterior; S, superior; I, inferior.

VISUAL ACUITY AND VISION RELATED RSNS (NETWORKS C-F)

There were no differences in visual networks between groups when assessing unimpaired greater than impaired VA, however for the converse contrast (impaired greater than

unimpaired), increased activity was shown in the L wing of the central lobule of the cerebellum associated with the medial visual resting-state network (Network E).

For PAG-seeded resting state data, patients versus controls highlighted similar areas to high-pain versus low-pain comparisons

The whole-brain mean resting-state activity for patients (n=26) and controls (n=19) temporally coincident with PAG resting-state activity (from here on, referred to as 'PAG-seeded functional connectivity') was notably different; on visual inspection of the raw z-statistic map (Figure 6, A & B), patients exhibited widespread PAG-seeded functional connectivity compared to controls, with relative sparing of the orbitofrontal cortices, the cerebellum and dorsal cortex, with very little in the way of negative associations for either group.

Despite the visually florid differences on the z-stat image, statistical contrasts revealed no significant differences between patients and controls for whole brain or descending pain modulatory network (DPMN) masked analyses.

With patients subdivided into low (n=8) and meaningful (n=18) pain, the raw z-stats showed meaningful pain associated with greater PAG-seeded functional connectivity (Figure 6, C & D), strikingly similar to that seen in patients versus controls (Figure 6, A-D). Again, statistical comparisons failed to show significance for brain-wide or DPMS-masked group comparisons.

Figure 6: Mean PAG-seeded functional connectivity

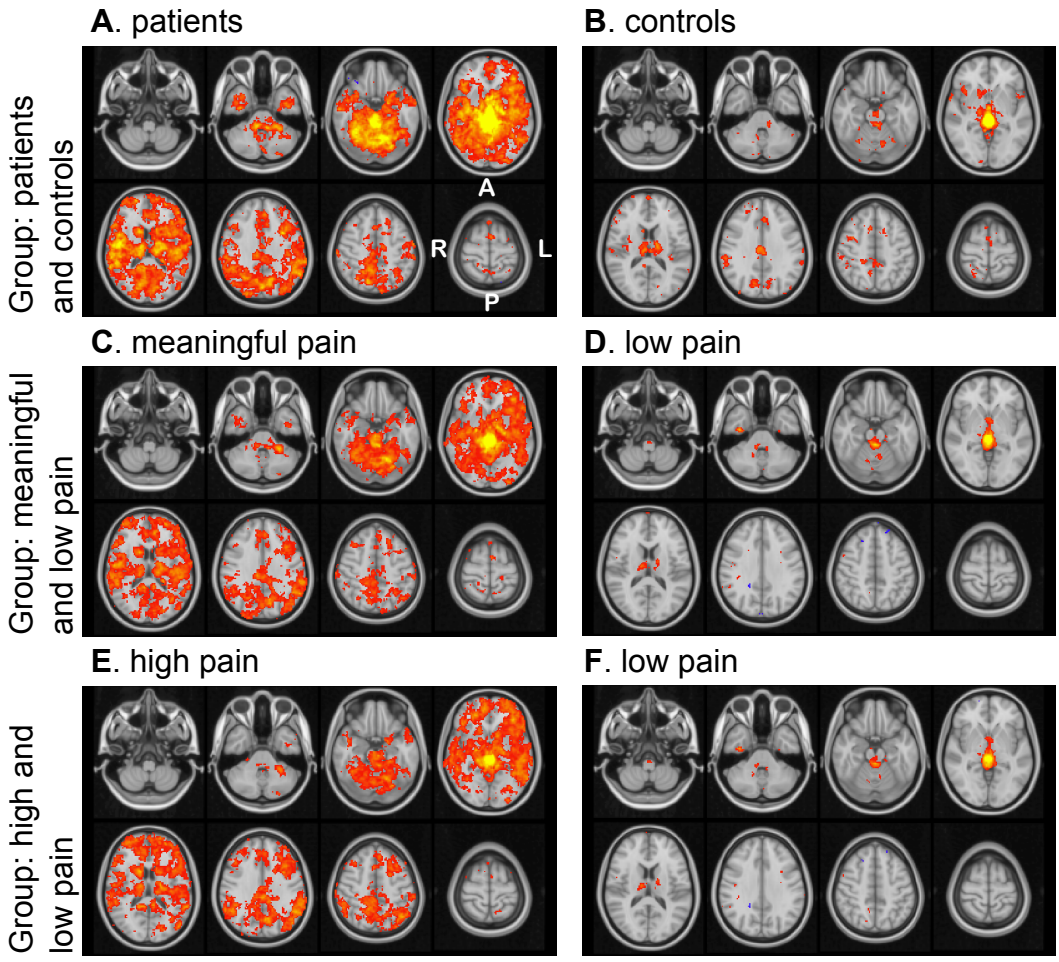

PAG-seeded functional connectivity was visually greater and more widespread for patients over controls (A & B), meaningful over low pain groups (C & D) and high over low pain groups (E & F). Raw z-stat image thresholded at z>2.3; red-yellow = activations, blue-lightblue = deactivations; no multiple comparisons correction. Image orientation in 6A applicable to whole figure; R, right; L, left; A, anterior; P, posterior.

When only the high-pain subgroup (n=12) of the meaningful pain group are compared with the low pain (n=8) group, a similar pattern was again apparent across the z-statistic maps (Figure 6, E & F). In this high-pain low-pain model however, a statistical contrast for high greater than low pain revealed a region of significance in the L angular gyrus (Figure 7).

Figure 7. PAG-seeded activation: severe pain > low pain

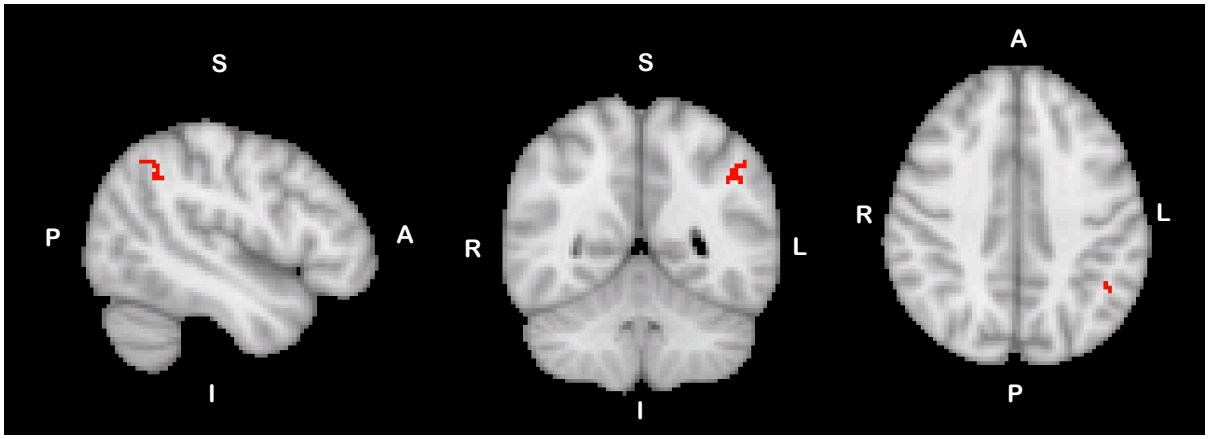

Significant PAG-seeded functional connectivity seen in the L angular gyrus for severe pain greater than low pain contrast. TFCE image, p<0.05. L, left; A, anterior; P, posterior; S, superior; I, inferior.

PSI as a continuous variable associated positively with PAG-seeded functional connectivity in the L frontal pole and negatively with an area in the rostral medulla

When PSI was incorporated into GLM analyses as a continuous variable (including modelling mean resting-state activity), the relationship to PAG-seeded functional connectivity was statistically significant in an area of the L frontal pole within the dlPFC (Figure 8B). There was no significant negative PSI effect seen brain-wide however in an area within the rostral medulla a negative association with PAG-seeded functional connectivity was noted on the raw z-statistic image (Figure 8A, blue region).

DPMS-masked statistics revealed two discrete statistically significant areas in the L dlPFC associated with PAG-seeded functional connectivity (Figure 9A), and when a brainstem-only statistical mask was employed, the negative association between PAG-seeded functional connectivity and PSI in the rostral medulla noted above became significant (maximal p=0.031, therefore only borderline after multiple comparisons correction; Figure 9B).

Figure 8. PAG-seeded activation: PSI effect

A. PSI effect Z-statistic map

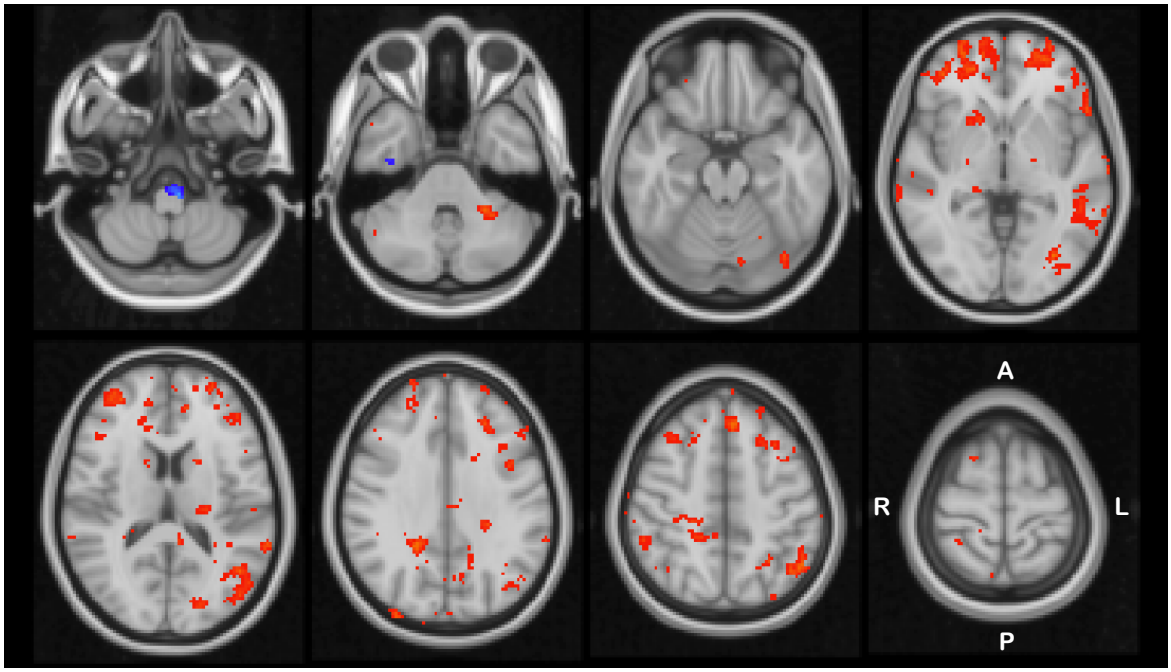

B. PSI TFCE map

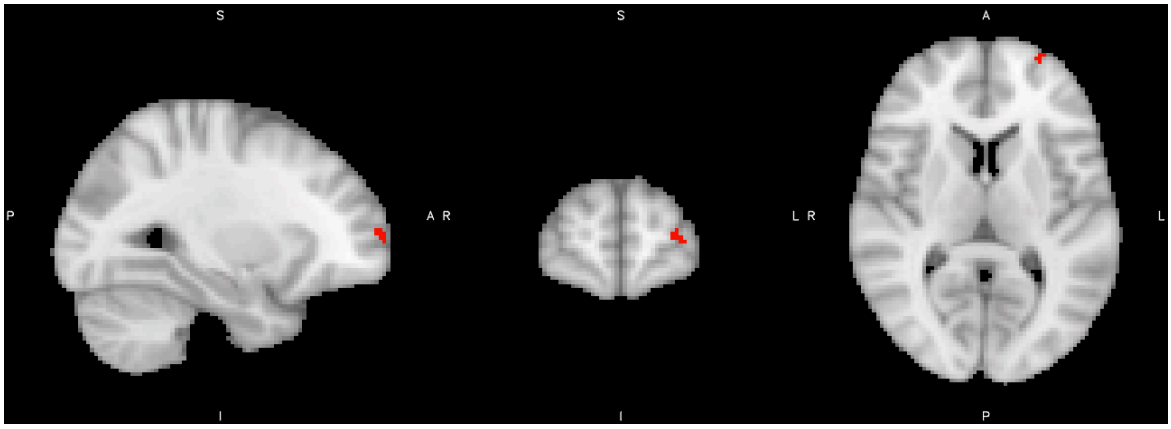

PAG-seeded functional connectivity inversely correlated with pain was seen in the medulla on raw z-stat (A); significant PAG-seeded functional connectivity correlated with pain was found in the L frontal pole. L, left; A, anterior; P, posterior; S, superior; I, inferior. Z-stat, z>2.3; TFCE image, p<0.05.

Figure 9. PAG-seeded activation: PSI effect

A. DPMS mask (positive PSI effect)

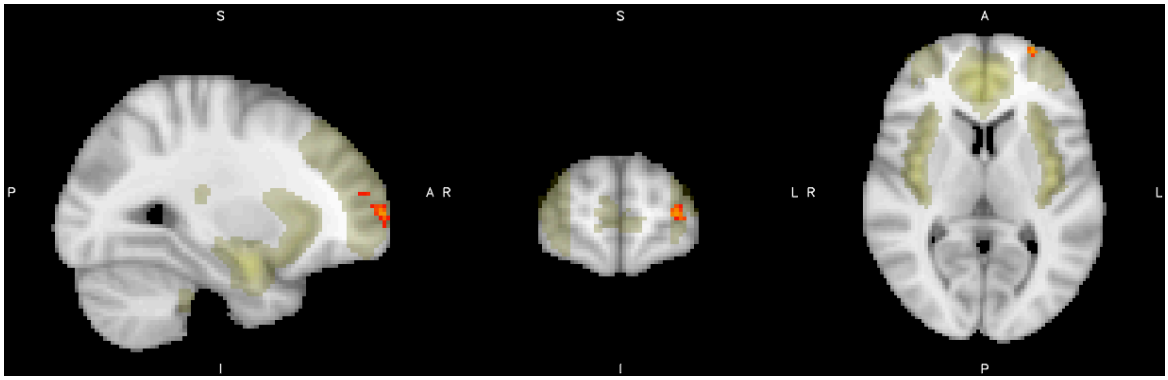

B. brainstem mask (negative PSI effect)

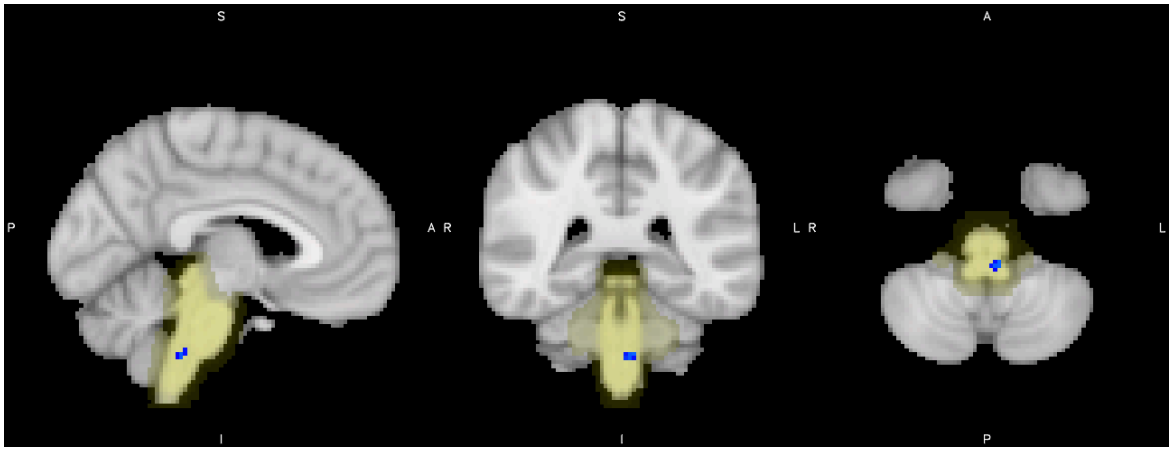

Significant PAG-seeded functional connectivity correlated with pain was found in the L frontal pole in DPMN-masked statistics. Significant PAG-seeded functional connectivity inversely correlated with pain was seen in the medulla (compatible with RVM) in brainstem masked region (B). L, left; A, anterior; P, posterior; S, superior; I, inferior. TFCE image, $p<0.05$.

Temporal covariates strengthened PSI relationship with PAG-seeded functional connectivity

Adding the temporal covariates of age, disease duration and time since first relapse enhanced the relationship seen with PSI for the whole brain and for DPMN-masked statistics (Figure 10).

Figure 10. PAG-seeded activation with temporal covariates

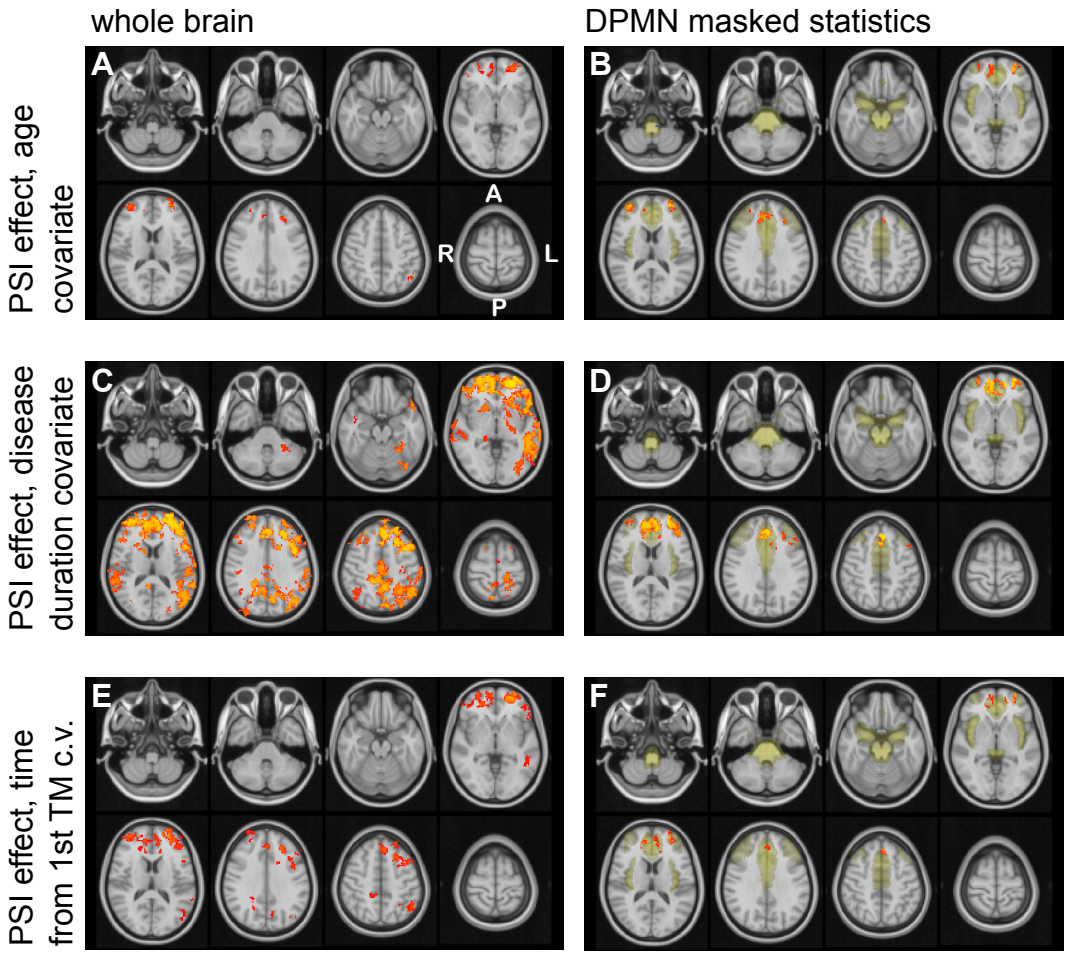

The effect of controlling for age (A & B), disease duration (C & D) and time from 1st relapse (E & F) was dramatic and revealed multiple significant regions of PAG-seeded functional connectivity associated with pain score (PSI) for whole brain (A, C & E) and DPMN-masked (B, D & F) statistics, most notably bilateral prefrontal cortices, R rostral ACC (A-F) and a medullary area of inverse correlation (B). R, right; L, left; A, anterior; P, posterior. TFCE image, $p<0.05$. Yellow transparency, DPMN mask; c.v., covariate

Controlling for age considerably enhanced the already seen L prefrontal cortex relationship but also revealed additional associated areas within the prefrontal cortex, the R paracingulate abutting and just overlapping the R rostral ACC, and the L angular and supramarginal gyri (Figure 10, A & B). The inverse PSI relationship with PAG-seeded functional connectivity in the brainstem became significant for DPMN-masked statistics (Figure 19B, small blue area in brainstem of top-left slice); the maximally associated voxel in this cluster aligned with that of the uncorrected PSI comparison brainstem-masked analysis (Figure 9B); the voxel's activation (by participant) is plotted against participant's PSI in Figure 11.

Figure 11. Plot of participant series for maximally associated brainstem voxel (48, 45, 9) vs PSI

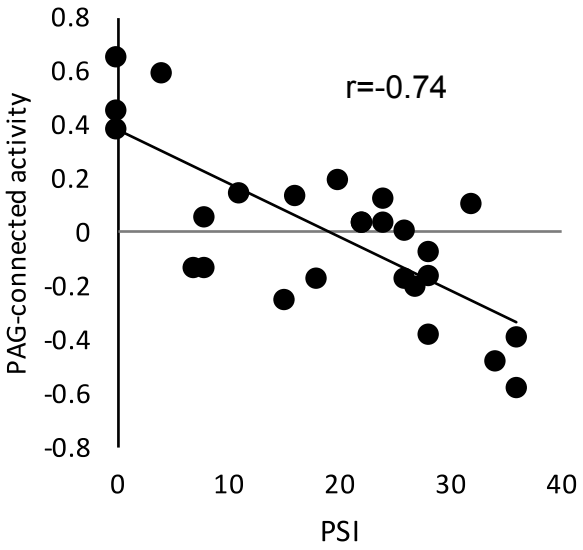

Correlation plot of the PAG-seeded functional connectivity of a voxel of interest in the medulla, compatible anatomically with the rostral ventromedial medulla (RVM), against pain score: a strong negative correlation is seen. r, Pearson's correlation coefficient; PAG, periaqueductal grey; PSI, pain severity index.

Controlling for disease duration also had an enhancing effect on PAG-seeded PSI related connectivity, producing widespread new areas of significant association, including but not limited to the rostral ACC and rostral PCC, bilateral putamen and caudate, the R thalamus, the L insula and operculum (bilateral in parietal lobes), extensive areas of the dorsolateral and dorsomedial PFC and extensive areas of the L temporal cortices (Figure 10, C & D). Further thresholding at $p<0.01$ revealed well defined areas in the L dlPFC and the R paracingulate (not shown). In this model, the inverse PSI to PAG-seeded connectivity relationship in the brainstem (RVM) described above failed to reach significance (maximum $p=0.0574$).

Time from first transverse myelitis, although not identical to disease duration, was highly correlated ($r^2=0.77$) and consequently produced similar, if somewhat more select, areas of related connectivity (Figure 10, E & F). No brain-wide or DPMN-masked effects were found for 'time from latest transverse myelitis (TM)'.

With 'time since chronic pain onset' (for those with chronic pain, n=22) as a covariate in the PSI-related PAG-seeded functional connectivity analyses, a small area in the L angular gyrus was shown to be significantly associated (almost identical in location to that in Figure 7).

<u>Depression and disability covariates</u>

Including EDMUS as a covariate abolished all significant brain-wide and DPMN-masked PSI effects, most probably because of PSI and EDMUS's collinearity (see Chapter 3). No significant effects were seen on brain-wide or DPMS masked analyses when HADS-A or HADS-D were added as covariates. Once more, including CESD as a covariate abolished the significance of PSI effects for brain-wide analyses, again perhaps due to covariance,

however a small area of significant PAG-seeded functional connectivity was shown for DPMN-masked statistics in the L dorsolateral prefrontal cortex (not shown).

A two-covariate model with disease duration and age produced robust effects of PSI on PAG-seeded functional connectivity seen in the rostral ACC and dlPFC

To try and build the least confounded model for PSI effects, disease duration and age were both included as covariates and as with earlier analyses they improved the strength of PSI relationships. The model produced highly significant ($p<0.01$) effects for PSI in the brain-wide analysis including the ACC (R>L, including rostral pregenual areas and dorsal ACC), dlPFC, L superior frontal gyrus and adjacent paracingulate (Figure 12).

Figure 12. PAG-seeded functional connectivity: PSI effect with age and disease duration covariates

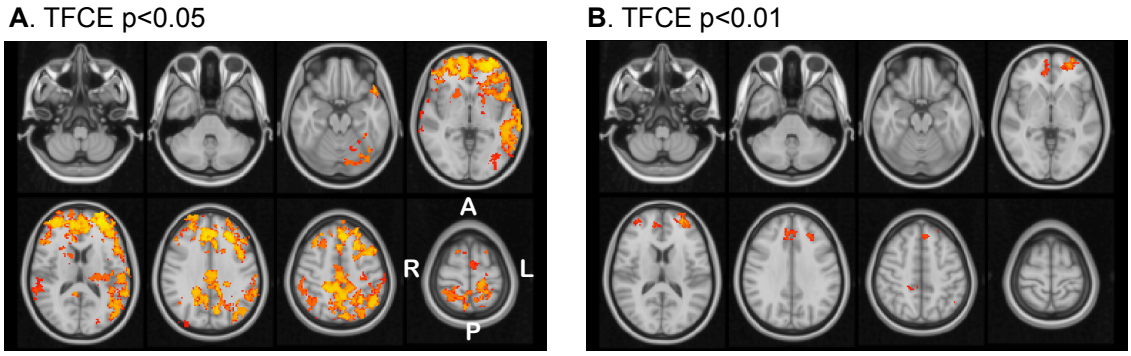

The effect of controlling for age and disease duration revealed multiple significant regions of PAG-seeded functional connectivity associated with pain score (PSI) for whole brain statistics, most notably bilateral dorsolateral prefrontal cortices and rostral pregenual ACC both surviving low p-value ($p<0.01$) thresholded TFCE maps (B). R, right; L, left; A, anterior; P, posterior.

Needless to say, these highly significant associations were reflected in the DPMN masked statistics within the same areas; the negatively associated rostral medullary activity

(described above; see figures 11 and 9B) was borderline significant (p=0.08) for DPMS masked statistics and significant (p=0.01) for brainstem-only masked statistics.

The covariates, age and disease duration, were also used to extend the earlier analysis of meaningful vs. low pain however this produced no new significant brain-wide or DPMN-masked results.

Spatially small PAG glutamate concentration associated effects in PAG-seeded resting state data

No brain-wide or DPMN-masked effects were seen for MRS determined PAG glutamate concentration related PAG-seeded functional connectivity (see Chapter 7). When corrected for age, whole-brain analysis of patient PAG-seeded functional connectivity associated with PAG-glutamate concentration showing a small significant negative association in the L superior division of the lateral occipital cortex bordering the precuneus, whilst DPMN-masked analysis of controls revealed a small borderline significant positive association (p=0.1) apparent in the R ventromedial prefrontal cortex.

Discussion

Statistically robust areas of PAG-seeded functional connectivity positively related to pain severity (PSI) are shown in the anterior cingulate cortex (ACC, R>L) and dorsolateral and ventrolateral pre-frontal cortices (dlPFC & vlPFC, L>R). Additionally, an area of the brainstem, anatomically compatible with the rostroventral medulla (RVM), consistently shows an inverse relationship between PAG-seeded functional connectivity and pain

severity (PSI). In other words, higher pain associates with more ACC/PFC PAG-seeded functional connectivity and with less RVM PAG-seeded functional connectivity.

The PFC and ACC are posited to have a central role in descending pain modulation, initiating downstream analgesic activity and effecting emotional modulation of pain (Cooper, 1975; Lorenz et al., 2003; Pastoriza et al., 1996; Patrick Hardy and Haigler, 1985; Petrovic et al., 2000; Ploghaus et al., 1999; Wager et al., 2004; Zhang et al., 1998). Many recent insights into the functional organisation of these rostral elements of descending pain modulatory activity are gleaned from fMRI placebo experiments in humans; broadly, these show increased dlPFC and rostral ACC (rACC) to brainstem (PAG and RVM) connectivity in anticipation of placebo and during delivery of placebo (Eippert et al., 2009a; Wager et al., 2004). In a single study by Eippert et al, a subtle differential activation of the rostral ACC (rACC) was found with relation to placebo experience: the pregenual rACC *de*-activated and the subgenual rACC activated during placebo administration (Bingel et al., 2006; Eippert et al., 2009a; Wager et al., 2004). Although my rACC results might be compatible with a differential PAG-rACC connectivity hinted at in Eippert et al's work (appearing pre-genual), the PAG-seeded pain related functional connectivity with the PFC and rACC in general are at odds with the rest of the literature. Clearly, the NMO chronic pain model differs substantially from that of an acute placebo or pain-expectation experiment on healthy participants, and perhaps this is where the explanation lies. This is further discussed in Chapter 9.

Resting-state network ICA revealed multiple networks consistent with those found in the literature and serves to reinforce the robustness of my data. On dual-regression analysis a

network involved in salience and executive function demonstrated multiple large significant clusters of greater connectivity in patients compared to controls, the largest of which was located in the pregenual-rostral anterior cingulate; an area, as discussed above, that is deactivated during placebo analgesia (Eippert et al., 2009a). When analysing networks with respect to PSI scores, a visuospatial network, involving many areas posited to underlie introspection, showed connectivity in the PCC positively related to PSI score (Beckmann et al., 2005); one can hypothesise that this connectivity somehow relates to the interoceptive monitoring of the spatial extent of subjective chronic pain. It is difficult to draw definite conclusions from the data-driven ICA of resting-state networks, suffice to say meaningful differences were found across patients, pain groups and controls.

The visually apparent increased spatial extent of mean PAG-seeded functional connectivity for patients compared to controls, and for higher versus lower pain scores is visually interesting but statistically lacks power. The PAG plays a host of roles in relation to emotional or aversive events (including respiratory control, fear processing, and defensive behaviour) that could all conceivably be modified by a disease state or chronic pain (Carrive, 1993; Faull et al., 2015). The small significant area in the L angular gyrus apparent for PAG-seeded functional connectivity greater in patients than controls is reliably shown as part of the DMN in studies where proposals about its exact function range from manipulation of acquired knowledge or mental projections of the future (Seghier, 2013).

An interesting result was the enhancing effect that controlling for age and disease duration measures had on PSI effects. It is known that age has complicated effects on resting state networks, including DMN connectivity, that are often difficult to unravel from associated

structural age-related changes (Goldstone et al., 2016). It is possible that these age-related changes are accounted for when correcting for age, however this does not explain why correcting for disease duration should have such an impact. It is feasible and probable that the chronicity of NMO has some correlates with brain function, and indeed there is some evidence for accumulating damage (both T2-hyperintense and 'unseen'; see Chapter 1b), but exactly how these might playout is far from clear.

Another interesting result is the lateralisation of significant effects: predominantly right ACC and left DFC. It is possible that the subtle differences in the average laterality of pain distribution (see Chapter 3 for participant pain maps) can explain this given that the contralateral differences are hidden just below the threshold of significance (and in light of the small significant contralateral effects seen).

A number of areas reduce the interrogative power of the above analyses. No control measures of T2 brain lesion location or volume, brain atrophy or measure of NAGM loss were acquired; these could conceivably influence the functional networks studied. An additional longitudinal arm assessing changes in pain measures over time would have been a useful adjunct able to corroborate some of the findings. Furthermore, techniques of resting-state network analyses confer no information regarding directionality and although it is possible to determine if two areas are 'firing' together, it is impossible to comment of causation.

Conclusion

ICA revealed robust resting-state network data consistent with the existing literature. PAG-seed based analyses showed connections inversely related to pain intensity in an area of the brainstem, anatomically compatible with the rostroventromedial medulla, a finding that fits well with existing studies, however, pre-frontal and rostral anterior cingulate cortices showed positive associations with the PAG-seed in relation to pain severity which are in stark contrast to findings from placebo effect studies: dorsolateral pre-frontal cortices and the rACC have previously been reported to show greater connectivity with the PAG in the anticipation and experience of placebo analgesia, postulated as evidence of opioidergic descending pain modulatory system activation, and thus connectivity between these and the PAG is usually associated with analgesia (Eippert et al., 2009a; Wager et al., 2004).

Chapter 7

Experimental chapter: 3T MRS of the periaqueductal grey and NMO pain homeostasis

Introduction

^{1}H magnetic resonance spectroscopy (MRS) of the central nervous system is a powerful technique that allows spatially localised in-vivo quantification of a limited set of metabolites. The background to MRS is discussed in Chapter 2.

In this chapter MRS is applied to the periaqueductal grey (PAG) of NMO participants as a novel technique to investigate the chronic pain aetiology of this disease. Previous MRS studies in NMO have neither looked at pain nor imaged the PAG, but show the following general features in CNS tissue: normal N-acetylaspartate (NAA) and myo-inositol (mI) concentrations (the commonly assessed metabolites in neuroinflammatory disease) in normal appearing CNS tissue (i.e. grey and white matter without T2-hyperintense lesions), and low mI with relatively preserved NAA within NMO cord lesions (Ciccarelli et al., 2013; De Seze et al., 2010).

MRS has also been applied in chronic pain, across diverse conditions including chronic back pain and fibromyalgia, and in general shows reduced NAA in areas including the dorsolateral prefrontal cortex (PFC) and anterior cingulate cortex (ACC), glutamate changes (positive and negative) in the ACC, ventrolateral PFC, insula and amygdala (Ito et al., 2017; Pyke et al., 2017; Zhao et al., 2017), and correlations between midbrain NAA and migraine frequency (Lai et al., 2012).

As discussed in detail in Chapters 1c and 6, the PAG plays a central role in descending pain modulation, with both facilitatory and inhibitory effects on dorsal horn pain processing via the rostroventral medulla (RVM) and probably also via reciprocal connections with the locus coeruleus (and other noradrenergic nuclei with projections to the dorsal horn) (Cameron et al., 1995; Cedarbaum and Aghajanian, 1978; Fields and Basbaum, 1978; Mantyh, 1983). Aside from a recent study in obstructive sleep apnoea (Macey et al., 2017) and an earlier study on episodic migraine (mentioned above) (Lai et al., 2012), few studies have performed MRS in the PAG and no studies known to the author have used MRS determined PAG glutamate to study chronic pain in humans. Therefore, in this chapter, a central component of the descending pain modulatory system, the PAG, is investigated using ^{1}H MRS in a population of NMO patients with varying degrees of chronic pain.

Objectives / Aims

1. Ascertain detectable PAG neurotransmitter (glutamate/GABA) concentrations and determine if differences correlate with pain severity.

2. Evaluate MRS evidence of underlying PAG damage in NMO patients and analyse if this relates to pain severity.

Methods

The full NMO Imaging Cohort underwent MRS at scan time and details of this cohort are provided in Chapter 3. Thirty of the 33 patients and all 24 controls had MRS data meeting data quality parameters and were included (see Table 1).

Table 1. Participant baseline characteristics

	Patients	**Controls**
n	30	24
Female, n(%)	24 (80)	15 (62.5)
Age, mean(sd)	53.5 (14.7)	53.6 (16.1)
Onset age, mean(sd)	43.9 (16.9)	
DD, mean(sd)	9.6 (6.1)	
No. of attacks, med(range)	3.5 (1-28)	
No. of TM attacks, med(range)	3 (1-28)	
EDMUS, med(range)	3 (1-28)	
PSI, mean(sd)	17.6 (11.7)	
Afro-Caribbean, n(%)	4 (13.3)	
Asian, n(%)	8 (26.7)	
Caucasian, n(%)	18 (60)	

sd, standard deviation; med, median

Imaging

All participants had 3D MPRAGE T1-weighted images of the brainstem acquired, over which the PAG voxel was positioned. Figure 1 shows an example of the PAG spectroscopy voxel placement. Imaging protocols can be found in Chapter 2.

Figure 1. Example PAG voxel placement (on T1-weighted image)

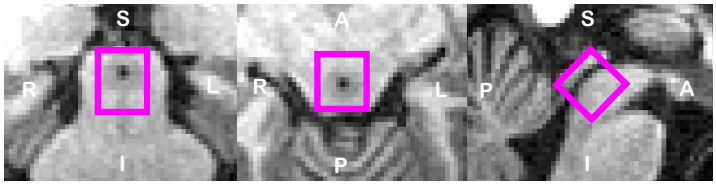

MRS PAG voxel placement overlaid on example participant's T1-weighted MRI. Pink outline = 10x10x10mm spectroscopy voxel; Orientation: coronal – axial – sagittal; S, superior; I, inferior; R, right; L, left; A, anterior; P, posterior

Metabolite quantification

Siemen's TWIX data were imported into MATLAB where MRS data were eddy-current corrected and phase corrected using a least-square algorithm in MRspa (https://www.cmrr.umn.edu/downloads/mrspa/), a semi-automated MATLAB routine. Data were corrected for T2 relaxation times, tissue water content and CSF contributions (determined by FSL's *FAST* segmentation in the PAG). The brainstem was segmented using FSL's *FIRST* (FMRIB's software library v5.0) and whole volume was calculated using FSL's *fslstats* (Jenkinson et al., 2012). Metabolites were then quantified with LCModel5 (Provencher, 2001) with water scaling on using simulated basis spectra with a measured macromolecule spectrum. The reliably of quantified metabolites was enforced by rejecting measures where modelled standard deviations (Cramér-Rao lower bounds, CRLB) were

>50% and where internal correlations (Pearson's r) were < -0.5. Each metabolite was then only used in subsequent analyses if ≥50% of participants had reliable measures.

Statistics

All two-group comparisons were performed using un-paired 2-sided Student's T-tests. Correlations were calculated using Pearson's r. Multiple linear regression analyses were performed with PSI, age or disease duration modelled as independent predictors of PAG glutamate concentration.

Results

Seven separate metabolites were reliably quantified (and 4 metabolite pairs; Table 2). Twenty-six patients and 23 controls had quantifiable concentrations of glutamate (Glu).

Borderline significant differences (p=0.1) were found between patients and controls for Glu and Glu+Gln, otherwise no statistically significant differences were found. Examples of spectra pre-baseline correction and with visibly different glutamate profiles are shown in Figure 2A and B.

No non-glutamate neurotransmitters were resolved with low enough standard deviation for meaningful inclusion (e.g. GABA).

Table 2. Metabolite concentrations

	all participants		patients		controls	
	n	mean (sd)	*n*	mean (sd)	*n*	mean (sd)
mI	*54*	9.5 (1.4)	*30*	9.7 (1.5)	*24*	9.2 (1.1)
NAA	*54*	8.5 (1.2)	*30*	8.6 (1.4)	*24*	8.4 (1)
NAAG	*36*	2.3 (0.8)	*17*	2.5 (1)	*19*	2.2 (0.6)
NAA + NAAG	*54*	10.4 (1.3)	*30*	10.4 (1.6)	*24*	10.4 (0.9)
Cr	*38*	5.4 (1.9)	*20*	5.4 (2.2)	*18*	5.3 (1.6)
Cr + PCr	*54*	7.6 (0.9)	*30*	7.8 (1)	*24*	7.5 (0.6)
Glu*	*49*	5.1 (1.6)	*26*	5.5 (1.8)	*23*	4.7 (1.2)
Glu + Gln*	*50*	6.7 (2.5)	*27*	7.2 (2.8)	*23*	6.1 (1.8)
GPC	*50*	2.2 (0.5)	*27*	2.2 (0.5)	*23*	2.3 (0.4)
PCh + GPC	*54*	2.4 (0.4)	*30*	2.3 (0.4)	*24*	2.4 (0.3)
Macromolecules	*54*	0.1 (0)	*30*	0.1 (0)	*24*	0.1 (0)

mI, myoinositol; NAA, N-acetylaspartate; NAAG, N-acetylaspartylglutamate; Cr, creatine; PCr, phosphocreatine; Glu, glutamate; Gln, glutamine; GPC, glycerophosphocholine; PCh, phosphocholine

* borderline significant differences (p=0.1) for patients vs. controls

Figure 2. (**A**) Example spectrum; (**B**) Comparison of two spectra with visually apparent glutamate differences

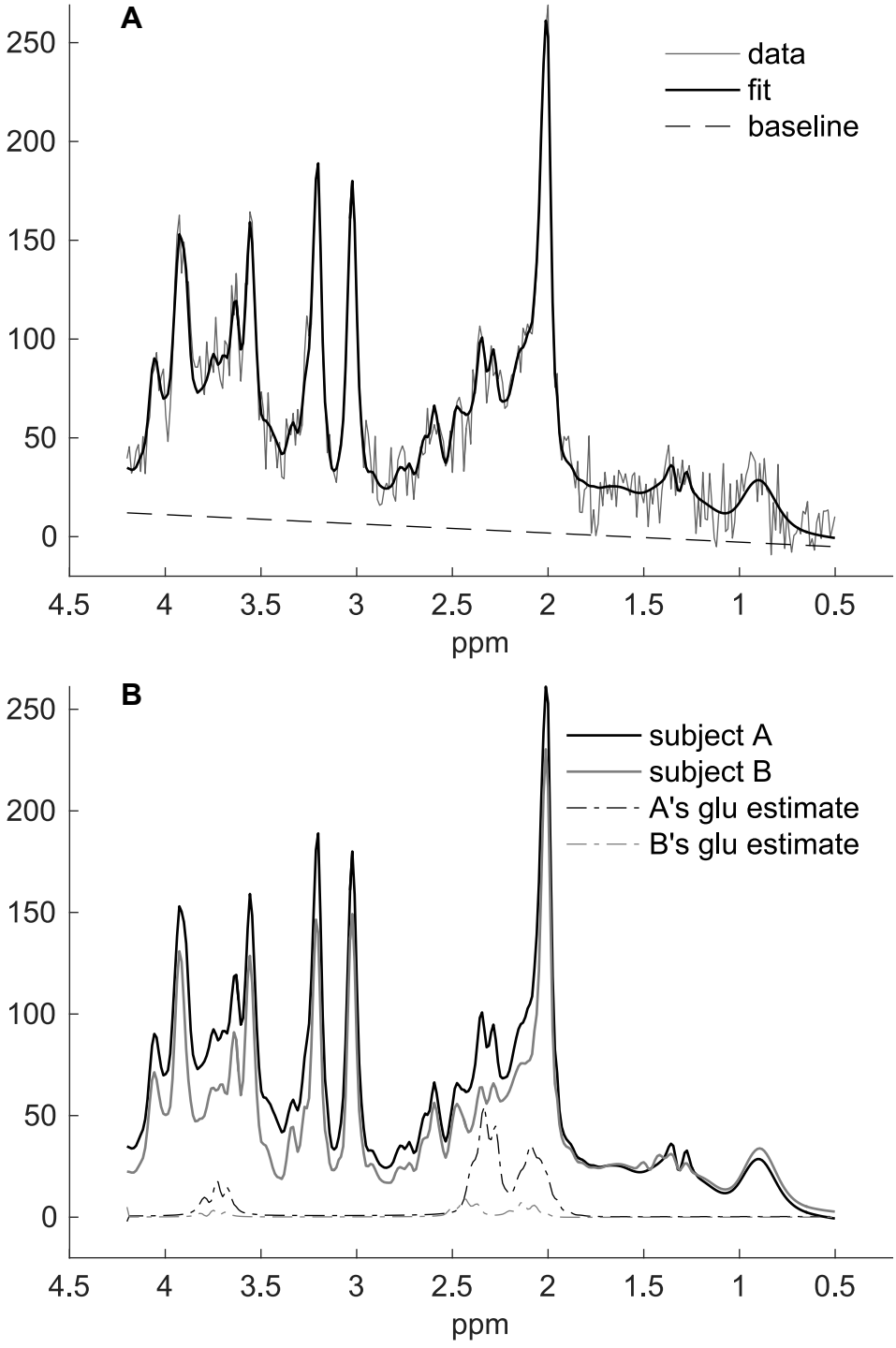

Example spectra from (A) a single subject showing good fit to data and linear baseline and (B) two subjects overlaid showing visible differences, especially in glutamate peaks. ppm, parts per million. In B data are baseline corrected; Glu, glutamate.

Glutamate levels predicted by pain severity

Glutamate showed a borderline-significant (p=0.05) correlation with PSI and a significant correlation (p=0.03) with painDetect (Figure 3; see discussion).

Figure 3. (**A**) PSI and (**B**) painDetect vs absolute glutamate concentration

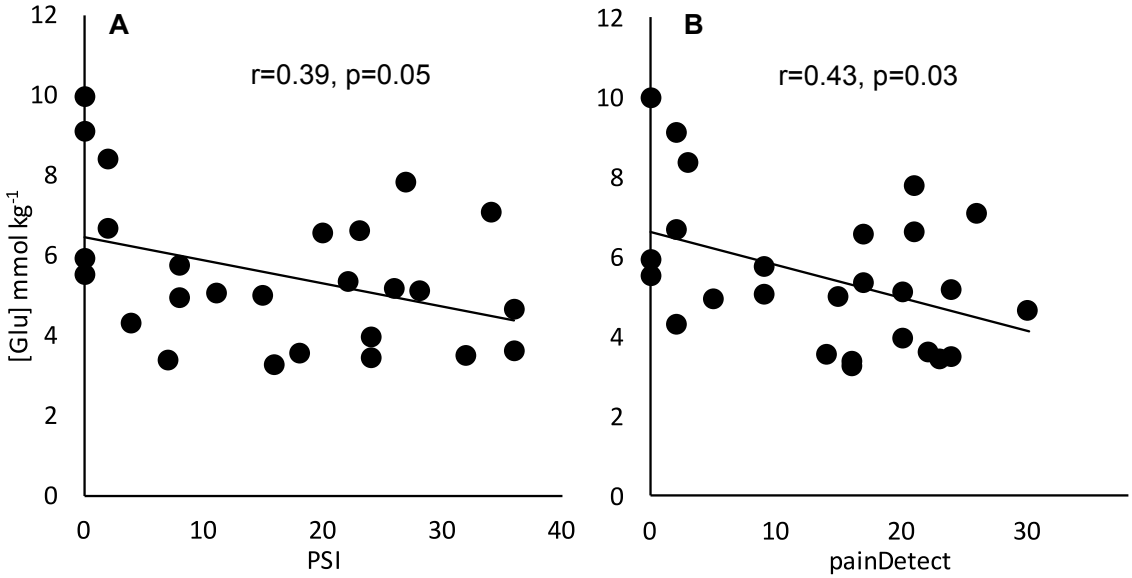

Glutamate showed negative correlations with pain measures, PSI (A) and painDetect (B). PSI, pain severity index; [Glu], absolute glutamate concentration.

Regression analysis was performed to see if any of PSI, age or disease duration were significant predictors of PAG glutamate concentration. Of these, PSI was uniquely predictive (p=0.026) with a standardised beta-coefficient of -0.49. The adjusted R-squared of the model was 0.139 and not significant, suggesting these three variables combined cannot reliably predict the glutamate concentration. EDMUS was not included as an independent variable because of its significant correlation with PSI (see Chapter 3).

PAG glutamate lower with higher pain and lower in controls

Figure 4. Box and whisker plot for glutamate concentrations by participant group

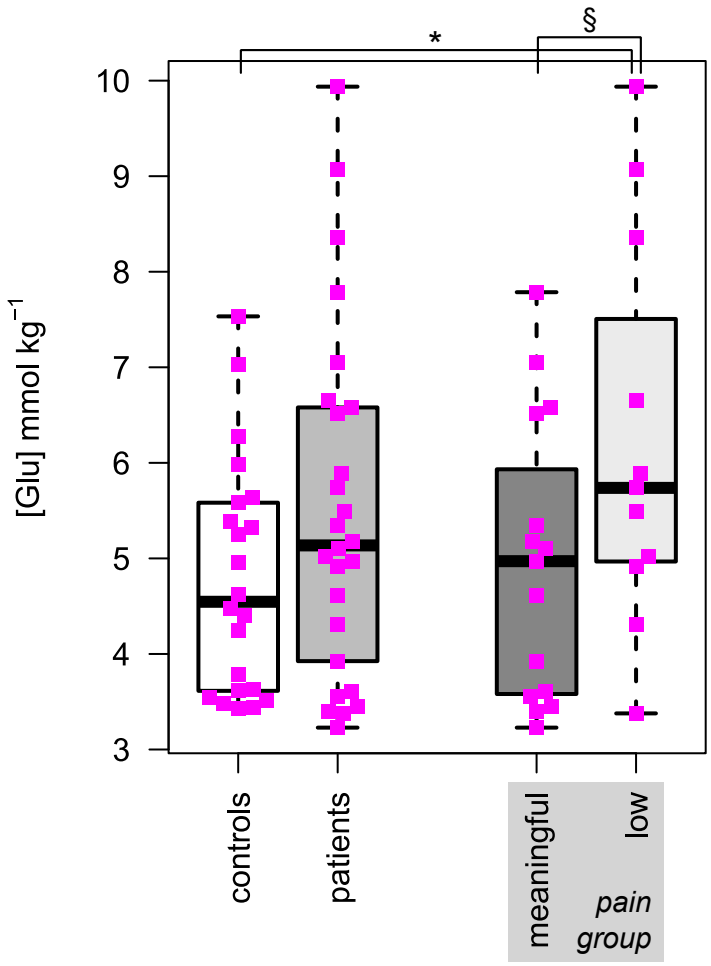

Glutamate concentration was visibly greater in patients compared to controls (not significant), however when patients were divided into meaningful and low pain subgroups, glutamate concentrations were lower for meaningful vs. low pain, and higher for low pain vs. controls. That is, low pain subjects had the highest level of PAG glutamate, greater than meaningful pain sufferers and controls (the latter two's glutamate concentrations appearing very similar). *p < 0.05 for unpaired t-test; § p=0.09 for unpaired t-test; [Glu], absolute glutamate concentration; Individual data-points superimposed in pink squares

The difference between patient and control concentrations of glutamate was borderline significant (p=0.1; Table 2 & Figure 4). Interestingly, the low pain group had higher PAG

glutamate concentrations compared to controls ($p<0.05$) and compared to the meaningful pain group ($p=0.09$; Figure 4).

At first glance, this is the opposite of what one might intuitively expect: low pain participants might be expected to look more like controls; this is addressed in the discussion below.

<u>No lesion location effect on glutamate concentration</u>

Figure 5. PAG glutamate concentration by lesion location group

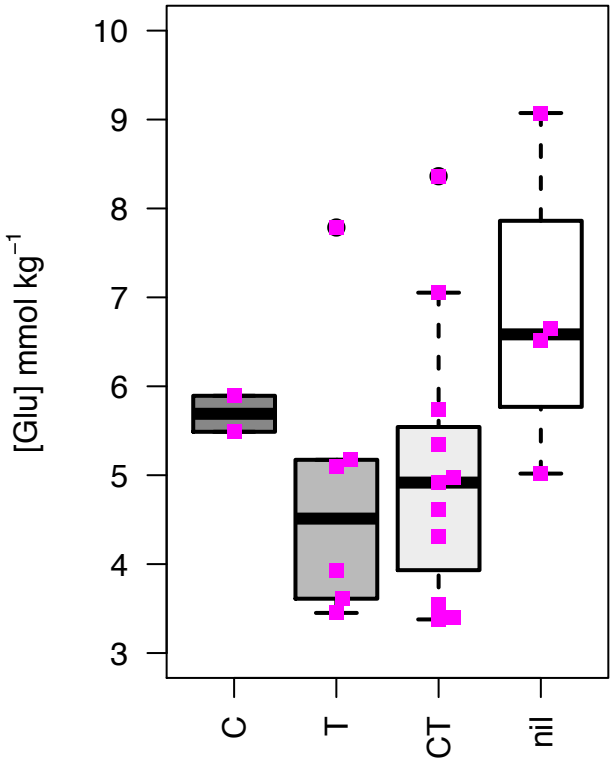

No significant differences were identified for participant glutamate concentrations organised by lesion location. C, cervical lesions only; T, thoracic lesions only; CT, cervicothoracic; nil, no current lesion; No significant difference across groups (ANOVA).

When subdivided by gross current lesion location, no significant differences were found between groups (Figure 5), although visually the absence of lesions seems to equate with high glutamate concentrations, this was not significant.

<u>There was no relationship between NAA and mI and patient or control group, age, disease duration or disability</u>

NAA and mI did not significantly correlate with any of PSI, EDMUS, disease duration or age. They did correlate with one another ($r=0.633$, $p<0.01$; Figure 6) however neither correlated with glutamate. Regression models with independent contributions from PSI, EDMUS, disease duration and age failed to find significant predictive factors for NAA or mI concentration (data not shown).

Figure 6. Correlation between PAG mI and NAA concentrations

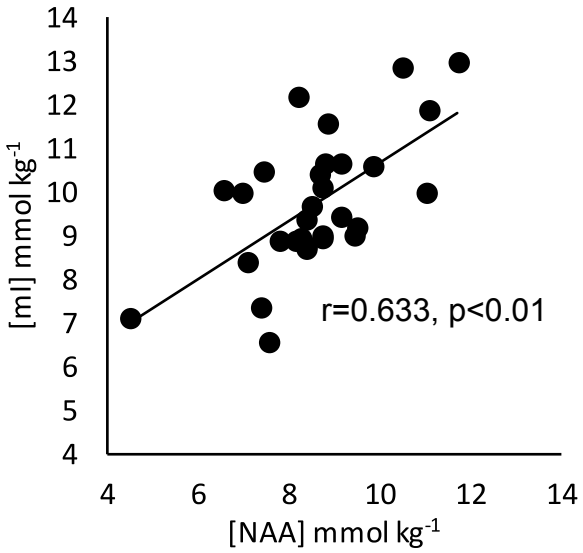

Metabolites myo-inositol and N-acetylaspartate correlated strongly with one another (as shown), but not with glutamate. [mI], absolute myoinositol concentration; [NAA], absolute N-acetylaspartate concentration.

No significant difference was found between patients and controls for either NAA or mI (Figure 7).

Figure 7. Relative concentrations in patients and controls for (**A**) mI and (**B**) NAA.

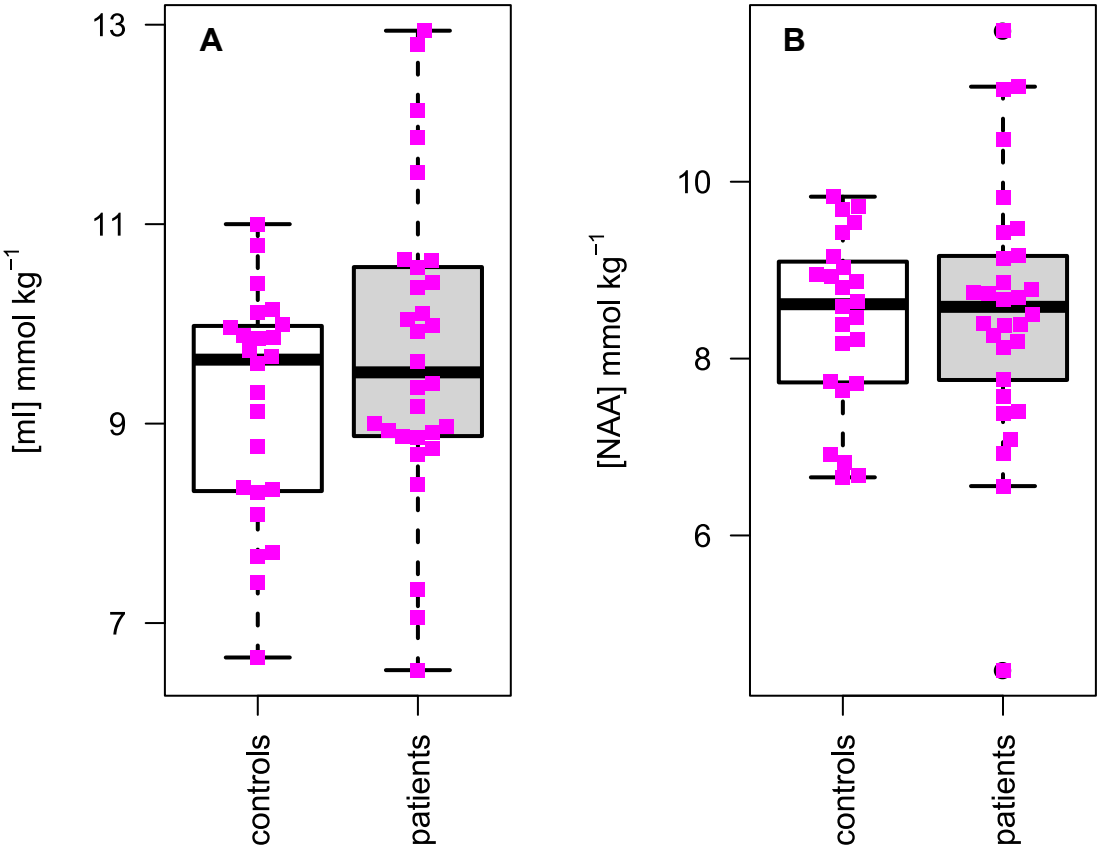

No difference was found between patients and controls for myo-inositol (A) or N-acetylaspartate (B) concentrations implying little 'hidden' damage to the PAG. [NAA], absolute N-acetyl aspartate concentration; [mI], absolute myoinositol concentration; Individual data-points superimposed in pink squares.

<u>Brainstem lesions associate with higher glutamate and myo-inositol levels</u>

Brainstem lesions were present in 42% (14/33), of the Imaging Cohort; 9% (3/33) had periaqueductal lesions. In those with viable glutamate measures, 35% (9/26) had brainstem lesions (three periaqueductal lesions included). The presence of lesions in the PAG was

associated with significantly higher mean Glu concentration and borderline-significantly higher mI levels compared to lesion-free participants (Figure 8).

Figure 8. Effect of PAG lesions on PAG metabolite concentrations

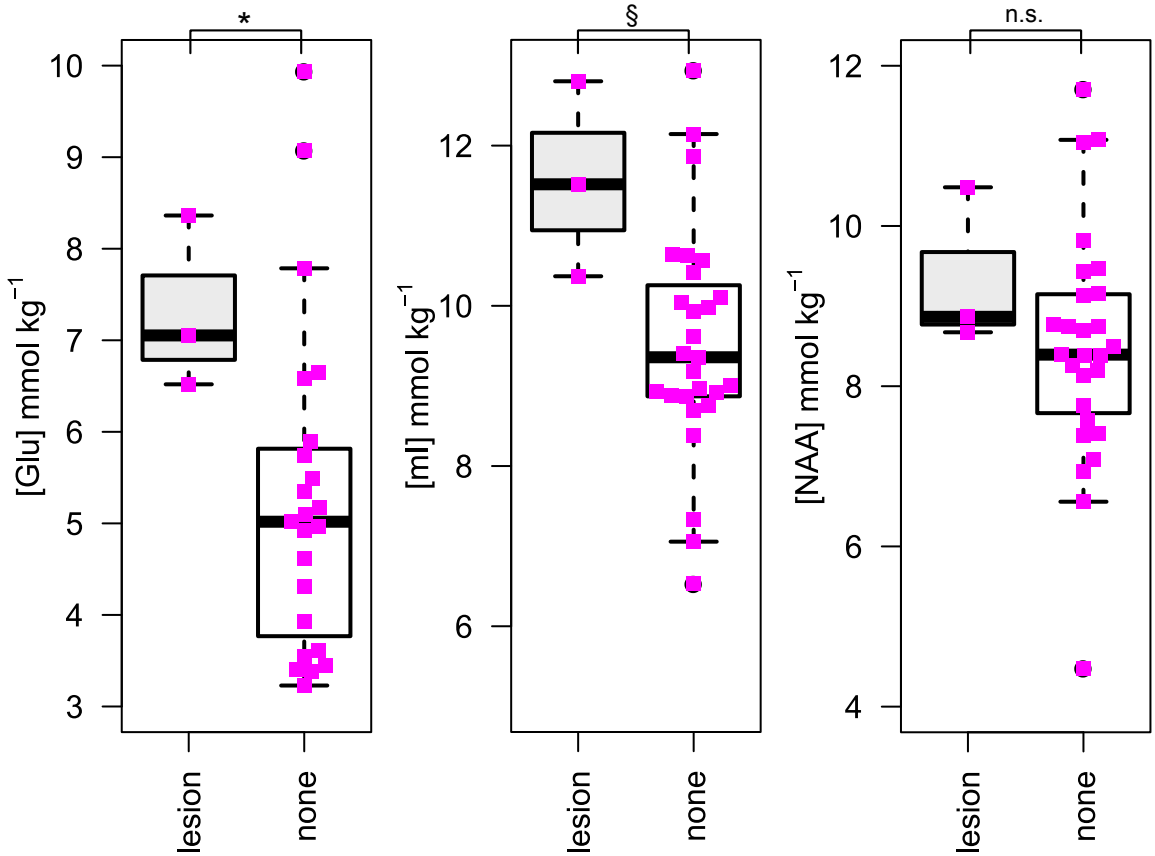

Significantly greater glutamate concentrations and higher, but not significant, myo-inositol concentrations were found in the PAG for those with lesions compared to those without. *, $p<0.05$; §, $p=0.08$; n.s., non-significant; [Glu], absolute glutamate concentration; [mI], absolute myo-inositol concentration; [NAA], absolute N-acetyl-cysteine concentration.

There was no relationship between the presence of PAG lesions and pain (data not shown).

Discussion

PAG glutamate concentration, corrected for age and disease duration, showed a significant negative correlation with chronic neuropathic pain severity in NMO patients. PAG

glutamate was also greater in low pain groups compared to meaningful pain groups and controls. Together, these two key results suggest that the PAG (or an anatomical portion thereof) exhibits excitatory activity in patients negatively correlated with the degree of chronic pain, whilst in controls this excitatory activity remains 'at baseline'. It is hypothesised therefore that those with higher pain are those who do not sufficiently 'activate' descending inhibition via the PAG (enough to overcome descending facilitation that is likely also present) in response to a neuropathic pain triggering insult (for example NMO myelitis).

This 'excitatory' activity of the PAG is potentially mediated by spinal afferent or rostral inputs, i.e. as direct feedback from noxious afferents to the PAG, from interconnected brainstem nuclei (including reciprocal connections from the RVM and locus coeruleus) or from more rostral sites integrating motivational and emotional processing (e.g. the rACC or PFC) (An et al., 1998; Ezra et al., 2015; Kwiat and Basbaum, 1990; Marchand and Hagino, 1983; Wiberg et al., 1987; Wyss and Sripanidkulchai, 1984). Direct injection of glutamate into the ventrolateral PAG in rats inhibits nociception at the level of the dorsal horn (Carstens et al., 1988; Jones and Gebhart, 1988), actions mediated through NMDA receptors (Jacquet, 1988) and balanced by tonic GABAergic inhibitory neurones (neurones *inhibited* by opioids with the consequence of releasing descending inhibition) (Vaughan et al., 1997), and it is likely that brain inputs to the PAG act on these receptors. Consequently, the increased glutamate concentrations observed here (posited as 'excitatory' activity of the PAG) are likely the result of increased excitatory input with the probable consequence of greater descending inhibition. Furthermore, no group differences between patients and controls were found for any other quantifiable metabolite, including N-acetylaspartate (NAA) and myo-inositol (mI), providing evidence that unseen NMO damage was not a

feature of NMO PAG tissue (although, see below regarding PAG lesions and metabolite concentrations). An NMO lesion in the PAG, with astrocytic damage and glutamate dysregulation, could in theory potentiate descending inhibition by increasing glutamate availability for descending facilitatory pathways, but this did not appear to be the dominant mode of action here (see discussion below) (Hinson et al., 2008). Overall these results suggest that 'pain vulnerability' may contribute to higher pain in certain NMO participants that is independent of NMO-related brainstem damage (Denk et al., 2014).

The neuropathic-potential of CNS insults (i.e. cord myelitis) was not directly assessed. In Chapters 4 and 5 the location of cord damage is shown to be highly relevant to pain severity; the same relationship is hinted at above (see Figure 5) but is far from statistically significant.

The PAG glutamate findings sit well with current literature. The PAG is important in a diverse range of survival essential behaviours dealing with stress or threat, not least pain related behaviours (Fields and Basbaum, 1978). Part of this response, mediated by the opiate-sensitive analgesia-producing ventrolateral PAG (Hosobuchi et al., 1977), seems to be amenable to both GABAergic inhibition (Depaulis et al., 1987) and glutamatergic stimulation (Siegfried and Nunes de Souza, 1989), with a GABA-disinhibition hypothesis proposed as a mechanisms of action for cannabinoid and opioid analgesic effects (Lau and Vaughan, 2014; Samineni et al., 2017). The MRS findings of this chapter are consistent with the concept of PAG glutamate mediated descending inhibition of ascending pain information.

The suggestion above that lack of MRS evidence of NAA and mI differences between patients and controls in normal appearing tissue is indicative of the absence of NMO related

damage is supported by numerous examples in the literature where MRS has been used to demonstrate occult damage (Gustafsson et al., 2007; Sun et al., 2017; Wattjes et al., 2007) and the absence of damage (De Seze et al., 2010) in normal appearing white matter and grey matter of neuroinflammatory disease participants. Nevertheless, the present study did reveal a borderline significant relationship between current PAG lesions (albeit a small group of only 4 patients) and high myo-inositol concentrations, and interestingly also between current PAG lesions and high glutamate concentrations. There was however no direct relationship between PAG-lesions and pain, and indeed increased glutamate with lesions would be the wrong way around if the PAG-glutamate is reflecting increased descending inhibition. However, as alluded to above, there is the distinct possibility that increased glutamate in the PAG could reflect enhanced descending facilitation (or possibly a combination of the both in a delicate balance), however there is little by way of examples in current literature to support this phenomenon. The effect of lesions on these two metabolites might be explained by the unique pathology exhibited in NMO brainstem lesions. Brainstem lesions in NMO are generally non-necrotic, non-demyelinating and contain reactive astrocytes (Lucchinetti et al., 2014; Popescu et al., 2011; Roemer et al., 2007), i.e. they would show little damage (NAA loss) but these pathological astrocytic changes could hypothetically be reflected in high myoinositol and alterations in the glutamate-glutamine cycle.

A few limitations are recognised. The use of painDectect in correlations with glutamate may be inappropriate, and is included primarily for illustration purposes. The painDetect scale is not intended as a measure of pain intensity, but is a screening tool to detect neuropathic

disease (Freynhagen et al., 2006). That said, the components of the score are graded and one could argue that the total is a sum of neuropathic feature severity.

Another limitation is that, as alluded to above, the functions of PAG are diverse and include roles in respiration, anxiety, panic and fear processing, defensive behaviour and emotional expression (Bandler and Shipley, 1994; Faull et al., 2015; Graeff et al., 1993; Tovote et al., 2016; Watson et al., 2016). Additionally, although anatomically small, the substructure of the PAG is complex and modular (Carrive, 1993; Ezra et al., 2015). It thus brings into question exactly *where* I am finding glutamate changes in a 1ml voxel that envelops the whole PAG (and small amounts of surrounding tissue) and exactly *which* clinical parameters are exerting a glutamate specific effect. Future studies, perhaps with MRS at 7T, might better elucidate these unknowns and allow researchers to selectively probe the ventro-lateral PAG. Another consideration is the timescale at which local glutamate concentrations might change; that is, am I measuring something with terribly high intra-participant variance? A recent study linking fMRI BOLD signal with glutamate concentration shows >3% variations in glutamate over minutes (Ip et al., 2017), not a large enough percentage change to affect my results but over longer timescales a conceivable confounder. Future studies investigating chronic pain measuring PAG fMRI BOLD and real-time glutamate would almost certainly be enlightening.

Conclusion

PAG glutamate concentration is negatively correlated with chronic neuropathic pain severity in NMO patients. Additionally, PAG glutamate is also greater in low pain groups compared to meaningful pain groups and controls and it is hypothesised that the results may indicate an inability in 'vulnerable' participants to activate descending pain control in the present of CNS damage.

Chapter 8

Experimental chapter: The ^{1}H-NMR NMO plasma metabolome and pain

Introduction and Background

^{1}H NMR (or MR) spectroscopy is a non-invasive technique that can determine the metabolomic profile of biofluids (Holmes et al., 1994) and has a wide range of applications across disparate disciplines, including within the food and drink industry where for example it has been used to differentiate horse meat from beef (Jakes et al., 2015) and to determine a coffee's country of origin (Arana et al., 2014), but also in the medical world with applications from amyotrophic lateral sclerosis (Gray et al., 2015) to cancer biomarker discovery (Serkova and Glunde, 2009). A single NMR spectrum is able to detect every hydrogen-containing metabolite present in a biofluid above micro-molar concentrations. Therefore, the NMR spectrum represents a molecular fingerprint of an individual at a given point in time.

Data-driven analysis techniques

Invariably, metabolomics datasets contain many more data points (metabolites, e.g. amino acids, lipoproteins, glucose) than samples (participants) and breaking-down and making sense of this multivariate data can be challenging. Straight-forward logistic regression in these circumstances is usually unhelpful: with so many variables, a predictive model is easily built but usually one without unique independent variable contributions and consequently little added inference. Herein lie the strengths of multivariate techniques such as principle component analysis (PCA) and partial least squares discriminant analysis (PLSDA). Both PCA and PLSDA reduce the complexity of the data by creating linear combinations of variables, called principle components, which explain the greatest variation in the data. In the case of PLSDA, the component explaining the greatest variance in the data that aligns to the greatest variance in the dependent categorical variable is selected as the first principle component. The second principle component is the one orthogonal to the first that represents the next greatest variation in data and category. Theoretically, if all components are modelled, the model fits the data perfectly, however the advantage of restructuring the data in this way is that a large proportion of variance in the data can now be represented in terms of the first few principle components. For example, we might be able to use three high-variance components of the data (predictive components) to estimate the dependent categorical variable with considerable accuracy (having discarded the lesser variance-explaining components). The result provides some inference as to what is most important in determining the dependent categorical variable, and also allows one to predict the dependent variable given a set of new variables. A detailed account of the mathematics and principles of PLSDA are outside the scope of this chapter, but some helpful insights can be found in Brereton and Lloyd, 2014.

The power of metabolomics

Metabolomics is the study of biological system-wide metabolite profiles, or metabolomes. Metabolomes have a close relationship with both genotype and phenotype (Rochfort, 2005). Using metabolomics, subtle changes in an organism's "biochemical matrix" can be detected and used to investigate diverse influences from the effects of pharmaceuticals and the environment to that of differing disease states (Mitchell et al., 2002).

Recently, the technique has been used to successfully differentiate multiple sclerosis (MS) subtypes (Dickens et al., 2014), and to differentiate MS from AQP4Ab positive NMO (Moussallieh et al., 2013). The studies further explored the most important metabolites driving the separation; the differentiating metabolites for MS subtypes included fatty acids, phosphocholine, N-acetyl species glucose and β-hydroxybutyrate, and for NMO versus MS included scyllo-inositol and acetate.

There is clearly utility in metabolomics for NMO diagnosis and there have been numerous and wide-ranging applications to pain in general, from targeted metabolomics of the murine dorsal horn showing altered sphingolipid metabolism (Patti et al., 2012) to human CSF studies of chronic regional pain syndrome showing catabolism related changes in keto-acids and glucose (Meissner et al., 2014).

In this chapter, the aim was to differentiate NMO patients with meaningful pain from those with low pain, and if successful, to interrogate the important metabolites driving the separation, hoping to glimpse insights into the aetiology of pain in NMO. Although the NMO pain differentiation was largely unsuccessful, the power of the technique is demonstrated

in the proof-of-principle relapsing-remitting MS (RRMS) versus NMO discrimination below.

Objectives / Aims

1. Separate NMO and RRMS patients using only blood plasma spectra (as a proof of principle for the metabolomics PLS-DA technique within the NMO cohort).

2. Separate NMO patients with differing pain scores using only blood plasma spectra and determine key metabolites driving the separation.

Methods

Sample preparation was performed in Prof Daniel Anthony's laboratory in the Department of Pharmacology, Oxford, with the help of Dr Fay Probert and Dr James Larkin; spectroscopy was performed in the Department of Chemistry, Oxford, under the auspices of Prof Tim Claridge. Dr Probert oversaw sample preparation and retrieval of spectrometer data; the sample preparation and analysis methods below are based on those of Dr Larkin (Dickens et al., 2014) with modifications by Dr Probert and myself; spectrometer parameters were optimised by Prof Claridge and Dr Probert at run time.

Participants

NMO and relapsing-remitting MS (RRMS) participants were recruited from Oxford's NMO national clinic and Oxford's local MS service, respectively, at the John Radcliffe Hospital; informed consent was obtained under the NMO tissue bank protocol (Oxford REC no: 10/H0606/56).

A subset of the NMO patients completed a Brief Pain Inventory (BPI) Pain Severity Index (PSI) score; this cohort includes 32 of the 33 participants in the Imaging Cohort (Chapter 3).

As with the Imaging Cohort, NMO participants were asked to score NMO-attributed chronic pain and not spasm-related NMO pain or pain due to other non-NMO pathologies (however, as discussed in Chapter 3, the influence of other pain conditions will certainly influence their experience of NMO pain and cannot be fully accounted for). NMO participants for whom pain scores were acquired had scores recorded outside of a relapse.

Sex differences between groups were compared using Chi-square; age differences were compared using Student's t-test and ANOVA.

Sample acquisition

Blood was drawn into lithium-heparin green-top BD Vacutainer™ tubes and within 30 minutes of acquisition, centrifuged for 10 minutes at 2,200 x g, after which the supernatant (blood plasma) was aliquoted and stored at -80°C. The time of draw and time of centrifugation were logged. See Figure 1 for a summary of the processing pipeline.

Sample Preparation

Samples were defrosted at room temperature and ultra-centrifuged at 100,000 x g for 30 minutes at 4°C. One-hundred and fifty microliters of the middle ('aqueous') phase was removed and diluted in 450µl of 75 mM sodium phosphate buffer prepared in D_2O (pH 7.4). Samples were further centrifuged at 16,000 x g for 3 minutes to remove precipitates, before transfer into 5mm NMR tubes, pre-cleaned with Virkon™.

Figure 1. Summary processing pipeline: plasma sample to NMR spectra analysis

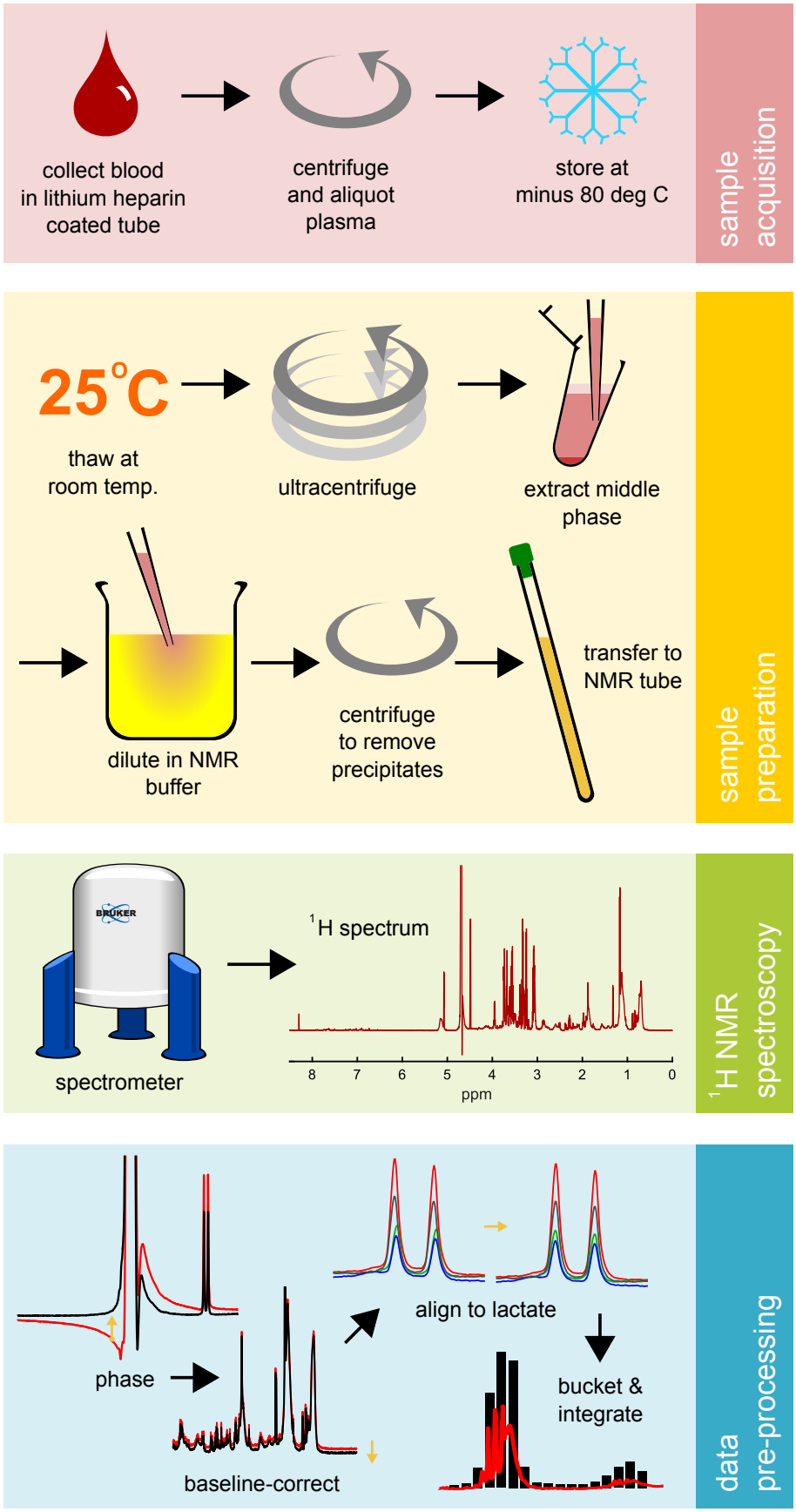

NMR Spectroscopy

Spectra were acquired on a 700-MHz Bruker AVII Spectrometer operating at 16.4T equipped with a ^{1}H ($^{13}C/^{15}N$) TCI cryo-probe, housed in the Department of Chemistry, Oxford. Samples were analysed at 310K. A spin-echo Carr-Purcell-Meiboom-Gill (CPMG) sequence with a τ interval of 400 μs, 80 loops, 32 data collections, an acquisition time of 1.5s, a relaxation delay of 2s, and a fixed receiver gain was used to supress broad signals arising from large molecular weight plasma components.

Data Processing

Free induction decay (FID) output from the CPMG spectrum was Fourier transformed after zero-filling by a factor of 2 and exponential function multiplication. Spectra were imported and visually inspected in MATLAB (MATLAB, 2015) using matNMR (van Beek, 2007). Spectra were re-imported into MATLAB (using 'rbnmr' script; Nyberg, 2013; modified by Dr James Larkin 2013), phased (Bao et al., 2013), baseline corrected with a third-order polynomial (matNMR script modified by Dr J Larkin 2013) and chemical shifts were referenced to the lactate-CH_3 doublet resonance at δ = 1.33 ppm (script by Dr J Larkin 2014, modified by Dr F Probert 2015). After removal of the water peak (4.3 – 4.9 ppm), spectra were split into 0.02ppm width 'buckets' and the integrals of each bucket were outputted as columns of comma-separated variables (i.e. '.csv' format).

Data Analysis

Bucketed integrals were imported into R (R Core Team, 2017) and all analyses were performed using R package *ropls* (Thevenot et al., 2015) and in-house scripts.

Principle component analysis (PCA) was used to inspect the data for structure and to identify outliers. Outliers were removed from further analysis if visual inspection of the spectra revealed distortion or contamination. Remaining spectra were subsequently analysed by PLS-DA (Brereton and Lloyd, 2014; Holmes et al., 1994).

All data points were used to find the number of principle components needed to optimise the Q^2Y of the PLS-DA models, and this number of predictive components was used for all subsequent models (including the null distribution, see below). The default minimum number of predictive components was set to two.

Models were cross-validated (x10) and compared with separately cross-validated 'null' models, created with randomly permuted class labels (see Figure 2 for analysis pipeline summary). The process was repeated (x100), each time matching class sizes by taking random samples from the larger class, and each time shuffling the data prior to folding into ten equal-sized blocks for cross-validation. Cross-validation was run on the ten unique 9:1 splits of the data, using 9 blocks to build a model and the remaining block to test each time. Accuracy was determined by how well the model predicted the classes of the testing block. The PLS-DA model was considered predictive if the accuracies of the model distribution were significantly different from that of the null distribution (p-value <0.05 as tested by the Kolmogorov-Smirnov test) and if the model distribution's mean accuracy was greater than 0.5 (p-value <0.05, one-tailed t-test).

Figure 2. Analysis Pipeline

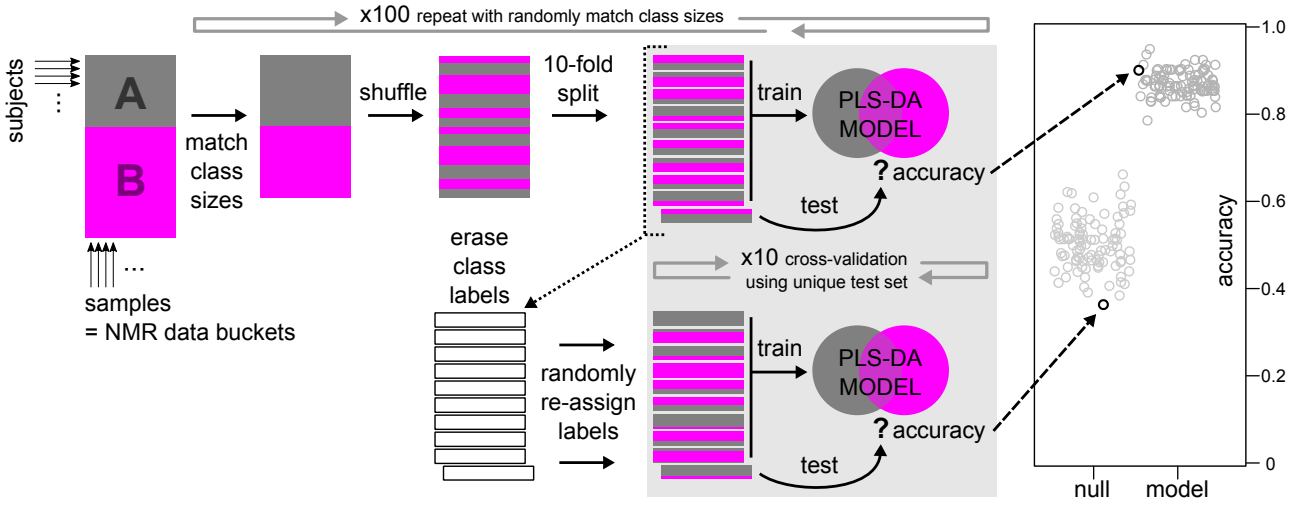

Schematic of the statistical analysis of bucketed NMR data points across subjects. Class sizes (e.g. pain / no-pain) are first matched using a random subset of the larger class. Subjects are then shuffled and folded into ten subsets. Nine of the subsets are used together to build the PLSDA model and the tenth is used to test the model (i.e. determine the model's accuracy), this is performed ten times for each unique 1:9 split. In parallel, the same 9/10 train 1/10 test sequence is performed 10 times for the same data with *randomly* assigned class labels (to generate a 'null' model). The whole process is performed 100 times with randomly selected matched size subsets of the larger class (Adapted from Jurynczyk et al., 2017b, supplemental data).

Results

Cohort characteristics

One hundred NMO patients and 42 RRMS patients donated plasma samples. Of the 100 NMO participants, 69 had contemporary BPI PSI scores.

RRMS VS NMO COHORT

The RRMS-NMO cohort were well matched for gender, but NMO patients were significantly older (see Table 1) which reflects the known demography of these diseases.

Table 1. Characteristics of RRMS vs NMO cohorts

	n	% female	age, mean(sd)
NMO	100	86.0[ns]	52(14)*
RRMS	42	71.4[ns]	41(10)*

NMO, Neuromyelitis optica; RRMS, relapsing-remitting multiple sclerosis

ns, not significant for chi-squared comparison; p<0.01 for t-test comparison

NMO PAIN COHORT

The pain sub-groups of the NMO pain cohort were well matched for age and gender. Their features are summarised in Table 2.

Table 2. Characteristics of NMO pain cohort

	n	% female	age, mean(sd)	PSI, mean(sd)
All	69	85.5	52(14)	13.2(11.2)
PSI category:				
low	32	84.4[ns]	52(14)[ns]	2.7(3.8)
moderate	21	85.7[ns]	52(17)[ns]	17.9(3.2)
high	16	87.5[ns]	54(11)[ns]	28.4(3.8)

PSI, pain severity index; sd, standard deviation

ns, not significant for comparison of PSI groups using chi-square for age and ANOVA for age

<u>PCA of all data helped to identify five participants with spectral anomalies that were removed from subsequent analyses</u>

The PCA plot for all NMO and all RRMS participants is shown in Figure 3. Five participants were identified with spectral anomalies and these were removed from subsequent analyses; they consisted of 4 NMO participants (one without pain scores, the others with PSIs of 0, 6 and 13) and 1 RRMS participant.

Figure 3. PCA plot of all data for outlier identification

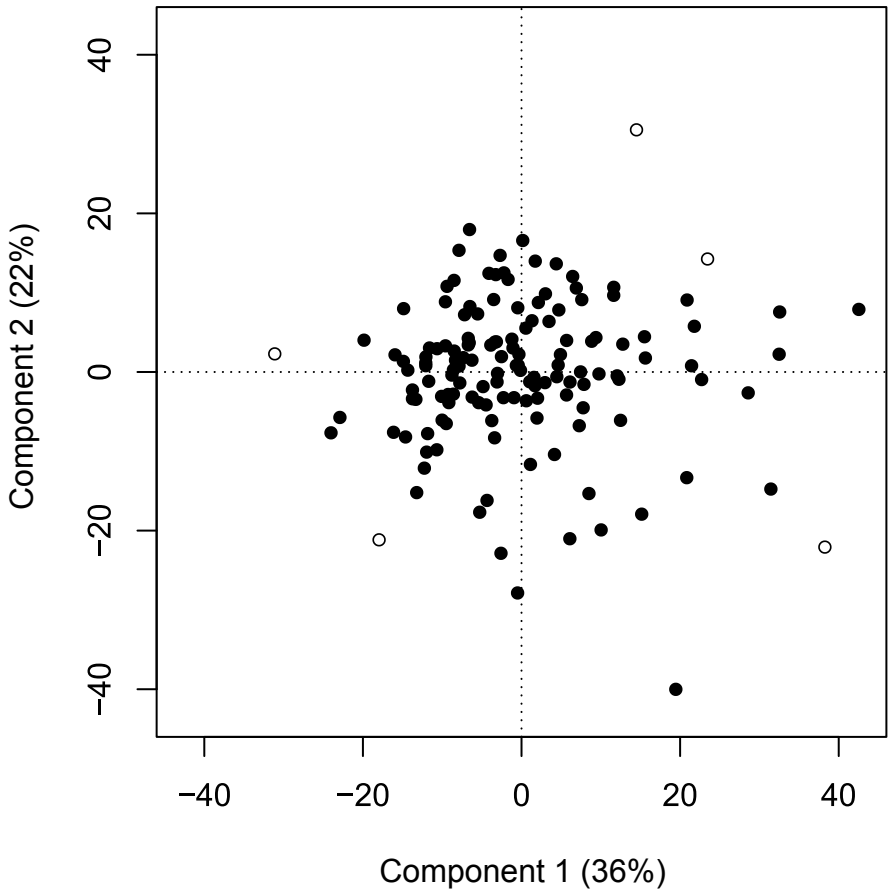

Principle component analysis of all NMO and RRMS data. PCA, principle component analysis; o, empty black circles, participants identified as having spectral anomalies and excluded; Percentages on axes represent variance explained by each component.

Plasma NMR spectra can be used to distinguish RRMS vs NMO: proof of principle

PCA of the RRMS and NMO metabolomics data, with disease classes labelled post-hoc, is shown in Figure 4.

Figure 4. PCA of RRMS vs NMO

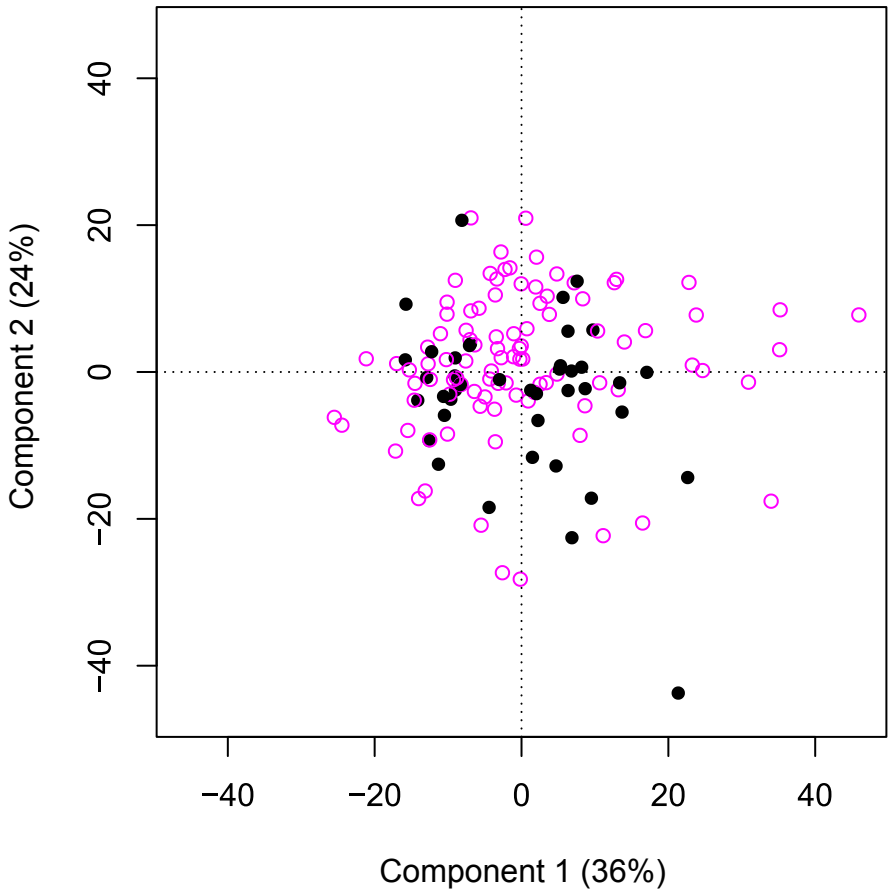

Principle component analysis of all NMO and RRMS data with post-hoc labelling of RRMS and NMO participants. • filled black circles, RRMS; o empty pink circles, NMO; Percentages on axes represent variance explained by each component; NB the data is plotted along its principle components, only then are the group labels applied.

PLS-DA showed good group clustering and separation on visual inspection (when plotted using the first two predictive components; Figure 5A) and with iterative testing produced a model distribution significantly different from the randomly permuted null distribution ($p<0.01$), able to accurately discriminate NMO from RRMS in 87% of cases (mean accuracy = 0.87, $p<0.01$; Figure 5B).

Figure 5. RRMS vs NMO (**A**) PLSDA with 7 predictive components (**B**) model and null distributions

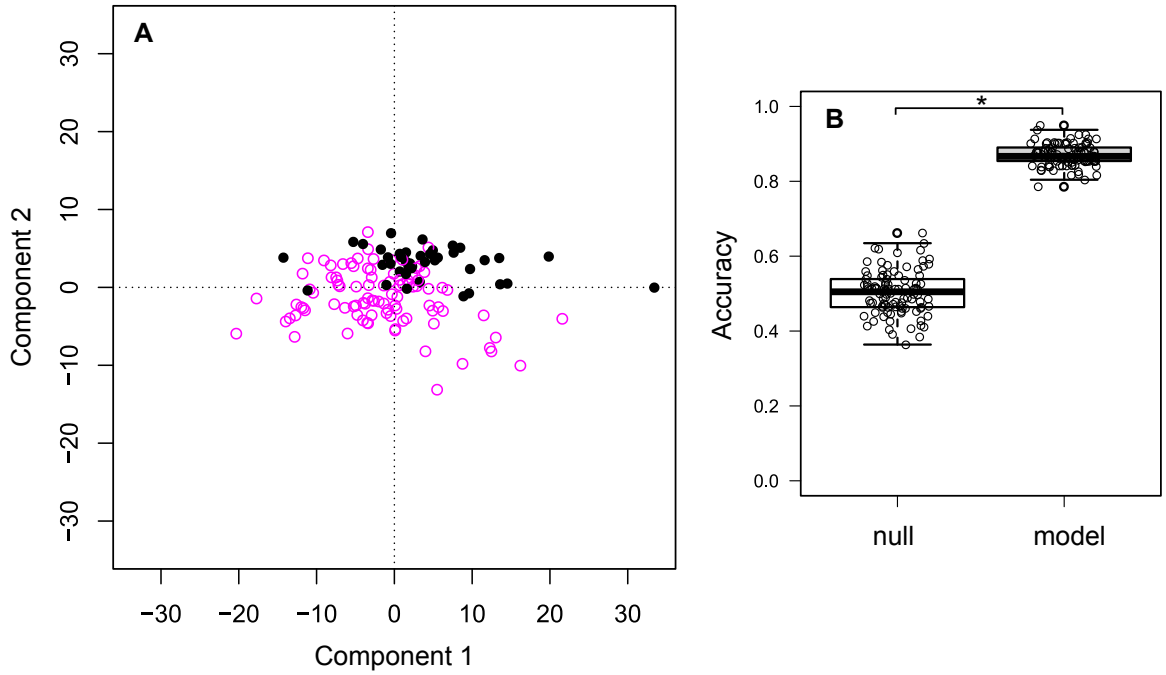

Parital least squares discriminant analysis (PLSDA) results of class-labelled data for NMO and RRMS, plotted on axes of greatest variance between groups (A). The resultant model distributions from permutation testing (B) were significantly different. *p<0.01 using Kolmogorov-Smirnov test; • filled black circles, RRMS; o empty pink circles, NMO; p1, first predictive component; p2, second predictive component.

Plasma NMR spectra had difficulty separating NMO patients divided by pain severity

LOW VERSUS MEANINGFUL PAIN

PCA of the low and meaningful NMO pain data was visibly more disorganised than for that of RRMS vs NMO, however there was still some apparent structure (Figure 6; low pain n=30, meaningful pain n=36).

Figure 6. PCA of low vs meaningful NMO pain

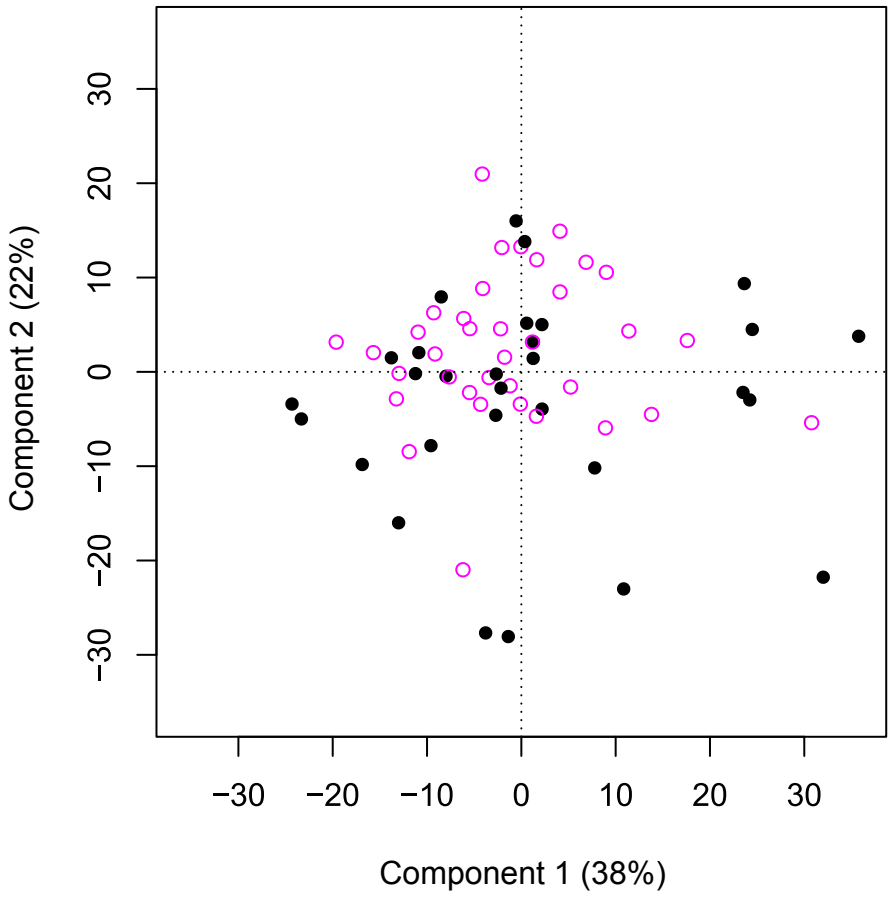

Principle component analysis of NMO meaningful and low pain subsets with post-hoc labelling of pain subgroups. • filled black circles, low-pain group; o empty pink circles, meaningful pain group; Percentages on axes represent variance explained by each component; NB the data is plotted along its principle components, only then are the group labels applied

The PLS-DA model performed slightly better than the 'null distribution' ($p<0.01$) and was significantly better than chance but with low accuracy (mean accuracy = 0.58, $p<0.01$; Figure 7).

Figure 7. Low vs meaningful NMO pain (**A**) PLSDA with 2 predictive components (**B**) model and null distributions

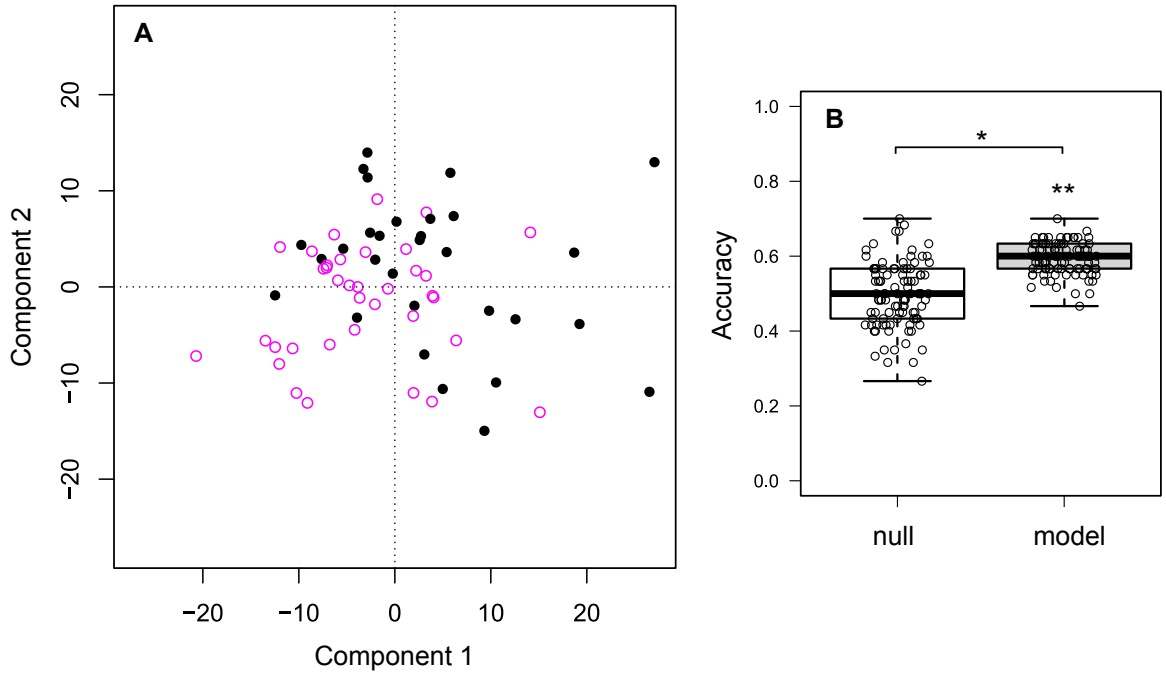

Parital least squares discriminant analysis (PLSDA) results of class-labelled data for NMO pain subgroups, plotted on axes of greatest variance between groups (A). The resultant model distributions from permutation testing (B), although significantly different and showing signifantly greater accuracy for the real-data PLSDA model compared to the null-data model, nonetheless showed only marginal accuracy differences and an accuracy for real-data only just above chance. • filled black circles, low-pain group; o empty pink circles, meaningful pain group; *p<0.01 using Kolmogorov-Smirnov test; **p<0.01 for one-way t-test comparing model mean accuracy to 0.5.

LOW VERSUS HIGH PAIN

Given that the predictive value of the low versus meaningful pain model was low, an attempt was made to polarise the difference between groups by selecting participants at the extremes of pain measures: low and high pain (see Chapter 3 for pain group definitions; low pain n=30, high pain n=8). PCA showed no better clustering and little structure (Figure 8)

Figure 8. PCA of low vs high NMO pain

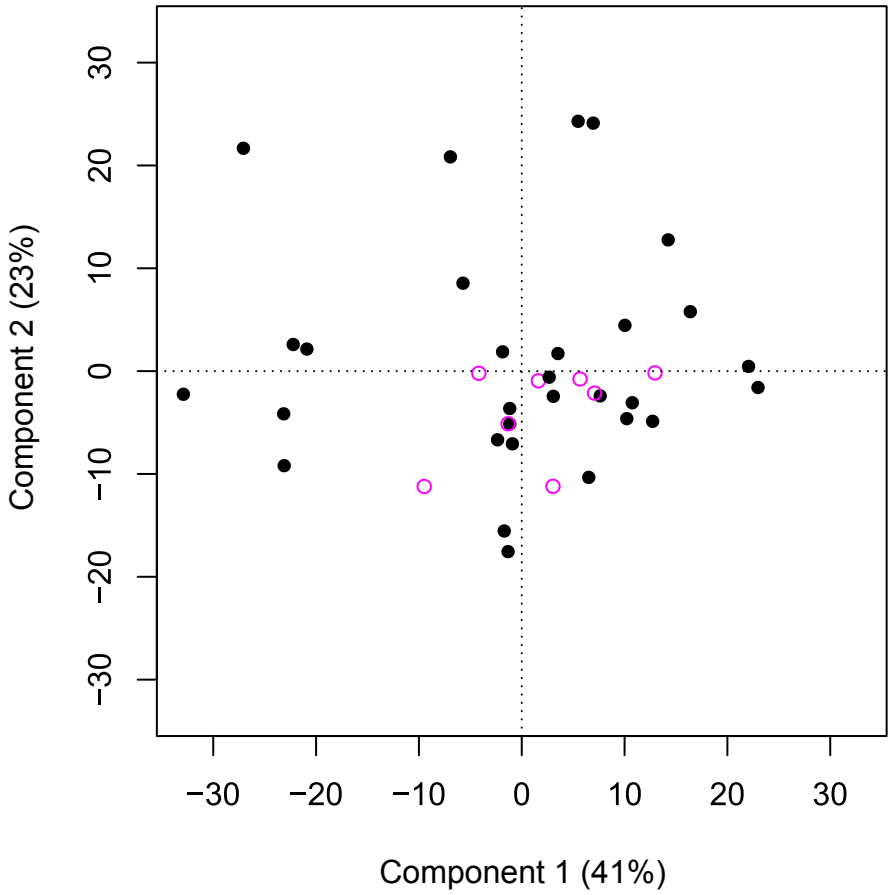

Principle component analysis of NMO high and low pain subsets with post-hoc labelling of pain subgroups. • filled black circles, low-pain group; o empty pink circles, high pain group; Percentages on axes represent variance explained by each component; NB the data is plotted along its principle components, only then are the group labels applied.

PLS-DA, again modelled with the default two predictive components, showed some visually promising clustering of groups, but no significant difference between the model distribution and chance (the null distribution; Figure 9).

Figure 9. Low vs high NMO pain (**A**) PLSDA with 2 predictive components (**B**) model and null distributions

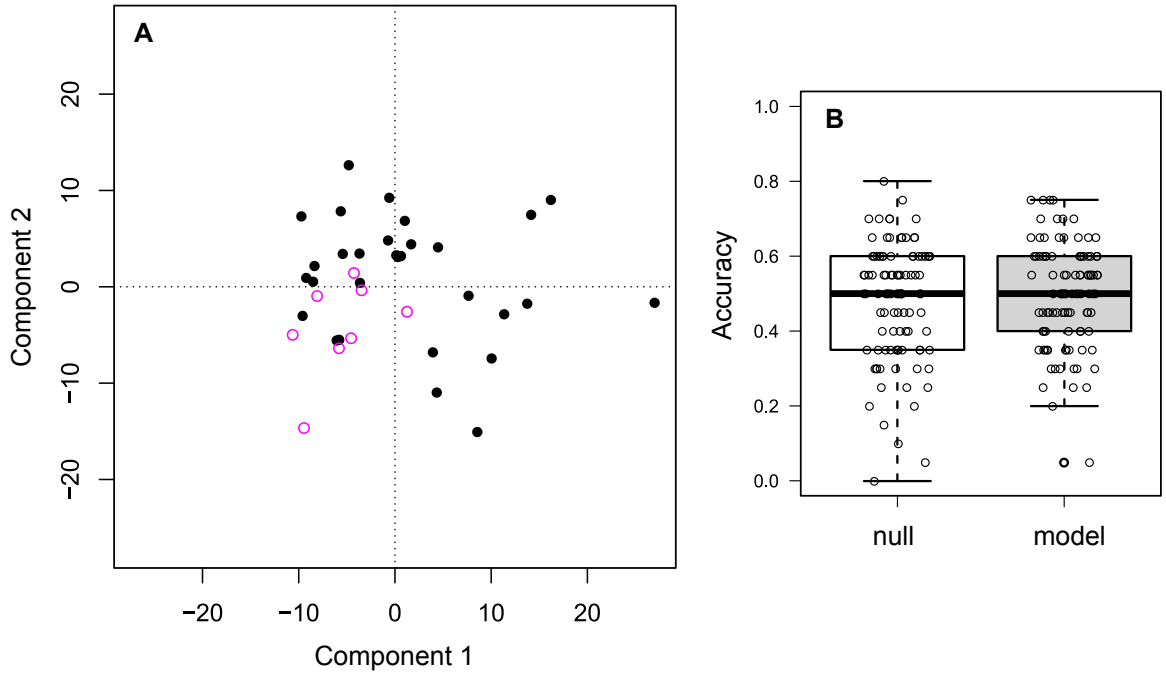

Parital least squares discriminant analysis (PLSDA) results of class-labelled data for NMO pain subgroups, plotted on axes of greatest variance between groups (A). The resultant model distributions from permutation testing (B) were not significantly different. • filled black circles, low-pain group; o empty pink circles, high pain group.

As the models for pain did not perform well, it was not deemed valid to further interrogate them as the metabolites identified would have no predictive value.

Discussion

^{1}H NMR spectroscopic metabolomics of blood plasma was unable to separate pain subgroups of NMO. This is unlikely to be a fault in methodology: the same NMO participants and a parallel RRMS cohort, processed simultaneously and with the same protocol, were readily differentiated with an accuracy of 0.87.

It has been shown before that NMR metabolomics can differentiate NMO from MS (Moussallieh et al., 2013) however no study has tried to differentiate degrees of clinical symptoms, such as pain, within neuroinflammatory disease. Metabolomics studies in human pain have either compared participants to healthy controls (for example in arthritis; Young et al., 2013) or differentiated different pain phenotypes or conditions (for example nociceptive versus neuropathic pain participants; Finco et al., 2016).

Metabolomics was considered a sensible methodology and used herein to seek differences in the downstream sequelae of neuroinflammatory damage that might associate with higher and lower pain states. These higher and lower pain states might however be driven by differing descending modulation. For example, in an imaging study of osteoarthritis where there is a discordance between the degree of pathology (e.g. joint damage) and experienced pain, PAG activation is shown to be activated in patients vs. controls in response to acute pain but also correlated within patients with the number of neuropathic pain features the acute pain elicited, suggesting PAG-activity is driving the increased neuropathic symptoms in a subset of patients, possibly as a consequence of increased descending facilitation. In line with this, the determinant of an NMO patient's level of pain might not lie in neuroinflammatory damage, but may be a function of individual pain vulnerability and the ability to modulate one's descending pain network (Denk et al., 2014). Or perhaps most likely, a combination of the both. I therefore suggest a reason for the failure to differentiate groups might have a basis in their common neuroinflammatory aetiology; that is, those with and without pain have very similar (NMO) disease (as in the osteoarthritis example above), with a similar metabolome, and it is either something compartmentally separate from the sampled plasma metabolome (e.g. differences in CNS

glutamate, GABA, noradrenaline or serotonin), or something unrelated to metabolomics (e.g. differences in physical brainstem networks such as white matter tract integrity between PAG and its ascending and descending pain modulating connections) that underlies different pain experiences in these participants. Another potential pitfall is that the pain groupings herein are not truly dichotomous but based on a continuous pain scale; where this was pushed to its extremes (with high and low pain comparisons) the numbers in the high pain group may have been prohibitively low (n=8). Larger, more polarised cohorts might solve this, but given that NMO is a very rare disorder, a multinational effort would likely be required (Pandit et al., 2015) and if the former hypothesis is correct, might again fail to show any difference in the plasma metabolome.

Metabolomics must be used with caution. Structured noise (e.g. post-prandial / late afternoon blood sampling) that in any way correlates with your categorical variable of interest (e.g. pain / no-pain) will likely be incorporated in the model (e.g. plasma glucose levels relate to time since lunch predicting the separation of pain / no pain groups). It is also important to validate PLS-DA models with a method not reliant on internal 'best-fit' parameters that create self-fulfilling predictions (and are often packaged with metabolomics software, see Golbraikh and Tropsha, 2002). One way to avoid these errors is to build null-distribution models with all data as I have used above. Furthermore, to prove a model's worth beyond reasonable doubt, it needs to be tested with a completely independent set of data.

^{1}H NMR metabolomics may have potential for investigating pain and perhaps with different biofluids, for example CSF samples, the investigation of NMO pain might prove fruitful.

However, using any biofluid metabolome to unravel pain effects versus epiphenomenon (biochemical, behavioural, mood changes as but a few examples) could prove extremely challenging.

Conclusion

^{1}H NMR spectroscopic metabolomics of blood plasma was unable to separate pain subgroups of NMO. It is possible that CNS changes in the cord or brainstem networks might not have downstream metabolic effects discernible in blood plasma. Future work in NMO pain metabolomics using CSF samples might be enlightening.

CHAPTER 9
Discussion

Three broad and overlapping mechanisms of pain in NMO were proposed as candidate aetiologies in Chapter 1c: (1) sensory pathway disruption, (2) pain modulatory system dysfunction, and (3) direct effects of neuroinflammation. The results presented in this thesis strongly implicate the first and second, but the third to a lesser extent due to limitations of experimental methods to explore neuroinflammatory mechanisms in detail. Sensory pathway disruption, in particular damage to the spinothalamic tract caused by thoracic lesions, along with a recently proposed novel form of 'spinal pain generator' mechanism, again related to thoracic lesions (see below), are supported by the results of Chapters 4 and 5. Pain modulatory system dysfunction, with notable changes in the PAG-seeded brain activity and PAG-glutamate concentrations are shown in relation to pain severity in Chapters 6 and 7. The mechanism of inflammatory mediated pain in NMO was not illuminated by results from the plasma metabolome (Chapter 8) that showed no differences between high and low pain patients or by PAG magnetic resonance spectroscopy (MRS) measurement of N-acetylaspartate (NAA) and myo-inositol (mI). However, a key area where inflammatory changes almost certainly contribute was not studied: the inflammatory milieu

at sites of cord lesions, and further work is needed. The main results are discussed under subheadings below.

Thoracic lesions and spinothalamic tract damage

The foremost finding of the thesis is that higher pain scores are associated with T2-hyperintense lesions (especially persistent lesions) in the thoracic cord when compared to cervicothoracic and especially when compared to cervical cord lesions. Indeed, the presence of cervical lesions predicts lower pain scores. Furthermore, within participants with only historical thoracic lesions or those with only current thoracic lesions, the degree of isolated cervical spinothalamic tract damage, as measured by reduced fractional anisotropy, strongly correlates with pain.

Outside of a single paper suggesting thoracic spinal cord lesions might have relevance in the aetiology of multiple sclerosis (MS) chronic pain, very little has been published (Okuda et al., 2014). Okuda and colleagues hypothesise that bilateral pain in MS, where lesion tend to be small, is not due to bilateral ascending pathway damage (which would be uncommon), but via small off-central thoracic lesions affecting bilaterally projecting pain modulating neurones from the interomediomedial and intermediolateral nuclei to lamina I. It is not clear if lesions of the spinal autonomic nuclei are sufficient to cause pain and Okuda's mechanism could be considered a remote form of 'spinal pain generator' whereby lesions in the spinal autonomic nuclei "sensitise" other levels of the cord. This type of mechanism is best suited to explain the evoked pain (hyperaesthesia and allodynia) seen in NMO participants (Chapter 3, Figure 5), and indeed this resembles the phenotypes of patients recruited in Okuda's cohort. Although the methods of the current study preclude comment

on the detailed axial extent of thoracic lesions, NMO lesions are commonly central and thus the thoracic lesions identified as important to pain could easily involve the same pathway. Assuming my cohort has a similar sensory phenotype to that of Pellkofer's NMO population (Pellkofer et al., 2013), i.e. thermal hypoeasthesia and heat-induced hyperalgesia, the diffusion results showing damage to the spinothalamic tract (STT) might fit with Craig's theory of disrupted thermosensory integration (Craig, 1998) positing that noxious and 'cool' STT neurones are in some way differentially affected (Craig, 2003), and that the degree of disruption (but not obliteration) mediates the severity of pain experienced. This theory would explain the constant burning dysaesthesia that is common in NMO participants (Chapter 3, Figure 5), however the evidence for quite why components of the STT might be differentially affected in NMO is not apparent and requires further thoracic-focussed study. It is also clearly possible that damage to STT tracts could occur anywhere along the cord and provide the ingredients for thermosensory disinhibition, or that focal neuroinflammatory damage could conceivably create a 'spinal pain generator' at any level (Finnerup et al., 2007). However, isolated cervical lesions in my cohort associate with very little pain, and so I tentatively suggest that a combined aetiology is at work: a combination of 'Okuda sensitised' dorsal horns and the possible addition of modally disrupted ascending STT fibres. A protective effect of cervical lesions must also be considered: it is possible that large cervical lesions obliterate STTs and prevent the development of significant chronic pain similar to findings in spinal cord injury where complete cord lesions are associated with less pain (Davidoff et al., 1987).

Descending pain modulatory network perturbations

A number of findings within this thesis implicate key components of the descending pain modulatory network (DPMN) in the aetiology of NMO pain, with evidence for the disease invoking inhibitory and probably facilitatory effects. PAG-seeded resting state BOLD activity shows a correlation with resting state BOLD activity in the pregenual rostral anterior cingulate cortex (ACC) and dorsolateral prefrontal cortex (dlPFC) that positively associates with pain severity, and a negative association with pain severity and PAG connectivity in a region resembling the rostroventromedial medulla (RVM). Magnetic resonance spectroscopy (MRS) of the PAG revealed a negative correlation of glutamate with pain, with lower glutamate concentrations in both high pain patients and controls, compared to low pain patients. There was minimal MRS evidence of hidden NMO damage to the PAG and indeed PAG lesions or surrogate measures of damage (i.e. mI and NAA concentrations) did not correlate with pain.

The ACC is part of the limbic network of the brain (MacLean, 1949) and implicated in affective components of pain processing (Johansen and Fields, 2004; Tölle et al., 1999; Zubieta et al., 2005). The dorsolateral prefrontal cortices receive a barrage of afferent pain information via the medial thalamus (Monconduit and Villanueva, 2005) and are well placed to modulate higher cortical processes as a result of noxious input. Both areas show pain modality-specific activation to heat allodynia compared to normal heat-evoked pain (Lorenz et al., 2002). Within non-pain disciplines, these areas are commonly ascribed the functions of error monitoring (ACC) and episodic memory retrieval (dlPFC) and are heavily interconnected (Wood and Grafman, 2003).

These two cortical areas thus clearly serve a function for 'bottom-up' pain processing, but their influence is bidirectional. Projections exist from the PFC to all sub-regions of the PAG: a PFC retrograde tracer experiment in monkeys showed direct connections from the dlPFC to the ventrolateral, dorsolateral and lateral columns of the PAG (more so to the latter) (An et al., 1998) and a recent diffusion imaging study in humans has shown significant connectivity between the dlPFC and ventrolateral columns of the PAG, with less but still evident connectivity to the lateral PAG (and almost none to the dorsal PAG) (Ezra et al., 2015). Conceivably therefore, activity seen on resting state could resemble dlPFC connectivity to differing PAG sub-regions. However the ventrolateral PAG is implicated in opioid-mediated analgesia (which presumably is the target of the dlPFC-PAG pathway activated in placebo experiments, see below), whereas stimulation of the lateral column of the PAG, although analgesic, is not opioid dependent and is associated with strong emotional reactions and confrontational behaviour (Bandler and Shipley, 1994), characteristics not seemingly portrayed by the NMO population.

In an early human brain imaging study of pain expectation, painful stimuli activated the caudal ACC whereas its anticipation activated the perigenual rostral ACC and adjacent frontal cortex (and this activity increased with subsequent trials; Ploghaus et al., 1999). A recent study has reproduced these ACC effects, and also implicated the PAG in computing an aversive stimulus prediction error (Roy et al., 2014). Their experiment, involving pain and no-pain trials with differing learned pain expectancy, showed that the PAG is the only brain region (on brain-wide analysis) to encode effects of both the pain stimulus and expectancy parameters. They suggest that forebrain regions (including the ventromedial PFC, anatomically equivalent to the current pregenual ACC / paracingulate findings) might encode the expected value of signals which are then compared with primary nociceptor

inputs within the PAG to generate an aversive prediction error that is projected back to prefrontal-temporal-striatal systems to update stimulus-related pain expectations. Emphasis is placed by the authors on the PAG's ideal anatomical location for comparing top-down expectations and bottom-up aversive sensations and its various rostral connections (including multiple PFC sites) available for value updating, sites which may then also make behavioural decisions (Roy et al., 2014). In a chronic pain condition, such as NMO, the role of the PAG in computing aversive prediction errors in concert with PFC / rostral ACC activity is unknown; the present findings showing PAG and rostral ACC connectivity correlated with pain scores might be partially unmasking chronic activation of this complex system.

In a complementary paradigm to pain expectation experiments, a placebo analgesia study by Eippert and colleagues has shown deactivation in the pregenual rostral ACC and activation in the subgenual rostral ACC, dlPFC, and also the PAG and RVM, the latter two remaining active into 'late pain' (that is, the second half of a 20 second pain stimulus) (Eippert et al., 2009a). They hypothesise that during the expectation of pain, via opioid-dependent signalling, the dlPFC recruits areas (including the rostral ACC) that can activate brainstem descending pain modulatory systems, such as the PAG and RVM. The authors suggest that this inhibitory brainstem activity may remain tonically active "until the nociceptive input is terminated" (without ongoing dlPFC and subgenual ACC). This study serves to highlight the relevance of the PAG, under the influence of higher cortical areas (the subgenual ACC and dlPFC), in inhibiting pain transmission whilst expecting and receiving placebo (presumably this inhibition is occurring at the level of the dorsal horn, see Eippert et al., 2009b).

So, the PAG, under the instruction of the rostral ACC (subgenual and pregenual) and dlPFC, has diverse roles important for both determining the expectedness of pain, but also for modifying it.

The findings of my work fit with the concepts of concerted RVM-PAG activation modulating pain via descending inhibition (herein, correlating with lower pain scores), however the PAG-seeded dlPFC and rACC activity positively associated with pain severity is harder to explain and is certainly the opposite to what one would expect from placebo experiments in response to *acute* pain-evoking stimuli (Eippert et al., 2009a). One can speculate that the surprisingly low PAG connectivity with the rACC and dlPFC during low pain (brain areas that are usually active during pain and show increased connectivity with the PAG during analgesia, at least in the acute setting) might be explained by the very fact that less pain information is arriving at rostral sites in participants for whom the PAG-RVM descending inhibitory circuitry wins out over facilitation, thus inhibiting nociceptive information at the point of entry to the CNS: the dorsal horn. For the opposite scenario where high pain measures associate with high PAG connectivity to rostral cortical areas (rACC and dlPFC), one can speculate about the often bidirectional interconnectivity between various nodes of the pain modulatory network, and the possibility of indirect pathways modulating PAG connectivity; for example the role of the dlPFC modulating PAG-thalamic and subsequently thalamic-rACC connectivity shown by Lorenz in a human PET imaging study (Lorenz et al., 2003). But these are speculations and examples in the literature are lacking.

I suggest therefore that increased dlPFC-PAG and increased PAG-RVM connectivity that drives descending inhibition and so less clinical pain is not witnessed here but is very likely present, though masked by other dlPFC related changes due to chronic pain (Baliki et al.,

2010; Vachon-Presseau et al., 2016) that are separately influencing outputs to other brainstem regions including elements of PAG function.

Further work will isolate separable networks more precisely related to the analgesic influences of the DPMN, and also address the overriding additional complication that there is almost certainly descending facilitation contributing to the NMO chronic pain phenotype, which might well explain the dlPFC-PAG increased connectivity, however as mentioned above there is currently no literature to support this being the case.

For future studies one must also bear in mind that the dissociated nature of PFC-PAG and PAG-RVM connectivity, for example the potential to show greater PFC-PAG connectivity during high pain states indicative of engaging descending facilitation *and* in low-pain states indicative of engaging descending inhibition, might ultimately mean that resting-state MRI of these regions in certain chronic pain conditions will always produce ambiguous results.

A helpful addition to future studies of NMO pain would be a stimulus paradigm whereby the response of descending pain modulatory network components to a simple pain stimulus during an fMRI scan, for example, could provide information, both from functional MRI and clinical measures (e.g. pain ratings), about the state of descending inhibition and facilitation and its capacity to be modified by acute painful stimuli.

Towards a unified theory of chronic pain aetiology in NMO

I propose a testable theory: chronic pain severity in NMO is dependent on an interrelationship between (a) thoracic lesions 'severe' enough to cause lasting T2-weighted MRI changes and demonstrate remote STT damage with diffusion imaging, (b) predetermined pain vulnerability evidenced by participant differences in PAG-RVM

connectivity and PAG glutamate levels, and (c) a possible protective effect of cervical lesions (at least for thoracic-lesion induced pain).

To begin to test this theory, in groups with well-matched ethnicity and gender variables, it is essential for imaging of the *whole* cord to be undertaken to document the three-dimensional details of T2-hyperintence lesions alongside diffusion measures and targeted MRS (where possible) as clearly the thoracic cord is an important area in the genesis of pain in NMO (and perhaps also other neuroinflammatory disorders). Furthermore, advances in magnetic resonance spectroscopy, particularly at higher field strengths now allow the reliable quantification of other CNS neurotransmitters (notably GABA), and this could provide further information about the balance of inhibition and excitation in a PAG-targeted study .Unfortunately, serotonin and noradrenaline, the predominant neurotransmitters that mediate brainstem to dorsal horn descending facilitation and inhibition, respectively, are not quantifiable using MRS. MRS of the cord and brainstem, with quantified GABA and glutamate, along with further fMRI brain studies in NMO, perhaps including attempts to modulate known pain networks with known therapies (e.g. opiates or duloxetine acting on the DPMN, or cannabinoid GABA effects) or stimulus paradigms, might start to unravel the complicated interplay of pain expectation, pain modulation and pain vulnerability that undoubtedly exist in this chronic pain condition.

Concluding remarks

Chronic pain can devastate lives. I hope the findings of this thesis, in particular the association of pain with thoracic lesions and of functional and metabolic changes in key pain modulatory areas of the brain, will serve as a stepping-stone on the route to a better understanding of chronic pain in NMO and the path to effective treatments.

References

Absoud, M., Lim, M.J., Appleton, R., Jacob, A., Kitley, J., Leite, M.I., Pike, M.G., Vincent, A., Wassmer, E., Waters, P., Woodhall, M., Hemingway, C., Palace, J., 2015. Paediatric neuromyelitis optica: clinical, MRI of the brain and prognostic features. J Neurol Neurosurg Psychiatry 86, 470–472. https://doi.org/10.1136/jnnp-2014-308550

Aicher, S.A., Silverman, M.B., Winkler, C.W., Bebo Jr, B.F., 2004. Hyperalgesia in an animal model of multiple sclerosis. Pain 110, 560–570. https://doi.org/10.1016/j.pain.2004.03.025

Al-Chaer, E.D., Lawand, N.B., Westlund, K.N., Willis, W.D., 1996. Visceral nociceptive input into the ventral posterolateral nucleus of the thalamus: a new function for the dorsal column pathway. J. Neurophysiol. 76, 2661–2674. https://doi.org/10.1152/jn.1996.76.4.2661

Alschuler, K.N., Ehde, D.M., Jensen, M.P., 2013. Co-occurring Depression and Pain in Multiple Sclerosis. Phys. Med. Rehabil. Clin. N. Am., Multiple Sclerosis Rehabilitation 24, 703–715. https://doi.org/10.1016/j.pmr.2013.06.001

Amato, M.P., Grimaud, J., Achiti, I., Bartolozzi, M.L., Adeleine, P., Hartung, H.-P., Kappos, L., Thompson, A., Trojano, M., Vukusic, S., Confavreux, C., 2004. European validation of a standardized clinical description of multiple sclerosis. J. Neurol. 251, 1472–1480. https://doi.org/10.1007/s00415-004-0567-0

Amiry-Moghaddam, M., Ottersen, O.P., 2003. The molecular basis of water transport in the brain. Nat. Rev. Neurosci. 4, 991–1001. https://doi.org/10.1038/nrn1252

An, X., Bandler, R., Öngür, D., Price, J. l., 1998. Prefrontal cortical projections to longitudinal columns in the midbrain periaqueductal gray in Macaque monkeys. J. Comp. Neurol. 401, 455–479. https://doi.org/10.1002/(SICI)1096-9861(19981130)401:4<455::AID-CNE3>3.0.CO;2-6

Apiwattanakul, M., Popescu, B.F., Matiello, M., Weinshenker, B.G., Lucchinetti, C.F., Lennon, V.A., McKeon, A., Carpenter, A.F., Miller, G.M., Pittock, S.J., 2010. Intractable vomiting as the initial presentation of neuromyelitis optica. Ann. Neurol. 68, 757–761. https://doi.org/10.1002/ana.22121

Apkarian, A.V., Bushnell, M.C., Treede, R.-D., Zubieta, J.-K., 2005. Human brain mechanisms of pain perception and regulation in health and disease. Eur. J. Pain 9, 463–463. https://doi.org/10.1016/j.ejpain.2004.11.001

Araki, M., Matsuoka, T., Miyamoto, K., Kusunoki, S., Okamoto, T., Murata, M., Miyake, S., Aranami, T., Yamamura, T., 2014. Efficacy of the anti–IL-6 receptor antibody tocilizumab in neuromyelitis optica A pilot study. Neurology 82, 1302–1306. https://doi.org/10.1212/WNL.0000000000000317

Arana, V.A., Medina, J., Alarcon, R., Moreno, E., Heintz, L., Schäfer, H., Wist, J., 2014. Coffee's country of origin determined by NMR: The Colombian case. Food Chem. https://doi.org/10.1016/j.foodchem.2014.11.160

Asgari, N., Skejoe, H.P.B., Lillevang, S.T., Steenstrup, T., Stenager, E., Kyvik, K.O., 2013. Modifications of longitudinally extensive transverse myelitis and brainstem lesions in the course of neuromyelitis optica (NMO): a population-based, descriptive study. BMC Neurol. 13, 33. https://doi.org/10.1186/1471-2377-13-33

Aston-Jones, G., Waterhouse, B., 2016. Locus coeruleus: From global projection system to adaptive regulation of behavior. Brain Res., 50th Anniversary Issue 1645, 75–78. https://doi.org/10.1016/j.brainres.2016.03.001

Bajic, D., Proudfit, H.K., 1999. Projections of neurons in the periaqueductal gray to pontine and medullary catecholamine cell groups involved in the modulation of nociception. J. Comp. Neurol. 405, 359–379.
Baliki, M.N., Geha, P.Y., Apkarian, A.V., Chialvo, D.R., 2008. Beyond Feeling: Chronic Pain Hurts the Brain, Disrupting the Default-Mode Network Dynamics. J. Neurosci. 28, 1398–1403. https://doi.org/10.1523/JNEUROSCI.4123-07.2008
Baliki, M.N., Geha, P.Y., Fields, H.L., Apkarian, A.V., 2010. Predicting value of pain and analgesia: nucleus accumbens response to noxious stimuli changes in the presence of chronic pain. Neuron 66, 149–160. https://doi.org/10.1016/j.neuron.2010.03.002
Bandler, R., Shipley, M.T., 1994. Columnar organization in the midbrain periaqueductal gray: modules for emotional expression? Trends Neurosci. 17, 379–389.
Bannister, K., Dickenson, A.H., 2017. The plasticity of descending controls in pain: translational probing. J. Physiol. 595, 4159–4166. https://doi.org/10.1113/JP274165
Bannister, K., Dickenson, A.H., 2016. What do monoamines do in pain modulation? Curr. Opin. Support. Palliat. Care 10, 143–148. https://doi.org/10.1097/SPC.0000000000000207
Bao, Q., Feng, J., Chen, L., Chen, F., Liu, Z., Jiang, B., Liu, C., 2013. A robust automatic phase correction method for signal dense spectra. J. Magn. Reson. San Diego Calif 1997 234, 82–89. https://doi.org/10.1016/j.jmr.2013.06.012
Barakat, N., Gorman, M.P., Benson, L., Becerra, L., Borsook, D., 2015. Pain and spinal cord imaging measures in children with demyelinating disease. NeuroImage Clin. 9, 338–347. https://doi.org/10.1016/j.nicl.2015.08.019
Barbas, H., 1995. Anatomic basis of cognitive-emotional interactions in the primate prefrontal cortex. Neurosci. Biobehav. Rev. 19, 499–510. https://doi.org/10.1016/0149-7634(94)00053-4
Barnett, Y., Sutton, I.J., Ghadiri, M., Masters, L., Zivadinov, R., Barnett, M.H., 2014. Conventional and advanced imaging in neuromyelitis optica. AJNR Am. J. Neuroradiol. 35, 1458–1466. https://doi.org/10.3174/ajnr.A3592
Basbaum, A.I., Fields, H.L., 1979. The origin of descending pathways in the dorsolateral funiculus of the spinal cord of the cat and rat: Further studies on the anatomy of pain modulation. J. Comp. Neurol. 187, 513–531. https://doi.org/10.1002/cne.901870304
Bauer, C.S., Rahman, W., Tran-van-Minh, A., Lujan, R., Dickenson, A.H., Dolphin, A.C., 2010. The anti-allodynic alpha(2)delta ligand pregabalin inhibits the trafficking of the calcium channel alpha(2)delta-1 subunit to presynaptic terminals in vivo. Biochem. Soc. Trans. 38, 525–528. https://doi.org/10.1042/BST0380525
Beaulieu, C., 2002. The basis of anisotropic water diffusion in the nervous system – a technical review. NMR Biomed. 15, 435–455. https://doi.org/10.1002/nbm.782
Beckmann, C.F., DeLuca, M., Devlin, J.T., Smith, S.M., 2005. Investigations into resting-state connectivity using independent component analysis. Philos. Trans. R. Soc. B Biol. Sci. 360, 1001–1013. https://doi.org/10.1098/rstb.2005.1634
Beckmann, C.F., Smith, S.M., 2004. Probabilistic independent component analysis for functional magnetic resonance imaging. IEEE Trans. Med. Imaging 23, 137–152. https://doi.org/10.1109/TMI.2003.822821

Bederson, J.B., Fields, H.L., Barbaro, N.M., 1990. Hyperalgesia during Naloxone-Precipitated Withdrawal from Morphine Is Associated with Increased On-Cell Activity in the Rostral Ventromedial Medulla. Somatosens. Mot. Res. 7, 185–203. https://doi.org/10.3109/08990229009144706

Bennett, D.L.H., 2015. Informed drug choices for neuropathic pain. Lancet Neurol. 14, 129–130. https://doi.org/10.1016/S1474-4422(14)70329-1

Berić, A., Dimitrijević, M.R., Lindblom, U., 1988. Central dysesthesia syndrome in spinal cord injury patients. Pain 34, 109–116.

Berkley, K.J., Budell, R.J., Blomqvist, A., Bull, M., 1986. Output systems of the dorsal column nuclei in the cat. Brain Res. 396, 199–225.

Bingel, U., Lorenz, J., Schoell, E., Weiller, C., Büchel, C., 2006. Mechanisms of placebo analgesia: racc recruitment of a subcortical antinociceptive network. Pain 120, 8–15. https://doi.org/10.1016/j.pain.2005.08.027

Biswal, B., Zerrin Yetkin, F., Haughton, V.M., Hyde, J.S., 1995. Functional connectivity in the motor cortex of resting human brain using echo-planar mri. Magn. Reson. Med. 34, 537–541. https://doi.org/10.1002/mrm.1910340409

Blanc, F., Noblet, V., Jung, B., Rousseau, F., Renard, F., Bourre, B., Longato, N., Cremel, N., Di Bitonto, L., Kleitz, C., Collongues, N., Foucher, J., Kremer, S., Armspach, J.-P., de Seze, J., 2012. White Matter Atrophy and Cognitive Dysfunctions in Neuromyelitis Optica. PLoS ONE 7, e33878. https://doi.org/10.1371/journal.pone.0033878

Bradl, M., Kanamori, Y., Nakashima, I., Misu, T., Fujihara, K., Lassmann, H., Sandkühler, J., 2014. Pain in neuromyelitis optica--prevalence, pathogenesis and therapy. Nat. Rev. Neurol. 10, 529–536. https://doi.org/10.1038/nrneurol.2014.129

Brereton, R.G., Lloyd, G.R., 2014. Partial least squares discriminant analysis: taking the magic away. J. Chemom. 28, 213–225. https://doi.org/10.1002/cem.2609

Bymaster, F.P., Lee, T.C., Knadler, M.P., Detke, M.J., Iyengar, S., 2005. The dual transporter inhibitor duloxetine: a review of its preclinical pharmacology, pharmacokinetic profile, and clinical results in depression. Curr. Pharm. Des. 11, 1475–1493.

Cabrera-Gomez, J.A., Kister, I., 2012. Conventional brain MRI in neuromyelitis optica. Eur. J. Neurol. Off. J. Eur. Fed. Neurol. Soc. 19, 812–819. https://doi.org/10.1111/j.1468-1331.2011.03565.x

Cadotte, D.W., Cadotte, A., Cohen-Adad, J., Fleet, D., Livne, M., Wilson, J.R., Mikulis, D., Nugaeva, N., Fehlings, M.G., 2015. Characterizing the Location of Spinal and Vertebral Levels in the Human Cervical Spinal Cord. Am. J. Neuroradiol. 36, 803–810. https://doi.org/10.3174/ajnr.A4192

Calabrese, M., Oh, M.S., Favaretto, A., Rinaldi, F., Poretto, V., Alessio, S., Lee, B.-C., Yu, K.-H., Ma, H.-I., Perini, P., Gallo, P., 2012. No MRI evidence of cortical lesions in neuromyelitis optica. Neurology 79, 1671–1676. https://doi.org/10.1212/WNL.0b013e31826e9a96

Calvo, Á.C., Martínez, M.A.M., Alentorn-Palau, A., Escuer, J.B., Pinel, L.R., Martínez-Yélamos, S., 2013. Idiopathic acute transverse myelitis: outcome and conversion to multiple sclerosis in a large series. BMC Neurol. 13, 135. https://doi.org/10.1186/1471-2377-13-135

Cameron, A.A., Khan, I.A., Westlund, K.N., Willis, W.D., 1995. The efferent projections of the periaqueductal gray in the rat: a Phaseolus vulgaris-leucoagglutinin study. II. Descending projections. J. Comp. Neurol. 351, 585–601. https://doi.org/10.1002/cne.903510408

Campbell, C.M., Edwards, R.R., 2012. Ethnic differences in pain and pain management. Pain Manag. 2, 219–230. https://doi.org/10.2217/pmt.12.7
Campbell, C.M., Edwards, R.R., Fillingim, R.B., 2005. Ethnic differences in responses to multiple experimental pain stimuli. Pain 113, 20–26. https://doi.org/10.1016/j.pain.2004.08.013
Campbell, C.M., France, C.R., Robinson, M.E., Logan, H.L., Geffken, G.R., Fillingim, R.B., 2008. Ethnic differences in the nociceptive flexion reflex (NFR). Pain 134, 91–96. https://doi.org/10.1016/j.pain.2007.03.035
Campbell, J.N., Raja, S.N., Meyer, R.A., Mackinnon, S.E., 1988. Myelinated afferents signal the hyperalgesia associated with nerve injury. Pain 32, 89–94. https://doi.org/10.1016/0304-3959(88)90027-9
Carnero Contentti, E., Leguizamón, F., Hryb, J.P., Celso, J., Pace, J.L.D., Ferrari, J., Knorre, E., Perassolo, M.B., 2016. Neuromyelitis optica: association with paroxysmal painful tonic spasms. Neurol. Barc. Spain 31, 511–515. https://doi.org/10.1016/j.nrl.2014.12.001
Carrive, P., 1993. The periaqueductal gray and defensive behavior: Functional representation and neuronal organization. Behav. Brain Res. 58, 27–47. https://doi.org/10.1016/0166-4328(93)90088-8
Carstens, E., Stelzer, B., Zimmermann, M., 1988. Microinjections of glutamate or morphine at coincident midbrain sites have different effects on nociceptive dorsal horn neurons in the rat. Neurosci. Lett. 95, 185–191.
Cedarbaum, J.M., Aghajanian, G.K., 1978. Afferent projections to the rat locus coeruleus as determined by a retrograde tracing technique. J. Comp. Neurol. 178, 1–15. https://doi.org/10.1002/cne.901780102
Chacur, M., Lambertz, D., Hoheisel, U., Mense, S., 2009. Role of spinal microglia in myositis-induced central sensitisation: an immunohistochemical and behavioural study in rats. Eur. J. Pain Lond. Engl. 13, 915–923. https://doi.org/10.1016/j.ejpain.2008.11.008
Chalumeau-Lemoine, L., Chretien, F., Larbi, A.G.S., Brugieres, P., Gray, F., Brun-Buisson, C., Creange, A., 2006. Devic Disease With Brainstem Lesions. Arch. Neurol. 63, 591–593. https://doi.org/10.1001/archneur.63.4.591
Ciccarelli, O., Thomas, D.L., De Vita, E., Wheeler-Kingshott, C.A.M., Kachramanoglou, C., Kapoor, R., Leary, S., Matthews, L., Palace, J., Chard, D., Miller, D.H., Toosy, A.T., Thompson, A.J., 2013. Low Myo-inositol indicating astrocytic damage in a case series of neuromyelitis optica: Astrocytic Damage in NMO. Ann. Neurol. n/a-n/a. https://doi.org/10.1002/ana.23909
Ciccarelli, O., Wheeler-Kingshott, C.A., McLean, M.A., Cercignani, M., Wimpey, K., Miller, D.H., Thompson, A.J., 2007. Spinal cord spectroscopy and diffusion-based tractography to assess acute disability in multiple sclerosis. Brain J. Neurol. 130, 2220–2231. https://doi.org/10.1093/brain/awm152
Cleeland, C.S., Ryan, K.M., 1994. Pain assessment: global use of the Brief Pain Inventory. Ann. Acad. Med. Singapore 23, 129–138.
Cohen-Adad, J., 2017. Functional Magnetic Resonance Imaging of the Spinal Cord: Current Status and Future Developments. Semin. Ultrasound CT MRI, Spinal Cord Imaging, Part 2 38, 176–186. https://doi.org/10.1053/j.sult.2016.07.007
Confavreux, C., Compston, D.A., Hommes, O.R., McDonald, W.I., Thompson, A.J., 1992. EDMUS, a European database for multiple sclerosis. J. Neurol. Neurosurg. Psychiatry 55, 671–676. https://doi.org/10.1136/jnnp.55.8.671

Confavreux, C., Vukusic, S., Moreau, T., Adeleine, P., 2000. Relapses and Progression of Disability in Multiple Sclerosis. N. Engl. J. Med. 343, 1430–1438. https://doi.org/10.1056/NEJM200011163432001
Cooper, S.J., 1975. Anaesthetisation of prefrontal cortex and response to noxious stimulation. Nature 254, 439–440. https://doi.org/10.1038/254439a0
Cosgrove, J., Alli, S., Ramadan, H., Ford, H.L., 2014. Myocarditis and diffuse skeletal muscle oedema: new features of neuromyelitis optica spectrum disorder? A case report. Mult. Scler. Houndmills Basingstoke Engl. 20, 120–122. https://doi.org/10.1177/1352458513495939
Craig, A., 2003. Interoception: the sense of the physiological condition of the body. Curr. Opin. Neurobiol. 13, 500–505. https://doi.org/10.1016/S0959-4388(03)00090-4
Craig, A.D., 2002. How do you feel? Interoception: the sense of the physiological condition of the body. Nat. Rev. Neurosci. 3, 655–666. https://doi.org/10.1038/nrn894
Craig, A.D., 1998. A new version of the thalamic disinhibition hypothesis of central pain. Pain Forum 7, 1–14. https://doi.org/10.1016/S1082-3174(98)70004-2
Craig, A.D. (Bud), 2003. PAIN MECHANISMS: Labeled Lines Versus Convergence in Central Processing. Annu. Rev. Neurosci. 26, 1–30. https://doi.org/10.1146/annurev.neuro.26.041002.131022
Craig, A.D. (Bud), 1995. Distribution of brainstem projections from spinal lamina I neurons in the cat and the monkey. J. Comp. Neurol. 361, 225–248. https://doi.org/10.1002/cne.903610204
Craig, A.D., Bushnell, M.C., 1994. The thermal grill illusion: unmasking the burn of cold pain. Science 265, 252–255. https://doi.org/10.1126/science.8023144
Craig, A.D., Reiman, E.M., Evans, A., Bushnell, M.C., 1996. Functional imaging of an illusion of pain. Nature 384, 258–260. https://doi.org/10.1038/384258a0
Cree, B.A., Bennett, J.L., Sheehan, M., Cohen, J., Hartung, H.-P., Aktas, O., Kim, H.J., Paul, F., Pittock, S., Weinshenker, B., Wingerchuk, D., Fujihara, K., Cutter, G., Patra, K., Flor, A., Barron, G., Madani, S., Ratchford, J.N., Katz, E., 2016. Placebo-controlled study in neuromyelitis optica-Ethical and design considerations. Mult. Scler. Houndmills Basingstoke Engl. 22, 862–872. https://doi.org/10.1177/1352458515620934
Daams, M., Weiler, F., Steenwijk, M.D., Hahn, H.K., Geurts, J.J., Vrenken, H., van Schijndel, R.A., Balk, L.J., Tewarie, P.K., Tillema, J.-M., Killestein, J., Uitdehaag, B.M., Barkhof, F., 2014. Mean upper cervical cord area (MUCCA) measurement in long-standing multiple sclerosis: relation to brain findings and clinical disability. Mult. Scler. Houndmills Basingstoke Engl. 20, 1860–1865. https://doi.org/10.1177/1352458514533399
Dalal, S., Hui, D., Nguyen, L., Chacko, R., Scott, C., Roberts, L., Bruera, E., 2012. Achievement of personalized pain goal in cancer patients referred to a supportive care clinic at a comprehensive cancer center. Cancer 118, 3869–3877. https://doi.org/10.1002/cncr.26694
Damoiseaux, J.S., Rombouts, S.A.R.B., Barkhof, F., Scheltens, P., Stam, C.J., Smith, S.M., Beckmann, C.F., 2006. Consistent resting-state networks across healthy subjects. Proc. Natl. Acad. Sci. U. S. A. 103, 13848–13853. https://doi.org/10.1073/pnas.0601417103
Danzebrink, R.M., Gebhart, G.F., 1990. Antinociceptive effects of intrathecal adrenoceptor agonists in a rat model of visceral nociception. J. Pharmacol. Exp. Ther. 253, 698–705.

DaSilva, A.F., Becerra, L., Pendse, G., Chizh, B., Tully, S., Borsook, D., 2008. Colocalized Structural and Functional Changes in the Cortex of Patients with Trigeminal Neuropathic Pain. PLOS ONE 3, e3396. https://doi.org/10.1371/journal.pone.0003396

Davidoff, G., Roth, E., Guarracini, M., Sliwa, J., Yarkony, G., 1987. Function-limiting dysesthetic pain syndrome among traumatic spinal cord injury patients: a cross-sectional study. Pain 29, 39–48.

Davie, C.A., Hawkins, C.P., Barker, G.J., Brennan, A., Tofts, P.S., Miller, D.H., McDonald, W.I., 1994. Serial proton magnetic resonance spectroscopy in acute multiple sclerosis lesions. Brain 117, 49–58. https://doi.org/10.1093/brain/117.1.49

De Leener, B., Kadoury, S., Cohen-Adad, J., 2014. Robust, accurate and fast automatic segmentation of the spinal cord. NeuroImage 98, 528–536. https://doi.org/10.1016/j.neuroimage.2014.04.051

De Leener, B., Lévy, S., Dupont, S.M., Fonov, V.S., Stikov, N., Louis Collins, D., Callot, V., Cohen-Adad, J., 2017. SCT: Spinal Cord Toolbox, an open-source software for processing spinal cord MRI data. NeuroImage 145, 24–43. https://doi.org/10.1016/j.neuroimage.2016.10.009

De Seze, J., Blanc, F., Kremer, S., Collongues, N., Fleury, M., Marcel, C., Namer, I.-J., 2010. Magnetic resonance spectroscopy evaluation in patients with neuromyelitis optica. J. Neurol. Neurosurg. Psychiatry 81, 409–411. https://doi.org/10.1136/jnnp.2008.168070

Defrin, R., Ohry, A., Blumen, N., Urca, G., 2002. Pain following spinal cord injury. Spinal Cord 40, 96–97; author reply 98-99. https://doi.org/10.1038/sj.sc.3101245

Denk, F., McMahon, S.B., Tracey, I., 2014. Pain vulnerability: a neurobiological perspective. Nat. Neurosci. 17, 192–200. https://doi.org/10.1038/nn.3628

Denuelle, M., Fabre, N., Payoux, P., Chollet, F., Geraud, G., 2008. Posterior cerebral hypoperfusion in migraine without aura. Cephalalgia Int. J. Headache 28, 856–862. https://doi.org/10.1111/j.1468-2982.2008.01623.x

Depaulis, A., Morgan, M.M., Liebeskind, J.C., 1987. GABAergic modulation of the analgesic effects of morphine microinjected in the ventral periaqueductal gray matter of the rat. Brain Res. 436, 223–228. https://doi.org/10.1016/0006-8993(87)91665-9

Desikan, R.S., Ségonne, F., Fischl, B., Quinn, B.T., Dickerson, B.C., Blacker, D., Buckner, R.L., Dale, A.M., Maguire, R.P., Hyman, B.T., Albert, M.S., Killiany, R.J., 2006. An automated labeling system for subdividing the human cerebral cortex on MRI scans into gyral based regions of interest. NeuroImage 31, 968–980. https://doi.org/10.1016/j.neuroimage.2006.01.021

Dib-Hajj, S.D., Black, J.A., Waxman, S.G., 2009. Voltage-Gated Sodium Channels: Therapeutic Targets for Pain. Pain Med. 10, 1260–1269. https://doi.org/10.1111/j.1526-4637.2009.00719.x

Dickens, A.M., Larkin, J.R., Griffin, J.L., Cavey, A., Matthews, L., Turner, M.R., Wilcock, G.K., Davis, B.G., Claridge, T.D.W., Palace, J., Anthony, D.C., Sibson, N.R., 2014. A type 2 biomarker separates relapsing-remitting from secondary progressive multiple sclerosis. Neurology 83, 1492–1499. https://doi.org/10.1212/WNL.0000000000000905

Dostrovsky, J.O., Deakin, J.F., 1977. Periaqueductal grey lesions reduce morphine analgesia in the rat. Neurosci. Lett. 4, 99–103.
Downer, J.J., Leite, M.I., Carter, R., Palace, J., Küker, W., Quaghebeur, G., 2012. Diagnosis of neuromyelitis optica (NMO) spectrum disorders: is MRI obsolete? Neuroradiology 54, 279–285. https://doi.org/10.1007/s00234-011-0875-x
Ducreux, D., Attal, N., Parker, F., Bouhassira, D., 2006. Mechanisms of central neuropathic pain: a combined psychophysical and fMRI study in syringomyelia. Brain 129, 963–976. https://doi.org/10.1093/brain/awl016
Duncan, N.W., Wiebking, C., Northoff, G., 2014. Associations of regional GABA and glutamate with intrinsic and extrinsic neural activity in humans—A review of multimodal imaging studies. Neurosci. Biobehav. Rev. 47, 36–52. https://doi.org/10.1016/j.neubiorev.2014.07.016
Dunne, K., Hopkins, I.J., Shield, L.K., 1986. Acute Transverse Myelopathy in Childhood. Dev. Med. Child Neurol. 28, 198–204. https://doi.org/10.1111/j.1469-8749.1986.tb03855.x
Eaton, W., Muntaner, C., Smith, C., Tien, A., Ybarra, M., 2004. Center for Epidemiologic Studies Depression Scale: Review and revision (CESD and CESD-R), in: The Use of Psychological Testing for Treatment Planning and Outcomes Assessment. pp. 363–377.
Edwards, C.L., Fillingim, R.B., Keefe, F., 2001. Race, ethnicity and pain. Pain 94, 133–137.
Edwards, R.R., Doleys, D.M., Fillingim, R.B., Lowery, D., 2001. Ethnic differences in pain tolerance: clinical implications in a chronic pain population. Psychosom. Med. 63, 316–323.
Eide, P.K., Hole, K., 1993. The Role of 5–Hydroxytryptamine (5–HT) Receptor Subtypes and Plasticity in the 5–HT Systems in the Regulation of Nociceptive Sensitivity. Cephalalgia 13, 75–85. https://doi.org/10.1046/j.1468-2982.1993.1302075.x
Eippert, F., Bingel, U., Schoell, E.D., Yacubian, J., Klinger, R., Lorenz, J., Büchel, C., 2009a. Activation of the Opioidergic Descending Pain Control System Underlies Placebo Analgesia. Neuron 63, 533–543. https://doi.org/10.1016/j.neuron.2009.07.014
Eippert, F., Finsterbusch, J., Bingel, U., Büchel, C., 2009b. Direct Evidence for Spinal Cord Involvement in Placebo Analgesia. Science 326, 404–404. https://doi.org/10.1126/science.1180142
Etemadifar, M., Nasr, Z., Khalili, B., Taherioun, M., Vosoughi, R., 2015. Epidemiology of neuromyelitis optica in the world: a systematic review and meta-analysis. Mult. Scler. Int. 2015, 174720. https://doi.org/10.1155/2015/174720
Ezra, M., Faull, O.K., Jbabdi, S., Pattinson, K.T., 2015. Connectivity-based segmentation of the periaqueductal gray matter in human with brainstem optimized diffusion MRI. Hum. Brain Mapp. 36, 3459–3471. https://doi.org/10.1002/hbm.22855
Fainsinger, R.L., Fairchild, A., Nekolaichuk, C., Lawlor, P., Lowe, S., Hanson, J., 2009. Is Pain Intensity a Predictor of the Complexity of Cancer Pain Management? J. Clin. Oncol. 27, 585–590. https://doi.org/10.1200/JCO.2008.17.1660
Falci, S., Best, L., Bayles, R., Lammertse, D., Starnes, C., 2002. Dorsal root entry zone microcoagulation for spinal cord injury-related central pain: operative intramedullary electrophysiological guidance and clinical outcome. J. Neurosurg. 97, 193–200.

Faull, O.K., Jenkinson, M., Clare, S., Pattinson, K.T.S., 2015. Functional subdivision of the human periaqueductal grey in respiratory control using 7 tesla fMRI. NeuroImage 113, 356–364. https://doi.org/10.1016/j.neuroimage.2015.02.026

Field, M.J., Cox, P.J., Stott, E., Melrose, H., Offord, J., Su, T.-Z., Bramwell, S., Corradini, L., England, S., Winks, J., Kinloch, R.A., Hendrich, J., Dolphin, A.C., Webb, T., Williams, D., 2006. Identification of the alpha2-delta-1 subunit of voltage-dependent calcium channels as a molecular target for pain mediating the analgesic actions of pregabalin. Proc. Natl. Acad. Sci. U. S. A. 103, 17537–17542. https://doi.org/10.1073/pnas.0409066103

Fields, H.L., Basbaum, A.I., 1978. Brainstem control of spinal pain-transmission neurons. Annu. Rev. Physiol. 40, 217–248. https://doi.org/10.1146/annurev.ph.40.030178.001245

Fields, H.L., Bry, J., Hentall, I., Zorman, G., 1983. The activity of neurons in the rostral medulla of the rat during withdrawal from noxious heat. J. Neurosci. Off. J. Soc. Neurosci. 3, 2545–2552.

Filippini, N., MacIntosh, B.J., Hough, M.G., Goodwin, G.M., Frisoni, G.B., Smith, S.M., Matthews, P.M., Beckmann, C.F., Mackay, C.E., 2009. Distinct patterns of brain activity in young carriers of the APOE-epsilon4 allele. Proc. Natl. Acad. Sci. U. S. A. 106, 7209–7214. https://doi.org/10.1073/pnas.0811879106

Finco, G., Locci, E., Mura, P., Massa, R., Noto, A., Musu, M., Landoni, G., d'Aloja, E., De-Giorgio, F., Scano, P., Evangelista, M., 2016. Can Urine Metabolomics Be Helpful in Differentiating Neuropathic and Nociceptive Pain? A Proof-of-Concept Study. PLoS ONE 11. https://doi.org/10.1371/journal.pone.0150476

Finnerup, N.B., 2013. Pain in patients with spinal cord injury. PAIN®, Biennial Review of Pain 154, Supplement 1, S71–S76. https://doi.org/10.1016/j.pain.2012.12.007

Finnerup, N.B., Attal, N., Haroutounian, S., McNicol, E., Baron, R., Dworkin, R.H., Gilron, I., Haanpää, M., Hansson, P., Jensen, T.S., Kamerman, P.R., Lund, K., Moore, A., Raja, S.N., Rice, A.S.C., Rowbotham, M., Sena, E., Siddall, P., Smith, B.H., Wallace, M., 2015. Pharmacotherapy for neuropathic pain in adults: a systematic review and meta-analysis. Lancet Neurol. 14, 162–173. https://doi.org/10.1016/S1474-4422(14)70251-0

Finnerup, N.B., Gyldensted, C., Nielsen, E., Kristensen, A.D., Bach, F.W., Jensen, T.S., 2003. MRI in chronic spinal cord injury patients with and without central pain. Neurology 61, 1569–1575. https://doi.org/10.1212/01.WNL.0000096016.29134.FA

Finnerup, N.B., Pedersen, L.H., Terkelsen, A.J., Johannesen, I.L., Jensen, T.S., 2007. Reaction to topical capsaicin in spinal cord injury patients with and without central pain. Exp. Neurol. 205, 190–200. https://doi.org/10.1016/j.expneurol.2007.01.026

Finsterbusch, J., 2012. Improving the performance of diffusion-weighted inner field-of-view echo-planar imaging based on 2D-Selective radiofrequency excitations by tilting the excitation plane. J. Magn. Reson. Imaging 35, 984–992. https://doi.org/10.1002/jmri.23522

Flanagan, E.P., Weinshenker, B.G., Krecke, K.N., Lennon, V.A., Lucchinetti, C.F., McKeon, A., Wingerchuk, D.M., Shuster, E.A., Jiao, Y., Horta, E.S., Pittock, S.J., 2015. Short myelitis lesions in aquaporin-4-IgG-positive neuromyelitis optica spectrum disorders. JAMA Neurol. 72, 81–87. https://doi.org/10.1001/jamaneurol.2014.2137

Flor, H., Braun, C., Elbert, T., Birbaumer, N., 1997. Extensive reorganization of primary somatosensory cortex in chronic back pain patients. Neurosci. Lett. 224, 5–8. https://doi.org/10.1016/S0304-3940(97)13441-3

Fontaine, D., Hamani, C., Lozano, A., 2009. Efficacy and safety of motor cortex stimulation for chronic neuropathic pain: critical review of the literature. J. Neurosurg. 110, 251–256. https://doi.org/10.3171/2008.6.17602

Freynhagen, R., Baron, R., Gockel, U., Tölle, T.R., 2006. painDETECT: a new screening questionnaire to identify neuropathic components in patients with back pain. Curr. Med. Res. Opin. 22, 1911–20.

Frohman, E.M., Wingerchuk, D.M., 2010. Transverse Myelitis. N. Engl. J. Med. 363, 564–572. https://doi.org/10.1056/NEJMcp1001112

Frostell, A., Hakim, R., Thelin, E.P., Mattsson, P., Svensson, M., 2016. A Review of the Segmental Diameter of the Healthy Human Spinal Cord. Front. Neurol. 7. https://doi.org/10.3389/fneur.2016.00238

Gao, Y.-J., Zhang, L., Samad, O.A., Suter, M.R., Yasuhiko, K., Xu, Z.-Z., Park, J.-Y., Lind, A.-L., Ma, Q., Ji, R.-R., 2009. JNK-induced MCP-1 production in spinal cord astrocytes contributes to central sensitization and neuropathic pain. J. Neurosci. Off. J. Soc. Neurosci. 29, 4096–4108. https://doi.org/10.1523/JNEUROSCI.3623-08.2009

Gebhart, G.F., 2004. Descending modulation of pain. Neurosci. Biobehav. Rev., Foundations and Innovations in the Neuroscience of Drug Abuse 27, 729–737. https://doi.org/10.1016/j.neubiorev.2003.11.008

Goadsby, P.J., 2005. Migraine, allodynia, sensitisation and all of that .. Eur. Neurol. 53 Suppl 1, 10–16. https://doi.org/10.1159/000085060

Golbraikh, A., Tropsha, A., 2002. Beware of q2! J. Mol. Graph. Model., QSAR in vivo 20, 269–276. https://doi.org/10.1016/S1093-3263(01)00123-1

Goldstone, A., Mayhew, S.D., Przezdzik, I., Wilson, R.S., Hale, J.R., Bagshaw, A.P., 2016. Gender Specific Re-organization of Resting-State Networks in Older Age. Front. Aging Neurosci. 8. https://doi.org/10.3389/fnagi.2016.00285

Graeff, F.G., Silveira, M.C.L., Nogueira, R.L., Audi, E.A., Oliveira, R.M.W., 1993. Role of the amygdala and periaqueductal gray in anxiety and panic. Behav. Brain Res. 58, 123–131. https://doi.org/10.1016/0166-4328(93)90097-A

Gray, E., Larkin, J.R., Claridge, T.D.W., Talbot, K., Sibson, N.R., Turner, M.R., 2015. The longitudinal cerebrospinal fluid metabolomic profile of amyotrophic lateral sclerosis. Amyotroph. Lateral Scler. Front. Degener. 16, 456–463. https://doi.org/10.3109/21678421.2015.1053490

Greenberg, B.M., 2015. Placebo studies should not be undertaken in NMO – No. Mult. Scler. J. 21, 691–693. https://doi.org/10.1177/1352458515579217

Griffin, C.M., Chard, D.T., Parker, G.J.M., Barker, G.J., Thompson, A.J., Miller, D.H., 2002. The relationship between lesion and normal appearing brain tissue abnormalities in early relapsing remitting multiple sclerosis. J. Neurol. 249, 193–199.

Guo Y, Lennon VA, Popescu Bh, et al, 2014. Autoimmune aquaporin-4 myopathy in neuromyelitis optica spectrum. JAMA Neurol. https://doi.org/10.1001/jamaneurol.2014.775

Gustafsson, M.C., Dahlqvist, O., Jaworski, J., Lundberg, P., Landtblom, A.-M.E., 2007. Low Choline Concentrations in Normal-Appearing White Matter of Patients with Multiple Sclerosis and Normal MR Imaging Brain Scans. Am. J. Neuroradiol. 28, 1306–1312. https://doi.org/10.3174/ajnr.A0580

Gwilym, S.E., Keltner, J.R., Warnaby, C.E., Carr, A.J., Chizh, B., Chessell, I., Tracey, I., 2009. Psychophysical and functional imaging evidence supporting the presence of central sensitization in a cohort of osteoarthritis patients. Arthritis Rheum. 61, 1226–1234. https://doi.org/10.1002/art.24837

Hains, B.C., Saab, C.Y., Waxman, S.G., 2005. Changes in electrophysiological properties and sodium channel Nav1.3 expression in thalamic neurons after spinal cord injury. Brain J. Neurol. 128, 2359–2371. https://doi.org/10.1093/brain/awh623

Hains, B.C., Waxman, S.G., 2006. Activated Microglia Contribute to the Maintenance of Chronic Pain after Spinal Cord Injury. J. Neurosci. 26, 4308–4317. https://doi.org/10.1523/JNEUROSCI.0003-06.2006

Hanley, M., Jensen, M., Cardenas, D., Turner, J., 2004. Clinical outcomes measurement: Pain interference in persons with spinal cord injury: Classification of mild, moderate, and severe pain. J. Pain, Supplement to The Journal of Pain 5, S113. https://doi.org/10.1016/j.jpain.2004.02.423

Hatem, S.M., Attal, N., Ducreux, D., Gautron, M., Parker, F., Plaghki, L., Bouhassira, D., 2010. Clinical, functional and structural determinants of central pain in syringomyelia. Brain 133, 3409–3422. https://doi.org/10.1093/brain/awq244

Hayes, D.J., Northoff, G., 2012. Common brain activations for painful and non-painful aversive stimuli. BMC Neurosci. 13, 60. https://doi.org/10.1186/1471-2202-13-60

Head, H., Holmes, G., 1911. SENSORY DISTURBANCES FROM CEREBRAL LESIONS. Brain 34, 102–254. https://doi.org/10.1093/brain/34.2-3.102

Healy, B.C., Arora, A., Hayden, D.L., Ceccarelli, A., Tauhid, S.S., Neema, M., Bakshi, R., 2012. Approaches to normalization of spinal cord volume: application to multiple sclerosis. J. Neuroimaging 22, e12–e19. https://doi.org/10.1111/j.1552-6569.2011.00629.x

Hendrich, J., Van Minh, A.T., Heblich, F., Nieto-Rostro, M., Watschinger, K., Striessnig, J., Wratten, J., Davies, A., Dolphin, A.C., 2008. Pharmacological disruption of calcium channel trafficking by the alpha2delta ligand gabapentin. Proc. Natl. Acad. Sci. U. S. A. 105, 3628–3633. https://doi.org/10.1073/pnas.0708930105

Hentall, I.D., Mesigil, R., Pinzon, A., Noga, B.R., 2003. Temporal and spatial profiles of pontine-evoked monoamine release in the rat's spinal cord. J. Neurophysiol. 89, 2943–2951. https://doi.org/10.1152/jn.00608.2002

Herwerth, M., Kalluri, S.R., Srivastava, R., Kleele, T., Kenet, S., Illes, Z., Merkler, D., Bennett, J.L., Misgeld, T., Hemmer, B., 2016. In vivo imaging reveals rapid astrocyte depletion and axon damage in a model of neuromyelitis optica-related pathology. Ann. Neurol. 79, 794–805. https://doi.org/10.1002/ana.24630

Hinson, S.R., Roemer, S.F., Lucchinetti, C.F., Fryer, J.P., Kryzer, T.J., Chamberlain, J.L., Howe, C.L., Pittock, S.J., Lennon, V.A., 2008. Aquaporin-4–binding autoantibodies in patients with neuromyelitis optica impair glutamate transport by down-regulating EAAT2. J. Exp. Med. 205, 2473–2481. https://doi.org/10.1084/jem.20081241

Hinson, S.R., Romero, M.F., Popescu, B.F.G., Lucchinetti, C.F., Fryer, J.P., Wolburg, H., Fallier-Becker, P., Noell, S., Lennon, V.A., 2012. Molecular outcomes of neuromyelitis optica (NMO)-IgG binding to aquaporin-4 in astrocytes. Proc. Natl. Acad. Sci. U. S. A. 109, 1245–1250. https://doi.org/10.1073/pnas.1109980108

Hirshberg, R.M., Al-Chaer, E.D., Lawand, N.B., Westlund, K.N., Willis, W.D., 1996. Is there a pathway in the posterior funiculus that signals visceral pain? Pain 67, 291–305.

Holden, J.E., Schwartz, E.J., Proudfit, H.K., 1999. Microinjection of morphine in the A7 catecholamine cell group produces opposing effects on nociception that are mediated by α1- and α2-adrenoceptors. Neuroscience 91, 979–990. https://doi.org/10.1016/S0306-4522(98)00673-3

Holmes, E., Foxall, P.J.D., Nicholson, J.K., Neild, G.H., Brown, S.M., Beddell, C.R., Sweatman, B.C., Rahr, E., Lindon, J.C., Spraul, M., Neidig, P., 1994. Automatic Data Reduction and Pattern Recognition Methods for Analysis of 1H Nuclear Magnetic Resonance Spectra of Human Urine from Normal and Pathological States. Anal. Biochem. 220, 284–296. https://doi.org/10.1006/abio.1994.1339

Holtås, S., Basibüyük, N., Fredriksson, K., 1993. MRI in acute transverse myelopathy. Neuroradiology 35, 221–226.

Hosobuchi, Y., Adams, J.E., Linchitz, R., 1977. Pain relief by electrical stimulation of the central gray matter in humans and its reversal by naloxone. Science 197, 183–186. https://doi.org/10.1126/science.301658

Houghton, A.K., Hewitt, E., Westlund, K.N., 1999. Dorsal column lesion prevents mechanical hyperalgesia and allodynia in osteotomy model. Pain 82, 73–80. https://doi.org/10.1016/S0304-3959(99)00034-2

Hua, L.H., Donlon, S.L., Sobhanian, M.J., Portner, S.M., Okuda, D.T., 2015. Thoracic spinal cord lesions are influenced by the degree of cervical spine involvement in multiple sclerosis. Spinal Cord 53, 520–525. https://doi.org/10.1038/sc.2014.238

Huh, S.-Y., Min, J.-H., Kim, W., Kim, S.-H., Kim, H.J., Kim, B.-J., Kim, B.J., Lee, K.H., 2013. The usefulness of brain MRI at onset in the differentiation of multiple sclerosis and seropositive neuromyelitis optica spectrum disorders. Mult. Scler. J. https://doi.org/10.1177/1352458513506953

Iannetti, G.D., Zambreanu, L., Wise, R.G., Buchanan, T.J., Huggins, J.P., Smart, T.S., Vennart, W., Tracey, I., 2005. Pharmacological modulation of pain-related brain activity during normal and central sensitization states in humans. Proc. Natl. Acad. Sci. U. S. A. 102, 18195–18200. https://doi.org/10.1073/pnas.0506624102

IASP Taxonomy - IASP [WWW Document], 2016. URL http://www.iasp-pain.org/Taxonomy#Peripheralneuropathicpain (accessed 9.26.16).

Inglese, M., Bester, M., 2010. Diffusion imaging in multiple sclerosis: research and clinical implications. NMR Biomed. 23, 865–872. https://doi.org/10.1002/nbm.1515

Ip, I.B., Berrington, A., Hess, A.T., Parker, A.J., Emir, U.E., Bridge, H., 2017. Combined fMRI-MRS acquires simultaneous glutamate and BOLD-fMRI signals in the human brain. NeuroImage 155, 113–119. https://doi.org/10.1016/j.neuroimage.2017.04.030

Ito, S., Mori, M., Makino, T., Hayakawa, S., Kuwabara, S., 2009. "Cloud-like enhancement" is a magnetic resonance imaging abnormality specific to neuromyelitis optica. Ann. Neurol. 66, 425–428.

Ito, T., Tanaka-Mizuno, S., Iwashita, N., Tooyama, I., Shiino, A., Miura, K., Fukui, S., 2017. Proton magnetic resonance spectroscopy assessment of metabolite status of the anterior cingulate cortex in chronic pain patients and healthy controls. J. Pain Res. 10, 287–293. https://doi.org/10.2147/JPR.S123403

Jacquet, Y.F., 1988. The NMDA receptor: central role in pain inhibition in rat periaqueductal gray. Eur. J. Pharmacol. 154, 271–276.

Jakes, W., Gerdova, A., Defernez, M., Watson, A.D., McCallum, C., Limer, E., Colquhoun, I.J., Williamson, D.C., Kemsley, E.K., 2015. Authentication of beef versus horse meat using 60MHz 1H NMR spectroscopy. Food Chem. 175, 1–9. https://doi.org/10.1016/j.foodchem.2014.11.110

Jarius, S., Ruprecht, K., Wildemann, B., Kuempfel, T., Ringelstein, M., Geis, C., Kleiter, I., Kleinschnitz, C., Berthele, A., Brettschneider, J., Hellwig, K., Hemmer, B., Linker, R.A., Lauda, F., Mayer, C.A., Tumani, H., Melms, A., Trebst, C., Stangel, M., Marziniak, M., Hoffmann, F., Schippling, S., Faiss, J.H., Neuhaus, O., Ettrich, B., Zentner, C., Guthke, K., Hofstadt-van Oy, U., Reuss, R., Pellkofer, H., Ziemann, U., Kern, P., Wandinger, K.P., Bergh, F.T., Boettcher, T., Langel, S., Liebetrau, M., Rommer, P.S., Niehaus, S., Münch, C., Winkelmann, A., Zettl U, U.K., Metz, I., Veauthier, C., Sieb, J.P., Wilke, C., Hartung, H.P., Aktas, O., Paul, F., 2012. Contrasting disease patterns in seropositive and seronegative neuromyelitis optica: A multicentre study of 175 patients. J. Neuroinflammation 9, 14. https://doi.org/10.1186/1742-2094-9-14

Jenkinson, M., Beckmann, C.F., Behrens, T.E.J., Woolrich, M.W., Smith, S.M., 2012. FSL. NeuroImage 62, 782–790. https://doi.org/10.1016/j.neuroimage.2011.09.015

Jensen, M.P., Smith, D.G., Ehde, D.M., Robinsin, L.R., 2001. Pain site and the effects of amputation pain: further clarification of the meaning of mild, moderate, and severe pain. Pain 91, 317–322. https://doi.org/10.1016/S0304-3959(00)00459-0

Johansen, J.P., Fields, H.L., 2004. Glutamatergic activation of anterior cingulate cortex produces an aversive teaching signal. Nat. Neurosci. 7, 398–403. https://doi.org/10.1038/nn1207

Jones, M.V., Collongues, N., de Seze, J., Kinoshita, M., Nakatsuji, Y., Levy, M., 2012. Review of Animal Models of Neuromyelitis Optica. Mult. Scler. Relat. Disord. 1, 174–179. https://doi.org/10.1016/j.msard.2012.06.003

Jones, S.L., Gebhart, G.F., 1988. Inhibition of spinal nociceptive transmission from the midbrain, pons and medulla in the rat: activation of descending inhibition by morphine, glutamate and electrical stimulation. Brain Res. 460, 281–296. https://doi.org/10.1016/0006-8993(88)90373-3

Jones, S.L., Gebhart, G.F., 1986. Characterization of coeruleospinal inhibition of the nociceptive tail-flick reflex in the rat: Mediation by spinal α2-adrenoceptors. Brain Res. 364, 315–330. https://doi.org/10.1016/0006-8993(86)90844-9

Jurynczyk, M., Geraldes, R., Probert, F., Woodhall, M.R., Waters, P., Tackley, G., DeLuca, G., Chandratre, S., Leite, M.I., Vincent, A., Palace, J., 2017a. Distinct brain imaging characteristics of autoantibody-mediated CNS conditions and multiple sclerosis. Brain 140, 617–627. https://doi.org/10.1093/brain/aww350

Jurynczyk, M., Probert, F., Yeo, T., Tackley, G., Claridge, T.D.W., Cavey, A., Woodhall, M.R., Arora, S., Winkler, T., Schiffer, E., Vincent, A., DeLuca, G., Sibson, N.R., Isabel Leite, M., Waters, P., Anthony, D.C., Palace, J., 2017b. Metabolomics reveals distinct, antibody-independent, molecular signatures of MS, AQP4-antibody and MOG-antibody disease. Acta Neuropathol. Commun. 5, 95. https://doi.org/10.1186/s40478-017-0495-8

Juryńczyk, M., Zaleski, K., Selmaj, K., 2013. Natalizumab and the development of extensive brain lesions in neuromyelitis optica. J. Neurol. 260, 1919–1921. https://doi.org/10.1007/s00415-013-6965-4

Kalita, J., Shah, S., Kapoor, R., Misra, U.K., 2002. Bladder dysfunction in acute transverse myelitis: magnetic resonance imaging and neurophysiological and urodynamic correlations. J. Neurol. Neurosurg. Psychiatry 73, 154–159. https://doi.org/10.1136/jnnp.73.2.154

Kalous, A., Osborne, P.B., Keast, J.R., 2007. Acute and chronic changes in dorsal horn innervation by primary afferents and descending supraspinal pathways after spinal cord injury. J. Comp. Neurol. 504, 238–253. https://doi.org/10.1002/cne.21412
Kanamori, Y., Nakashima, I., Takai, Y., Nishiyama, S., Kuroda, H., Takahashi, T., Kanaoka-Suzuki, C., Misu, T., Fujihara, K., Itoyama, Y., 2011. Pain in neuromyelitis optica and its effect on quality of life: a cross-sectional study. Neurology 77, 652–658. https://doi.org/10.1212/WNL.0b013e318229e694
Karl, A., Birbaumer, N., Lutzenberger, W., Cohen, L.G., Flor, H., 2001. Reorganization of Motor and Somatosensory Cortex in Upper Extremity Amputees with Phantom Limb Pain. J. Neurosci. 21, 3609–3618.
Kawachi, I., Lassmann, H., 2017. Neurodegeneration in multiple sclerosis and neuromyelitis optica. J Neurol Neurosurg Psychiatry 88, 137–145. https://doi.org/10.1136/jnnp-2016-313300
Khanna, S., Sharma, A., Huecker, J., Gordon, M., Naismith, R.T., Van Stavern, G.P., 2012. Magnetic resonance imaging of optic neuritis in patients with neuromyelitis optica versus multiple sclerosis. J. Neuro-Ophthalmol. Off. J. North Am. Neuro-Ophthalmol. Soc. 32, 216–220. https://doi.org/10.1097/WNO.0b013e318254c62d
Kidd, D., Barkhof, F., McConnell, R., Algra, P.R., Allen, I.V., Revesz, T., 1999. Cortical lesions in multiple sclerosis. Brain 122, 17–26. https://doi.org/10.1093/brain/122.1.17
Kim, D.H., Fields, H.L., Barbaro, N.M., 1990. Morphine analgesia and acute physical dependence: rapid onset of two opposing, dose-related processes. Brain Res. 516, 37–40. https://doi.org/10.1016/0006-8993(90)90894-H
Kim, H.J., Paul, F., Lana-Peixoto, M.A., Tenembaum, S., Asgari, N., Palace, J., Klawiter, E.C., Sato, D.K., de Seze, J., Wuerfel, J., Banwell, B.L., Villoslada, P., Saiz, A., Fujihara, K., Kim, S.-H., 2015. MRI characteristics of neuromyelitis optica spectrum disorder. Neurology 84, 1165–1173. https://doi.org/10.1212/WNL.0000000000001367
Kim, S.-M., Go, M.J., Sung, J.-J., Park, K.S., Lee, K.-W., 2012. Painful tonic spasm in neuromyelitis optica: incidence, diagnostic utility, and clinical characteristics. Arch. Neurol. 69, 1026–1031. https://doi.org/10.1001/archneurol.2012.112
Kim, S.-M., Kim, S.-J., Lee, H.J., Kuroda, H., Palace, J., Fujihara, K., 2017. Differential diagnosis of neuromyelitis optica spectrum disorders. Ther. Adv. Neurol. Disord. 10, 265–289. https://doi.org/10.1177/1756285617709723
Kim, W., Lee, J.E., Kim, S.-H., Huh, S.-Y., Hyun, J.-W., Jeong, I.H., Park, M.-S., Cho, J.Y., Lee, S.-H., Lee, K.S., Kim, H.J., 2016. Cerebral Cortex Involvement in Neuromyelitis Optica Spectrum Disorder. J. Clin. Neurol. Seoul Korea 12, 188–193. https://doi.org/10.3988/jcn.2016.12.2.188
Kim, W., Park, M.S., Lee, S.H., Kim, S.-H., Jung, I.J., Takahashi, T., Misu, T., Fujihara, K., Kim, H.J., 2010. Characteristic brain magnetic resonance imaging abnormalities in central nervous system aquaporin-4 autoimmunity. Mult. Scler. J. 16, 1229–1236. https://doi.org/10.1177/1352458510376640
Kimbrough, D.J., Fujihara, K., Jacob, A., Lana-Peixoto, M.A., Leite, M.I., Levy, M., Marignier, R., Nakashima, I., Palace, J., de Seze, J., Stuve, O., Tenembaum, S.N., Traboulsee, A., Waubant, E., Weinshenker, B.G., Wingerchuk, D.M., GJCF-CC&BR, 2012. Treatment of Neuromyelitis Optica: Review and Recommendations. Mult. Scler. Relat. Disord. 1, 180–187. https://doi.org/10.1016/j.msard.2012.06.002
Kister, I., Herbert, J., Zhou, Y., Ge, Y., 2013. Ultrahigh-Field MR (7 T) Imaging of Brain Lesions in Neuromyelitis Optica. Mult. Scler. Int. 2013, 1–7. https://doi.org/10.1155/2013/398259

Kitley, J., 2013. Longitudinally Extensive Transverse Myelitis With and Without Aquaporin 4 Antibodies. JAMA Neurol. https://doi.org/10.1001/jamaneurol.2013.3890

Kitley, J., Leite, M.I., George, J.S., Palace, J.A., 2012a. The differential diagnosis of longitudinally extensive transverse myelitis. Mult. Scler. Houndmills Basingstoke Engl. 18, 271–285. https://doi.org/10.1177/1352458511406165

Kitley, J., Leite, M.I., Nakashima, I., Waters, P., McNeillis, B., Brown, R., Takai, Y., Takahashi, T., Misu, T., Elsone, L., Woodhall, M., George, J., Boggild, M., Vincent, A., Jacob, A., Fujihara, K., Palace, J., 2012b. Prognostic factors and disease course in aquaporin-4 antibody-positive patients with neuromyelitis optica spectrum disorder from the United Kingdom and Japan. Brain J. Neurol. 135, 1834–1849. https://doi.org/10.1093/brain/aws109

Kitley, J., Palace, J., 2016. Therapeutic options in neuromyelitis optica spectrum disorders. Expert Rev. Neurother. 16, 319–329. https://doi.org/10.1586/14737175.2016.1150178

Kıyat-Atamer, A., Ekizoğlu, E., Tüzün, E., Kürtüncü, M., Shugaiv, E., Akman-Demir, G., Eraksoy, M., 2013. Long-term MRI findings in neuromyelitis optica: seropositive versus seronegative patients. Eur. J. Neurol. 20, 781–787. https://doi.org/10.1111/ene.12058

Klawiter, E.C., Xu, J., Naismith, R.T., Benzinger, T.L.S., Shimony, J.S., Lancia, S., Snyder, A.Z., Trinkaus, K., Song, S.-K., Cross, A.H., 2012. Increased radial diffusivity in spinal cord lesions in neuromyelitis optica compared with multiple sclerosis. Mult. Scler. Houndmills Basingstoke Engl. 18, 1259–1268. https://doi.org/10.1177/1352458512436593

Ko, H.-Y., Park, J.H., Shin, Y.B., Baek, S.Y., 2004. Gross quantitative measurements of spinal cord segments in human. Spinal Cord 42, 35–40. https://doi.org/10.1038/sj.sc.3101538

Kong, Y., Eippert, F., Beckmann, C.F., Andersson, J., Finsterbusch, J., Büchel, C., Tracey, I., Brooks, J.C.W., 2014. Intrinsically organized resting state networks in the human spinal cord. Proc. Natl. Acad. Sci. 111, 18067–18072. https://doi.org/10.1073/pnas.1414293111

Kong, Y., Okoruwa, H., Revis, J., Tackley, G., Leite, M.I., Lee, M., Tracey, I., Palace, J., 2016. Pain in patients with transverse myelitis and its relationship to aquaporin 4 antibody status. J. Neurol. Sci. 368, 84–88. https://doi.org/10.1016/j.jns.2016.06.041

Kremer, S., Renard, F., Achard, S., Lana-Peixoto, M.A., Palace, J., Asgari, N., Klawiter, E.C., Tenembaum, S.N., Banwell, B., Greenberg, B.M., Bennett, J.L., Levy, M., Villoslada, P., Saiz, A., Fujihara, K., Chan, K.H., Schippling, S., Paul, F., Kim, H.J., de Seze, J., Wuerfel, J.T., Guthy-Jackson Charitable Foundation (GJCF) Neuromyelitis Optica (NMO) International Clinical Consortium and Biorepository, Cabre, P., Marignier, R., Tedder, T., van Pelt, D., Broadley, S., Chitnis, T., Wingerchuk, D., Pandit, L., Leite, M.I., Apiwattanakul, M., Kleiter, I., Prayoonwiwat, N., Han, M., Hellwig, K., van Herle, K., John, G., Hooper, D.C., Nakashima, I., Sato, D., Yeaman, M.R., Waubant, E., Zamvil, S., Stüve, O., Aktas, O., Smith, T.J., Jacob, A., O'Connor, K., 2015. Use of Advanced Magnetic Resonance Imaging Techniques in Neuromyelitis Optica Spectrum Disorder. JAMA Neurol. 72, 815–822. https://doi.org/10.1001/jamaneurol.2015.0248

Kucyi, A., Salomons, T.V., Davis, K.D., 2013. Mind wandering away from pain dynamically engages antinociceptive and default mode brain networks. Proc. Natl. Acad. Sci. U. S. A. 110, 18692–18697. https://doi.org/10.1073/pnas.1312902110

Kurtzke, J.F., 1983. Rating neurologic impairment in multiple sclerosis: an expanded disability status scale (EDSS). Neurology 33, 1444–1452.

Kwiat, G.C., Basbaum, A.I., 1990. Organization of tyrosine hydroxylase- and serotonin-immunoreactive brainstem neurons with axon collaterals to the periaqueductal gray and the spinal cord in the rat. Brain Res. 528, 83–94. https://doi.org/10.1016/0006-8993(90)90198-K

Lai, T.-H., Fuh, J.-L., Lirng, J.-F., Lin, C.-P., Wang, S.-J., 2012. Brainstem 1H-MR spectroscopy in episodic and chronic migraine. J. Headache Pain 13, 645–651. https://doi.org/10.1007/s10194-012-0491-0

LaMotte, R.H., Shain, C.N., Simone, D.A., Tsai, E.F., 1991. Neurogenic hyperalgesia: psychophysical studies of underlying mechanisms. J. Neurophysiol. 66, 190–211.

Lau, B.K., Vaughan, C.W., 2014. Descending modulation of pain: the GABA disinhibition hypothesis of analgesia. Curr. Opin. Neurobiol., SI: Neuromodulation 29, 159–164. https://doi.org/10.1016/j.conb.2014.07.010

Lee, M.C., Zambreanu, L., Menon, D.K., Tracey, I., 2008. Identifying brain activity specifically related to the maintenance and perceptual consequence of central sensitization in humans. J. Neurosci. Off. J. Soc. Neurosci. 28, 11642–11649. https://doi.org/10.1523/JNEUROSCI.2638-08.2008

Lennon, V.A., Kryzer, T.J., Pittock, S.J., Verkman, A.S., Hinson, S.R., 2005. IgG marker of optic-spinal multiple sclerosis binds to the aquaporin-4 water channel. J. Exp. Med. 202, 473–477. https://doi.org/10.1084/jem.20050304

Lennon, V.A., Wingerchuk, D.M., Kryzer, T.J., Pittock, S.J., Lucchinetti, C.F., Fujihara, K., Nakashima, I., Weinshenker, B.G., 2004. A serum autoantibody marker of neuromyelitis optica: distinction from multiple sclerosis. The Lancet 364, 2106–2112. https://doi.org/10.1016/S0140-6736(04)17551-X

Lenz, F.A., Kwan, H.C., Dostrovsky, J.O., Tasker, R.R., 1989. Characteristics of the bursting pattern of action potentials that occurs in the thalamus of patients with central pain. Brain Res. 496, 357–360. https://doi.org/10.1016/0006-8993(89)91088-3

Lindblom, U.F., Ottosson, J.O., 1957. Influence of Pyramidal Stimulation upon the Relay of Coarse Cutaneous Afferents in the Dorsal Horn. Acta Physiol. Scand. 38, 309–318. https://doi.org/10.1111/j.1748-1716.1957.tb01394.x

Lorenz, J., Cross, D.J., Minoshima, S., Morrow, T.J., Paulson, P.E., Casey, K.L., 2002. A Unique Representation of Heat Allodynia in the Human Brain. Neuron 35, 383–393. https://doi.org/10.1016/S0896-6273(02)00767-5

Lorenz, J., Minoshima, S., Casey, K.L., 2003. Keeping pain out of mind: the role of the dorsolateral prefrontal cortex in pain modulation. Brain 126, 1079–1091. https://doi.org/10.1093/brain/awg102

Losseff, N.A., Webb, S.L., O'Riordan, J.I., Page, R., Wang, L., Barker, G.J., Tofts, P.S., McDonald, W.I., Miller, D.H., Thompson, A.J., 1996. Spinal cord atrophy and disability in multiple sclerosisA new reproducible and sensitive MRI method with potential to monitor disease progression. Brain 119, 701–708. https://doi.org/10.1093/brain/119.3.701

Lucchinetti, C.F., Guo, Y., Popescu, B.F.G., Fujihara, K., Itoyama, Y., Misu, T., 2014. The Pathology of an Autoimmune Astrocytopathy: Lessons Learned from Neuromyelitis Optica. Brain Pathol. Zurich Switz. 24, 83–97. https://doi.org/10.1111/bpa.12099

Lucchinetti, C.F., Mandler, R.N., McGavern, D., Bruck, W., Gleich, G., Ransohoff, R.M., Trebst, C., Weinshenker, B., Wingerchuk, D., Parisi, J.E., Lassmann, H., 2002. A role for humoral mechanisms in the pathogenesis of Devic's neuromyelitis optica. Brain 125, 1450–1461. https://doi.org/10.1093/brain/awf151

Luo, Z.D., Chaplan, S.R., Higuera, E.S., Sorkin, L.S., Stauderman, K.A., Williams, M.E., Yaksh, T.L., 2001. Upregulation of Dorsal Root Ganglion α2δ Calcium Channel Subunit and Its Correlation with Allodynia in Spinal Nerve-Injured Rats. J. Neurosci. 21, 1868–1875.

Macey, P.M., Sarma, M.K., Prasad, J.P., Ogren, J.A., Aysola, R., Harper, R.M., Thomas, M.A., 2017. Obstructive sleep apnea is associated with altered midbrain chemical concentrations. Neuroscience. https://doi.org/10.1016/j.neuroscience.2017.09.001

MacLean, P.D., 1949. Psychosomatic disease and the visceral brain; recent developments bearing on the Papez theory of emotion. Psychosom. Med. 11, 338–353.

Maier, C., Baron, R., Tölle, T.R., Binder, A., Birbaumer, N., Birklein, F., Gierthmühlen, J., Flor, H., Geber, C., Huge, V., Krumova, E.K., Landwehrmeyer, G.B., Magerl, W., Maihöfner, C., Richter, H., Rolke, R., Scherens, A., Schwarz, A., Sommer, C., Tronnier, V., Üçeyler, N., Valet, M., Wasner, G., Treede, R.-D., 2010. Quantitative sensory testing in the German Research Network on Neuropathic Pain (DFNS): Somatosensory abnormalities in 1236 patients with different neuropathic pain syndromes. PAIN 150, 439–450. https://doi.org/10.1016/j.pain.2010.05.002

Mandler, R.N., Davis, L.E., Jeffery, D.R., Kornfeld, M., 1993. Devic's neuromyelitis optica: A clinicopathological study of 8 patients. Ann. Neurol. 34, 162–168. https://doi.org/10.1002/ana.410340211

Mann, R.S., Constantinescu, C.S., Tench, C.R., 2007. Upper cervical spinal cord cross-sectional area in relapsing remitting multiple sclerosis: application of a new technique for measuring cross-sectional area on magnetic resonance images. J. Magn. Reson. Imaging JMRI 26, 61–65. https://doi.org/10.1002/jmri.20959

Mantyh, P.W., 1983. Connections of midbrain periaqueductal gray in the monkey. II. Descending efferent projections. J. Neurophysiol. 49, 582–594. https://doi.org/10.1152/jn.1983.49.3.582

Marchand, J.E., Hagino, N., 1983. Afferents to the periaqueductal gray in the rat. A horseradish peroxidase study. Neuroscience 9, 95–106.

Marek, R., Strobel, C., Bredy, T.W., Sah, P., 2013. The amygdala and medial prefrontal cortex: partners in the fear circuit. J. Physiol. 591, 2381–2391. https://doi.org/10.1113/jphysiol.2012.248575

Marignier, R., Nicolle, A., Watrin, C., Touret, M., Cavagna, S., Varrin-Doyer, M., Cavillon, G., Rogemond, V., Confavreux, C., Honnorat, J., Giraudon, P., 2010. Oligodendrocytes are damaged by neuromyelitis optica immunoglobulin G via astrocyte injury. Brain J. Neurol. 133, 2578–2591. https://doi.org/10.1093/brain/awq177

Masters-Israilov, A., Robbins, M.S., 2017. Headache in Neuromyelitis Optica. Curr. Pain Headache Rep. 21, 20. https://doi.org/10.1007/s11916-017-0620-1

MATLAB, 2015. version 8.6.0 (R2015b). The MathWorks Inc., Natick, Massachusetts.

Matsushita, T., Isobe, N., Matsuoka, T., Shi, N., Kawano, Y., Wu, X., Yoshiura, T., Nakao, Y., Ishizu, T., Kira, J., 2009. Aquaporin-4 autoimmune syndrome and anti-aquaporin-4 antibody-negative opticospinal multiple sclerosis in Japanese. Mult. Scler. 15, 834–847. https://doi.org/10.1177/1352458509104595

Matthews, L., Kolind, S., Brazier, A., Leite, M.I., Brooks, J., Traboulsee, A., Jenkinson, M., Johansen-Berg, H., Palace, J., 2015. Imaging Surrogates of Disease Activity in Neuromyelitis Optica Allow Distinction from Multiple Sclerosis. PLOS ONE 10, e0137715. https://doi.org/10.1371/journal.pone.0137715

Matthews, L., Marasco, R., Jenkinson, M., Küker, W., Luppe, S., Leite, M.I., Giorgio, A., De Stefano, N., Robertson, N., Johansen-Berg, H., Evangelou, N., Palace, J., 2013. Distinction of seropositive NMO spectrum disorder and MS brain lesion distribution. Neurology 80, 1330–1337. https://doi.org/10.1212/WNL.0b013e3182887957

Matthews, L., Palace, J.A., 2014. The role of imaging in diagnosing neuromyelitis optica spectrum disorder. Mult. Scler. Relat. Disord. 3, 284–293. https://doi.org/10.1016/j.msard.2013.11.003

Mayer, D.J., Price, D.D., 1976. Central nervous system mechanisms of analgesia. Pain 2, 379–404.

McMahon, S.B. (Ed.), 2013. Wall and Melzack's textbook of pain, 6th ed. ed. Elsevier/Saunders, Philadelphia, PA.

Meisner, J.G., Marsh, A.D., Marsh, D.R., 2010. Loss of GABAergic interneurons in laminae I-III of the spinal cord dorsal horn contributes to reduced GABAergic tone and neuropathic pain after spinal cord injury. J. Neurotrauma 27, 729–737. https://doi.org/10.1089/neu.2009.1166

Meissner, A., van der Plas, A.A., van Dasselaar, N.T., Deelder, A.M., van Hilten, J.J., Mayboroda, O.A., 2014. 1H-NMR metabolic profiling of cerebrospinal fluid in patients with complex regional pain syndrome–related dystonia: Pain 155, 190–196. https://doi.org/10.1016/j.pain.2013.10.005

Melzack, R., 1987. The short-form McGill pain questionnaire. Pain 30, 191–197. https://doi.org/10.1016/0304-3959(87)91074-8

Melzack, R., Stotler, W.A., Livingston, W.K., 1958. Effects of discrete brainstem lesions in cats on perception of noxious stimulation. J. Neurophysiol. 21, 353–367. https://doi.org/10.1152/jn.1958.21.4.353

Meng, I.D., Manning, B.H., Martin, W.J., Fields, H.L., 1998. An analgesia circuit activated by cannabinoids. Nature 395, 381–383. https://doi.org/10.1038/26481

Meyer-Moock, S., Feng, Y.-S., Maeurer, M., Dippel, F.-W., Kohlmann, T., 2014. Systematic literature review and validity evaluation of the Expanded Disability Status Scale (EDSS) and the Multiple Sclerosis Functional Composite (MSFC) in patients with multiple sclerosis. BMC Neurol. 14, 58. https://doi.org/10.1186/1471-2377-14-58

Millan, M.J., 2002. Descending control of pain. Prog. Neurobiol. 66, 355–474.

Minami, T., Matsumura, S., Okuda-Ashitaka, E., Shimamoto, K., Sakimura, K., Mishina, M., Mori, H., Ito, S., 2001. Characterization of the glutamatergic system for induction and maintenance of allodynia. Brain Res. 895, 178–185. https://doi.org/10.1016/S0006-8993(01)02069-8

Misu, T., Fujihara, K., Kakita, A., Konno, H., Nakamura, M., Watanabe, S., Takahashi, T., Nakashima, I., Takahashi, H., Itoyama, Y., 2007. Loss of aquaporin 4 in lesions of neuromyelitis optica: distinction from multiple sclerosis. Brain 130, 1224–1234. https://doi.org/10.1093/brain/awm047

Misu, T., Fujihara, K., Nakashima, I., Sato, S., Itoyama, Y., 2005. Intractable hiccup and nausea with periaqueductal lesions in neuromyelitis optica. Neurology 65, 1479–1482. https://doi.org/10.1212/01.wnl.0000183151.19351.82

Misu, T., Höftberger, R., Fujihara, K., Wimmer, I., Takai, Y., Nishiyama, S., Nakashima, I., Konno, H., Bradl, M., Garzuly, F., Itoyama, Y., Aoki, M., Lassmann, H., 2013. Presence of six different lesion types suggests diverse mechanisms of tissue injury in neuromyelitis optica. Acta Neuropathol. (Berl.) 125, 815–827. https://doi.org/10.1007/s00401-013-1116-7

Mitchell, S., Holmes, E., Carmichael, P., 2002. Metabonomics and medicine: the Biochemical Oracle. Biol. Lond. Engl. 49, 217–221.

Monconduit, L., Villanueva, L., 2005. The lateral ventromedial thalamic nucleus spreads nociceptive signals from the whole body surface to layer I of the frontal cortex. Eur. J. Neurosci. 21, 3395–3402. https://doi.org/10.1111/j.1460-9568.2005.04160.x

Moussallieh, F.-M., Elbayed, K., Chanson, J., Rudolf, G., Piotto, M., De Seze, J., Namer, I., 2013. Serum analysis by 1H Nuclear Magnetic Resonance spectroscopy: a new tool for distinguishing neuromyelitis optica from multiple sclerosis. Mult. Scler. J. https://doi.org/10.1177/1352458513504638

Murchison, A., Kitley, J., George, J., Woodhall, M., Waters, P., Vincent, A., Leite, M., Kuker, W., Palace, J., 2013. Spinal cord MRI features in neuromyelitis optica (NMO): characteristics and relationship with severity and recovery in longitudinally extensive transverse myelitis (LETM) attacks. Mult. Scler. J. 19, 329–329.

Murchison, A., Kitley, J., Leite, M.I., Küker, W., Palace, J., 2015. Predictive value of MRI parameters in severity and recovery of first-episode myelitis in aquaporin-4 antibody disease. J. Neurol. Sci. 355, 49–53. https://doi.org/10.1016/j.jns.2015.05.011

Mutch, K., Methley, A., Zhao, S., Elsone, L., Emmanuel, A., Panicker, J., Jacob, A., 2014. Bladder, bowel and sexual function in neuromyelitis optica affects quality of life. Mult. Scler. J. 20, 978–978.

Naismith, R.T., Xu, J., Klawiter, E.C., Lancia, S., Tutlam, N.T., Wagner, J.M., Qian, P., Trinkaus, K., Song, S.-K., Cross, A.H., 2013. Spinal cord tract diffusion tensor imaging reveals disability substrate in demyelinating disease. Neurology 80, 2201–2209. https://doi.org/10.1212/WNL.0b013e318296e8f1

Nakae, A., Nakai, K., Yano, K., Hosokawa, K., Shibata, M., Mashimo, T., 2011. The Animal Model of Spinal Cord Injury as an Experimental Pain Model. BioMed Res. Int. 2011, e939023. https://doi.org/10.1155/2011/939023

Nakamura, M., Miyazawa, I., Fujihara, K., Nakashima, I., Misu, T., Watanabe, S., Takahashi, T., Itoyama, Y., 2008. Preferential spinal central gray matter involvement in neuromyelitis optica. J. Neurol. 255, 163–170. https://doi.org/10.1007/s00415-008-0545-z

Napadow, V., LaCount, L., Park, K., As-Sanie, S., Clauw, D.J., Harris, R.E., 2010. Intrinsic Brain Connectivity in Fibromyalgia is Associated with Chronic Pain Intensity. Arthritis Rheum. 62, 2545–2555. https://doi.org/10.1002/art.27497

Narayana, P.A., Doyle, T.J., Lai, D., Wolinsky, J.S., 1998. Serial proton magnetic resonance spectroscopic imaging, contrast-enhanced magnetic resonance imaging, and quantitative lesion volumetry in multiple sclerosis. Ann. Neurol. 43, 56–71. https://doi.org/10.1002/ana.410430112

Nyberg, N., 2013. RBNMR.

O'Connor, A.B., Schwid, S.R., Herrmann, D.N., Markman, J.D., Dworkin, R.H., 2008. Pain associated with multiple sclerosis: Systematic review and proposed classification. PAIN® 137, 96–111. https://doi.org/10.1016/j.pain.2007.08.024

Okuda, D.T., Melmed, K., Matsuwaki, T., Blomqvist, A., Craig, A.D.B., 2014. Central neuropathic pain in MS is due to distinct thoracic spinal cord lesions. Ann. Clin. Transl. Neurol. 1, 554–561. https://doi.org/10.1002/acn3.85

Oldenmenger, W.H., van der Rijt, C.C., 2016. Feasibility of assessing patients' acceptable pain in a randomized controlled trial on a patient pain education program. Palliat. Med. 0269216316664492. https://doi.org/10.1177/0269216316664492

Olechowski, C.J., Truong, J.J., Kerr, B.J., 2009. Neuropathic pain behaviours in a chronic-relapsing model of experimental autoimmune encephalomyelitis (EAE): Pain 141, 156–164. https://doi.org/10.1016/j.pain.2008.11.002

Österberg, A., Boivie, J., 2010. Central pain in multiple sclerosis – Sensory abnormalities. Eur. J. Pain 14, 104–110. https://doi.org/10.1016/j.ejpain.2009.03.003

Österberg, A., Boivie, J., Thuomas, K.-Å., 2005. Central pain in multiple sclerosis — prevalence and clinical characteristics. Eur. J. Pain 9, 531–531. https://doi.org/10.1016/j.ejpain.2004.11.005

Osterman, P.O., Westerberg, C.-E., 1975. PAROXYSMAL ATTACKS IN MULTIPLE SCLEROSIS. Brain 98, 189–202. https://doi.org/10.1093/brain/98.2.189

Oz, G., Tkáč, I., 2011. Short-echo, single-shot, full-intensity proton magnetic resonance spectroscopy for neurochemical profiling at 4 T: validation in the cerebellum and brainstem. Magn. Reson. Med. Off. J. Soc. Magn. Reson. Med. Soc. Magn. Reson. Med. 65, 901–910. https://doi.org/10.1002/mrm.22708

Palace, J., 2015. Placebo studies should not be undertaken in NMO – Yes. Mult. Scler. J. 21, 689–691. https://doi.org/10.1177/1352458515579446

Palace, J., Leite, I., Jacob, A., 2012. A practical guide to the treatment of neuromyelitis optica. Pract. Neurol. 12, 209–214. https://doi.org/10.1136/practneurol-2012-000237

Palace J, Leite M, Nairne A, Vincent A, 2010. Interferon beta treatment in neuromyelitis optica: Increase in relapses and aquaporin 4 antibody titers. Arch. Neurol. 67, 1016–1017. https://doi.org/10.1001/archneurol.2010.188

Palecek, J., 2004. The role of dorsal columns pathway in visceral pain. Physiol. Res. 53 Suppl 1, S125-130.

Pandit, L., Asgari, N., Apiwattanakul, M., Palace, J., Paul, F., Leite, M.I., Kleiter, I., Chitnis, T., GJCF International Clinical Consortium & Biorepository for Neuromyelitis Optica, 2015. Demographic and clinical features of neuromyelitis optica: A review. Mult. Scler. Houndmills Basingstoke Engl. 21, 845–853. https://doi.org/10.1177/1352458515572406

Papadopoulos, M.C., Verkman, A.S., 2011. Aquaporin 4 and neuromyelitis optica. Lancet Neurol. 11, 535–544. https://doi.org/10.1016/S1474-4422(12)70133-3

Pastoriza, L.N., Morrow, T.J., Casey, K.L., 1996. Medial frontal cortex lesions selectively attenuate the hot plate response: possible nocifensive apraxia in the rat. Pain 64, 11–17. https://doi.org/10.1016/0304-3959(95)00070-4

Patrick Hardy, S.G., Haigler, H.J., 1985. Prefrontal influences upon the midbrain: A possible route for pain modulation. Brain Res. 339, 285–293. https://doi.org/10.1016/0006-8993(85)90094-0

Patti, G.J., Yanes, O., Shriver, L.P., Courade, J.-P., Tautenhahn, R., Manchester, M., Siuzdak, G., 2012. Metabolomics implicates altered sphingolipids in chronic pain of neuropathic origin. Nat. Chem. Biol. 8, 232–234. https://doi.org/10.1038/nchembio.767

Paty, D.W., Oger, J.J.F., Kastrukoff, L.F., Hashimoto, S.A., Hooge, J.P., Eisen, A.A., Eisen, K.A., Purves, S.J., Low, M.D., Brandejs, V., Robertson, W.D., Li, D.K.B., 1988. MRI in the diagnosis of MS A prospective study with comparison of clinical evaluation, evoked potentials, oligoclonal banding, and CT. Neurology 38, 180–180. https://doi.org/10.1212/WNL.38.2.180

Pellkofer, H.L., Havla, J., Hauer, D., Schelling, G., Azad, S.C., Kuempfel, T., Magerl, W., Huge, V., 2013. The Major Brain Endocannabinoid 2-AG Controls Neuropathic Pain and Mechanical Hyperalgesia in Patients with Neuromyelitis Optica. PLoS ONE 8, e71500. https://doi.org/10.1371/journal.pone.0071500

Pertovaara, A., 2006. Noradrenergic pain modulation. Prog. Neurobiol. 80, 53–83. https://doi.org/10.1016/j.pneurobio.2006.08.001

Pessôa, F.M.C., Lopes, F.C.R., Costa, J.V.A., Leon, S.V.A., Domingues, R.C., Gasparetto, E.L., 2012. The cervical spinal cord in neuromyelitis optica patients: a comparative study with multiple sclerosis using diffusion tensor imaging. Eur. J. Radiol. 81, 2697–2701. https://doi.org/10.1016/j.ejrad.2011.11.026

Petrovic, P., Petersson, K.M., Ghatan, P.H., Stone-Elander, S., Ingvar, M., 2000. Pain-related cerebral activation is altered by a distracting cognitive task. Pain 85, 19–30. https://doi.org/10.1016/S0304-3959(99)00232-8

Pires, C.E., Silva, C.M.C. da, Lopes, F.C.R., Malfetano, F.R., Pereira, V.C.S.R., Kubo, T., Bahia, P.R.V., Alves-Leon, S.V., Gasparetto, E.L., 2012. Brain MRI abnormalities in Brazilian patients with neuromyelitis optica. J. Clin. Neurosci. Off. J. Neurosurg. Soc. Australas. 19, 969–974. https://doi.org/10.1016/j.jocn.2011.10.009

Pittock, S.J., 2006. Brain Abnormalities in Neuromyelitis Optica. Arch. Neurol. 63, 390. https://doi.org/10.1001/archneur.63.3.390

Pittock, S.J., Lucchinetti, C.F., 2016. Neuromyelitis optica and the evolving spectrum of autoimmune aquaporin-4 channelopathies: a decade later: NMO renamed: autoimmune AQP4 channelopathy. Ann. N. Y. Acad. Sci. 1366, 20–39. https://doi.org/10.1111/nyas.12794

Pittock, S.J., Weinshenker, B.G., Lucchinetti, C.F., Wingerchuk, D.M., Corboy, J.R., Lennon, V.A., 2006. Neuromyelitis Optica Brain Lesions Localized at Sites of High Aquaporin 4 Expression. Arch. Neurol. 63, 964–968. https://doi.org/10.1001/archneur.63.7.964

Pleger, B., Ragert, P., Schwenkreis, P., Förster, A.-F., Wilimzig, C., Dinse, H., Nicolas, V., Maier, C., Tegenthoff, M., 2006. Patterns of cortical reorganization parallel impaired tactile discrimination and pain intensity in complex regional pain syndrome. NeuroImage 32, 503–510. https://doi.org/10.1016/j.neuroimage.2006.03.045

Ploghaus, A., Tracey, I., Gati, J.S., Clare, S., Menon, R.S., Matthews, P.M., Rawlins, J.N.P., 1999. Dissociating Pain from Its Anticipation in the Human Brain. Science 284, 1979–1981. https://doi.org/10.1126/science.284.5422.1979

Pohl, M., Kawakami, N., Kitic, M., Bauer, J., Martins, R., Fischer, M.-T., Machado-Santos, J., Mader, S., Ellwart, J.W., Misu, T., Fujihara, K., Wekerle, H., Reindl, M., Lassmann, H., Bradl, M., 2013. T cell-activation in neuromyelitis optica lesions plays a role in their formation. Acta Neuropathol. Commun. 1, 85. https://doi.org/10.1186/2051-5960-1-85

Popescu, B.F.G., Lennon, V.A., Parisi, J.E., Howe, C.L., Weigand, S.D., Cabrera-Gómez, J.A., Newell, K., Mandler, R.N., Pittock, S.J., Weinshenker, B.G., Lucchinetti, C.F., 2011. Neuromyelitis optica unique area postrema lesions: Nausea, vomiting, and pathogenic implications. Neurology 76, 1229–1237. https://doi.org/10.1212/WNL.0b013e318214332c

Popescu, B.F.G., Parisi, J.E., Cabrera-Gómez, J.A., Newell, K., Mandler, R.N., Pittock, S.J., Lennon, V.A., Weinshenker, B.G., Lucchinetti, C.F., 2010. Absence of cortical demyelination in neuromyelitis optica. Neurology 75, 2103–2109. https://doi.org/10.1212/WNL.0b013e318200d80c

Porreca, F., Ossipov, M.H., Gebhart, G.F., 2002. Chronic pain and medullary descending facilitation. Trends Neurosci. 25, 319–325. https://doi.org/10.1016/S0166-2236(02)02157-4

Portenoy, R.K., Ugarte, C., Fuller, I., Haas, G., 2004. Population-based survey of pain in the United States: differences among white, African American, and Hispanic subjects. J. Pain Off. J. Am. Pain Soc. 5, 317–328. https://doi.org/10.1016/j.jpain.2004.05.005

Prieto, G.J., Cannon, J.T., Liebeskind, J.C., 1983. N. raphe magnus lesions disrupt stimulation-produced analgesia from ventral but not dorsal midbrain areas in the rat. Brain Res. 261, 53–57. https://doi.org/10.1016/0006-8993(83)91282-9

Provencher, S.W., 2001. Automatic quantitation of localized in vivo 1H spectra with LCModel. NMR Biomed. 14, 260–264.

Pu, S., Long, Y., Yang, N., He, Y., Shan, F., Fan, Y., Yin, J., Gao, Q., Cong, G., 2015. Syndrome of inappropriate antidiuretic hormone secretion in patients with aquaporin-4 antibody. J. Neurol. 262, 101–107. https://doi.org/10.1007/s00415-014-7537-y

Pyke, T.L., Osmotherly, P.G., Baines, S., 2017. Measuring Glutamate Levels in the Brains of Fibromyalgia Patients and a Potential Role for Glutamate in the Pathophysiology of Fibromyalgia Symptoms: A Systematic Review. Clin. J. Pain 33, 944–954. https://doi.org/10.1097/AJP.0000000000000474

Qian, P., Lancia, S., Alvarez, E., Klawiter, E.C., Cross, A.H., Naismith, R.T., 2012. Association of neuromyelitis optica with severe and intractable pain. Arch. Neurol. 69, 1482–1487. https://doi.org/10.1001/archneurol.2012.768

Qian, W., Chan, Q., Mak, H., Zhang, Z., Anthony, M.-P., Yau, K.K.-W., Khong, P.-L., Chan, K.H., Kim, M., 2011. Quantitative assessment of the cervical spinal cord damage in neuromyelitis optica using diffusion tensor imaging at 3 Tesla. J. Magn. Reson. Imaging JMRI 33, 1312–1320. https://doi.org/10.1002/jmri.22575

R Core Team, 2017. R: A Language and Environment for Statistical Computing. R Foundation for Statistical Computing, Vienna, Austria.

Radloff, L.S., 1977. The CES-D Scale: A Self-Report Depression Scale for Research in the General Population. Appl. Psychol. Meas. 1, 385–401. https://doi.org/10.1177/014662167700100306

Raichle, M.E., 2015. The Brain's Default Mode Network. Annu. Rev. Neurosci. 38, 433–447. https://doi.org/10.1146/annurev-neuro-071013-014030

Raichle, M.E., MacLeod, A.M., Snyder, A.Z., Powers, W.J., Gusnard, D.A., Shulman, G.L., 2001. A default mode of brain function. Proc. Natl. Acad. Sci. 98, 676–682. https://doi.org/10.1073/pnas.98.2.676

Ringelstein, M., Ayzenberg, I., Harmel, J., Lauenstein, A.-S., Lensch, E., Stögbauer, F., Hellwig, K., Ellrichmann, G., Stettner, M., Chan, A., Hartung, H.-P., Kieseier, B., Gold, R., Aktas, O., Kleiter, I., 2015. Long-term Therapy With Interleukin 6 Receptor Blockade in Highly Active Neuromyelitis Optica Spectrum Disorder. JAMA Neurol. 72, 756–763. https://doi.org/10.1001/jamaneurol.2015.0533

Rochfort, S., 2005. Metabolomics Reviewed: A New "Omics" Platform Technology for Systems Biology and Implications for Natural Products Research. J. Nat. Prod. 68, 1813–1820. https://doi.org/10.1021/np050255w

Roemer, S.F., Parisi, J.E., Lennon, V.A., Benarroch, E.E., Lassmann, H., Bruck, W., Mandler, R.N., Weinshenker, B.G., Pittock, S.J., Wingerchuk, D.M., Lucchinetti, C.F., 2007. Pattern-specific loss of aquaporin-4 immunoreactivity distinguishes neuromyelitis optica from multiple sclerosis. Brain 130, 1194–1205. https://doi.org/10.1093/brain/awl371

Rolke, R., Baron, R., Maier, C., Tölle, T.R., Treede, R.-D., Beyer, A., Binder, A., Birbaumer, N., Birklein, F., Bötefür, I.C., Braune, S., Flor, H., Huge, V., Klug, R., Landwehrmeyer, G.B., Magerl, W., Maihöfner, C., Rolko, C., Schaub, C., Scherens, A., Sprenger, T., Valet, M., Wasserka, B., 2006. Quantitative sensory testing in the German Research Network on Neuropathic Pain (DFNS): Standardized protocol and reference values. PAIN 123, 231–243. https://doi.org/10.1016/j.pain.2006.01.041

Rowell, L.N., Mechlin, B., Ji, E., Addamo, M., Girdler, S.S., 2011. Asians differ from non-Hispanic Whites in experimental pain sensitivity. Eur. J. Pain Lond. Engl. 15, 764–771. https://doi.org/10.1016/j.ejpain.2010.11.016

Roy, M., Shohamy, D., Daw, N., Jepma, M., Wimmer, E., Wager, T.D., 2014. Representation of aversive prediction errors in the human periaqueductal gray. Nat. Neurosci. 17, 1607–1612. https://doi.org/10.1038/nn.3832

Sabater, L., Giralt, A., Boronat, A., Hankiewicz, K., Blanco, Y., Llufriu, S., Alberch, J., Graus, F., Saiz, A., 2009. Cytotoxic effect of neuromyelitis optica antibody (NMO-IgG) to astrocytes: An in vitro study. J. Neuroimmunol. 215, 31–35. https://doi.org/10.1016/j.jneuroim.2009.07.014

Saini, H., Fernandez, G., Kerr, D., Levy, M., 2010. Differential expression of aquaporin-4 isoforms localizes with neuromyelitis optica disease activity. J. Neuroimmunol. 221, 68–72. https://doi.org/10.1016/j.jneuroim.2010.02.007

Saji, E., Arakawa, M., Yanagawa, K., Toyoshima, Y., Yokoseki, A., Okamoto, K., Otsuki, M., Akazawa, K., Kakita, A., Takahashi, H., Nishizawa, M., Kawachi, I., 2013. Cognitive impairment and cortical degeneration in neuromyelitis optica. Ann. Neurol. 73, 65–76. https://doi.org/10.1002/ana.23721

Salimi-Khorshidi, G., Douaud, G., Beckmann, C.F., Glasser, M.F., Griffanti, L., Smith, S.M., 2014. Automatic Denoising of Functional MRI Data: Combining Independent Component Analysis and Hierarchical Fusion of Classifiers. NeuroImage 90, 449–468. https://doi.org/10.1016/j.neuroimage.2013.11.046

Samad, T.A., Moore, K.A., Sapirstein, A., Billet, S., Allchorne, A., Poole, S., Bonventre, J.V., Woolf, C.J., 2001. Interleukin-1beta-mediated induction of Cox-2 in the CNS contributes to inflammatory pain hypersensitivity. Nature 410, 471–475. https://doi.org/10.1038/35068566

Samineni, V.K., Grajales-Reyes, J.G., Copits, B.A., O'Brien, D.E., Trigg, S.L., Gomez, A.M., Bruchas, M.R., Gereau, R.W., 2017. Divergent Modulation of Nociception by Glutamatergic and GABAergic Neuronal Subpopulations in the Periaqueductal Gray. eNeuro 4. https://doi.org/10.1523/ENEURO.0129-16.2017

Sedani, S., Absoud, M., Milford, D., Leite, M., Pike, M., Vincent, A., Palace, J., Wassmer, E., 2012. Abstract P675: Good response to Ofatumumab in a child with severe relapsing Neuromyelitis Optica. Mult. Scler. J. 18, 279–508. https://doi.org/10.1177/1352458512459021

Seghier, M.L., 2013. The Angular Gyrus. The Neuroscientist 19, 43–61. https://doi.org/10.1177/1073858412440596

Seixas, D., Foley, P., Palace, J., Lima, D., Ramos, I., Tracey, I., 2014. Pain in multiple sclerosis: A systematic review of neuroimaging studies. NeuroImage Clin. 5, 322–331. https://doi.org/10.1016/j.nicl.2014.06.014

Serkova, N.J., Glunde, K., 2009. Metabolomics of cancer. Methods Mol. Biol. Clifton NJ 520, 273–295. https://doi.org/10.1007/978-1-60327-811-9_20

Shah, S., Kellman, P., Greiser, A., Weale, P., Zuehlsdorff, S., Jerecic, R., 2009. Rapid Fieldmap Estimation for Cardiac Shimming. Proc. Intl. Soc. Mag. Reson. Med. 566.

Shimizu, J., Hatanaka, Y., Hasegawa, M., Iwata, A., Sugimoto, I., Date, H., Goto, J., Shimizu, T., Takatsu, M., Sakurai, Y., Nakase, H., Uesaka, Y., Hashida, H., Hashimoto, K., Komiya, T., Tsuji, S., 2010. IFNβ-1b may severely exacerbate Japanese optic-spinal MS in neuromyelitis optica spectrum. Neurology 75, 1423–1427. https://doi.org/10.1212/WNL.0b013e3181f8832e

Siddall, P.J., McClelland, J.M., Rutkowski, S.B., Cousins, M.J., 2003. A longitudinal study of the prevalence and characteristics of pain in the first 5 years following spinal cord injury. Pain 103, 249–257.

Siegfried, B., Nunes de Souza, R.L., 1989. NMDA receptor blockade in the periaqueductal grey prevents stress-induced analgesia in attacked mice. Eur. J. Pharmacol. 168, 239–242. https://doi.org/10.1016/0014-2999(89)90570-0

Sinnecker, T., Dörr, J., Pfueller, C.F., Harms, L., Ruprecht, K., Jarius, S., Brück, W., Niendorf, T., Wuerfel, J., Paul, F., 2012. Distinct lesion morphology at 7-T MRI differentiates neuromyelitis optica from multiple sclerosis. Neurology 79, 708–714. https://doi.org/10.1212/WNL.0b013e3182648bc8

Sivilotti, L., Woolf, C.J., 1994. The contribution of GABAA and glycine receptors to central sensitization: disinhibition and touch-evoked allodynia in the spinal cord. J. Neurophysiol. 72, 169–179.

Smith, S.M., Nichols, T.E., 2009. Threshold-free cluster enhancement: addressing problems of smoothing, threshold dependence and localisation in cluster inference. NeuroImage 44, 83–98. https://doi.org/10.1016/j.neuroimage.2008.03.061

Stanaway, F.F., Blyth, F.M., Cumming, R.G., Naganathan, V., Handelsman, D.J., Waite, L.M., Sambrook, P.N., Creasey, H.M., Seibel, M.J., Le Couteur, D.G., 2011. Back pain in older male Italian-born immigrants in Australia: the importance of socioeconomic factors. Eur. J. Pain Lond. Engl. 15, 70–76. https://doi.org/10.1016/j.ejpain.2010.05.009

Stanwell, P., Siddall, P., Keshava, N., Cocuzzo, D., Ramadan, S., Lin, A., Herbert, D., Craig, A., Tran, Y., Middleton, J., Gautam, S., Cousins, M., Mountford, C., 2010. Neuro magnetic resonance spectroscopy using wavelet decomposition and statistical testing identifies biochemical changes in people with spinal cord injury and pain. NeuroImage 53, 544–552. https://doi.org/10.1016/j.neuroimage.2010.06.051

Stellmann, J.-P., Krumbholz, M., Friede, T., Gahlen, A., Borisow, N., Fischer, K., Hellwig, K., Pache, F., Ruprecht, K., Havla, J., Kümpfel, T., Aktas, O., Hartung, H.-P., Ringelstein, M., Geis, C., Kleinschnitz, C., Berthele, A., Hemmer, B., Angstwurm, K., Young, K.L., Schuster, S., Stangel, M., Lauda, F., Tumani, H., Mayer, C., Zeltner, L., Ziemann, U., Linker, R.A., Schwab, M., Marziniak, M., Bergh, F.T., Oy, U.H., Neuhaus, O., Zettl, U., Faiss, J., Wildemann, B., Paul, F., Jarius, S., Trebst, C., Kleiter, I., 2017. Immunotherapies in neuromyelitis optica spectrum disorder: efficacy and predictors of response. J Neurol Neurosurg Psychiatry 88, 639–647. https://doi.org/10.1136/jnnp-2017-315603

Storoni, M., Davagnanam, I., Radon, M., Siddiqui, A., Plant, G.T., 2013. Distinguishing Optic Neuritis in Neuromyelitis Optica Spectrum Disease From Multiple Sclerosis: A Novel Magnetic Resonance Imaging Scoring System. J. Neuroophthalmol. 33, 123–127. https://doi.org/10.1097/WNO.0b013e318283c3ed

Suchdev, K., Razmjou, S., Venkatachalam, P., Khan, O.A., Mohamed, W., Ibrahim, M.S., 2017. Late onset neuromyelitis optica mimicking an acute stroke in an elderly patient. J. Neuroimmunol. 309, 1–3. https://doi.org/10.1016/j.jneuroim.2017.04.006

Sudoh, Y., Cahoon, E.E., Gerner, P., Wang, G.K., 2003. Tricyclic antidepressants as long-acting local anesthetics. Pain 103, 49–55.

Sun, J., Song, H., Yang, Y., Zhang, K., Gao, X., Li, X., Ni, L., Lin, P., Niu, C., 2017. Metabolic changes in normal appearing white matter in multiple sclerosis patients using multivoxel magnetic resonance spectroscopy imaging. Medicine (Baltimore) 96. https://doi.org/10.1097/MD.0000000000006534

Sung, B., Lim, G., Mao, J., 2003. Altered Expression and Uptake Activity of Spinal Glutamate Transporters after Nerve Injury Contribute to the Pathogenesis of Neuropathic Pain in Rats. J. Neurosci. 23, 2899–2910.

Susser, E., Sprecher, E., Yarnitsky, D., 1999. Paradoxical heat sensation in healthy subjects: peripherally conducted by Aδ or C fibres? Brain 122, 239–246. https://doi.org/10.1093/brain/122.2.239

Suzuki, R., Rahman, W., Hunt, S.P., Dickenson, A.H., 2004. Descending facilitatory control of mechanically evoked responses is enhanced in deep dorsal horn neurones following peripheral nerve injury. Brain Res. 1019, 68–76. https://doi.org/10.1016/j.brainres.2004.05.108

Suzuki, R., Rahman, W., Rygh, L.J., Webber, M., Hunt, S.P., Dickenson, A.H., 2005. Spinal-supraspinal serotonergic circuits regulating neuropathic pain and its treatment with gabapentin: Pain 117, 292–303. https://doi.org/10.1016/j.pain.2005.06.015

Svendsen, K.B., Jensen, T.S., Hansen, H.J., Bach, F.W., 2005. Sensory function and quality of life in patients with multiple sclerosis and pain. PAIN 114, 473–481. https://doi.org/10.1016/j.pain.2005.01.015

Svendsenl, K.B., Sørensenl, L., Jensenl, T.S., Hansenl, H.J., Bachl, F.W., 2011. MRI of the central nervous system in MS patients with and without pain. Eur. J. Pain 15, 395–401. https://doi.org/10.1016/j.ejpain.2010.09.006

Tackley, G., Kuker, W., Palace, J., 2014. Magnetic resonance imaging in neuromyelitis optica. Mult. Scler. J. 20, 1153–1164. https://doi.org/10.1177/1352458514531087

Tackley, G., O'Brien, F., Rocha, J., Woodhall, M., Waters, P., Chandratre, S., Halfpenny, C., Hemingway, C., Wassmer, E., Wasiewski, W., Leite, M.I., Palace, J., 2016. Neuromyelitis optica relapses: Race and rate, immunosuppression and impairment. Mult. Scler. Relat. Disord. 7, 21–25. https://doi.org/10.1016/j.msard.2016.02.014

Tahara, M., Ito, R., Tanaka, K., Tanaka, M., 2012. Cortical and leptomeningeal involvement in three cases of neuromyelitis optica. Eur. J. Neurol. Off. J. Eur. Fed. Neurol. Soc. 19, e47-48. https://doi.org/10.1111/j.1468-1331.2012.03667.x

Tan, G., Jensen, M.P., Thornby, J., Anderson, K.O., 2005. Ethnicity, control appraisal, coping, and adjustment to chronic pain among black and white Americans. Pain Med. Malden Mass 6, 18–28. https://doi.org/10.1111/j.1526-4637.2005.05008.x

Thevenot, E.A., Roux, A., Xu, Y., Ezan, E., Junot, C., 2015. Analysis of the human adult urinary metabolome variations with age, body mass index and gender by implementing a comprehensive workflow for univariate and OPLS statistical analyses. J. Proteome Res. 14, 3322–3335.

Tölle, T.R., Kaufmann, T., Siessmeier, T., Lautenbacher, S., Berthele, A., Munz, F., Zieglgänsberger, W., Willoch, F., Schwaiger, M., Conrad, B., Bartenstein, P., 1999. Region-specific encoding of sensory and affective components of pain in the human brain: a positron emission tomography correlation analysis. Ann. Neurol. 45, 40–47.

Tovote, P., Esposito, M.S., Botta, P., Chaudun, F., Fadok, J.P., Markovic, M., Wolff, S.B.E., Ramakrishnan, C., Fenno, L., Deisseroth, K., Herry, C., Arber, S., Lüthi, A., 2016. Midbrain circuits for defensive behaviour. Nature 534, 206–212. https://doi.org/10.1038/nature17996

Twork, S., Wiesmeth, S., Spindler, M., Wirtz, M., Schipper, S., Pöhlau, D., Klewer, J., Kugler, J., 2010. Disability status and quality of life in multiple sclerosis: non-linearity of the Expanded Disability Status Scale (EDSS). Health Qual. Life Outcomes 8, 55. https://doi.org/10.1186/1477-7525-8-55

Urban, M.O., Gebhart, G.F., 1999. Supraspinal contributions to hyperalgesia. Proc. Natl. Acad. Sci. 96, 7687–7692. https://doi.org/10.1073/pnas.96.14.7687

Uzawa, A., Mori, M., Arai, K., Sato, Y., Hayakawa, S., Masuda, S., Taniguchi, J., Kuwabara, S., 2010. Cytokine and chemokine profiles in neuromyelitis optica: significance of interleukin-6. Mult. Scler. Houndmills Basingstoke Engl. 16, 1443–1452. https://doi.org/10.1177/1352458510379247

Vachon-Presseau, E., Tétreault, P., Petre, B., Huang, L., Berger, S.E., Torbey, S., Baria, A.T., Mansour, A.R., Hashmi, J.A., Griffith, J.W., Comasco, E., Schnitzer, T.J., Baliki, M.N., Apkarian, A.V., 2016. Corticolimbic anatomical characteristics predetermine risk for chronic pain. Brain 139, 1958–1970. https://doi.org/10.1093/brain/aww100

van Beek, J.D., 2007. matNMR: a flexible toolbox for processing, analyzing and visualizing magnetic resonance data in Matlab. J. Magn. Reson. San Diego Calif 1997 187, 19–26. https://doi.org/10.1016/j.jmr.2007.03.017

Vaughan, C.W., Ingram, S.L., Connor, M.A., Christie, M.J., 1997. How opioids inhibit GABA-mediated neurotransmission. Nature 390, 611–614. https://doi.org/10.1038/37610

Viegas, S., Weir, A., Esiri, M., Kuker, W., Waters, P., Leite, M.I., Vincent, A., Palace, J., 2009. Symptomatic, radiological and pathological involvement of the hypothalamus in neuromyelitis optica. J. Neurol. Neurosurg. Psychiatry 80, 679–682. https://doi.org/10.1136/jnnp.2008.157693

Vierck, C.J., Whitsel, B.L., Favorov, O.V., Brown, A.W., Tommerdahl, M., 2013. Role of primary somatosensory cortex in the coding of pain. Pain 154, 334–344. https://doi.org/10.1016/j.pain.2012.10.021

Viisanen, H., Pertovaara, A., 2010. Roles of the rostroventromedial medulla and the spinal 5-HT1A receptor in descending antinociception induced by motor cortex stimulation in the neuropathic rat. Neurosci. Lett. 476, 133–137. https://doi.org/10.1016/j.neulet.2010.04.014

Von Heijne, M., Hao, J.-X., Sollevi, A., Xu, X.-J., 2001. Effects of intrathecal morphine, baclofen, clonidine and R-PIA on the acute allodynia-like behaviours after spinal cord ischaemia in rats. Eur. J. Pain 5, 1–10. https://doi.org/10.1053/eujp.2000.0212

Vrethem, M., Boivie, J., Arnqvist, H., Holmgren, H., Lindström, T., Thorell, L.H., 1997. A comparison a amitriptyline and maprotiline in the treatment of painful polyneuropathy in diabetics and nondiabetics. Clin. J. Pain 13, 313–323.

Wager, T.D., Rilling, J.K., Smith, E.E., Sokolik, A., Casey, K.L., Davidson, R.J., Kosslyn, S.M., Rose, R.M., Cohen, J.D., 2004. Placebo-Induced Changes in fMRI in the Anticipation and Experience of Pain. Science 303, 1162–1167. https://doi.org/10.1126/science.1093065

Wagner-Johnston, N.D., Carson, K.A., Grossman, S.A., 2010. High Outpatient Pain Intensity Scores Predict Impending Hospital Admissions in Patients with Cancer. J. Pain Symptom Manage. 39, 180–185. https://doi.org/10.1016/j.jpainsymman.2009.06.012

Wang, G., Thompson, S.M., 2008. Maladaptive Homeostatic Plasticity in a Rodent Model of Central Pain Syndrome: Thalamic Hyperexcitability after Spinothalamic Tract Lesions. J. Neurosci. 28, 11959–11969. https://doi.org/10.1523/JNEUROSCI.3296-08.2008

Wang, G.K., Strichartz, G.R., 2001. Therapeutic Na+ channel blockers beneficial for pain syndromes. Drug Dev. Res. 54, 154–158. https://doi.org/10.1002/ddr.10014

Wang, M., Offord, J., Oxender, D.L., Su, T.Z., 1999. Structural requirement of the calcium-channel subunit alpha2delta for gabapentin binding. Biochem. J. 342 (Pt 2), 313–320.

Wang, Y., Wu, A., Chen, X., Zhang, L., Lin, Y., Sun, S., Cai, W., Zhang, B., Kang, Z., Qiu, W., Hu, X., Lu, Z., 2014. Comparison of clinical characteristics between neuromyelitis optica spectrum disorders with and without spinal cord atrophy. BMC Neurol. 14. https://doi.org/10.1186/s12883-014-0246-4

Wanigasekera, V., Lee, M.C.H., Rogers, R., Hu, P., Tracey, I., 2011. Neural Correlates of an Injury-Free Model of Central Sensitization Induced by Opioid Withdrawal in Humans. J. Neurosci. Off. J. Soc. Neurosci. 31, 2835–2842. https://doi.org/10.1523/JNEUROSCI.5412-10.2011

Wanigasekera, V., Mezue, M., Andersson, J., Kong, Y., Tracey, I., 2016. Disambiguating pharmacodynamic efficacy from behaviour with neuroimaging: implications for analgesic drug development. Anesthesiology 124, 159–168. https://doi.org/10.1097/ALN.0000000000000924

Waters, P.J., McKeon, A., Leite, M.I., Rajasekharan, S., Lennon, V.A., Villalobos, A., Palace, J., Mandrekar, J.N., Vincent, A., Bar-Or, A., Pittock, S.J., 2012. Serologic diagnosis of NMO: a multicenter comparison of aquaporin-4-IgG assays. Neurology 78, 665–671; discussion 669. https://doi.org/10.1212/WNL.0b013e318248dec1

Watson, T.C., Cerminara, N.L., Lumb, B.M., Apps, R., 2016. Neural Correlates of Fear in the Periaqueductal Gray. J. Neurosci. 36, 12707–12719. https://doi.org/10.1523/JNEUROSCI.1100-16.2016

Wattjes, M.P., Harzheim, M., Lutterbey, G.G., Klotz, L., Schild, H.H., Träber, F., 2007. Axonal Damage But No Increased Glial Cell Activity in the Normal-Appearing White Matter of Patients with Clinically Isolated Syndromes Suggestive of Multiple Sclerosis Using High-Field Magnetic Resonance Spectroscopy. Am. J. Neuroradiol. 28, 1517–1522. https://doi.org/10.3174/ajnr.A0594

Weinshenker, B.G., 2015. Placebo Studies should not be Undertaken in Neuromyelitis Optica: Commentary. Mult. Scler. J. 21, 693–694. https://doi.org/10.1177/1352458515580402

Weinshenker, B.G., Wingerchuk, D.M., Pittock, S.J., Lucchinetti, C.F., Lennon, V.A., 2006. NMO-IgG: A Specific Biomarker for Neuromyelitis Optica. Dis. Markers 22, 197–206. https://doi.org/10.1155/2006/586306

White, S.R., Vyas, D., Bieger, D., 1985. Serotonin immunoreactivity in spinal cord axons and terminals of rodents with experimental allergic encephalomyelitis. Neuroscience 16, 701–709.

Wiberg, M., Westman, J., Blomqvist, A., 1987. Somatosensory projection to the mesencephalon: an anatomical study in the monkey. J. Comp. Neurol. 264, 92–117. https://doi.org/10.1002/cne.902640108

Wingerchuk, D.M., Banwell, B., Bennett, J.L., Cabre, P., Carroll, W., Chitnis, T., Seze, J. de, Fujihara, K., Greenberg, B., Jacob, A., Jarius, S., Lana-Peixoto, M., Levy, M., Simon, J.H., Tenembaum, S., Traboulsee, A.L., Waters, P., Wellik, K.E., Weinshenker, B.G., 2015. International consensus diagnostic criteria for neuromyelitis optica spectrum disorders. Neurology 85, 177–189. https://doi.org/10.1212/WNL.0000000000001729

Wingerchuk, D.M., Hogancamp, W.F., O'Brien, P.C., Weinshenker, B.G., 1999. The clinical course of neuromyelitis optica (Devic's syndrome). Neurology 53, 1107–1107. https://doi.org/10.1212/WNL.53.5.1107

Wingerchuk, D.M., Lennon, V.A., Lucchinetti, C.F., Pittock, S.J., Weinshenker, B.G., 2007. The spectrum of neuromyelitis optica. Lancet Neurol. 6, 805–815. https://doi.org/10.1016/S1474-4422(07)70216-8

Wingerchuk, D.M., Lennon, V.A., Pittock, S.J., Lucchinetti, C.F., Weinshenker, B.G., 2006. Revised diagnostic criteria for neuromyelitis optica. Neurology 66, 1485–1489. https://doi.org/10.1212/01.wnl.0000216139.44259.74

Wood, J.N., Grafman, J., 2003. Human prefrontal cortex: processing and representational perspectives. Nat. Rev. Neurosci. 4, 139–147. https://doi.org/10.1038/nrn1033

Woolf, C.J., 2011. Central sensitization: Implications for the diagnosis and treatment of pain. Pain 152, S2-15. https://doi.org/10.1016/j.pain.2010.09.030

Woolf, C.J., 1983. Evidence for a central component of post-injury pain hypersensitivity. Nature 306, 686–688.

Woolf, C.J., Shortland, P., Coggeshall, R.E., 1992. Peripheral nerve injury triggers central sprouting of myelinated afferents. Nature 355, 75–78. https://doi.org/10.1038/355075a0

Woolf, C.J., Thompson, S.W., 1991. The induction and maintenance of central sensitization is dependent on N-methyl-D-aspartic acid receptor activation; implications for the treatment of post-injury pain hypersensitivity states. Pain 44, 293–299.

Woolrich, M.W., Jbabdi, S., Patenaude, B., Chappell, M., Makni, S., Behrens, T., Beckmann, C., Jenkinson, M., Smith, S.M., 2009. Bayesian analysis of neuroimaging data in FSL. NeuroImage 45, S173-186. https://doi.org/10.1016/j.neuroimage.2008.10.055

Wu, C.W., Chen, C.-L., Liu, P.-Y., Chao, Y.-P., Biswal, B.B., Lin, C.-P., 2011. Empirical evaluations of slice-timing, smoothing, and normalization effects in seed-based, resting-state functional magnetic resonance imaging analyses. Brain Connect. 1, 401–410. https://doi.org/10.1089/brain.2011.0018

Wyss, J.M., Sripanidkulchai, K., 1984. The topography of the mesencephalic and pontine projections from the cingulate cortex of the rat. Brain Res. 293, 1–15.

Yaksh, T.L., Al-Rodhan, N.R., Jensen, T.S., 1988. Sites of action of opiates in production of analgesia. Prog. Brain Res. 77, 371–394.

Yalcin, I., Choucair-Jaafar, N., Benbouzid, M., Tessier, L.-H., Muller, A., Hein, L., Freund-Mercier, M.-J., Barrot, M., 2009. β2-adrenoceptors are critical for antidepressant treatment of neuropathic pain. Ann. Neurol. 65, 218–225. https://doi.org/10.1002/ana.21542

Yao, X., Verkman, A.S., 2017. Complement regulator CD59 prevents peripheral organ injury in rats made seropositive for neuromyelitis optica immunoglobulin G. Acta Neuropathol. Commun. 5. https://doi.org/10.1186/s40478-017-0462-4

Yeomans, D.C., Proudfit, H.K., 1990. Projections of substance P-immunoreactive neurons located in the ventromedial medulla to the A7 noradrenergic nucleus of the rat demonstrated using retrograde tracing combined with immunocytochemistry. Brain Res. 532, 329–332.

Yezierski, R.P., Liu, S., Ruenes, G.L., Kajander, K.J., Brewer, K.L., 1998. Excitotoxic spinal cord injury: behavioral and morphological characteristics of a central pain model. Pain 75, 141–155. https://doi.org/10.1016/S0304-3959(97)00216-9

Yezierski, R.P., Yu, C.-G., Mantyh, P.W., Vierck, C.J., Lappi, D.A., 2004. Spinal neurons involved in the generation of at-level pain following spinal injury in the rat. Neurosci. Lett., Festschrift dedicated to Prof. Manfred Zimmermann on the occasion of his 70th birthday 361, 232–236. https://doi.org/10.1016/j.neulet.2003.12.035

Yiannakas, M.C., Mustafa, A.M., De Leener, B., Kearney, H., Tur, C., Altmann, D.R., De Angelis, F., Plantone, D., Ciccarelli, O., Miller, D.H., Cohen-Adad, J., Gandini Wheeler-Kingshott, C.A.M., 2015. Fully automated segmentation of the cervical cord from T1-weighted MRI using PropSeg: Application to multiple sclerosis. NeuroImage Clin. 10, 71–77. https://doi.org/10.1016/j.nicl.2015.11.001

Yonezu, T., Ito, S., Mori, M., Ogawa, Y., Makino, T., Uzawa, A., Kuwabara, S., 2013. "Bright spotty lesions" on spinal magnetic resonance imaging differentiate neuromyelitis optica from multiple sclerosis. Mult. Scler. J. https://doi.org/10.1177/1352458513495581

Yonezu, T., Ito, S., Mori, M., Ogawa, Y., Makino, T., Uzawa, A., Kuwabara, S., 2012. Evaluating spinal cord MRI findings in neuromyelitis optica. Neuroradiology 54.

Young, S.P., Kapoor, S.R., Viant, M.R., Byrne, J.J., Filer, A., Buckley, C.D., Kitas, G.D., Raza, K., 2013. The Impact of Inflammation on Metabolomic Profiles in Patients With Arthritis. Arthritis Rheum. 65, 2015–2023. https://doi.org/10.1002/art.38021

Yu, C.S., Lin, F.C., Li, K.C., Jiang, T.Z., Zhu, C.Z., Qin, W., Sun, H., Chan, P., 2006. Diffusion Tensor Imaging in the Assessment of Normal-Appearing Brain Tissue Damage in Relapsing Neuromyelitis Optica. Am. J. Neuroradiol. 27, 1009–1015.

Zakrzewska, J.M., 2010. Medical management of trigeminal neuropathic pains. Expert Opin. Pharmacother. 11, 1239–1254. https://doi.org/10.1517/14656561003767449

Zambreanu, L., Wise, R.G., Brooks, J.C. w, Iannetti, G.D., Tracey, I., 2005. A role for the brainstem in central sensitisation in humans. Evidence from functional magnetic resonance imaging. Pain 114, 397–407. https://doi.org/10.1016/j.pain.2005.01.005

Zelman, D.C., Dukes, E., Brandenburg, N., Bostrom, A., Gore, M., 2005. Identification of cut-points for mild, moderate and severe pain due to diabetic peripheral neuropathy: Pain 115, 29–36. https://doi.org/10.1016/j.pain.2005.01.028

Zemlan, F.P., Behbehani, M.M., 1988. Nucleus cuneiformis and pain modulation: anatomy and behavioral pharmacology. Brain Res. 453, 89–102. https://doi.org/10.1016/0006-8993(88)90146-1

Zhang, S., Tang, J.-S., Yuan, B., Jia, H., 1998. Inhibitory effects of electrical stimulation of ventrolateral orbital cortex on the rat jaw-opening reflex. Brain Res. 813, 359–366. https://doi.org/10.1016/S0006-8993(98)01050-6

Zhao, S., Mutch, K., Elsone, L., Nurmikko, T., Jacob, A., 2014. Neuropathic pain in neuromyelitis optica affects activities of daily living and quality of life. Mult. Scler. Houndmills Basingstoke Engl. 20, 1658–1661. https://doi.org/10.1177/1352458514522103

Zhao, S., Mutch, K., Elsone, L., Nurmikko, T., Jacob, A., 2013. Pain in Neuromyelitis Optica Is an Under–Recognised but Disabling Symptom. J. Neurol. Neurosurg. Psychiatry 84, e2–e2. https://doi.org/10.1136/jnnp-2013-306573.195

Zhao, X., Xu, M., Jorgenson, K., Kong, J., 2017. Neurochemical changes in patients with chronic low back pain detected by proton magnetic resonance spectroscopy: A systematic review. NeuroImage Clin. 13, 33–38. https://doi.org/10.1016/j.nicl.2016.11.006

Zhong, X., Wang, H., Bao, J., Li, R., Long, Y., Lu, Z., Dai, Y., Qiu, W., Hu, X., 2012. Relationship between neuromyelitis optica-IgG status and spinal cord magnetic resonance imaging in patients with neuromyelitis optica. Chin Med J 125, 270–274.

Zhu, H., Barker, P.B., 2011. MR Spectroscopy and Spectroscopic Imaging of the Brain. Methods Mol. Biol. Clifton NJ 711, 203–226. https://doi.org/10.1007/978-1-61737-992-5_9

Ziegler, E.A., Magerl, W., Meyer, R.A., Treede, R.D., 1999. Secondary hyperalgesia to punctate mechanical stimuli. Central sensitization to A-fibre nociceptor input. Brain J. Neurol. 122 (Pt 12), 2245–2257.

Zigmond, A.S., Snaith, R.P., 1983. The Hospital Anxiety and Depression Scale. Acta Psychiatr. Scand. 67, 361–370. https://doi.org/10.1111/j.1600-0447.1983.tb09716.x

Zubieta, J.-K., Bueller, J.A., Jackson, L.R., Scott, D.J., Xu, Y., Koeppe, R.A., Nichols, T.E., Stohler, C.S., 2005. Placebo Effects Mediated by Endogenous Opioid Activity on μ-Opioid Receptors. J. Neurosci. 25, 7754–7762. https://doi.org/10.1523/JNEUROSCI.0439-05.2005

Zubieta, J.K., Smith, Y.R., Bueller, J.A., Xu, Y., Kilbourn, M.R., Jewett, D.M., Meyer, C.R., Koeppe, R.A., Stohler, C.S., 2001. Regional mu opioid receptor regulation of sensory and affective dimensions of pain. Science 293, 311–315. https://doi.org/10.1126/science.1060952

Appendix

Common abbreviations

Ab, antibody

ACC, anterior cingulate cortex

AQP4, aquaporin 4

AQP4Ab, anti-aquaporin 4 antibody

BBB, blood-brain barrier

BPI, brief pain inventory score

CNS, central nervous system

CSF, cerebroscpinal fluid

CST, corticospinal tract

CSA, cross-sectional area (of spinal cord)

DH, dorsal horn

dlPFC, dorsolateral pre-frontal cortex

DMN, default mode network

DPMN, descending pain modulatory network

EDMUS, European Database for Multiple Sclerosis (EDMUS) grading scale

EDSS, expanded disability status scale

EV, explanatory variable used in GLM

FA, fractional anisotropy

FC, fasciculus cuneatus (lateral dorsal column)

FG, fasciculus gracilis (medial dorsal column)

FOV, field of view

GABA, γ-aminobutyric acid

GLM, general linear model

GM, grey matter

HADS, hospital anxiety and depression scale

ICA, independent component analysis

LC, locus coeruleus

LETM, longitudinally extensive transverse myelitis. Spinal cord lesions greater ≥3 spinal segments

MD, mean diffusivity

mI, *myo*-inositol

MS, multiple sclerosis

NAA, N-acetylaspartate

NMO, neuromyelitis optica (AQP4Ab positive unless otherwise stated)

NNT, number needed to treat

ON, optic neuritis

PAG, periaqueductal grey

PCA, principle component analysis

PCC, posterior cingulate cortex

PFC, pre-frontal cortex

PLSDA, partial least-squares discriminant analysis

PSI, pain severity index (taken from the BPI unless otherwise stated)

QST, quantitative sensory testing

RSN, resting state network

SCI, spinal cord injury

SNR, signal-to-noise ration

STT, spino-thalamic tract

vlPFC, ventrolateral pre-frontal cortex

WM, white matter